ABSTRACT

WON, JONGHO. Natural and Enhanced Attenuation of High Explosives in Soil. (Under the direction of Dr. Robert C. Borden and Dr. Detlef Knappe)

The high explosive (HE) compounds 2,4,6-trinitrotoluene (TNT), hexahydro-1,3,5-trinitro-1,3,5-triazine (RDX; royal demolition explosive), and octahydro-1,3,5,7-tetranitro-1,3,5,7-tetrazine (HMX; high melting explosive) are commonly used in military munitions and can be deposited on military ranges during training activities. HEs deposited on ranges can be transported into groundwater by rainfall and migrate off the ranges, potentially causing adverse health impacts. However, only limited research has been conducted to identify cost effective technologies for treating explosives deposited on ranges. In this study, soil conditions controlling HEs natural attenuation were investigated, and the impact of mixed organic amendment (waste glycerin and lignosulfonate) in HE leaching was evaluated to improve our understanding of processes controlling HE leaching in grenade range soil.

Soil microcosms composed of grenade range soil and water showed that TNT extensively degraded under both aerobic and anaerobic conditions with or without organic amendment addition. While RDX and HMX did not biodegrade under aerobic conditions, they were significantly biodegraded under anaerobic conditions, without accumulation of TNT or RDX degradation products. Microcosm results also showed that addition of glycerin (GL) and lignosulfonate (LS) significantly increased oxygen consumption rates in soil, indicating that addition of organic amendment can potentially be effective in generating anoxic conditions and stimulating anaerobic HEs biodegradation.

Batch sorption studies were performed to identify the extent of HEs sorption and impact of LS addition. Experimental results indicate that both LS and HEs nonlinearly sorb to the soils examined in this study. Norlig A (NA, lignosulfonate) weakly binds to soil initially, with potential desorption and migration into the deeper soil. Ultrazine CA (UCA) more strongly sorbed to field sand (FS) than NA. Greater sorption of RDX was observed in range soil (RS) than in FS. RDX sorption was similar to TNT in both FS and RS, inconsistent with prior research. NA amendment was not effective in enhancing overall TNT and RDX sorption in both FS and RS. Nonlinear sorption of explosives needs to be considered as an important factor in predicting transport since sorption to soil is concentration dependent.

Transport and fate of HEs were examined in laboratory columns containing soils from two adjoining hand grenade throwing bays. Experimental treatments included amendment with GL + LS and parallel untreated controls. Experimental results showed extensive TNT degradation under both aerobic and anaerobic conditions, consistent with prior microcosm results. A portion of the RDX naturally attenuated in soil columns that were aerobic for much of the monitoring period. However, RDX degradation was more extensive under anoxic conditions. In one column, the soil remained anoxic for about a year after amendment addition, reducing RDX leaching. RDX was reduced to lower concentrations when elevated TOC concentrations were present in the column effluent.

A 26-month field study was conducted to evaluate the effect of monitored natural attenuation (MNA) and organic substrate enhanced attenuation (OSEA) on the transport and attenuation of HEs in two adjoining hand grenade throwing bays. Field monitoring results

demonstrated that relatively minor changes in soil properties resulted in substantial differences in geophysical and geochemical conditions on the ranges, influencing RDX leaching. Occasional periods when the soil becomes anoxic can substantially reduce RDX leaching. Addition of GL + LS resulted in transition of redox conditions from aerobic to anoxic, reducing RDX leaching. However, additional research will be needed to develop this technology and improve our understanding of how soil properties and amendment addition control leaching.

Natural and Enhanced Attenuation of High Explosives in Soil

by
Jongho Won

A dissertation submitted to the Graduate Faculty of
North Carolina State University
in partial fulfillment of the
requirements for the degree of
Doctor of Philosophy

Civil Engineering

Raleigh, North Carolina

2016

APPROVED BY:

Dr. Robert C. Borden Co-chair of Advisory Committee	Dr. Detlef Knappe Co-chair of Advisory Committee
Dr. Francis Lajara de los Reyes	Dr. Joshua Heitman

BIOGRAPHY

Jongho Won was born in Jinan, South Korea on December 2, 1978. He received his B.E. degree in Environmental Engineering from Korea University, South Korea in 2003 and M.S. degree in Environmental Science and Engineering from Gwangju Institute of Science and Technology (GIST), South Korea in 2006. After receiving his M.S. degree, he worked at Korea Water Resource Corporation (K-Water) for one year and then worked at Korea Environmental Industry and Technology Institute (KEITI) for three years. He started as a Graduate Research Assistant in the Department of Civil, Construction, and Environmental Engineering at North Carolina State University in August 2011. He received his Ph.D. degree in Civil Engineering with a minor in Soil Science in August 2016.

ACKNOWLEDGMENTS

First of all, I truly thanks to God. Without his guidance I could not achieve this work.

I would like to thank my advisor Dr. Robert C. Borden for his guidance, support, encouragement, and advice for all the time of my journey to pursue a Ph.D. degree. His advice and guidance enabled me to have wider sight to see problems and experimental results. I also wish to thank Dr. Detlef Knappe for being my co-advisor and his precious advice on my research. I would like to acknowledge other committee members, Dr. Francis Lajara de los Reyes and Dr. Joshua Heitman for accepting to be in my doctoral committee and providing invaluable comments on my research.

I wish to thank lab and office mates, Jason, Tino, Jonathan, Andrew, Della, and Erika for their helps and friendship in and out of the laboratory. I also would like to thank my research colleagues Bilgen and Stewart for their efforts and helps in my research project. I am also thankful to David and Lisa for their big helps in the laboratory, including chemical analysis and troubleshooting of analytical instruments.

Very special thanks are given to my wife, Youjin. Without her incredible support, sacrifice, and faith in me, I would not finish my journey for a Ph.D. degree. Also my huge thanks extend to my lovely daughter, Haein. I wish to express my true sorry to her for not sharing enough time with her during my graduate study. I also wish to appreciate my parents for their endless encouragement and praying for me.

TABLE OF CONTENTS

LIST OF TABLES viii

LIST OF FIGURES X

CHAPTER 1. INTRODUCTION 1

1.1 Problems and Research Needs 1

1.2 Research Objectives 3

1.3 Dissertation Organization 4

CHAPTER 2. LITERATURE REVIEW 5

2.1 Introduction of High Explosives 5

2.2 Sorption of High Explosives 9

2.3 Biotic Degradation of High Explosives 10

2.4 Abiotic Degradation of High Explosives 16

2.4.1 Reductive Transformation of High Explosives by Reduced Iron Species 17

2.4.2 Abiotic Degradation of High Explosives by Electron Shuttles 18

2.5 Current Remediation Technologies 21

2.6 Proposed Remediation Approach 23

2.6.1 Proposed Remediation Technology 23

2.6.2 Prior Work 24

2.7 References 26

CHAPTER 3. IMPACT OF GLYCERIN AND LIGNOSULFONATE ON BIODEGRADATION OF HIGH EXPLOSIVES IN SOIL 34

3.1 Introduction 34
3.2 Material and Methods 39
3.2.1 Chemicals 39
3.2.2 Active Range Soils Used in Experiments 39
3.2.3 Biodegradation of HEs in Soil Slurry Microcosms 40
3.2.4 Oxygen Consumption in Soil Slurry Microcosms 42
3.2.5 Sample Extraction and Analytical Methods 43
3.3 Experimental Results 45
3.3.1 HEs Biodegradation 45
3.3.2 Oxygen Consumption in Soil 50
3.4 Discussion 57
3.5 Conclusions 60
3.6 References 61
CHAPTER 4. BATCH STUDIES OF TNT AND RDX SORPTION IN NATURAL AND LIGNOSULFONATE AMENDED SOILS 69
4.1 Introduction 69
4.2 Material and Methods 71
4.3 Experimental Results 77
4.3.1 Sorption of Lignosulfonates in Soils 77
4.3.2 TNT and RDX Sorption to FS and RS 82
4.3.3 TNT and RDX Sorption to Lignosulfonate Treated Soil 89
4.4 Discussion 93

4.5 Conclusions 96
4.6 References 96
CHAPTER 5. LABORATORY COLUMN EVALUATION OF HIGH EXPLOSIVES DEGRADATION IN GRENADE RANGE SOILS 103
5.1 Introduction 103
5.2 Material and Methods 106
5.3 Experimental Results 110
5.3.1 Leaching Columns 110
5.3.2 Soil Column Hydraulics 114
5.3.3 Oxygen Distribution in Soil Columns 118
5.3.4 Soil Column Geochemistry 120
5.3.5 Explosives in Soil Columns 126
5.4 Discussion 132
5.5 Conclusions 136
5.6 References 136
CHAPTER 6. NATURAL AND ENHANCED ATTENUATION OF EXPLOSIVES ON A HAND GRENADE RANGE 142
6.1 Introduction 142
6.2 Material and Methods 145
6.3 Experimental Results 148
6.3.1 Field Site Characteristics 148
6.3.2 Site Hydrology and Biogeochemistry 150

6.3.3 Explosives 155
6.4 Discussion 159
6.5 Conclusions 161
6.6 References 161
CHAPTER 7. CONCLUSIONS AND RECOMMENDATIONS FOR FURTHER RESEARCH 166
7.1 Conclusions 166
7.2 Recommendations for Further Research 168
APPENDICES 170
APPENDIX I. Experimental and Analytical Methods 171
APPENDIX II. Supplementary Material for Batch Study 177
APPENDIX III. Supplementary Material for Sorption Study 182
APPENDIX IV. Supplementary Material for Column Study 197
APPENDIX V. Supplementary Material for Field Study 208

LIST OF TABLES

Table 2.1. Physical and chemical properties of HE compounds (Brannon and Pennington 2002; Pichtel 2012). 7

Table 3.1. Average lag periods and degradation rates of RDX and HMX in Bay C and T soil microcosms with different treatments assuming first-order degradation of the components. Values in parentheses are standard deviations of replicates. Bold values are statistically different from live control (*p-value* < 0.05). 50

Table 3.2. First- and second-order degradation coefficients, ratios of oxygen to substrate consumed, and RMSE between observed and modeling results assuming complete mineralization of organic substrates. The best fit parameter values for each treatment are shown in bold. 56

Table 4.1. Selected properties of soils used in sorption isotherm study. 72

Table 4.2. Chemical composition of artificial groundwater. 73

Table 4.3. Regression parameters for Ultrazine CA and Norlig A sorption to field sand (FS) and/or range soil (RS) with 14-day equilibration period (± 95 % confidence limit). Bold values are parameters for the model with the best fit. 79

Table 4.4. Regression parameters for TNT and RDX sorption to field sand (FS) and range soil (RS) with 14-day equilibration period (± 95 % confidence limit). Bold values are parameters for the model with the best fit. 83

Table 4.5. Regression parameters of TNT and RDX sorption to washed (WFS) and amended field sand (AFS), intact (IRS), washed (WRS), and amended range soils (ARS) (±

95 % confidence limit). Bold values are parameters for the model with the best fit. 93
Table 5.1. Average column hydraulic properties. 115
Table S-1. Main physicochemical properties of Ultrazine CA and Norlig A (Farling 2013). 182
Table S-2. Main physicochemical properties of TNT and RDX (Brannon and Pennington 2002). 183
Table S-3. Regression parameters for experimental lignosulfonate sorption results in field sand (FS) and range soil (RS). 186
Table S-4. Regression parameters of 2,6-DNT, 2,4-DNT, and 2-ADNT sorption to intact (IRS), washed (WRS), and amended range soils (ARS). 192
Table S-5. Regression parameters of TNT and RDX sorption to washed (WFS) and amended field sand (AFS), intact (IRS), washed (WRS), and amended range soils (ARS) (± 95 % confidence limit). Bold values are parameters for the model with the best fit. 193
Table S-6. Hydraulics of soil columns measured at the termination of monitoring. 198
Table S-7. Water balance in soil columns over monitoring period. 199
Table S-8. Mass balance results of nitrogen in soil columns. 201
Table S-9. Masses of OC, RDX, TNT, HMX, and RDX degradation products (MNX, DNX, and TNX) in soil columns. 206
Table S-10. Characterization results of different depth grenade range soils. 212

LIST OF FIGURES

Figure 2.1. Major contaminated sites with explosives in the U.S. and Canada (Kalderis et al. 2011). 8

Figure 2.2. Structures of common explosives found on soil (Kalderis et al. 2011)..... 9

Figure 2.3. Anaerobic biodegradation pathway for RDX (Pennington and Brannon 2002). . 13

Figure 2.4. Biodegradation pathways of HMX (Pichtel 2012). 14

Figure 2.5. Biodegradation pathways and metabolites for TNT under anaerobic conditions (Kalderis et al. 2011). 15

Figure 2.6. Schematic representation of biotic and abiotic degradation pathways for explosives (Bhushan et al. 2006). 16

Figure 2.7. A series of two-electron transfer steps for RDX degradation (Kwon and Finneran 2006). 16

Figure 2.8. Model of humic material aid in Fe(III) reduction in tight pore spaces in soil and sediments (Lovley et al. 1998). 20

Figure 3.1. Concentrations of TNT and RDX in autoclaved, live (no added substrate) controls, and substrates-treated (GL+UCA or GL+NA) microcosms with field sand under aerobic and anaerobic conditions. Error bars represent range of values in replicate columns. Where not visible, error bars are smaller than symbol size. 46

Figure 3.2. Concentrations of high explosives (TNT, RDX, and HMX) and RDX nitroso derivatives (MNX, DNX, and TNX) in autoclaved, live (no added substrate) controls, and GL+NA added microcosms with Bay C and T soils respectively

under aerobic and anaerobic conditions. Error bars represent range of values in replicate columns. Where not visible, error bars are smaller than symbol size. ... 49

Figure 3.3. Cumulative oxygen consumption and carbon dioxide production in gas phase in live control (untreated) and GL+NA treated microcosms with Bay C or T soils. Error bars represent range of values in replicate microcosms. Where not visible, error bars are smaller than symbol size. ... 52

Figure 3.4. Correlations between cumulative masses of oxygen consumed and carbon dioxide produced in untreated microcosms (□), microcosms treated with GL only (◊), microcosms treated with NA only (Δ), and microcosms treated with GL+NA (○). Dash lines represent linear correlation for each treatment. ... 53

Figure 3.5. Experiment and modeling results of cumulative oxygen consumption in gas phase under 1st and 2nd order degradation of organic substrates in Bay C and T soil microcosms treated with crude glycerin (GL), Norlig A (NA), and crude glycerin + Norlig A (GL + NA). Error bars represent range of values in replicate columns. Where not visible, error bars are smaller than symbol size. ... 55

Figure 3.6. Predicted oxygen consumption rates over time with varying amounts of glycerin (GL) and Norlig A(NA). ... 59

Figure 4.1. Concentrations of Ultrazine CA (UCA) sorbed to field sand (FS) for varying equilibration times and initial concentrations. ... 78

Figure 4.2. Freundlich and Langmuir sorption isotherms for Ultrazine CA (UCA) and Norlig A (NA) on field sand (FS). ... 80

Figure 4.3. Freundlich isotherms for Ultrazine CA (UCA) and Norlig A (NA) on field sand (FS) and range soil (RS). 81

Figure 4.4. Linear, Freundlich, and Langmuir sorption isotherms for TNT and RDX on field sand (FS). 84

Figure 4.5. Linear, Freundlich, and Langmuir sorption isotherms for TNT and RDX on intact range soil (RS). 85

Figure 4.6. Freundlich sorption isotherms for TNT and RDX on field sand (FS) and range soil (RS). Dotted lines are upper and lower 95 % confidence intervals for each estimated Freundlich isotherm model. 86

Figure 4.7. Sorption isotherms for TNT and RDX on field sand (FS) and range soil (RS). Dotted lines are upper and lower 95 % confidence intervals for each estimated Freundlich isotherm model. 88

Figure 4.8. Freundlich sorption isotherms for TNT and RDX on intact (IRS) and amended range soil (ARS). Dotted lines are upper and lower 95 % confidence intervals for each estimated Freundlich isotherm model. 91

Figure 4.9. Langmuir sorption isotherms for TNT and RDX on washed (WFS), and amended field sand (AFS). Dotted lines are upper and lower 95 % confidence intervals for each estimated Langmuir isotherm model. 92

Figure 4.10. Retardation factors for varying concentrations of TNT and RDX in range soil (RS) which were computed with regression parameters determined by Freundlich sorption isotherm model. 95

Figure 5.1. Average biweekly effluent volume and average concentrations of total organic carbon (TOC), nitrate (NO_3), nitrite (NO_2), RDX, and TNT in effluents of the duplicate leaching columns. Error bars represent range of values in duplicate columns. Where not visible, error bars are smaller than symbol size. 113

Figure 5.2. Masses of RDX, TNT, HMX, and degradation products in effluent and soils of duplicate leaching columns. HMX degradation products were not monitored in this study. 114

Figure 5.3. Total porosities (closed marks) and water-filled porosities (open marks) along the vertical soil profile in soil columns at the end of monitoring period. Error bars represent range of values in duplicate columns. Where not visible, error bars are smaller than symbol size. 116

Figure 5.4. Soil column water balance over 695 day operating period. [Evaporated = Applied - (Effluent + Ponded + Δ Soil moisture)]. 117

Figure 5.5. Oxygen concentrations at 25, 50, 75, and 100 cm below the soil surface in soil columns over the monitoring period. 119

Figure 5.6. Average chloride (Cl), TOC, nitrate (NO_3), and manganese (Mn) concentrations in effluents of soil columns over monitoring period. 122

Figure 5.7. Organic carbon (OC) contents along the vertical soil profile in columns at the end of monitoring period. Error bars represent range of values in replicate columns. Where not visible, error bars are smaller than symbol size. 123

Figure 5.8. Masses of nitrogen in effluent and soils of laboratory columns. Inoganic-N (Eff.) = (NO_2-N + NO_3-N) discharged. Exploisive-N (Eff.) = explosives-N discharged. Exploisive -N (Soil) = explosives-N sorbed to soils. 125

Figure 5.9. Concentrations of poorly crystallized and crystallized Fe(II) along the vertical soil profile in columns at the end of monitoring period. Error bars represent range of values in replicate columns. Where not visible, error bars are smaller than symbol size..... 126

Figure 5.10. Concentrations of RDX and RDX nitroso degradation products (MNX, DNX, and TNX) in column effluents over the monitoring period. TNT and TNT degradation products were less than 36 µg/L in all effluent samples. 128

Figure 5.11. Vertical distribution of HEs in column soils at the end of monitoring period. Error bars represent range of values in replicate columns. Where not visible, error bars are smaller than symbol size..... 129

Figure 5.12. Masses of RDX, TNT, HMX, and degradation products in effluent and soils of laboratory columns. HMX degradation products were not monitored in this study. 131

Figure 6.1. Saturated hydraulic conductivity (K_{sat}), silt fraction, clay fraction, organic carbon content, poorly-crystalline and crystalline Fe(II) fraction and total Fe versus depth in Bays T and C. 149

Figure 6.2. Cumulative infiltration measured in bucket lysimeters in throwing bays in comparison to cumulative rainfall. 150

Figure 6.3. Precipitation, potential ET, and soil moisture for December 2012 to June 2015. 152

Figure 6.4. Temporal variations in chloride (Cl), bromide (Br) and TOC in throwing bays at 0.9, 1.2 and 1.5 m bgs. 153

Figure 6.5. Temporal variations in Eh, nitrate (NO_3), manganese (Mn), and iron (Fe) in throwing bays at 0.9, 1.2 and 1.5 m bgs. 154

Figure 6.6. Number of grenades thrown per Bay per month. Dashed line presents a linear trend of the numbers. 156

Figure 6.7. Temporal variations in TNT, RDX, HMX, MNX, DNX, and TNX in throwing bays at 0.9, 1.2 and 1.5 m bgs. 157

Figure 6.8. TNT and RDX concentrations in soil in Bays T and C in Marcy 2013 - prior to amendment application and July 2015 – two years after amendment application. 158

Figure S-1. Example of first-order RDX degradation rate estimated by searching for regression that generated highest F-statistic. 177

Figure S-2. Concentrations of TNT and RDX in field sand microcosms with various treatments under aerobic and anaerobic conditions. Error bars represent range of values in replicate columns. Where not visible, error bars are smaller than symbol size. 178

Figure S-3. Concentrations of high explosives (RDX, TNT, and HMX) in Bay C and T soil microcosms for all treatments under aerobic and anaerobic conditions. Error bars

represent range of values in replicate columns. Where not visible, error bars are smaller than symbol size. 179

Figure S-4. Cumulative oxygen consumption and carbon dioxide production in Bay C and T soil microcosms for all treatments. Error bars represent range of values in replicate microcosms. Where not visible, error bars are smaller than symbol size. 180

Figure S-5. Correlations between cumulative masses of oxygen consumed and carbon dioxide produced during first 27 days (top) and last 57 days (bottom) of monitoring period in Bay C soil microcosms with no treatment (□), addition of GL only (◊), NA only (Δ), and GL+NA (○). Dash lines represent linear correlation for each treatment. 181

Figure S-6. Zeta potentials of field sand (FS) and lignosulfonates (Norlig A and Ultrazine CA) over pH 2 - 12..... 184

Figure S-7. pH effect in sorption of Norlig A (NA) in field sand (FS). Low pH; Initial pH = 2.53 ± 0.05 (after 2hrs for equilibrium), final pH 4.14 ± 0.09 (after 14-day sorption period). High pH; Initial pH 7.89 ± 1.10, final pH 6.59 ± 0.55. 185

Figure S-8. Freundlich sorption isotherms for Ultrazine CA (UCA) on autoclaved and untreated field sand (FS). Dotted lines are upper and lower 95 % confidence intervals for each estimated Freundlich isotherm model. 187

Figure S-9. Freundlich sorption isotherms for Ultrazine CA (UCA) and Norlig A (NA) on field sand (FS). Dotted lines are upper and lower 95 % confidence intervals for each estimated Freundlich isotherm model..... 188

Figure S-10. Freundlich and Langmuir sorption isotherms for TNT and RDX on field sand (FS). Dotted lines are upper and lower 95 % confidence intervals for each estimated isotherm model. 189

Figure S-11. Freundlich and Langmuir sorption isotherms for TNT and RDX on range soil (RS). Dotted lines are upper and lower 95 % confidence intervals for each estimated isotherm model. 190

Figure S-12. Freundlich sorption isotherms for TNT and 2-ADNT on range soil (RS). Dotted lines are upper and lower 95 % confidence intervals for each estimated Freundlich isotherm model. 191

Figure S-13. Freundlich sorption isotherms for TNT and RDX on intact (IRS), washed (WRS), and amended range soil (ARS). 194

Figure S-14. Freundlich sorption isotherms for TNT and RDX on intact (IRS) and washed range soil (WRS). Dotted lines are upper and lower 95 % confidence intervals for each estimated Freundlich isotherm model. 195

Figure S-15. Desorption of Norlig A (NA) during washing process in pretreatment of grenade range soil (RS) prior to sorption experiment for TNT and RDX. 196

Figure S-16. Photographs of soil columns. Column series included: 1) Bay C soils with no amendment, (2) Bay C soils with GL + NA, (3) Bay T soils with no amendment, and (4) Bay T soils with GL + NA. Relatively smaller columns on top of the rack were leaching columns with a water drainage layer only (0.15 m coarse sand + 0.1 m fine sand). 197

Figure S-17. Cumulative volumes of column effluents and volumes of water ponded on the top of column soils over the monitoring period. Error bars in cumulative volumes of effluent represent range of values in replicate columns. Where not visible, error bars are smaller than symbol size..... 200
Figure S-18. Concentrations of RDX, MNX, DNX, TNX and HMX in column effluents over the monitoring period..... 202
Figure S-19. Concentrations of TNT, 2,6-DNT, 2,4-DNT, 2-ADNT and 4-ADNT in column effluents over the monitoring period..... 203
Figure S-20. Cumulative masses of RDX, TNT, HMX, and RDX degradation products (MNX, DNX, and TNX) over the monitoring period. 204
Figure S-21. Masses of MNX, DNX, and TNX in effluent and soils of laboratory columns. 205
Figure S-22. Vertical variation of explosives concentrations in soil columns at the end of monitoring period..... 207
Figure S-23. Hand grenade range (RG40) at Fort Bragg..... 208
Figure S-24. Trench excavation and open trench in hand grenade range at Fort Bragg..... 209
Figure S-25. Monitoring instrumentation during installation in grenade bays and sampling access point. 210
Figure S-26. Craters in grenade throwing bay, organic amendment application by impact sprinkler, and organic amendment application by spray nozzle. 211

CHAPTER 1. INTRODUCTION

1.1 Problems and Research Needs

2,4,6-trinitrotoluene (TNT), Hexahydro-1,3,5-trinitro-1,3,5-triazine (RDX; Royal Demolition Explosive), and octahydro-1,3,5,7-tetranitro-1,3,5,7-tetrazine (HMX; High Melting Explosive) are high explosive (HE) compounds, commonly used for military applications. HE compounds have been typically detected in areas where they were manufactured, stored, disposed, or used in military training (Lynch et al. 2001; Brannon and Pennington 2002). Groundwater contamination with HE compounds has been confirmed at 583 sites and suspected at other 88 sites in the U.S. (Wani et al. 2003). Sites contaminated with HE compounds have been observed all around the world, including Canada, Germany, the U.K., Australia, and Asia. However to date, only few sites have been cleaned up (Spain et al. 2000).

TNT, RDX, HMX, and their degradation products are the major source of explosives related contamination in soil and groundwater due to their low soil partition coefficients and limited biodegradation (Brannon and Pennington 2002; Davis et al. 2006). When the explosives undergo high-order (complete) detonation, the mass of explosives deposited on the ranges are low. However, low-order (partial) detonation of HE munitions and leaching of HE from unexploded ordnance (UXO) are potential long-term sources for the explosives contamination in active ranges (Brannon and Pennington 2002; Fuller et al. 2004). HE compounds can be transported to groundwater in permeable soils due to their moderate

aqueous solubility and weak binding affinity to soil. Exposure of humans to HE compounds can generate significant health issues. TNT and RDX are classified as possible human carcinogens (C classification) by U.S. Environmental Protection Agency (EPA 2014). In contrast, HMX is not currently classified as a human carcinogen, but does result in adverse impacts to the liver and nervous system (ATSDR 1997).

Extensive research results have shown that HE compounds are biodegradable, but rapid degradation typically only occurs under anoxic/anaerobic conditions. RDX and HMX degradation were low or zero in aerobic environment (Boopathy and Manning 1996; Hawari et al. 2000; Pennington and Brannon 2002; Bhushan et al. 2006; Kwon and Finneran 2008; Kalderis et al. 2011). Sorption of RDX and HMX is typically lower than TNT sorption and is less affected by soil organic content and cation exchange capacity (CEC) (Brannon and Pennington 2002; Hatzinger et al. 2004; Jaramillo et al. 2011). As a result, natural attenuation of RDX and HMX is expected to be limited, especially in aerobic sandy soils.

Several approaches have been studied for remediation of HE compounds on military ranges. Lime application and peat moss/soybean oil (PMSO) addition were the most effective approaches in degradation of HE compounds. However, both remediation technologies have some operational issues. For the best performance of these technologies, the lime and PMSO should be tilled into the soil, requiring UXO clearance with associated cost and safety issues. Periodic reapplication of lime and PMSO is needed to maintain performance, increasing remediation costs.

For efficient management of explosives contaminated ranges, better understanding of HEs transport and fate in soils is needed. This information can aid in identifying sites where

natural attenuation is sufficient to prevent adverse impacts and to develop more efficient and effective technologies for controlling HEs leaching when natural attenuation is limited. This need is especially critical to reduce the high costs and safety issues associated with treating active ranges containing UXO.

1.2 Research Objectives

The overall objective of this study is to improve our understanding of processes controlling leaching of high explosives (HE) on military training ranges and develop remediation methods for reducing leaching and enhancing degradation of these compounds. Specific objectives of this research include the following.

1) Evaluate the impact of crude glycerin (GL) and lignosulfonate (LS) addition to soils on HEs biodegradation under aerobic and anaerobic conditions.
2) Determine the kinetics of oxygen consumption by GL and LS added to soils.
3) Determine the extent of TNT and RDX sorption in representative soils, and evaluate the impact of LS addition on sorption of TNT and RDX.
4) Examine the transport and fate of HEs in hand grenade range soil, and evaluate the impact of GL and LS addition on oxygen consumption and HEs biodegradation using laboratory scale columns.
5) Evaluate the transport and attenuation of HEs in variably saturated soils at a hand grenade range using two different management approaches: a) monitored natural attenuation (MNA); and b) organic substrate enhanced attenuation (OSEA).

1.3 Dissertation Organization

This dissertation is composed of seven chapters. Chapter 1 documents the problem, research needs, and objectives of this study. A literature review of explosives degradation processes and current remediation technologies is presented in Chapter 2. Chapter 3 summarizes results of a microcosm study examining the impact of organic amendment on biodegradation of HEs in soil. Sorption of lignosulfonate and explosives to soil is presented in Chapter 4. Chapter 5 presents results of a laboratory column study of HEs degradation in grenade range soils. In Chapter 6, natural and enhanced attenuation of explosives on a hand grenade range is described. Conclusion and recommendations for future work are presented in Chapter 7.

CHAPTER 2. LITERATURE REVIEW

2.1 Introduction of High Explosives

Explosives are classified in two groups, primary and secondary explosives, depending on their initiation susceptibility. The HEs, TNT, RDX, and HMX, are classified as secondary explosives that are ignited by primary explosives (Kalderis et al. 2011; Pichtel 2012). HE compounds are ubiquitous in subsurface environments near military areas since they have been extensively used in military training with mortar, rockets, and hand grenades. HE compounds remain in surface soil when munitions are incompletely detonated or unexploded. The explosive residues and UXO are potential long-term sources of explosive contamination to soil and groundwater. Table 2.1 shows physical and chemical properties of HE compounds. Their moderate solubility, low sorption coefficients, and low biodegradability in typical condition have led to migration of these compounds into groundwater (Spain et al. 2000; Brannon and Pennington 2002; Fuller et al. 2004; Pichtel 2012).

According to Talley and Sleeper (1997), the U.S. Departments of Defense (DoD) and Energy (DoE) have more than 21,000 contaminated sites with most sites contaminated with explosives. Thiboutot et al. (1998) reported that the Department of Defense Canada has over 100 sites contaminated with TNT, RDX, and HMX. Figure 2.1 shows sites in the U.S. and Canada where military ranges have been monitored for the presence of HE residues. Contamination with explosives is not limited only to North America. Explosives

contaminated sites have also be identified in Germany, the U.K., and Australia. However, few of these sites have been remediated (Spain et al. 2000).

Exposure of humans to these contaminants can generate significant adverse health effects. TNT can cause liver and blood damage, anorexia, and anemia. RDX and HMX can result in systematic poisoning generally affecting bone marrow and the liver (Lynch et al. 2001). These compounds are also toxic to mammalian system and bioaccumulate in crop plants, leading to potential exposure by eating or direct contact (Spain et al. 2000; Pennington and Brannon 2002). TNT and RDX are classified as possible human carcinogen by U.S. EPA (EPA 2014). In contrast, HMX is not currently classified as human carcinogen, but does have adverse impacts on the liver and nervous system (ATSDR 1997).

The chemical structure of common HEs are shown in Figure 2.2. HE compounds include three or four nitro functional groups ($-NO_2$). During reductive degradation, the nitro groups are often reduced to nitroso groups (-NO), hydroxylamine (-NHOH), and then amino groups ($-NH_2$) by both biotic and abiotic processes (Hawari et al. 2000). Moreover, the electrons produced from microbial transformation facilitate the reduction of nitro groups under both aerobic and anaerobic conditions (Spain et al. 2000).

TNT is one of the most common bulk explosives used in military ordnance and mining/quarrying operations due to its chemical/thermal stability and insensitivity to shock and friction. TNT is used alone and in mixtures with other HE compounds (RDX and HMX) in explosive formulations. TNT is moderately soluble in water (130 mg/L at 20 ºC) and weakly sorbed to soils due to its low octanol-water partition coefficient (log K_{ow} = 1.86). RDX is a highly stable nitramine compound and generally used in mixtures with other

explosive compounds. RDX is slightly soluble (42 mg/L at 20 ºC) than TNT. However, it has a lower octanol-water partitioning coefficient (log K_{ow} = 0.86) which explains the weaker sorption of RDX onto soils. HMX is commonly used as burster charges for artillery shells and a component of plastic explosives. HMX has a relatively low water solubility (5 mg/L at 25 ºC) and octanol-water partitioning coefficient (log K_{ow} = 0.061) (Brannon and Pennington 2002; Pichtel 2012).

Table 2.1. Physical and chemical properties of HE compounds (Brannon and Pennington 2002; Pichtel 2012).

Compound	**TNT**	**RDX**	**HMX**
Chemical formula	$C_7H_5N_3O_6$	$C_3H_6N_6O_6$	$C_4H_8N_8O_8$
Molecular weight	227.13	222.26	296.16
Melting point (ºC)	80-82	204	276-280
Boiling point (ºC)	240 (exploded)	(decomposes)	(decomposes)
Solubility in water (mg/L)	130 (20 ºC)	42 (20 ºC)	5 (25 ºC)
Specific gravity	1.5-1.6	1.89	1.96
Vapor pressure (1 bar, 20 ºC)	7.2×10^{-9}	5.3×10^{-12}	4.3×10^{-17}
Henry's Law Constant (bar m^3 mol^{-1})	4.57×10^{-7} to 1.1×10^{-8}	6.3×10^{-8} to 1.96×10^{-11}	2.6×10^{-15}
Octanol/water partitioning coefficient	1.86	0.86	0.061
Sorption coefficient (L/kg)	0 to11	0 to 8.4	1 to 18

HE compounds are subject to transport to groundwater in high permeable soils due to their moderate aqueous solubility and weak sorption affinity to soils. Since they are

carcinogenic and/or toxic, management strategies are required to reduce leaching of HEs to groundwater, including identifying sites where HEs will naturally attenuate and developing remediation technologies for sites where natural attenuation is limited.

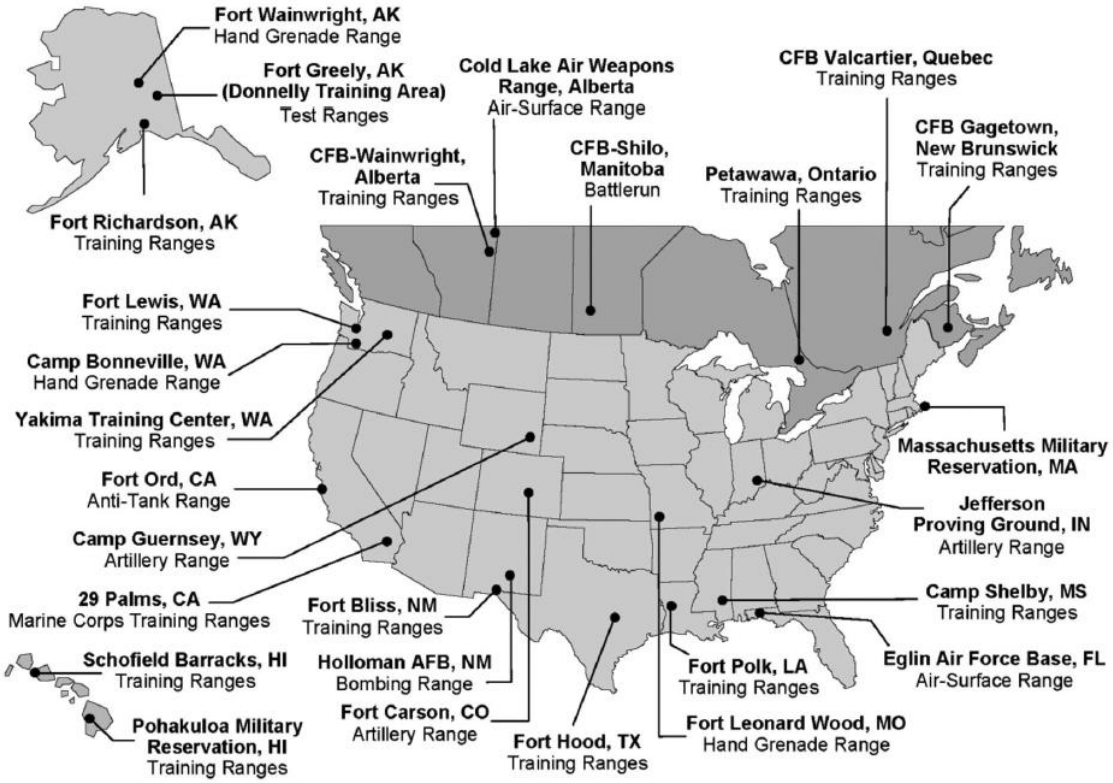

Figure 2.1. Major contaminated sites with explosives in the U.S. and Canada (Kalderis et al. 2011).

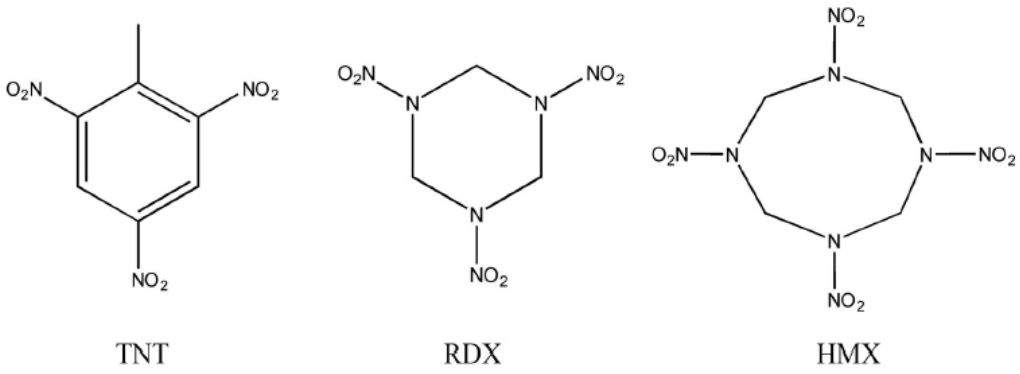

Figure 2.2. Structures of common explosives found on soil (Kalderis et al. 2011)

2.2 Sorption of High Explosives

Sorption processes results in accumulation of a dissolved solute on the surface of a solid sorbent, including humic substances, metal oxides and hydroxides, and microorganisms. Sorption processes may include hydrophobic partitioning, hydrogen bonding, ion exchange, and chemisorption (Pichtel 2012). These processes can be influenced by physicochemical properties of the solute/sorbent, e.g., HE compounds and soils, and environmental factors, such as ionic strength, pH, and cation exchange capacity (CEC), resulting in variable extent of sorption (Kalderis et al. 2011).

TNT is reversibly sorbed to soils through hydrogen bonding and ion exchange between the nitro functional groups and soil surfaces (Pennington and Patrick 1990). However, sorption of certain reduction products of TNT to humic acid and clay minerals is irreversible (Spain et al 2000). Soil/water partition coefficients (K_d) for TNT in surface soils ranged from 0 to 11 L/kg (Brannon and Pennington 2002). RDX is generally more weakly sorbed to soils than TNT. RDX sorption mechanisms have been described by linear isotherms (Selim and Iskandar 1994; Myers et al. 1998; Brannon et al. 2002). Brannon and

Pennington (2002) demonstrated that sorption coefficient for RDX in surface soil ranged from 0 to 8.4 L/kg. HMX sorption coefficients are varied, but it is obvious that HMX is less sorbed to soils than TNT. HMX sorption coefficient in surface soil ranged from 1 to 18 L/kg (Brannon and Pennington 2002).

Sheremata et al. (1999) demonstrated that sorption coefficients increased with the increase of the number of amino groups, for example, 2,4-diamino-6-nitrotoluene (2,4-DANT) > 4-amino-2,6-dinitrotoluene (4-ADNT) > TNT. Yamamoto et al. (2004) showed that organic carbon fraction influenced the surface partition coefficient (K_d) for TNT, 2,4-DNT, and RDX with higher sorption of TNT and 2,4-DNT than RDX. However, HMX sorption was not significantly affected by soil organic carbon content. Hatzinger et al. (2004) showed that addition of peat moss enhanced sorption of TNT and RDX, resulting in approximately 90 % removal. Cattaneo et al. (2000) showed that clay minerals play an important role in sorption of HE compounds, where sorption of TNT to montmorillonite was two orders of magnitude greater than TNT sorption to kaolinite.

2.3 Biotic Degradation of High Explosives

Biodegradation is a remediation technique that uses microbial metabolism and/or cometabolism to remove organic contaminants (Lee and Brodman 2004). It has been widely used to treat a wide variety of pollutants, including nitroaromatic compounds (NACs), polychlorinated biphenyls (PCBs), trichloroethylene (TCE), perchloroethylene (PCE), BTEX (benzene, toluene, ethylbenzene, and xylenes), and other organic contaminants. When

biodegradation results in the complete conversion of target compounds to their inorganic components, the process is referred to as mineralization (Spain et al. 2000).

Lee and Brodman (2004) showed limited biodegradation of RDX under aerobic condition. However, under anaerobic condition, RDX was biodegraded through initial transformation of nitro groups ($-NO_2$) to nitroso groups (-NO) (Kwon and Finneran 2006). Hawari et al. (2000) also demonstrated that RDX biodegradation under anaerobic conditions was faster than aerobic biodegradation. Figure 2.3 shows the pathways of anaerobic mineralization process for RDX. RDX is microbially transformed to hexahydro-1-nitroso-3,5-dinitro-1,3,5-triazine (MNX), hexahydro-1,3-dinitroso-5-nitro-1,3,5-triazine (DNX), and then hexahydro-1,3,5-trinitroso-1,3,5-triazine (TNX) sequentially. These intermediate nitroso compounds are eventually degraded to nitrous oxide (N_2O) and formaldehyde (HCHO).

Figure 2.4 shows the biodegradation pathways for HMX. Similar to RDX biodegradation, HMX also can be degraded by reduction of nitro groups ($-NO_2$) to nitroso groups (-NO). The intermediates can be subsequently transformed to nitrous oxide (N_2O) and formaldehyde (HCHO) that are indicators of ring cleavage (Bhushan et al. 2006; Pichtel 2012). Relatively less information on HMX biodegradation are available compared to RDX and TNT degradation. HMX and RDX were effectively degraded in Makua Military Reservation in Oahu, Hawaii, by application of molasses-water mixture as a carbon source (Payne et al. 2013). Fournier et al. (2004) showed that 97 % of HMX was degraded after 25 days by reduction under nitrogen-limiting conditions. Morley et al. (2002) also demonstrated use of HMX and RDX as a nitrogen source under anaerobic conditions.

TNT can be biodegraded by a wide variety of microorganisms under both of aerobic and anaerobic conditions. TNT can be used as carbon source and/or nitrogen source for microorganisms (Kalderis et al. 2011). TNT transformation is significantly enhanced under anaerobic conditions compared to slow transformation under aerobic conditions (Pennington and Brannon 2002). Under both conditions, TNT is generally transformed to amino derivatives via nonspecific extracellular enzymes, such as nitroreductase. As shown in Figure 2.5, the predominant derivatives are 2-amino-4,6-dinitrotoluene (2-ADNT), 4-amino-2,6-dinitrotoluene (4-ADNT), and 2,4-diamino-6-nitrotoluene (2,4-DANT). These intermediate compounds can be further transformed through biotic and/or abiotic processes. However, mineralization of TNT is relatively low compared to RDX mineralization (Kalderis et al. 2011).

Although the HEs can be used primary substrates by microorganisms, addition of co-substrates may lead to more rapid degradation (Boopathy and Manning 1996). TNT removal was more effective when pyruvate was provided as co-substrate compared to when TNT was the sole carbon source. Various substrates, including acetate, glucose, volatile fatty acid, formate, methanol, and soybean oil, have been used to stimulate microbial activities in the presence of HE compounds.

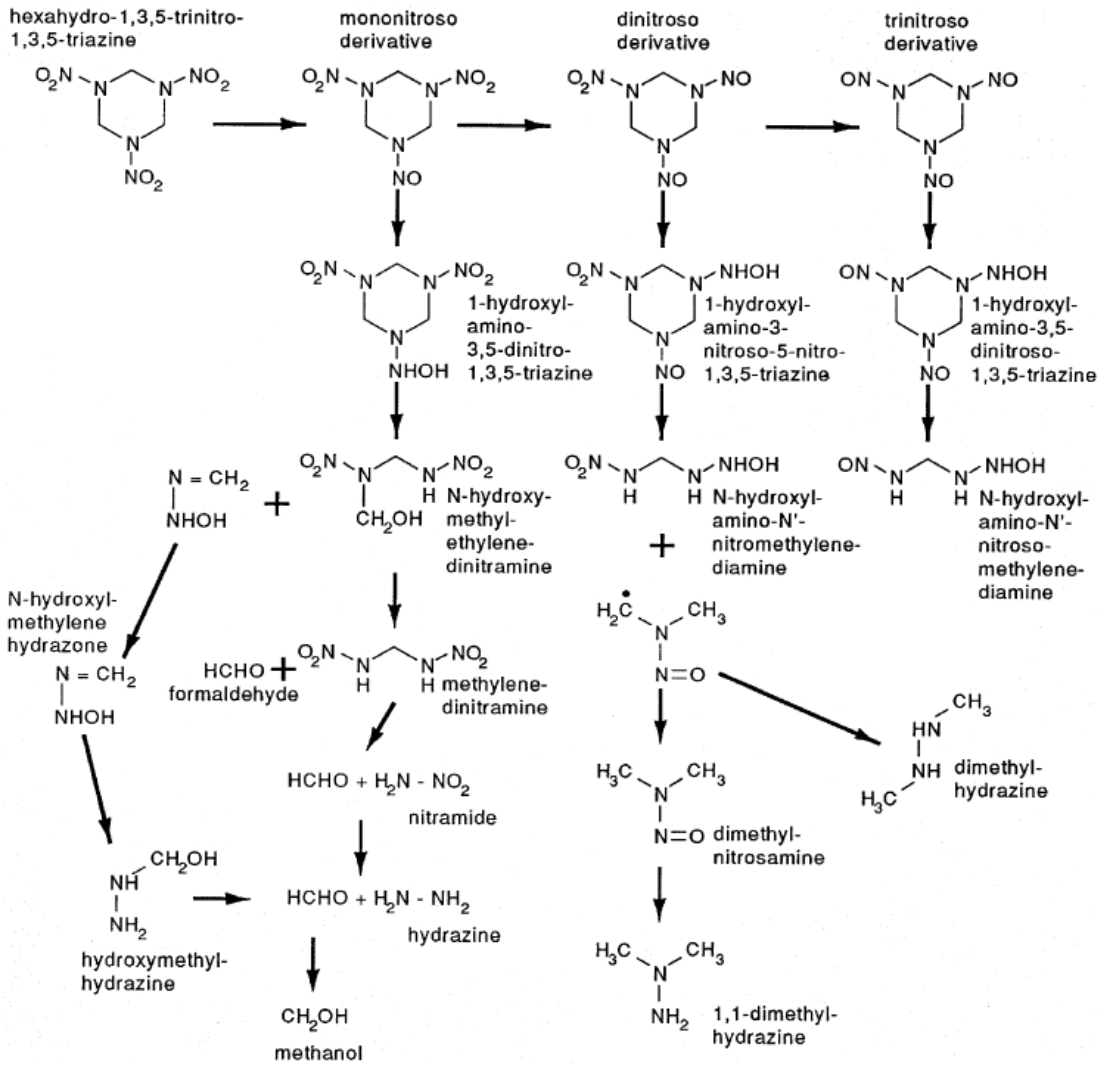

Figure 2.3. Anaerobic biodegradation pathway for RDX (Pennington and Brannon 2002).

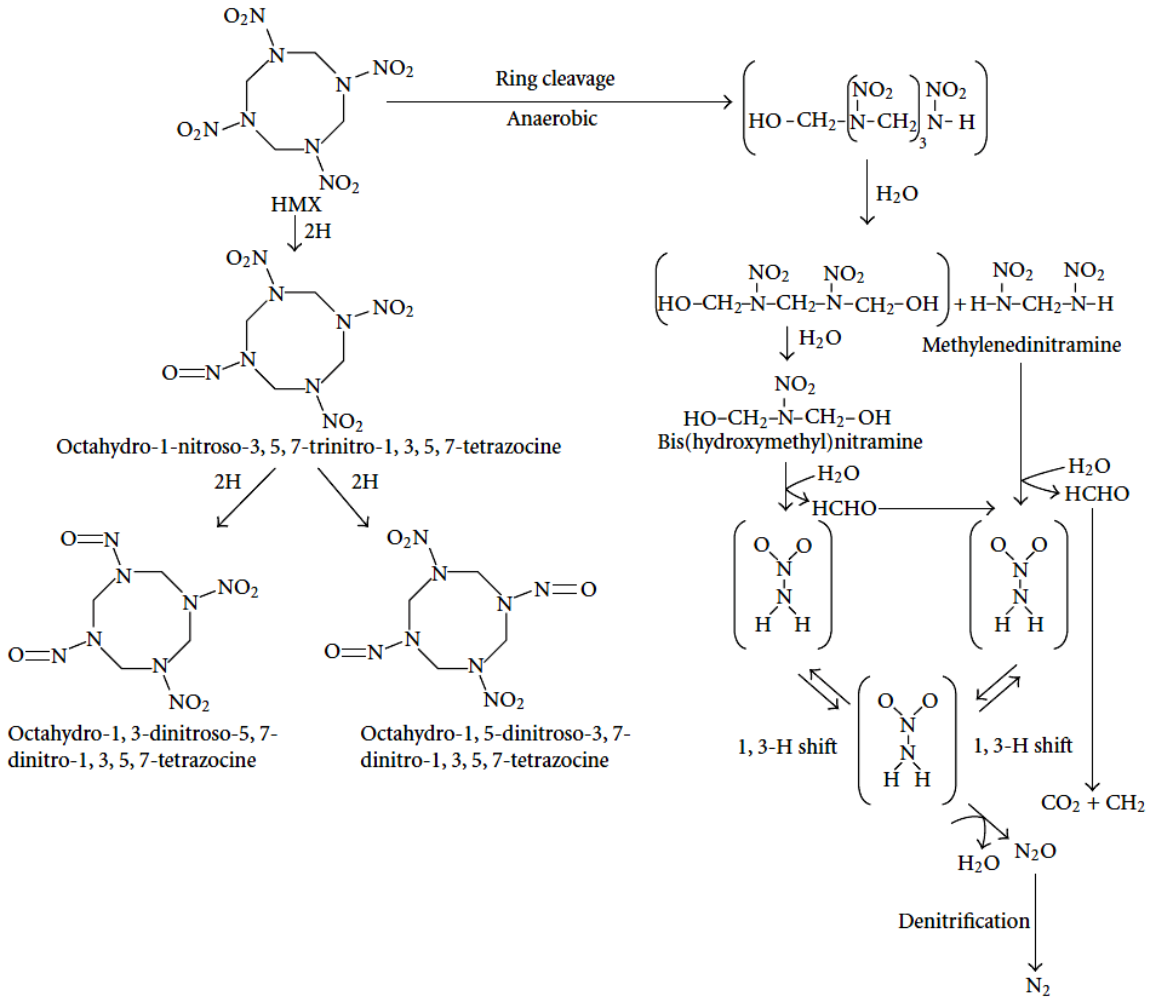

Figure 2.4. Biodegradation pathways of HMX (Pichtel 2012).

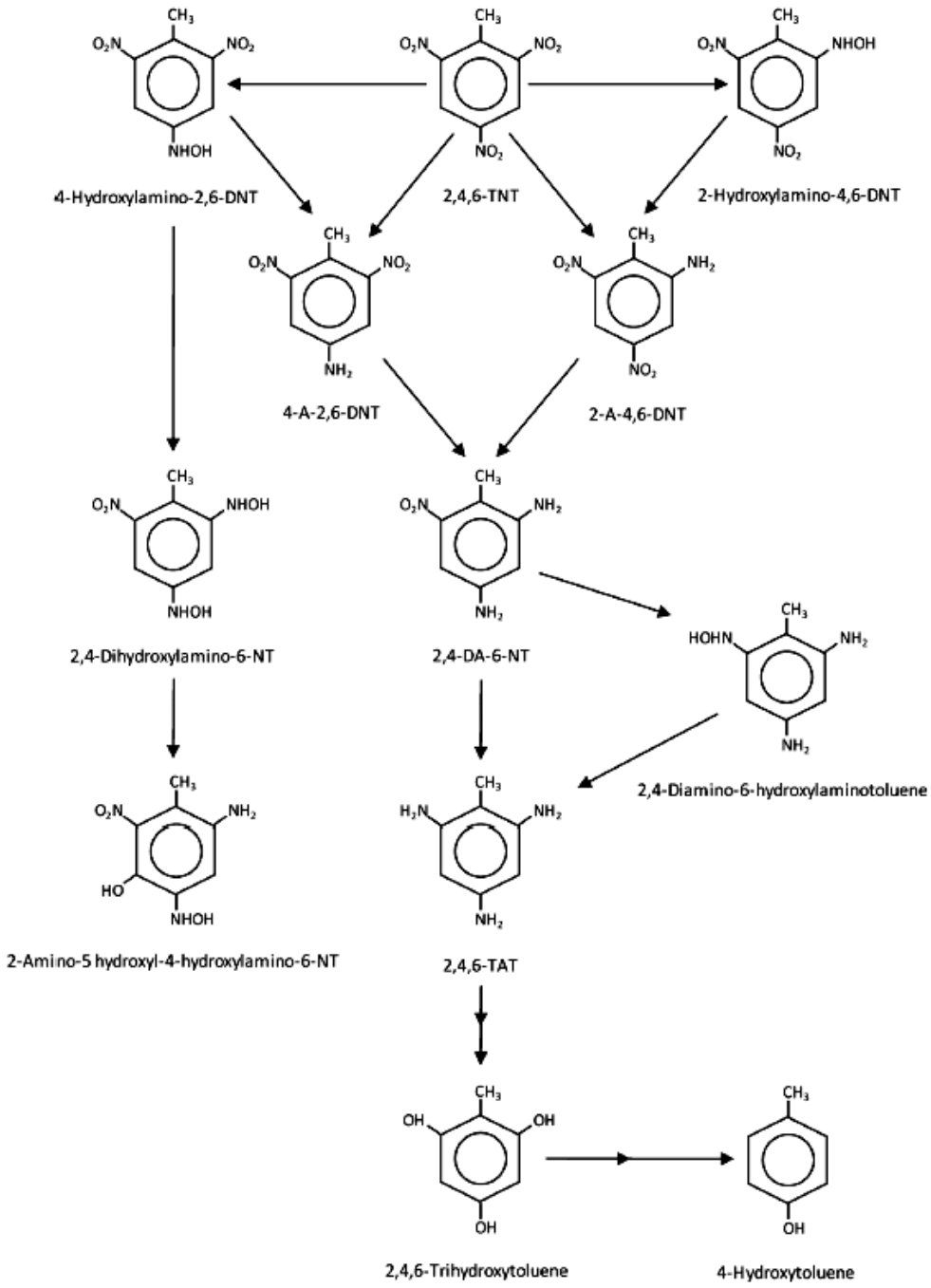

Figure 2.5. Biodegradation pathways and metabolites for TNT under anaerobic conditions (Kalderis et al. 2011).

2.4 Abiotic Degradation of High Explosives

HE compounds can be degraded by both biotic and abiotic processes. As shown in Figure 2.6, HE compounds can be degraded by biodegradation; by reducing electron shuttles that transfer electrons to the HE compounds; and by reducing Fe(III) to Fe(II) which is reactive to the compounds (Bhushan et al. 2006). Figure 2.7 shows abiotic RDX degradation pathways by a series of two-electron transfer steps.

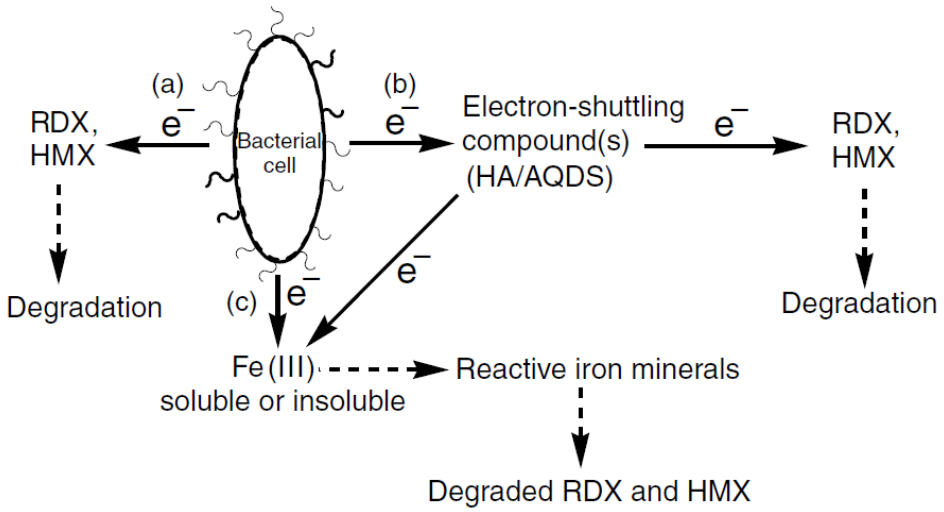

Figure 2.6. Schematic representation of biotic and abiotic degradation pathways for explosives (Bhushan et al. 2006).

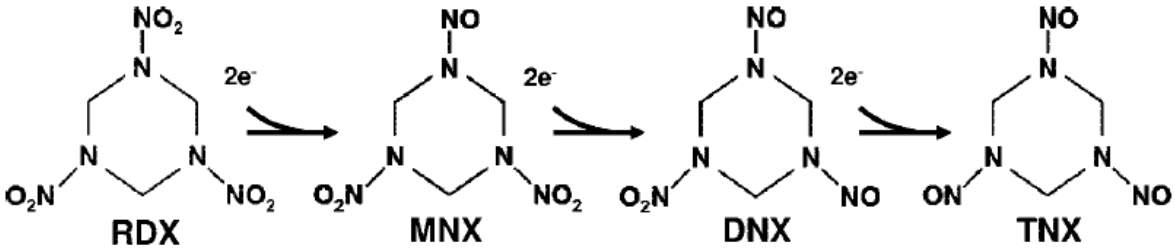

Figure 2.7. A series of two-electron transfer steps for RDX degradation (Kwon and Finneran 2006).

2.4.1 *Reductive Transformation of High Explosives by Reduced Iron Species*

Several studies have demonstrated that Fe(III) reduction had an important role in abiotic reductive transformation of HE compounds. Brannon et al. (1998) showed that Fe(II) increased the transformation rate of TNT with pH increase in the presence of montmorillonite or kaolinite. Bhushan et al. (2006) showed that RDX and HMX were abiotically degraded by microbially reduced Fe(III), humic acid, and AH2QDS, resulting in formaldehyde (HCHO) production. Boparai et al. (2010) showed that RDX, HMX, and TNT were successfully transformed in iron-rich contaminated sediments by dithionite treatment and their transformation kinetics relied on the dithionite concentration, solid-solution ratio, pH, and the buffer concentration. Thomas et al. (2012) found that RDX degradation was the most efficient in acidic or neutral pH conditions when the soil contains sufficient iron oxides and iron-bearing clay minerals. Hofstetter et al. (1999) concluded that reduced sulfur and iron species were the most important reductants for abiotic transformation of HE compounds in anoxic subsurface environments.

Not all species of Fe(II) are equally effective in abiotic reduction of the HE compounds. According to Gregory et al. (2004) and Bhushan et al. (2006), free Fe(II) alone did not react with RDX or HMX, but Fe(II) bound to specific minerals such as magnetite, siderite, hematite, and goethite were reactive with both RDX and HMX. Elsner et al. (2004) demonstrated that the Fe(II)-bearing minerals such as siderite ($FeCO_3$), goethite (α-FeOOH), and hematite (Fe_2O_3) react with nitroaromatic compounds (NACs) and polyhalogenated alkanes. Hofstetter et al. (1999) showed that reduction of TNT and other NACs by dissolved free Fe(II) was extremely slow in columns containing *Geobacter metallireducens* and

FeOOH-coated sand, whereas Fe(II) surface species significantly contributed to the degradation of NACs. These experimental results showed that reactive Fe(II) surface species can be formed by either adsorption of aqueous Fe(II) to minerals including Fe(III) oxides or microbial/abiotic reduction of Fe(III) (Hofstetter et al. 1999).

2.4.2 *Abiotic Degradation of High Explosives by Electron Shuttles*

In addition to direct abiotic reduction of HEs by reduced Fe, certain compounds can accelerate HE degradation by acting as shuttles to transport electrons from Fe(II) and/or other sources of reducing equivalents to the HE compounds (Lovley and Blunt-Harris 1999). Numerous studies have shown that humic substances can act as electron shuttles, accelerating reduction of soil and groundwater contaminants including chromium, arsenate, uranium, and explosives (Bhushan et al. 2006; Hoferkamp and Weber 2006; Van der Zee and Cervantes 2009; Palmer and Wandruszka 2010; Chen et al. 2011; Barlett et al. 2012).

Humic substances are chemically heterogeneous, polymeric organic compounds that are ubiquitous in aquatic and soil environments. These materials contain redox active functional groups that play a significant role in the reductive transformation processes, including cytochromes, flavines, cobalamins, porphyrins, pyridines, phenazines, and quinones (Kappler et al. 2004; Van der Zee and Cervantes 2009). Quinones are often the most important redox mediator for reductive biotic and abiotic transformation because they are abundant, stable, and non-toxic (Field and Cervantes 2005).

The abiotic degradation processes of HE compounds are strongly associated with Fe(III) reduction to Fe(II) which can be accelerated by addition of humic substances or

quinone analogues (Nevin and Lovley 2000; Peretyazhko and Sposito 2006; Rakshit et al. 2009). Kappler et al. (2004) demonstrated numbers of humic reducing bacteria were two orders of magnitude greater than Fe reducing bacteria in lake sediments, indicating electrons were initially transferred to the humic material, and then subsequently transferred from the humic materials to Fe(III). Jiang and Kappler (2008) showed that reduced humic substances facilitated the microbial-mediated reduction of poorly crystalline Fe(III) oxide by shuttling electrons from humic substances to Fe(III). Iron complexation with humic substances is also able to accelerate Fe(III) reduction by expediting dissolution of Fe(III) mineral and formation of readily reducible Fe(III)-humic substances complexes. Furthermore, iron complexes prevent coating the dissolved iron oxide surface by produced Fe(II), further enhancing Fe(III) reduction (Royer et al. 2002).

During Fe(III) reduction, iron-reducing bacteria utilize humic substances as electron acceptor in the microbial oxidation of their substrates (Lovley and Blunt-Harris 1999). Iron- or sulfur-reducing microorganisms transfer electrons to dissolved humic substances, including *Geobacter metallireducens*, *Geobacter sulfurreducens*, and *Shewanella putrefaciens*, followed by shuttling electrons to Fe(III) for its reduction (Lovley et al. 1998; Roden et al. 2010). Soluble humic materials also increase the contact opportunity between microorganisms and insoluble Fe(III) for its microbial reduction (Lovley et al. 1996). As shown in Figure 2.8, humic substances transfer electrons to Fe(III) in tight pore spaces in sediment, where iron- or sulfur-reducing microbes cannot approach due to their relatively large size (Lovley et al. 1998). In microbially-mediated Fe(III) reduction, electron transfer

dominates initially, but Fe(II) complexation dominates later (Royer et al. 2002; Rakshit et al. 2009).

Solid-phase humic substances in sediment can also enhance Fe(III) oxide reduction, indicating identical ability with dissolved humic materials (Roden et al. 2010). Moreover, chemical Fe(III) reduction was approximately two-fold higher than microbial reduction (Roden et al. 2010). However, Jiang and Kappler (2008) demonstrated that biological and chemical Fe(III) reduction rates were almost same in the presence of dissolved humic substances.

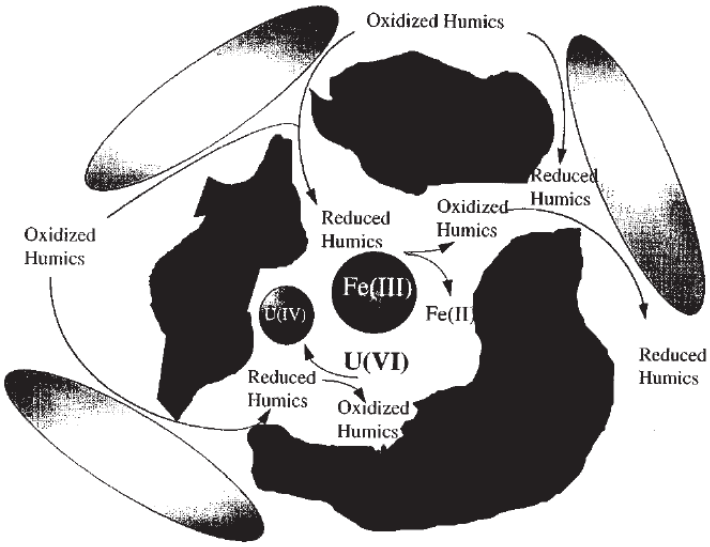

Figure 2.8. Model of humic material aid in Fe(III) reduction in tight pore spaces in soil and sediments (Lovley et al. 1998).

2.5 Current Remediation Technologies

Ex situ remediation technologies for soil and groundwater contaminated with explosives include composting, bioslurry reactors, and land-farming (Fuller et al. 2004). However, these approaches are impractical and excessively expensive to apply over large areas with explosives related-contamination. Potential existence of unexploded ordnance (UXO) also impedes the application of these technologies or requires additional cost for UXO clearance. Two approaches that are potentially applicable to treatment of explosive impacted ranges include application of lime to stimulate base hydrolysis and addition of peat moss/soybean oil to enhance sorption and biodegradation.

Hansen et al. (2003) showed that TNT and RDX were degraded within 24 hours in soil microcosms amended with lime to increase the pH to over 10.5. Davis et al. (2006) reported 99.9 % removal of TNT, 74 % removal of RDX, and 57 % removal of HMX within 21 days in soil slurry microcosms with pH > 12. In bench-scale columns and mesocosm-scale laboratory lysimeters containing hand-grenade range soil, Martin et al. (2012) showed hydrated lime addition reduced RDX leaching by over 90%. For the best performance, the lime should be well mixed into the soil to bring the hydroxide ion into direct contact with the explosive compounds (Brooks et al. 2003; Martin et al. 2012). However, mixing lime into the soil may cause safety issues due to UXO or require additional costs for UXO removal. Furthermore, large amounts of lime are required to raise the soil pH to the optimum range for effective alkaline hydrolysis, especially in acidic soils containing alumino-silicates and iron hydroxides. According to Brooks et al. (2003), approximately 100 to 200 tons of hydrated lime is required for an area of 100 m X 100 m to raise the soil pH for desired range.

Additional lime must be periodically applied to maintain performance since soil pH decreases over time due to downward transport by infiltrating rainfall and reaction with atmospheric carbon dioxide. Use of quicklime may reduce the required application amount because quicklime raises the soil pH slightly higher than the hydrated lime. However, use of quicklime can produce safety issues due to its large exothermic reaction (Brooks et al. 2003). In soils with high clay content, the reaction rates of alkaline hydrolysis can be slow due to high cation exchange capacity (CEC) in the soil (Martin et al. 2012). Moreover, the high pH condition resulted from the lime treatment may kill most vegetation at the target site.

Addition of peat moss and soybean oil can also be effective in stimulating sorption and biodegradation to reduce explosives leaching. Fuller et al. (2004) showed that Sphagnum peat moss addition in soil slurry microcosm was effective in stimulating RDX mineralization and crude soybean oil addition stimulated TNT, RDX, and HMX mineralization. The combination of peat moss and crude soybean oil (PMSO) stimulated removal of RDX and its degradation product MNX (Schaefer et al. 2005; Fuller et al. 2009). However, application of PMSO to ranges has some operational issues including: a) increased dust problems in arid areas; b) increased fire hazard; c) challenges in distributing the material without exposing workers to UXO hazards; and d) disturbance of the PMSO amendment by ordinance detonation, potentially reducing treatment effectiveness.

Ideally, remediation technologies for large, heterogeneously contaminated areas should be effective in reducing explosives leaching and be easy to apply, reducing operational costs and potential safety issues.

2.6 Proposed Remediation Approach

2.6.1 *Proposed Remediation Technology*

A potential alternative that overcomes some of the limitations of the PSMO approach developed by Fuller et al. (2009) is spray application of a mixture of water soluble, easily biodegradable organic substrate and humic material, followed by water application to transport the material into the soil.

Waste glycerin (GL), a byproduct of biodiesel production, could be a useful soluble substrate due to its low cost ($ 0.02 to 0.10 / lb.), high aqueous solubility, relatively high flash point (176 ºC), and high chemical oxygen demand (1.1 g/g). These characteristics may lead to easy distribution of substrate, preventing fire hazards during open burn (OB)/open detonation (OD) activities, and maintaining a relatively long-lasting, reducing environment. Behrooz and Borden (2012) showed that waste GL added to the acid mine tailing with a single surface application resulted in strongly reducing conditions for over 15 months. From this example, it is expected that GL could generate sustainable reducing condition in subsurface environment, resulting in anaerobic biodegradation of HE compounds.

Humic materials will also maintain reducing conditions by slowly consuming oxygen, increasing hydrophobic sorption and covalent binding of TNT, and may potentially serve as electron shuttles, enhancing abiotic degradation by Fe(II) (Kwon and Finneran 2006). Lignosulfonates (LS) produced through reaction with metal bisulfites and other reagents during wood pulping for paper production, could be good candidates for enhancing HE degradation due to their low cost ($ 0.5 to 1.05 / lb.), high solubility, easy spray application, and low fire hazard. LS contains high molecular weight polymeric organic carbon, similar to

natural soil humics, and this slowly biodegradable material could provide a large reservoir of reducing power and electron shuttles to enhance biotic and abiotic HE degradation.

Transport of the organic amendments into the soil profile will be important. By transporting these materials at least 15 cm into the soil profile: (a) fire hazards are reduced; (b) oxygen flux is reduced resulting in more strongly reducing conditions for contaminant degradation; and (c) the lower oxygen flux limits aerobic degradation of the humic materials, greatly increasing treatment longevity.

2.6.2 *Prior Work*

In prior work, Farling (2013) characterized different lignins to identify commercially available materials that could potentially be used to enhance HE degradation and sorption. The humic substances characterized included Norlig A, Ultrazine CA, Borresperse CA, BorreGro HA1, BorreGro HA 2, Dry Soluble 80, Organo Liquid Hume, REAX 83A, REAX 85A, and Indulin AT. Dry Soluble 80 and Indulin AT contain the lowest and highest TOC content, respectively, with a range from 0.32 to 0.62. Indulin AT has the lowest moisture content (0.040) and Organic Liquid Hume has the highest (8.538). The lignosulfonates Norlig A and Borresperse CA have the lowest ambient pH (≈ 4.0) while the Kraft lignin REAX 83A is the most basic with pH > 10. The test for pH effect on the aqueous solubility of humic materials showed that Norlig A, Ultrazine CA, Borresperse CA, Dry Soluble 80, and Indulin AT required significant amounts of base to raise the pH, indicating these materials have a significant buffering capacity. Complete solubilization of Indulin AT required pH $\geq$ 10. Dry Soluble 80

contained insoluble component over the pH range tested. Solubility of all other lignins was over 95 % at the pH range of 7-11.

Leaching experiments conducted by Farling (2013) showed that the LS (Norlig A, Ultrazine CA, and Borresperse CA) were more strongly retained (50 - 30% discharged) than other materials tested. The soluble humates (Dry Soluble 80, Organo Liquid Hume, and BorreGro HA-1, HA-2) were very poorly retained, indicating these materials would not be appropriate for our proposed application. Kraft lignins produced through reaction with NaOH and Na_2S during pulping processes, could also transported into the soil by raising the pH to above 10 using a mixture of NaOH and $Ca(OH)_2$. While this approach can be effective in the laboratory, it will be more complicated to implement in the field. Based on the ease of field implementation and retention in soil, LS appeared to be most suitable for reducing leaching and enhancing degradation of HE compounds.

Laboratory soil column experiments monitored by Farling (2013) showed that lignosulfonates were strongly retained by the soil, but glycerin rapidly migrated through the columns with 70 - 82 % of the applied GL discharged in the column effluent. TNT leaching was significantly reduced in columns treated with GL alone and GL+LS treated columns, resulting in discharge < 5 % of TNT amount applied. However, RDX degradation was limited in all treated columns. Monitoring data showed that oxygen was rapidly transported through the sandy soil, preventing establishment of anaerobic conditions required to enhance RDX degradation.

2.7 References

Barlett, M., Moon, H.S., Peacock, A.A., Hedrick, D.B., Williams, K.H., Long, P.E., Lovley. D., Jaffe, P.R., 2012. Uranium reduction and microbial community development in response to stimulation with different electron donors. Biodegradation. 23(4), 535-546.

Behrooz, M., Borden, R.C., 2012. Waste glycerol addition to reduce AMD production in unsaturated mine tailings. Mine Water Environ. 31(3), 161-171.

Bhushan, B., Halasz, A., Hawari, J., 2006. Effect of iron(III), humic acids and anthraquinone-2,6-disulfonate on biodegradation of cyclic nitramines by Clostridium sp. EDB2. J. Appl. Microbiol. 100(3), 555-563.

Boopathy, R., Manning, J.F., 1996. Characterization of partial anaerobic metabolic pathway for 2,4,6-trinitrotoluene degradation by a sulfate-reducing bacterial consortium. Can. J. Microbiol. 42(12), 1203-1208.

Boparai, H.K., Comfort, S.D., Satapanajaru, T., Szecsody, J.E., Grossl, P.R., Shea, P.J. 2010. Abiotic transformation of high explosives by freshly precipitated iron minerals in aqueous Fe(II) solutions. Chemosphere. 79(8), 865-872.

Brannon, J.M., Pennington, J.C., 2002. Environmental fate and transport process descriptors for explosives. Final report for Strategic Environmental Research and Development Program. ERDC/EL TR-02-10. U.S. Army Engineer Research and Development Center. Vicksburg, MS.

Brannon, J.M., Price, C.B., Hayes, C., Yost, S.L., 2002. Aquifer soil cation substitution and adsorption of TNT, RDX, and HMX. Soil Sediment Contam. 11(3), 327-338.

Brannon, J.M., Price, C.B., Hayes, C., 1998. Abiotic transformation of TNT in montmorillonite and soil suspensions under reducing conditions. Chemosphere. 36(6), 1453-1462.

Brooks, M.C., Davis, J.L., Larson, S.L., Felt, D.R., Nestler, C.C., 2003. Topical lime treatment for containment of source zone energetics contamination. USACE, ERDC/EL TR-03-19, U.S. Army Environmental Research and Development Center, Vicksburg, MS.

Cattaneo, M.V., Pennington, J.C., Brannon, J.M., Gunnison, D., Harrelson, D.W., Zakikhani, M., 2000. Natural attenuation of explosives in remediation of hazardous waste contaminated soils. Marcel Dekker, New York, NY.

Chen, H., Li, X., Xu, Z., 2011. Cr(VI) remediation by enriched sediment with anthraquinone-2,6-disulfonate as electron shuttles. Phys. Chem. Earth. 36(9), 451-454.

Davis, J.L., Brooks, M.C., Larson, S.L., Nestler, C.C., Felt, D.R., 2006. Lime treatment of explosives-contaminated soil from munitions plants and firing ranges. Soil Sediment Contam. 15(6), 565-580.

Elsner, M., Schwarzenbach, R.P., Haderlein, S.B., 2004. Reactivity of Fe(II)-bearing minerals toward reductive transformation of organic contaminants. Environ. Sci. Technol. 38(3), 799-807.

Farling, S.R., 2013. Generation of biodegradation-sorption barriers for munitions constituents. MS thesis. North Carolina State University, Raleigh, NC.

Field, J.A., Cervantes, F.J., 2005. Microbial redox reactions mediated by humus and structurally related quinones. In Perminova, I.V., Hatfield, K., Hertkorn, N., Use of humic

substances to remediate polluted environments: from theory to practice, Chapter 17. Dordrecht, The Netherlands. Springer. 343-352.

Fournier, D., Halasz, A., Thiboutot, S., Ampleman, G., Manno, D., Hawari, J., 2004. Biodegradation of Octahydro-1,3,5,7-tetranitro-1,3,5,7-tetrazocine (HMX) by *Phanerochaete chrysosporium*: New Insight into the Degradation Pathway. Environ. Sci. Technol. 38(15), 4130-4133.

Fuller, M.E., Hatzinger, P.B., Rungmakol, D., Schuster, R.L., Steffan, R.J., 2004. Enhancing the attenuation of explosives in surface soils at military facilities: combined sorption and biodegradation. Environ. Toxicol. Chem. 23(2), 313-324.

Fuller, M.E., Schaefer, C.E., Steffan, R.J., 2009. Evaluation of a peat moss plus soybean oil (PMSO) technology for reducing explosive residue transport to groundwater at military training ranges under field conditions. Chemosphere. 77(8), 1076-1083.

Gregory, K.B., Larese-Casanova, P., Parkin, G.F., Scherer, M.M., 2004. Abiotic transformation of hexahydro-1,3,5-trinitro-1,3,5-triazine by Fe(II) bound to magnetite. Environ. Sci. Technol. 38(5), 1408-1414.

Hansen, L.D., Larson, S.L., Davis, J.L., Cullinane, M.J., Nestler, C.C., Felt, D.R., 2003. Lime treatment of 2,4,6-trinitrotoluene contaminated soils: Proof of Concept study. USACE, ERDC/EL TR-03-15, U.S. Army Environmental Research and Development Center, Vicksburg, MS.

Hatzinger, P.B., Fuller, M.E., Rungmakol, D., Schuster, R.L., Steffan, R.J., 2004. Enhancing the attenuation of explosives in surface soils at military facilities: Sorption-desorption isotherms. Environ. Toxicol. Chem. 23(2), 306-312.

Hawari, J., Beaudet, S., Halasz, A., Thiboutot, S., Ampleman, G., 2000. Microbial degradation of explosives: biotransformation versus mineralization. Appl. Microbiol. Biotechnol. 54(5), 605-618.

Hoferkamp, L.A., Weber E.J., 2006. Nitroaromatic reduction kinetics as a function of dominant terminal electron acceptor processes in natural sediments. Environ. Sci. Technol. 40(7), 2206-2212.

Hofstetter, T.B., Heijman, C.G., Haderlein, S.B., Holliger, C., Schwarzenbach, R.P., 1999. Complete reduction of TNT and other (poly)nitroaromatic compounds under iron-reducing subsurface conditions. Environ. Sci. Technol. 33(9), 1479-1487.

Jaramillo, A.M., Douglas, T.A., Walsh, M.E., Trainor, T.P., 2011. Dissolution and sorption of hexahydro-1,3,5-trinitro-1,3,5-triazine (RDX) and 2,4,6-trinitrotoluene (TNT) residues from detonated mineral surfaces. Chemosphere. 84(8), 1058-1065.

Jiang, J., Kappler, A., 2008. Kinetics of microbial and chemical reduction of humic substances: Implications for electron shuttling. Environ. Sci. Technol. 42(10), 3563-3569.

Kalderis, D., Juhasz, A.L., Boopathy, R., Comfort, S., 2011. Soils contaminated with explosives: Environmental fate and evaluation of state-of-the-art remediation processes. Pure Appl. Chem. 83(7), 1407-1484.

Kappler, A., Benz, M., Schink, B., Brune, A., 2004. Electron shuttling via humic acids in microbial iron(II) reduction in freshwater sediment. FEMS Microbiol. Ecol. 47(1), 85-92.

Kwon, M.J., Finneran, K.T., 2006. Microbially mediated biodegradation of hexahydro-1,3,5-trinitro-1,3,5-triazine by extracellular electron shuttling compounds. Appl. Environ. Microbiol. 72(9), 5933-5941.

Kwon, M.J., Finneran, K.T., 2008. Biotransformation products and mineralization potential for hexahydro-1,3,5-trinitro-1,3,5-triazine (RDX) in abiotic versus biological degradation pathways with anthraquinone-2,6-disulfonate (AQDS) and Geobacter metallireducens. Biodegradation. 19(5), 705-715.

Lee, S.Y., Brodman, B.W., 2004. Biodegradation of 1,3,5-Trinitro-1,3,5-triazine (RDX). J. Environ. Sci. Health A Tox. Hazard. Subst. Environ. Eng. 39(1), 61-75.

Lovley, D.R., Blunt-Harris, E.L., 1999. Role of humic-bound iron as an electron transfer agent in dissimilatory Fe(III) reduction. Appl. Environ. Microbiol. 65(9), 4252-4254.

Lovley, D.R., Coates, J.D., Blunt-Harris, E.L., Phillips, E.J.P., Woodward, J.C., 1996. Humic substances as electron acceptors for microbial respiration. Nature. 382(1): 445-448.

Lovley, D.R., Fraga, J.L., Blunt-Harris, E.L., Hayes, L.A., Phillips, E.J.P., Coates, J.D., 1998. Humic substances as a mediator for microbially catalyzed metal reduction. Acta hydrochim. Hydrobiol. 26(3), 152-157.

Lynch, J.C., Myers, K.F., Brannon, J.M., Delfino, J.J., 2001. Effects of pH and temperature on the aqueous solubility and dissolution rate of 2,4,6-trinitrotoluene (TNT), hexahydro-1,3,5-trinitro-triazine (RDX), and octahydro-1,3,5,7-tetranitro-1,3,5,7-tetrazocine (HMX). J. Chem. Eng. Data. 46(6), 1549-1555.

Martin, W.A., Larson, S.L., Nestler, C.C., Fabian, G., O'Connor, G., Felt, D.R., 2012. Hydrated lime for metals immobilization and explosives transformation: Treatability study. J. Hazard. Mater. 215-216, 280-286.

Morley, M.C., Shammas, S.N., Speitel, G.E., 2002. Biodegradation of RDX and HMX mixtures: Batch screening experiments and sequencing batch reactors. Environ. Eng. Sci. 19(4), 237-250.

Myers, T.E., Brannon, J.M., Pennington, J.C., Davis, W.M., Myers, K.F., Townsend, D.M., Ochman, M.K., Hayes, C.A., 1998. Laboratory studies of soil sorption/transformation of TNT, RDX, and HMX. Tech. Rep. IRRP-98-8. US Army Engineer Waterways Experiment Station. Vicksburg, MS.

Nevin, K.P., Lovley, D.R., 2000. Potential for nonenzymatic reduction of Fe(III) via electron shuttling in subsurface sediments. Environ. Sci. Technol. 34(12), 2472-2478.

Palmer, N.E., von Wandruszka, R., 2010. Humic acids as reducing agents: the involvement of quinoid moieties in arsenate reduction. Environ. Sci. Pollut. Res. Int. 17(7), 1362-1370.

Payne, Z.M., Lamichhane, K.M., Babcock, R.W., Turnbull, S.J., 2013. Pilot-scale in situ bioremediation of HMX and RDX in soil pore water in Hawaii. Environ. Sci. Process Impacts. 15(11), 2023-2029.

Pennington, J.C., Brannon, J.M., 2002. Environmental fate of explosives. Thermochimica acta. 384(1), 163-172.

Pennington, J.C., Patrick, W.H., 1990. Adsorption and desorption of 2,4,6-trinitrotoluene by soils. J. Environ. Quality. 19(3), 559-567.

Peretyazhko, T., Sposito, G., 2006. Reducing capacity of terrestrial humic acids. Geoderma. 137(1), 140-146.

Pichtel, J., 2012. Distribution and fate of military explosives and propellants in soil: A review. Appl. Environ. Soil Sci. 2012. 1-33.

Rakshit, S., Uchimiya, M., Sposito, G., 2009. Iron(III) bioreduction in soil in the presence of added humic substances. Soil Sci. Soc. Am. J. 73(1), 65-71.

Roden, E.E., Kappler, A., Bauer, I., Jiang, J., Paul, A., Stoesser, R., Konishi, H., Xu, H., 2010. Extracellular electron transfer through microbial reduction of solid-phase humic substances. Nature Geoscience. 3(6), 417-421.

Royer, A.R., Burgos, W.D., Fisher, A.S., Unz, R.F., Dempsey, B.A., 2002. Enhancement of biological reduction of hematite by electron shuttling and Fe(II) complexation. Environ. Sci. Technol. 36(9), 1939-1946.

Schaefer, C.E., Fuller, M.E., Lowey, J.M., Steffan, R.J., 2005. Use of peat moss amended with soybean oil for mitigation of dissolved explosive compounds leaching into the subsurface: Insight into mass transfer mechanisms. Environ. Eng. Sci. 22(3), 337-349.

Selim, H.M., Iskandar, I.K., 1994. Sorption-desorption and transport of TNT and RDX in soils. CRREL Report 94-7. US Army Cold regions Research and Engineering Laboratory, Hanover, NH.

Sheremata, T.W., Thiboutot, S., Ampleman, G., Paquet, L., Halasz, A., Hawari, J., 1999. Fate of 2,4,6-trinitrotoluene and its metabolites in natural and model soil systems. Environ. Sci. Technol. 33(22), 4002-4008.

Spain, J.C., Hughes, J.B., Knackmuss, H.J., 2000. Biodegradation of nitroaromatic compounds and explosives. Lewis Publishers.

Talley, J.W., Sleeper, P.M., 1997. Roadblocks to the implementation of biotreatment strategies. Ann. N. Y. Acad. Sci. 829, 16-29.

Thiboutot, S., Ampleman, G., Gagnon, A., Marois, A., Jenkins, T.F., Walsh, M.E., Thorne, P.G., Ranney, T.A., 1998. Characterization of anti-tank firing ranges at CFB Valcartier. Report DREV-R-9809. WATC Wainwright and CFAD Dundurn, Quebec, Canada.

Thomas, T., Caldwell, B., Britto, R., Arnseth, R., 2012. Iron-mediated abiotic degradation of RDX in a contaminated aquifer. Remediation. 22(3), 29-41.

U.S. Agency for Toxic Substances and Disease Registry (ATSDR). 1997. HMX Fact Sheet (on-line), available from URL http://www.atsdr.cdc.gov/toxfaqs/tfacts98.pdf

U.S. Environmental Protection Agency (EPA). 2014. RDX Fact Sheet (on-line), available from URL http://www2.epa.gov/sites/production/files/2014-03/documents/ffrrofactsheet _contaminant _rdx_january2014_final.pdf

U.S. Environmental Protection Agency (EPA). 2014. TNT Fact Sheet (on-line), available from URL http://www2.epa.gov/sites/production/files/2014-03/documents/ffrrofactsheet _contaminant _tnt_january2014_final.pdf

Van der Zee, F.P., Cervantes, F.J., 2009. Impact and application of electron shuttles on the redox (bio)transformation of contaminants: A review. Biotechnol. Adv. 27(3), 256-277.

Wani, A.H., Felt, D.R., Davis, J.L., 2003. Biologically active zone enhancement (BAZE) supplemental study: Mass balance of RDX biotransformation and influence of aquifer temperature on RDX biodegradation in groundwater. ERDC/EL TR-03-11. U.S. Army Engineer Research and Development Center. Vicksburg. MS.

Yamamoto, H., Morley, M.C., Speitel, G.E. Jr., Clausen, J., 2004. Fate and transport of high explosives in a sandy soil: adsorption and desorption. Soil Sediment Contam. 13(5), 361-379.

CHAPTER 3. IMPACT OF GLYCERIN AND LIGNOSULFONATE ON BIODEGRADATION OF HIGH EXPLOSIVES IN SOIL

3.1 Introduction

The high explosives (HEs) compounds 2,4,6-trinitrotoluene (TNT), hexahydro-1,3,5-trinitro-1,3,5-triazine (RDX; royal demolition explosive), and octahydro-1,3,5,7-tetranitro-1,3,5,7-tetrazine (HMX; high melting explosive) are commonly used in military munitions and can be deposited on military ranges as a result of training activities. While greater than 99.99% of the explosive load is consumed when munitions detonate as intended (high-order detonation), substantial amounts of HEs may remain on the range as unexploded ordinance (UXO) or be deposited on the range as chunks or small particles following partial or low-order detonation (Brannon and Pennington 2002; Fuller et al. 2004; Walsh et al. 2006). Over time, the HE compounds can be dissolved by rainwater, infiltrate through the vadose zone, and potentially migrate off the range with flowing groundwater. TNT and RDX are classified as possible human carcinogens (C classification) by U.S. Environmental Protection Agency (EPA 2014). HMX is not currently classified as human carcinogen, but exposure can have adverse impacts to the liver and nervous system (ATSDR 1997).

Biodegradation can limit migration of dissolved TNT through the vadose zone. TNT can be degraded by a wide variety of microorganisms under both of aerobic and anaerobic conditions (Fuller and Manning 1997; Singh 2012). However, TNT degradation is often

more rapid under anaerobic conditions (Pennington and Brannon, 2002). TNT is typically degraded to amino derivatives including 2-amino-4,6-dinitrotoluene (2-ADNT), 4-amino-2,6-dinitrotoluene (4-ADNT), 2,6-diamino-4-nitrotoluene (2,6-DANT), and 2,4-diamino-6-nitrotoluene (2,4-DANT) (McCormick et al. 1981; Hawari et al. 2000). These intermediate compounds can be further transformed through biotic and/or abiotic processes.

In general, RDX is more resistant to aerobic biodegradation than TNT (Bradley and Chapelle 1995; Felt et al. 2009; Halasz et al. 2012). However, RDX can be utilized as a source of nitrogen under aerobic conditions when other nitrogen sources are limited (Binks et al. 1995; Fuller et al. 2010a). 4-nitro-2,4-diazabutanal (4-NDAB) and methylenedinitramine (MEDINA) are typically produced in aerobic biodegradation of RDX associated with the XplA/XplB enzymes (Fournier et al. 2004; Fuller et al. 2010a; Crocker et al. 2015). Despite the potential for RDX biodegradation under aerobic conditions, several studies have reported that aerobic RDX degraders may not be widespread in soil and groundwater, resulting in little or no RDX degradation under aerobic conditions (Fuller et al. 2010b; Crocker et al. 2015; Fuller et al. 2015).

RDX is readily biodegraded under anaerobic conditions (McCormick et al. 1981; Hawari et al. 2000; Halasz et al. 2012). A common anaerobic degradation pathway for RDX involves the reduction of nitro functional groups ($-NO_2$) to nitroso groups (-NO) where RDX is sequentially reduced to hexahydro-1-nitroso-3,5-dinitro-1,3,5-triazine (MNX), hexahydro-1,3-dinitroso-5-nitro-1,3,5-triazine (DNX), and then hexahydro-1,3,5-trinitroso-1,3,5-triazine (TNX) (McCormick et al. 1981; Fuller et al. 2004; Kwon and Finneran 2006). These intermediate nitroso compounds can then be transformed to nitrous oxide (N_2O) and carbon

dioxide (CO_2) (Hawari et al. 2001). Hawari et al. also reported that RDX can also be degraded by direct ring cleavage, yielding MEDINA and bis(hydroxymethyl)nitramine. The intermediate nitramines are further degraded to nitrous oxide (N_2O) and formaldehyde (HCHO) by spontaneous chemical decomposition. However, the factors controlling these degradation pathways are not well understood.

Redox conditions and the presence of different electron acceptors and donors can influence RDX biodegradation rates. RDX biodegradation was faster under mixed electron acceptor conditions compared to single select electron acceptor conditions including sulfate reducing, fermenting, methanogenic, and nitrate reducing conditions (Boopathy 2001). Enhanced biodegradation was observed under conditions with electron donors producing hydrogen (Adrian et al. 2003; Adrian and Arnett 2007) and under highly reducing conditions (Price et al. 2001). However, the presence of nitrate inhibited RDX degradation due to the preferential microbial utilization of nitrate as a nitrogen source and/or an electron acceptor (Cho et al. 2015).

Biodegradation of HMX is analogous to RDX biodegradation due to its similar structure. HMX is resistant to aerobic biodegradation and its degradation is enhanced under anaerobic conditions (Boopathy 2001; Singh 2012). Similar to RDX, HMX can be degraded by sequential reduction of nitro groups to nitroso groups (i.e., transformation of HMX to mononitroso-, dinitroso-, trinitroso-, and tetranitroso-HMX) and by direct ring cleavage. The nitroso intermediates can be subsequently transformed to nitrous oxide (N_2O) and formaldehyde (HCHO) that are indicators of ring cleavage (Bhushan et al. 2006; Pichtel 2012). The direct ring cleavage pathway yields 4-NDAB and MEDINA under aerobic

conditions, and MEDINA under anaerobic conditions (Zhao et al. 2004; Singh 2012). Degradation of HMX is typically slower than RDX and high concentration of RDX can inhibit biodegradation of HMX (Uchimiya et al. 2010). However, low RDX levels did not inhibit HMX degradation (Fuller et al. 2009).

Hatzinger et al. (2004) and Fuller et al. (2004) showed that addition of peat moss and soybean oil can also be effective in stimulating sorption and biodegradation to reduce explosives leaching. Sphagnum peat moss addition to soil slurries was effective in stimulating RDX mineralization and crude soybean oil addition stimulated TNT, RDX, and HMX mineralization (Fuller et al. 2004). The combination of peat moss and crude soybean oil (PMSO) reduced leaching of both RDX and MNX by two orders of magnitude (Schaefer et al. 2005; Fuller et al. 2009). However, application of PMSO to ranges may have some operational issues including: a) increased dust problems in arid areas; b) increased fire hazard; c) challenges in distributing the material without exposing workers to UXO hazards; and d) disturbance of the PMSO amendment by ordinance detonation, potentially reducing treatment effectiveness.

Farling (2013) proposed the use of lignosulfonate (LS) and glycerin (GL) as an alternative to peat moss and soybean oil for enhancing HEs sorption and biodegradation. The LS and GL could be mixed with water and spray applied to the range, eliminating the need to remove UXO, greatly reducing worker exposure. Once applied, natural rainfall or artificial irrigation would transport the amendments deeper into the soil. The readily biodegradable GL was intended to consume available oxygen in soil, generating anaerobic conditions and stimulating anaerobic biodegradation of the HEs. The LS was expected to

biodegrade more slowly, consuming oxygen, and helping to maintain anoxic conditions. GL, produced as a byproduct of biodiesel production, is an attractive substrate due to its low cost, high solubility in water, and relatively high flash point (176 °C). LS is produced during paper production through reaction with metal bisulfites and other reagents (Pearl 1967; Kirk et al. 1980) and is commonly used as a dust control agent, additive in concrete preparation, and dye and insecticides dispersant (Nelson and Northey 2004; Ouyang et al. 2006; Yang et al. 2008). Laboratory soil column experiments monitored by Farling (2013) showed that LS was strongly retained by the soil, but GL rapidly migrated through the columns with 70 - 82 % of the applied GL discharged in the column effluent. TNT leaching was significantly reduced in columns treated with GL alone and GL+LS treated columns, resulting in discharge < 5 % of TNT amount applied. However, RDX degradation was limited in all treated columns. Monitoring data showed that oxygen was rapidly transported through the sandy soil, preventing establishment of anaerobic conditions required to enhance RDX degradation.

Objectives of this work are to: 1) improve our understanding of HEs biodegradation in soil at an active hand grenade range; 2) evaluate the impact of GL and LS addition to these soils on HEs biodegradation under aerobic and anaerobic conditions; and 3) evaluate the kinetics of oxygen consumption by GL and LS. This information can aid in identifying sites where natural attenuation is sufficient to prevent adverse impacts and sites where GL and LS addition might be effective in increasing oxygen consumption rates to control HEs leaching.

3.2 Material and Methods

3.2.1 *Chemicals*

Calcium lignosulfonates (Ultrazine and Norlig A) were purchased from Lignotech USA (Rothschild, WI) and crude glycerin was obtained from Piedmont Biofuels (Pittsboro, NC). Acetonitrile and toluene used for soil and water extractions were HPLC grade and purchased from J.T. Baker and Fisher Scientific respectively.

Analytical standards for TNT, RDX, 2,4-DNT, 2,6-DNT, 2-ADNT, 4-ADNT, and HMX were purchased from AccuStandard, Inc. (New Haven, CT), and standards for RDX nitroso derivatives (MNX, DNX, and TNX) were purchased from SRI International (Menlo Park, CA). All standards were diluted in acetonitrile prior to use.

3.2.2 *Active Range Soils Used in Experiments*

Soils used in this work were collected from two hand grenade throwing bays at Fort Bragg, NC (Bay C and Bay T). The most recent soil survey indicates that the native soils at this site are primarily Vaucluse loamy sand. However, there has been significant re-grading of the site and much of the A soil horizon has been removed to form soil containment berms. Soil for use in the biodegradation tests was prepared by blending soil obtained from 0 to 1 m below ground surface (bgs) in the middle of each bay. Soil characterization results showed that RDX and TNT concentrations were relatively higher in Bay T than Bay C soil, and TNT concentrations were approximately an order of magnitude lower than RDX. While RDX concentrations were 0.03 - 0.24 mg/kg in Bay T and 0.01 - 0.08 mg/kg in Bay C soil, TNT concentrations were 0.008 - 0.012 mg/kg in Bay T and 0.005 - 0.008 mg/kg in Bay C soil.

Both organic carbon (OC) and clay content were significantly higher ($p < 0.05$) in Bay C (OC = 0.14 - 0.23 % and clay = 1.8 - 2.6%) compared to Bay T soil (OC = 0.06 - 0.15 %, clay = 1.4 - 2.3 %). However, Fe(II) concentrations were significantly higher ($p < 0.05$) in Bay T (1.5 - 2.4 g/kg) compared to Bay C soil (1.1 - 1.6 g/kg). Soil pH (5.4 ± 0.2), silt content (13.4 ± 2.7 %), and median grain size (296 ± 70 μm) were not statistically different between Bay C and T soils. Soil analytical methods are described in Appendix I.

3.2.3 *Biodegradation of HEs in Soil Slurry Microcosms*

An initial set of aerobic and anaerobic microcosms were constructed with 50 g of sand from a quarry near Fort Bragg, NC, 100 mL of groundwater, and composited effluent from laboratory columns amended with TNT, RDX, glycerin and lignosulfonates (Farling, 2013). Experimental treatments included: 1) autoclaved controls; 2) no amendment (live controls); 3) 0.256 g of glycerin (GL), 4) 0.032 g of Ultrazine CA (UCA), 5) 0.037 g of Norlig A (NA), 6) GL + UCA, and 7) GL + NA. UCA is a higher cost material where the lower molecular weight materials have been removed. NA is a relatively low cost lignosulfonate that is commonly used for dust control. The organic amendment loading rates were determined from the amendment loading rates in the field sand columns constructed by Farling (2013). Aerobic and anaerobic microcosms were constructed and monitored separately. Aerobic microcosms were shaken on a tumbler and the headspace was flushed each week with 500 mL of pure oxygen. The anaerobic microcosms were flushed with nitrogen gas for 30 min and incubated with no shaking since rapid oxygen exchange was not required.

A second set of microcosms were then constructed to simulate the transient aerobic and anaerobic conditions that might occur in grenade range soils. Microcosms were constructed by addition of 50 g of blended grenade range soil, 100 mL of pore water collected from bucket lysimeters at the site, and RDX/TNT stock solutions to generate approximately 1,000 µg/L of each component in the microcosm. The experimental treatments included: 1) autoclaved control, 2) no treatment (live control), 3) 0.074 g of crude glycerin (GL), 4) 0.074 g of Norlig A (NA, lignosulfonate), and 5) 0.074 g of both crude GL and NA. All treatments were run in triplicate. The organic amendment loading per g soil was identical to the substrate loading used in a field evaluation of organic substrate addition to the Fort Bragg hand grenade range (Chapter 6). Microcosms for the autoclaved controls were constructed by placing soil and groundwater into serum bottles, autoclaving at 121 ºC and 20 psi for an hour to remove viable microorganisms, and then spiking RDX and TNT stock solutions to avoid thermal decomposition of those explosives. Bottle controls were constructed without sediment by transferring groundwater and spiking explosives, and operated in parallel with other microcosms. For the first 56 days, all microcosms were shaken on a tumbler and the headspace was flushed each week with 500 mL of pure oxygen using a gas syringe to maintain aerobic conditions in aqueous phase. At Day 56, all bottles were flushed with pure nitrogen gas for 30 min to switch from aerobic conditions to anaerobic conditions in microcosms. After 56 days, the microcosms were incubated with no shaking since rapid oxygen exchange was no longer required. Gas samples from each microcosm were analyzed by gas chromatography (GC) with a thermal conductivity detector (TCD) and flame ionization detector (FID) in series to monitor changes in oxygen, carbon

dioxide, nitrogen, and methane concentrations. When gas samples were analyzed, gas pressure in each bottle was neutralized using a gas syringe, followed by adding 3 mL of pure nitrogen gas into the bottle prior to collecting 3 mL of gas sample for the analysis in order to avoid negative pressure inside bottles.

3.2.4 *Oxygen Consumption in Soil Slurry Microcosms*

Soil microcosms were constructed and monitored to evaluate the impact of organic substrates (crude GL and/or NA) on oxygen consumption in microcosms using sediment collected from both Bays C and T at Fort Bragg. The soil microcosms were constructed by transferring 100 g of air-dried, mixed soil and 100 mL of pore water into three different 250 mL serum bottles for each treatment. The microcosm headspace was flushed with 500 mL of pure oxygen to displace the air, sealed with a butyl rubber stopper, and shaken on a tumbler for two days to saturate the liquid phase with oxygen prior to oxygen consumption experiment. Each microcosm was flushed with another 500 mL of pure oxygen, followed by neutralizing gas pressure in bottles using a gas syringe. Experimental treatments were the same as in the HEs biodegradation incubations. The only difference between the HEs biodegradation and oxygen consumption experiments was the use of greater amount of soil with more amendment addition to evaluate the kinetics of oxygen consumption by organic amendments more efficiently. Gas samples from each microcosm were periodically analyzed by gas chromatography (GC-TCD) to monitor changes in concentrations of oxygen, carbon dioxide, and nitrogen. When gas samples were analyzed, gas pressure in each bottle was neutralized using a gas syringe, followed by adding 3 mL of pure nitrogen gas into the bottle

prior to collecting 3 mL of gas sample for the analysis to avoid negative pressure inside bottles. The added nitrogen gas was subtracted in the calculation of gaseous masses.

The amount of oxygen (O_2) consumed and carbon dioxide (CO_2) produced in each bottle was determined by accounting for the mass removed during sampling and correcting for gas partitioning to the aqueous phase based on the Henry's Law constant. Gas concentrations (%) by volume determined by GC-TCD were converted to mass using the molecular weight and ideal gas molar volume. Data collection ended once oxygen concentrations dropped below a level that might limit oxygen consumption (assumed to be 10 %). O_2 consumption in bottles containing a sodium sulfite solution matched within a range of 108 - 114% of the theoretical value, confirming the accuracy of this approach.

3.2.5 *Sample Extraction and Analytical Methods*

Water samples for explosives analysis were first extracted with toluene by frozen micro-extraction (FME) following procedures described by Li et al. (2011) followed by analysis of the toluene extract by GC with an electron captured detector (ECD) to minimize interferences with humic materials and lignin present in soil and aqueous samples. Water samples were first filtered through 0.2 μm PTFE syringe filters, liquid-liquid extracted with 1 mL of both sample and toluene placed in 4 mL Teflon-capped PTFE target vials, followed by shaking on a vortex for 30 seconds and mixing on a table shaker for 2 hours after packed in an insulated box filled with ice to minimize thermal decomposition of explosives. Vials were placed in a - 80 ºC freezer for 30 min to separate toluene by freezing water. The toluene was transferred to amber target vials and stored at - 20 ºC until analyzed by GC-ECD. 2 μL

extract in toluene was injected into an Agilent 7890A GC equipped with a cool-on-column inlet, 7.5 m long-0.53 mm diameter-1.5 μm film thickness DB-5ms column, and 1 m long Restek retention gap column, with helium as the carrier gas (10 mL/min) and nitrogen as the makeup gas (60 mL/min). The different analytes were separated with the following temperature program: 75 ºC for 0.1 min, increased at 15 °C per min to 200 ºC, then increased at 20 ºC per min to 300 °C, then held for 5.5 min, and the detector temperature was 325 ºC. The cool-on-column injector and the autosampler tray cooled to ~ 4 ºC were used to minimize thermal decomposition of the explosive components.

First-order RDX and HMX degradation rates during the anaerobic phase were calculated for each microcosm using the equation:

$$\ln C_{(t)} = \ln C_0 - kt$$

where, $C_{(t)}$ = concentration at time t, C_0 = initial concentration, k = rate constant, and t = time.

In several of the incubations, there was a lag prior to the onset of degradation and/or degradation slowed once concentrations dropped to near the analytical detection limit. To provide a consistent approach for estimating lag periods and degradation rates, the data that resulted in the highest F-statistic were used in the regression. Data prior to the period were assumed to be during the lag phase. Figure S-1 in Appendix II illustrates how this procedure was applied for a representative dataset.

3.3 Experimental Results

3.3.1 *HEs Biodegradation*

A series of initial microcosm incubations were conducted using sand from a quarry near Fort Bragg, NC to evaluate the impact of glycerin and two different types of lignosulfonate (Norlig A and Ultrazine CA) on TNT and RDX biodegradation. Figure 3.1 shows the effect of glycerin plus Norlig A (GL+NA) and glycerin plus Ultrazine CA (GL+UCA) on TNT and RDX biodegradation in field sand microcosms under aerobic and anaerobic conditions. Under aerobic conditions, both GL+NA and GL+UCA stimulated TNT biodegradation with TNT reduced to below detection (< 1 µg/L) in 28 days. However, in the live control incubations (no added substrate), degradation was more variable with TNT reduced by over 99 % in two of three incubations in 28 days. TNT also declined in the autoclaved incubations, either due to slow sorption to the soil or incomplete sterilization.

GL+NA and GL+UCA both stimulated TNT biodegradation in field sand under anaerobic conditions. However, TNT was also reduced to below detection in the live control incubations, indicating rapid biodegradation under anaerobic conditions with or without substrate addition.

Figure S-2 in Appendix II shows TNT concentrations versus time in aerobic and anaerobic field sand microcosms amended with GL, UCA, NA, GL+UCA, GL+NA, and both live and autoclaved controls. Under aerobic conditions, all of the organic substrates stimulated TNT biodegradation (*p-values* < 0.05). However, degradation was more rapid in treatments containing glycerin (GL, GL+UCA and GL+NA) than in those that only contained

lignosulfonate (UCA and NA). Under anaerobic conditions, TNT was reduced to below the analytical detection limit within 14 days in all amended incubations.

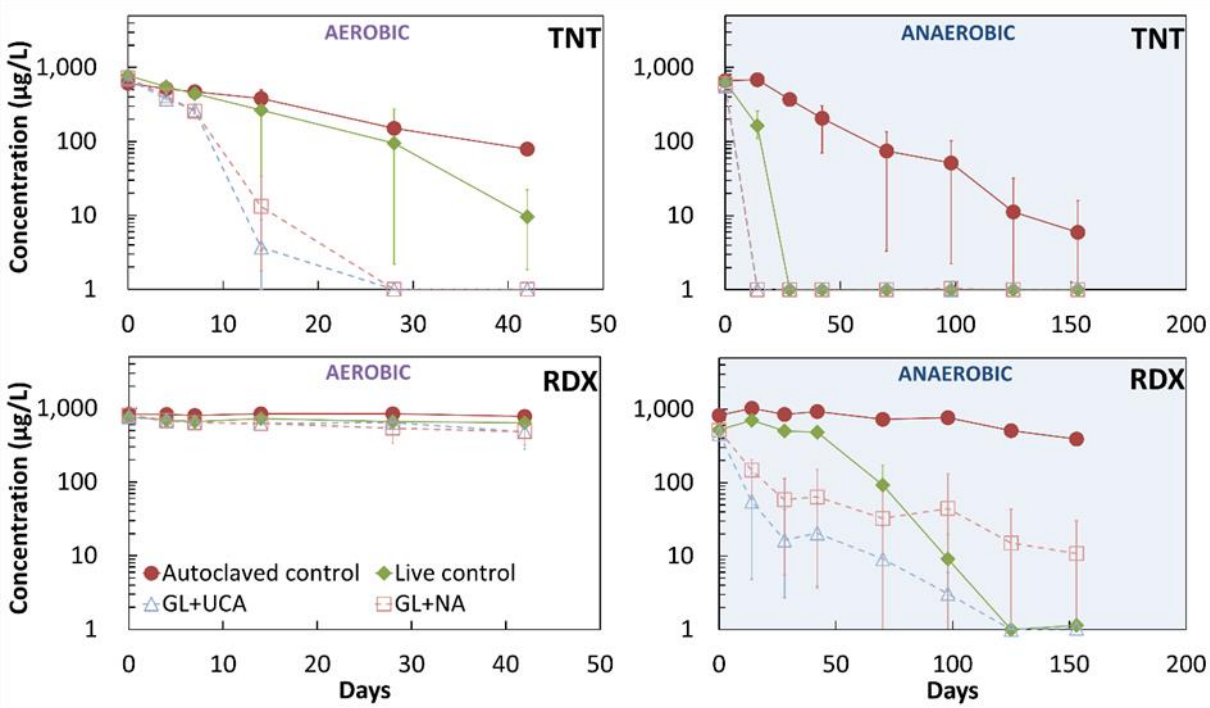

Figure 3.1. Concentrations of TNT and RDX in autoclaved, live (no added substrate) controls, and substrates-treated (GL+UCA or GL+NA) microcosms with field sand under aerobic and anaerobic conditions. Error bars represent range of values in replicate columns. Where not visible, error bars are smaller than symbol size.

Consistent with prior reports (Bradley and Chapelle 1995; Felt et al. 2009), RDX was not aerobically biodegraded in any field sand incubation. Under anaerobic conditions, RDX was significantly degraded in all live microcosms. Degradation was most rapid in the GL only incubations followed by NA, UCA, GL+UCA, then live control and GL+NA incubations. The apparently slower degradation in the GL+NA incubation may not be significant, since RDX was reduced to below detection in two of three bottles within 98 days.

Based on the successful treatment of both TNT and RDX in field sand microcosms under anaerobic conditions, additional experiments were conducted using soils from grenade Bays C and T at Fort Bragg, NC. In these experiments, the microcosms had an initial 56-day aerobic phase followed by an 85-day anaerobic phase. Treatments included autoclaved control, live control (no added substrate), GL, NA, and GL+NA. A combination of glycerin and lignosulfonate was selected to provide an easily biodegradable substrate (GL) to rapidly consume oxygen and a more slowly degradable substrate (NA) to maintain anaerobic conditions, while reducing the need for frequent substrate addition. NA was selected over UCA because of its much lower cost (approximately 38 % of UCA).

Figure 3.2 shows the variation in concentration of TNT, RDX, HMX and RDX degradation products (MNX, DNX, TNX) over time. Based on prior results, the HEs and degradation products were only monitored at the beginning and end of the aerobic phase. TNT was extensively degraded in soil from both Bays C and T under aerobic conditions. At the completion of the aerobic phase, 2,6-dinitrotoluene (2,6-DNT) and 2,4-dinitrotoluene (2,4-DNT) were below the analytical detection limit of 2.5 µg/L, whereas 2-ADNT and 4-ADNT were increased as TNT was degraded, followed by further degradation of the ADNTs under anaerobic conditions (data not shown).

Consistent with prior observations, RDX was not substantially degraded in the Bay C and T soils during the aerobic phase. HMX, MNX, DNX and TNX were not added to the incubations but were present at low levels in the soil used to construct the microcosms. Small increases in aqueous phase concentrations for each of these compounds were observed in some incubations during the aerobic phase, presumably due to release of this material from

the soil. There is no evidence of HMX, MNX, DNX or TNX degradation during the aerobic phase.

With the onset of anaerobic conditions, both RDX and HMX were extensively degraded in the Bay C and T microcosms. Both compounds were rapidly degraded in the soils amended with GL+NA and in the Bay T live control. However, degradation appeared to be somewhat slower in the Bay C live control. MNX, DNX and TNX concentrations increased during the period of most rapid RDX degradation, then declined as RDX became depleted.

To provide a more quantitative evaluation of the data, lag periods and first-order degradation rates were estimated for RDX and HMX as described under Methods and are shown in Table 3.1. For the live control incubations (no added GL+NA), RDX and HMX degradation rates were significantly higher (*p-value* < 0.05) in the Bay T soil microcosms compared to Bay C soil microcosms, possibly associated with the higher Fe(II) content of this soil. Addition of GL, NA, and GL+NA all significantly increased RDX and HMX degradation rates in the Bay C soil, but did not enhance degradation in the Bay T soil (Figure S-3). The small difference between the live control rates and amended rates is presumably due to the high degradation rates in the live control T soil.

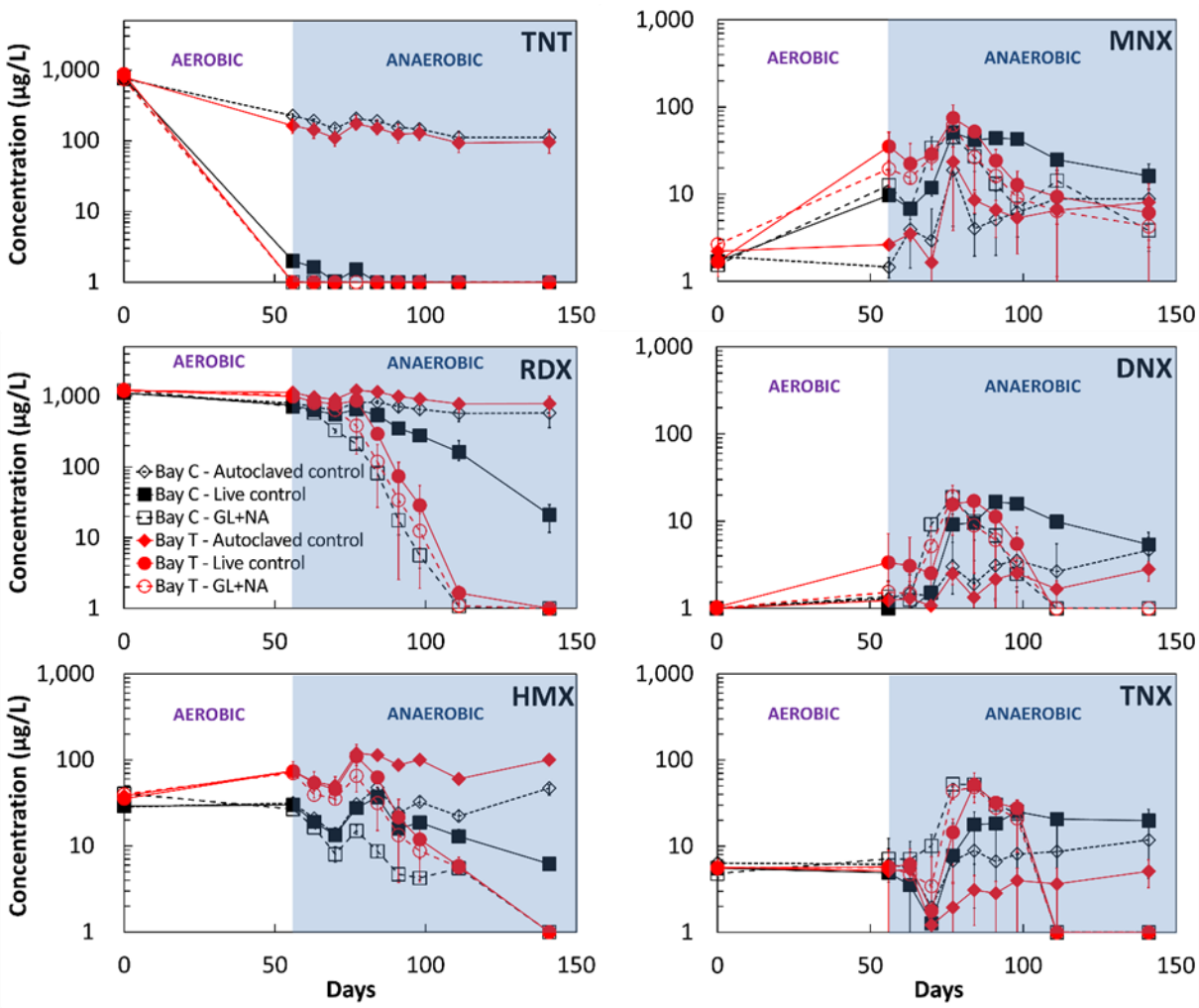

Figure 3.2. Concentrations of high explosives (TNT, RDX, and HMX) and RDX nitroso derivatives (MNX, DNX, and TNX) in autoclaved, live (no added substrate) controls, and GL+NA added microcosms with Bay C and T soils respectively under aerobic and anaerobic conditions. Error bars represent range of values in replicate columns. Where not visible, error bars are smaller than symbol size.

ANOVA analysis showed no significant difference (*p-values* > 0.05) in means of RDX and HMX degradation rates across groups of different microcosms in both the Bay C and Bay T soils, indicating that a type of substrate added did not significantly influence degradation rates, once anaerobic conditions were established. ANOVA analysis including groups of untreated (live controls) and treated microcosms also showed no significant

difference (*p-values* > 0.05) in means of their degradation rates in Bay T and HMX degradation rates in Bay C soils, but significant difference (*p-value* < 0.05) in means of RDX degradation rates in Bay C soil, suggesting enhanced RDX degradation with the presence of organic substrates even in anaerobic conditions in Bay C soil.

Table 3.1. Average lag periods and degradation rates of RDX and HMX in Bay C and T soil microcosms with different treatments assuming first-order degradation of the components. Values in parentheses are standard deviations of replicates. Bold values are statistically different from live control (*p-value* < 0.05).

	Treatment	**RDX**		**HMX**	
		Lag (d)	Rate (d^{-1})	Lag (d)	Rate (d^{-1})
Bay C	Autoclaved control	21 (0)	0.010 (0.002)	35 (0)	-0.011 (0.003)
	Live control	14 (12)	0.050 (0.020)	28 (12)	0.027 (0.003)
	GL*	0	**0.120 (0.020)**	14 (12)	**0.049 (0.006)**
	NA**	7 (12)	**0.100 (0.030)**	14 (12)	0.050 (0.02)
	GL + NA	0	**0.110 (0.020)**	7 (12)	**0.044 (0.005)**
Bay T	Autoclaved control	21 (0)	0.010 (0.004)	26 (8)	0.007 (0.011)
	Live control	14 (12)	0.130 (0.040)	14 (12)	0.076 (0.008)
	GL*	0	0.147 (0.006)	0	0.100 (0.040)
	NA**	5 (8)	0.130 (0.040)	0	**0.058 (0.001)**
	GL + NA	12 (11)	0.155 (0.007)	14 (12)	0.070 (0.010)

* GL - glycerin
** NA – Norlig A lignosulfonate

3.3.2 *Oxygen Consumption in Soil*

The HEs biodegradation microcosms with Bay T soil described above showed that addition of GL, NA, or GL+NA did not significantly increase degradation rates in

comparison to untreated live control microcosms, once anaerobic conditions were established. However, addition of these substrates could increase oxygen consumption rates, increasing the likelihood of anaerobic conditions.

Laboratory soil microcosms were constructed with blended soils plus pore water collected from Bay C and Bay T and monitored to estimate oxygen consumption in untreated and organic substrates-treated soils. Cumulative masses of oxygen consumed and carbon dioxide produced in untreated and amended microcosms with Bay C or T soils are shown in Figure 3.3. Overall, all three replicate microcosms for each treatment exhibited the same behavior in oxygen consumption. In untreated microcosms (live controls), cumulative mass of oxygen consumed was low (< 1.0 mmol), indicating low oxygen consumption by natural carbon and microbial respiration in soils. However, oxygen consumption was significantly enhanced by addition of GL+NA, resulting in increases of 367% in Bay C and 232% in Bay T soil microcosms. The increased oxygen consumption in substrates-treated microcosms is primarily due to addition of GL rather than NA. Microcosms treated with GL only showed 286% and 195% increased oxygen consumption in Bay C and T soils respectively, whereas NA-treated microcosms showed 33% higher and 7% lower oxygen consumption in Bay C and T soils compared to untreated live controls (data shown in Figure S-4). Oxygen consumption in the GL+NA treated Bay C soil was significantly higher than in the treated Bay T soil, possibly due to the higher initial organic carbon content of the Bay C soil.

Carbon dioxide (CO_2) production followed the same general pattern as oxygen consumption in both the untreated and treated microcosms. Addition of GL+NA to soils significantly enhanced CO_2 production compared to untreated microcosms, resulting in

higher production rates in treated Bay C soil than in treated Bay T soil (Figure 3.3). In microcosms treated with NA only, however, CO_2 production was significantly higher than live controls although O_2 consumption was not considerably different between live controls and NA treated microcosms (data shown in Figure S-4).

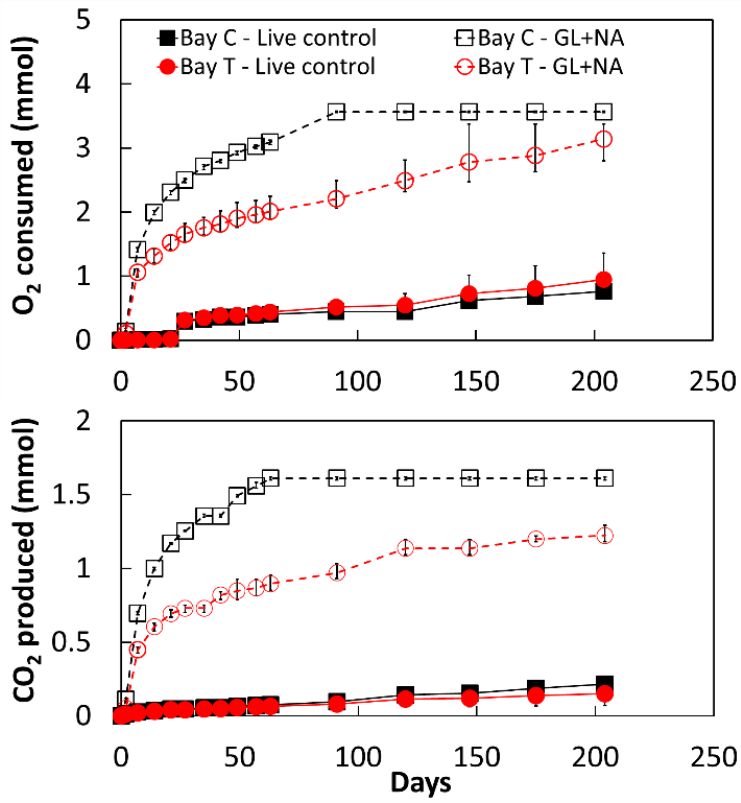

Figure 3.3. Cumulative oxygen consumption and carbon dioxide production in gas phase in live control (untreated) and GL+NA treated microcosms with Bay C or T soils. Error bars represent range of values in replicate microcosms. Where not visible, error bars are smaller than symbol size.

As shown in the equations below, complete mineralization of GL should result in production of 0.86 moles of CO_2 per mole O_2 consumed while mineralization of NA should result in 0.82 moles CO_2 per mole O_2.

GL: $C_3H_8O_3 + 3½\ O_2 \rightarrow 3\ CO_2 + 4\ H_2O$

NA: $C_{20}H_{24}CaO_{10}S_2 + 24½\ O_2 \rightarrow 11\ H_2O + 20\ CO_2 + CaSO_4 + H_2SO_4$

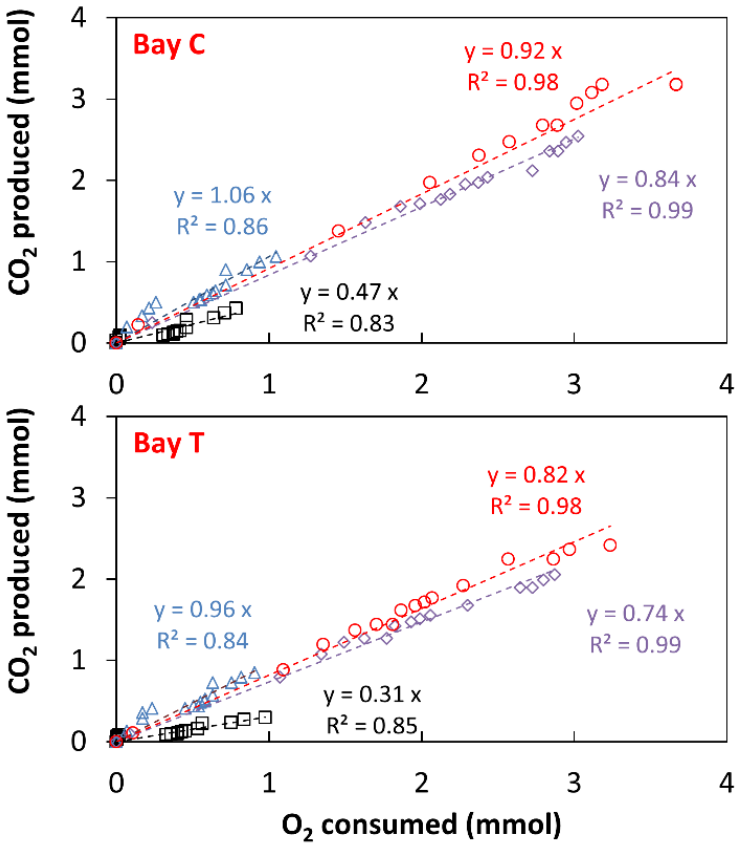

Figure 3.4. Correlations between cumulative masses of oxygen consumed and carbon dioxide produced in untreated microcosms (□), microcosms treated with GL only (◊), microcosms treated with NA only (Δ), and microcosms treated with GL+NA (○). Dash lines represent linear correlation for each treatment.

Figure 3.4 shows the relationship between the cumulative masses of O_2 consumed and CO_2 produced in microcosms for each treatment. The ratio of CO_2 produced to O_2 consumed for GL was 0.84 in Bay C and 0.74 in Bay T, consistent with near complete

mineralization of the GL. The CO_2:O_2 ratio for NA was 1.06 in Bay C and 0.96 in Bay T which are higher than expected based on complete mineralization. The cause of this higher than expected ratio is not known, but it may be associated with earlier release of carboxylic group (COOH) during aerobic degradation, ultimately producing carbon dioxide by decarboxylation, and accumulation of partially degraded intermediates of NA leading lower than expected oxygen consumption (Wang et al. 2013). Several studies showed increase of reactive phenolic intermediates during aerobic lignosulfonate degradation, which could be further biodegraded by oxidative aromatic ring cleavage (Colberg and Young 1985; Bugg and Winfield 1998). This postulation can be supported by decrease of the CO_2:O_2 ratio for NA over time. In Bay C soil microcosms, the ratio was 2.01 during first 21 days, but it decreased to 0.83 during last 57 days of the monitoring period, consistent with theoretical ratio by complete mineralization of NA (data shown in Figure S-5 in supplementary material).

To aid in planning substrate application to stimulate HE biodegradation, oxygen consumption over time was fit to 1st order (eq. 1) and 2nd order (eq. 2) models of substrate (S, mg/L in aqueous phase) and oxygen (O_2, mg/L in aqueous phase) consumption over time, where f is the ratio of oxygen to substrate consumed. k_1 (d^{-1}) and k_2 (L mg^{-1} d^{-1}) are the 1st and 2nd order degradation coefficients, respectively.

$$1^{st}\ \text{Order:}\quad dS/dt = -k_1 S \quad \text{and} \quad dO_2/dt = -f\, dS/dt \qquad \text{(eq. 1)}$$

$$2^{nd}\ \text{Order:}\quad dS/dt = -k_2 S O_2 \quad \text{and} \quad dO_2/dt = -f\, dS/dt \qquad \text{(eq. 2)}$$

f was estimated assuming complete mineralization of organic substrates since the correlation of CO_2 produced and O_2 consumed indicated that mineralization was the primary mechanism in substrate degradation.

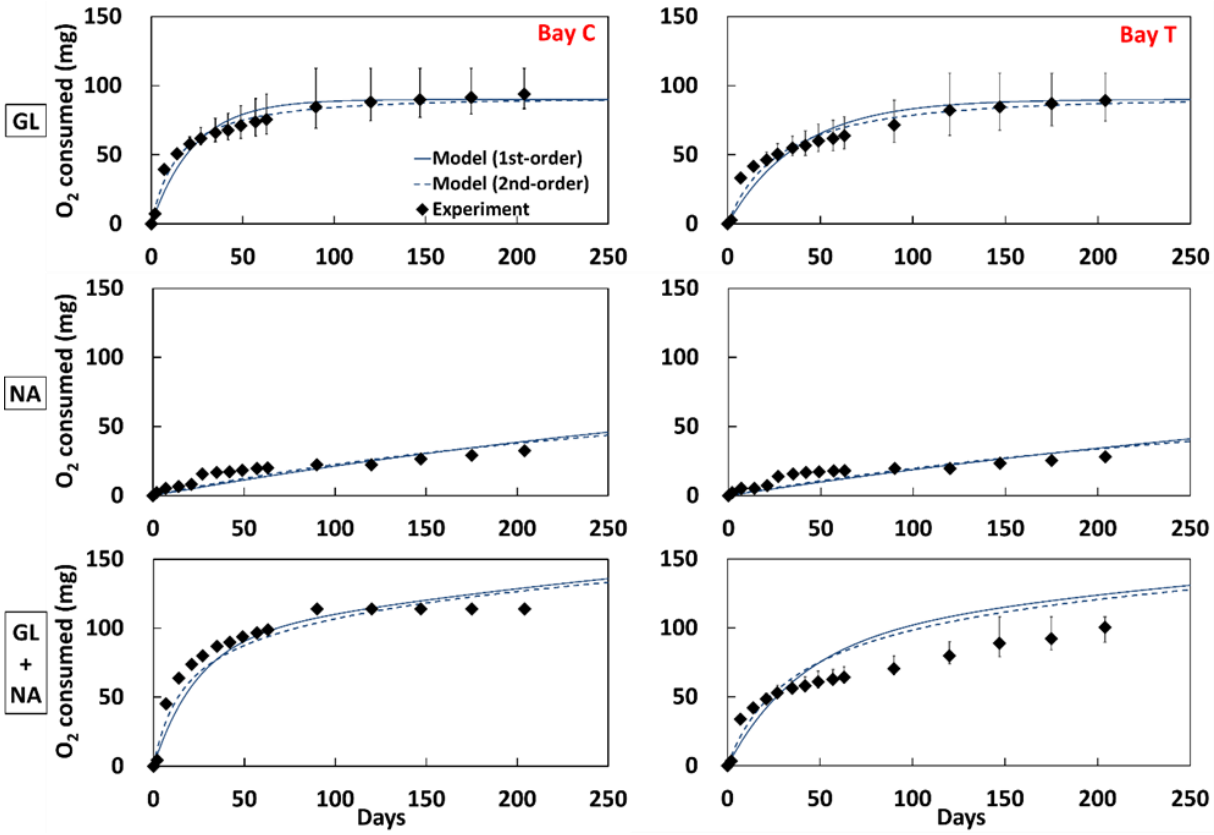

Figure 3.5. Experiment and modeling results of cumulative oxygen consumption in gas phase under 1st and 2nd order degradation of organic substrates in Bay C and T soil microcosms treated with crude glycerin (GL), Norlig A (NA), and crude glycerin + Norlig A (GL + NA). Error bars represent range of values in replicate columns. Where not visible, error bars are smaller than symbol size.

Figure 3.5 shows a comparison of simulated and observed O_2 consumption over time in the Bay C or T soil microcosms. Values of k_1 and k_2 for GL and LS were obtained by fitting the simulation model to the observed oxygen consumption in the GL-only and NA-

only microcosms using the GRG Nonlinear solver in MS Excel to minimize the root mean squared error (RMSE) between simulated and observed O_2 consumption. O_2 consumption in the GL+NA microcosms was then predicted using the best fit values of k_1 and k_2. Estimated model parameters and error statistics are presented in Table 3.2.

Table 3.2. First- and second-order degradation coefficients, ratios of oxygen to substrate consumed, and RMSE between observed and modeling results assuming complete mineralization of organic substrates. The best fit parameter values for each treatment are shown in bold.

	First-order				**Second-order**			
Soil	**Constant**	**GL***	**NA****	**GL+NA**	**Constant**	**GL**	**NA**	**GL+NA**
Bay C	k_1 (d^{-1})	0.042	0.002	N/A	k_2 (L mg^{-1} d^{-1})	1.8E-3	6.8E-5	N/A
	f	1.22	1.48	N/A	f	1.22	1.48	N/A
	RMSE	6.56	5.62	10.61	**RMSE**	**3.66**	**4.96**	**8.68**
Bay T	k_1 (d^{-1})	0.026	0.002	N/A	k_2 (L mg^{-1} d^{-1})	1.0E-3	5.7E-5	N/A
	f	1.22	1.48	N/A	f	1.22	1.48	N/A
	RMSE	7.65	5.50	17.83	**RMSE**	**5.19**	**4.99**	**15.67**

* GL: Glycerin
** NA: Norlig A lignosulfonate

Both 1st and 2nd order models provided a good fit to measured experiment results (Figure 3.5). However, the second-order model provided a slightly better fit to the oxygen consumption results with smaller values of RMSE. As expected, 1st and 2nd order rates were higher for GL than NA. Values of k_1 and k_2 for GL were relatively lower in Bay T soil (k_1 = 0.026 d^{-1} and $k_2 = 10^{-3}$ L mg^{-1} d^{-1}) than Bay C soil (k_1 = 0.042 d^{-1} and $k_2 = 1.8*10^{-3}$ L mg^{-1} d^{-1}). Predicted O_2 consumption in the Bay C microcosms with GL+NA closely matched observed values indicating the models have some predictive ability. However, the model prediction

was not as good for the Bay T microcosms treated with GL+NA. Actual oxygen consumption in GL+NA treated Bay T soil microcosms were significantly lower than oxygen consumption predicted by the best fit values of k_1 and k_2 for GL+NA treated microcosms, resulting in approximately two-fold higher RMSE (15.67) than in GL+NA-treated Bay C soil microcosms (8.68).

3.4 Discussion

Microcosm experiments using both field sand and soil from two active grenade throwing bays showed aerobic biodegradation of TNT, consistent with prior reports (Fuller and Manning 1997; Singh 2012). There was no evidence of RDX, MNX or HMX biodegradation under aerobic conditions. Biodegradation of RDX, HMX and RDX degradation products was enhanced under anaerobic conditions. Further, anaerobic Bay C microcosms showed enhanced RDX degradation in the presence of GL+NA (Figure 3.2). The enhanced RDX degradation with organic substrates is consistent with the prior work by Fuller et al. (2004; 2009), which showed enhanced mineralization of RDX and HMX by addition of molasses, crude soybean oil, and peat moss + soybean oil. In untreated Bay C soil microcosms (live controls) under anaerobic conditions, RDX was degraded with the rates of 0.05 ± 0.02 d^{-1}, however, the degradation rates were significantly increased up to 0.11 ± 0.02 d^{-1} by addition of GL+NA. HMX degradation rates were also enhanced from 0.027 ± 0.003 d^{-1} to 0.044 ± 0.005 d^{-1} by GL+NA addition (Table 3.2). These rates are much higher than the 1st order natural attenuation rate for RDX in groundwater ($8x10^{-6}$ d^{-1}) reported by Pennington et al. (2001). The 1st order decay constant for RDX of 0.17 d^{-1} reported by

Galloway (2015) by photosynthetic bacteria under anaerobic conditions is consistent with RDX degradation rates ($0.155 \pm 0.007\ d^{-1}$) in GL+NA treated Bay T soils during anaerobic phase.

Several previous studies have reported that HEs degradation products are resistant to further degradation in oxic conditions and can be accumulated in the environment although the parent compounds are degraded (Vorbeck et al. 1998; Singh 2012). Formation of these intermediates in degradation processes has become health and safety concerns due to their toxic potentials. It has been reported that TNT degradation products including 2,4-DNT, 2,6-DNT, 2-ADNT, and 4-ADNT were also toxic to most microorganisms and some species of both invertebrates and vertebrates (Dodard et al. 1999; Lachance et al. 2004; Lotufo and Lydy 2005; Karnjanapiboonwong et al. 2009). Zhang et al. (2008) showed toxicity to earthworms by the RDX nitroso derivatives (MNX, DNX, and TNX).

In this study, while 2,4-DNT and 2,6-DNT were not detected, 2-ADNT and 4-ADNT increased as TNT was degraded during the aerobic phase, then these intermediates were further degraded during the anaerobic phase, and were reduced below 2.5 µg/L within 42 days (data not shown). RDX nitroso derivatives initially increased then declined during anaerobic RDX degradation, resulting in final concentrations of DNX and TNX below 1 µg/L at the end of monitoring period (Figure 3.2). MNX concentrations were still detected at the end of monitoring in all microcosms. However, MNX concentrations were significantly lower in the GL+NA treated microcosms than the live controls, and MNX concentrations were continuing to decline. The sum of MNX, DNX, and TNX were always less than 10 % of the initial RDX concentration, with the exception of a single sample (data not shown).

Other RDX degradation products were not monitored in this study. However, MEDINA is not expected to accumulate in the environment since it is unstable in water and readily decomposed to nitrous oxide (N_2O) and formaldehyde (HCHO) (Halasz et al. 2010).

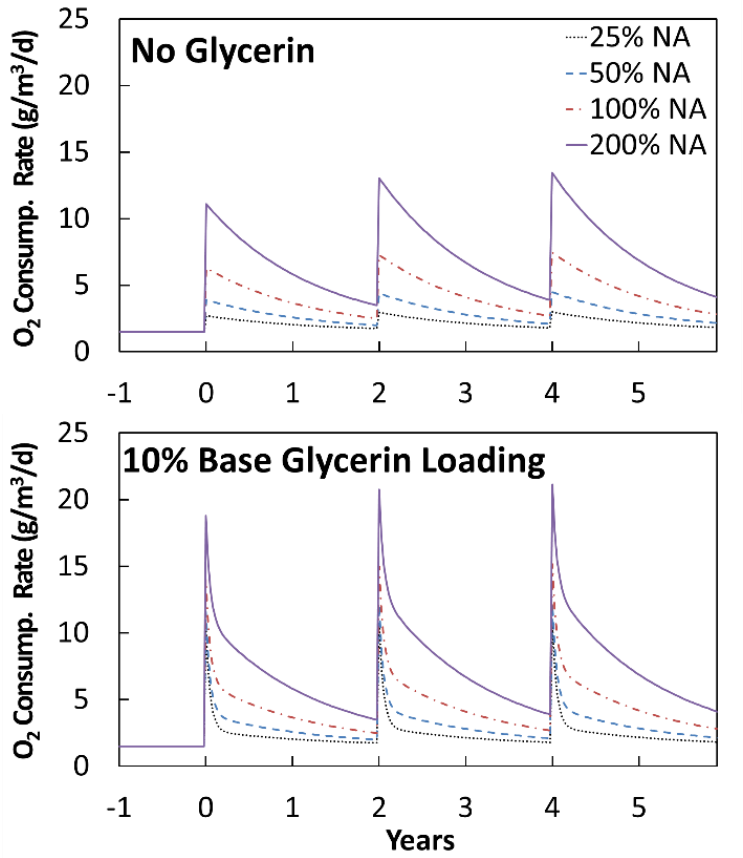

Figure 3.6. Predicted oxygen consumption rates over time with varying amounts of glycerin (GL) and Norlig A(NA).

The oxygen consumption experiments demonstrated the benefit of providing a mixture of a rapidly biodegradable substrate (GL) to quickly generate anaerobic conditions and a more slowly biodegradable substrate (NA) to slowly consume oxygen over time (Figure 3.5). The amount of GL and NA required to generate anoxic conditions will depend

on site specific conditions including the initial oxygen content of the soil and the rate of oxygen entry into the soil over time. Figure 3.6 shows oxygen consumption rates (g O_2/m^3 soil/day) in Bay C soil versus time for different amounts of GL and NA predicted with the first order model. Substrate loading rates used in these simulations are reported relative to the base loading rates used in the oxygen consumption studies (Figure 3.3) with substrate reapplication every other year. When only GL is added, oxygen consumption rates spike immediately after GL addition then decline rapidly, dropping below 1.5 $g/m^3/d$ (oxygen consumption rate by natural soil with no amendment) within 100 days. When only NA is added, oxygen consumption rates are more uniform, declining by 21 % over the two-year reapplication cycle. In some cases, it may be desirable to add a small amount of GL to rapidly consume oxygen, and then maintain reducing conditions with a larger amount of NA (illustrated in Figure 3.6). The amount of GL and NA required to generate and maintain anaerobic conditions will be site specific and depend on the soil characteristics and air filled porosity.

3.5 Conclusions

TNT rapidly biodegraded under aerobic and anaerobic conditions in microcosms constructed with both field sand and soil from two grenade throwing bays with and without organic amendments. However, there was no evidence of substantial RDX, HMX, or RDX daughter products biodegradation under aerobic conditions. Under anaerobic conditions, RDX, HMX and RDX daughter products were biodegraded. Addition of crude glycerin (GL) plus Norlig A (NA, lignosulfonate) resulted in more rapid RDX degradation in Bay C soil.

TNT and RDX daughter products (2-ADNT, 4-ADNT, MNX, DNX, and TNX) did not substantially accumulate and were degraded under anaerobic conditions.

The organic substrates (GL+NA) applied in this study increased oxygen consumption rates and can potentially be used to generate anaerobic conditions in the field. The ratio of CO_2 produced to O_2 consumed indicates both materials are mineralized. Mathematical model simulations indicate that oxygen consumption rates of 5 to 20 $g/m^3/d$ can be achieved with reasonable amendment application rates. However, further work is needed to determine the oxygen consumption rates required under field conditions.

3.6 References

Adrian, N.R., Arnett, C.M., 2007. Anaerobic biotransformation of explosives in aquifer slurries amended with ethanol and propylene glycol. Chemosphere. 66(10), 1849-1856.

Adrian, N.R., Arnett, C.M., Hickey, R.F., 2003. Stimulating the anaerobic biodegradation of explosives by the addition of hydrogen or electron donors that produce hydrogen. Water Res. 37(14), 3499-3507.

Bhushan, B., Halasz, A., Hawari, J., 2006. Effect of iron(III), humic acids and anthraquinone-2,6-disulfonate on biodegradation of cyclic nitramines by Clostridium sp. EDB2. J. Appl. Microbiol., 100(3), 555-563.

Binks, P.R., Nicklin, S., Bruce, N.C., 1995. Degradation of Hexahydro-1,3,5-Trinitro-1,3,5-Triazine (RDX) by *Stenotrophomonas maltophilia* PB1. Appl. Environ. Microbiol. 61(4). 1318-1322.

Boopathy, R., 2001. Enhanced biodegradation of cyclotetramethylenetetranitramine (HMX) under mixed electron-acceptor condition. Bioresource Technol. 76(3), 241-244.

Bradley, P.M., Chapelle, F.H., 1995. Factors affecting microbial 2,4,6-trinitrotoluene mineralization in contaminated soil. Environ. Sci. Technol. 29, 802-806.

Brannon, J.M., Pennington, J.C., 2002. Environmental fate and transport process descriptors for explosives. Final report for Strategic Environmental Research and Development Program. ERDC/EL TR-02-10. U.S. Army Engineer Research and Development Center, Vicksburg, MS.

Bugg, T.D., Winfield, C.J., 1998. Enzymatic cleavage of aromatic rings: mechanistic aspects of the catechol dioxygenases and later enzymes of bacterial oxidative cleavage pathways. Nat. Prod. Rep. 15(5), 513-530.

Cho, K.C., Lee, D.G., Fuller, M.E., Hatzinger, P.B., Condee, C.W., Chu, K.H., 2015. Application of ^{13}C and ^{15}N stable isotope probing to characterize RDX degrading microbial communities under different electron-accepting conditions. J. Hazard. Mater. 297, 42-51.

Colberg, P.J., Young, L.Y., 1985. Anaerobic degradation of soluble fractions of [14C-lignin] lignocellulose. Appl. Environ. Microbiol. 49(2), 345-349.

Crocker, F.H., Indest, K.J., Jung, C.M., Hancock, D.E., Fuller, M.E., Hatzinger, P.B., Vainberg, S., Istok, J.D., Wilson, E., Michalsen, M.M., 2015. Evaluation of microbial transport during aerobic bioaugmentation of an RDX-contaminated aquifer. Biodegradation. 26, 443-451.

Dodard, S.G., Renoux, A.Y., Hawari, J., Ampleman, G., Thiboutot, S., Sunahara, G.I., 1999. Ecotoxicity characterization of dinitrotoluenes and some of their reduced metabolites. Chemosphere, 38(9), 2071-2079.

Farling, S.R., 2013. Generation of biodegradation-sorption barriers for munitions constituents. MS thesis. North Carolina State University, Raleigh, NC.

Felt, D.R., Bednar, A., Arnett, C., Kirgan, R., 2009. Bio-geochemical factors that affect RDX degradation. Proceedings of the Annual International Conference on Soils, Sediments, Water and Energy. 14(17), 207-215.

Fournier, D., Halasz, A., Thiboutot, S., Ampleman, G., Manno, D., Hawari, J., 2004. Biodegradation of octahydro-1,3,5,7-tetranitro-1,3,5,7-tetrazocine (HMX) by Phanerochaete chrysosporium: New insight into the degradation pathway. Environ. Sci. Technol. 38(15), 4130-4133.

Fuller, M.E., Hatzinger, P.B., Condee, C.W., Andaya, C., Vainberg, S., Michalsen, M.M., Crocker, F.H., Indest, K.J., Jung, C.M., Eaton, H., Istok, J.D., 2015. Laboratory evaluation of bioaugmentation for aerobic treatment of RDX in groundwater. Biodegradation, 26(1), 77-89.

Fuller, M.E., Hatzinger, P.B., Rungmakol, D., Schuster, R.L., Steffan, R.J., 2004. Enhancing the attenuation of explosives in surface soils at military facilities: Combined sorption and biodegradation. Environ. Toxicol. Chem. 23(2), 313-324.

Fuller, M.E., Manning, J.F., 1997. Aerobic gram-positive and gram-negative bacteria exhibit differential sensitivity to and transformation of 2,4,6-trinitrotoluene (TNT). Curr. Microbiol. 35, 77-83.

Fuller, M.E., Perreault, N., Hawari, J., 2010a. Microaerophilic degradation of hexahydro-1,3,5-trinitro-1,3,5-triazine (RDX) by three *Rhodococcus* strains. Lett. Appl. Microbiol. 51(3), 313 – 318.

Fuller, M.E., McClay, K., Higham, M., Hatzinger, P.B., Steffan, R.J., 2010b. Hexahydro-1, 3, 5-trinitro-1, 3, 5-triazine (RDX) bioremediation in groundwater: are known RDX-degrading bacteria the dominant players? Bioremediat. J., 14(3), 121-134.

Fuller, M.E., Schaefer, C.E., Steffan, R.J., 2009. Evaluation of a peat moss plus soybean oil (PMSO) technology for reducing explosive residue transport to groundwater at military training ranges under field conditions. Chemosphere. 77(8), 1076-1083.

Galloway, S., 2015. Biodegradation of hexahydro-1, 3, 5-trinitro-1, 3, 5-triazine (RDX) using photosynthetic bacteria. MS thesis. Clemson University, Clemson, SC.

Halasz, A., Manno, D., Perreault, N.N., Sabbadin, F., Bruce, N.C., Hawari, J., 2012. Biodegradation of RDX nitroso products MNX and TNX by cytochrome P450 XplA. Environ. Sci. Technol. 46(13), 7245-7251.

Halasz, A., Manno, D., Strand, S.E., Bruce, N.C., Hawari, J., 2010. Biodegradation of RDX and MNX with *Rhodococcus* sp. strain DN22: new insights into the degradation pathway. Environ. Sci. Technol. 44(24), 9330-9336.

Hatzinger, P.B., Fuller, M.E., Rungmakol, D., Schuster, R.L., Steffan, R.J., 2004. Enhancing the attenuation of explosives in surface soils at military facilities: Sorption-desorption isotherms. Environ. Toxicol. Chem. 23(2), 306-312.

Hawari, J., Beaudet, S., Halasz, A., Thiboutot, S., Ampleman, G., 2000. Microbial degradation of explosives: biotransformation versus mineralization. Appl. Microbiol. Biotechnol. 54(5), 605-618.

Hawari, J., Halasz, A., Beaudet, S., Paquet, L., Ampleman, G., Thiboutot, S., 2001. Biotransformation routes of octahydro-1, 3, 5, 7-tetranitro-1, 3, 5, 7-tetrazocine by municipal anaerobic sludge. Environ. Sci. Technol. 35(1), 70-75.

Karnjanapiboonwong, A., Zhang, B., Freitag, C.M., Dobrovolny, M., Salice, C.J., Smith, P.N., Kendall, R.J., Anderson, T.A., 2009. Reproductive toxicity of nitroaromatics to the cricket, *Acheta domesticus*. Sci. Total Environ. 407(18), 5046-5049.

Kirk, T.K., Higuchi, T., Chang, H., 1980. Lignin biodegradation: microbiology, chemistry, and potential applications. CRC Press, Boca Raton, FL.

Kwon, M.J., Finneran, K.T., 2006. Microbially mediated biodegradation of hexahydro-1,3,5-trinitro-1,3,5-triazine by extracellular electron shuttling compounds. Appl. Environ. Microbiol. 72(9), 5933-5941.

Lachance, B., Renoux, A.Y., Sarrazin, M., Hawari, J., Sunahara, G.I., 2004. Toxicity and bioaccumulation of reduced TNT metabolites in the earthworm *Eisenia andrei* exposed to amended forest soil. Chemosphere, 55(10), 1339-1348.

Li, M.Y., Conlon, P., Fiorenza, S., Vitale, R.J., Alvarez, P.J.J., 2011. Rapid analysis of 1,4-Dioxane in groundwater by frozen micro-extraction with gas chromatography/mass spectrometry. Ground Water Monit. R. 31(4), 70-76.

Lotufo, G.R., Lydy, M.J., 2005. Comparative toxicokinetics of explosive compounds in sheepshead minnows. Arch. Environ. Contam. Toxicol. 49(2), 206-214.

McCormick, N.G., Cornell, J.H., Kaplan, A.M., 1981. Biodegradation of hexahydro-1,3,5-trinitro-1,3,5-triazine. App. Environ. Microbiol. 42, 817–823.

Nelson, J.B., Northey, R.A., 2004. Gaseous emissions from lignosulfonates in dust abatement applications. J. Environ. Manage. 73(4), 333-338.

Ouyang, X., Qiu, X., Chen, P., 2006. Physicochemical characterization of calcium lignosulfonate - A potentially useful water reducer. Colloid Surface A. 282-283(20), 489-497.

Pearl, I.A., 1967. The chemistry of lignin, M. Dekker, New York.

Pennington, J.C., Brannon, J.M., 2002. Environmental fate of explosives. Thermochim. Acta. 384(1), 163-172.

Pennington, J.C., Brannon, J.M., Gunnison, D., Harrelson, D.W., Zakikhani, M., Miyares, P., Jenkins, T.F., Clarke, J., Hayes, C., Ringleberg, D., Perkins, E., Fredrickson, H., 2001. Monitored natural attenuation of explosives. Soil Sediment Contam. 10,45-70.

Pichtel, J., 2012. Distribution and fate of military explosives and propellants in soil: A review. Appl. Environ. Soil Sci. 2012, 1-33.

Price, C.B., Brannon, J.M., Yost, S.L., Hayes, C.A., 2001. Relationship between redox potential and pH on RDX transformation in soil-water slurries. J. Environ. Eng-ASCE. 127(1), 26-31.

Schaefer, C.E., Fuller, M.E., Lowey, J.M., Steffan, R.J., 2005. Use of peat moss amended with soybean oil for mitigation of dissolved explosive compounds leaching into the subsurface: Insight into mass transfer mechanisms. Environ. Eng. Sci. 22(3), 337-349.

Singh, S.N., 2012. Microbial degradation of xenobiotics. Springer, Berlin, Germany.

Uchimiya, M., Gorb, L., Isayev, O., Qasim, M.M., Leszczynski, J., 2010. One-electron standard reduction potentials of nitroaromatic and cyclic nitramine explosives. Environ. Pollut. 158, 3048-3053.

U.S. Agency for Toxic Substances and Disease Registry (ATSDR). 1997. HMX Fact Sheet (on-line), available from URL http://www.atsdr.cdc.gov/toxfaqs/tfacts98.pdf

U.S. Environmental Protection Agency (EPA). 2014. RDX Fact Sheet (on-line), available from URL http://www2.epa.gov/sites/production/files/2014-03/documents/ffrrofactsheet _contaminant _rdx_january2014_final.pdf

U.S. Environmental Protection Agency (EPA). 2014. TNT Fact Sheet (on-line), available from URL http://www2.epa.gov/sites/production/files/2014-03/documents/ffrrofactsheet _contaminant _tnt_january2014_final.pdf

Vorbeck, C., Lenke, H., Fischer, P., Spain, J.C., Knackmuss, H.J., 1998. Initial reductive reactions in aerobic microbial metabolism of 2, 4, 6-trinitrotoluene. Appl. Environ. Microbiol. 64(1), 246-252.

Walsh, M.R., Walsh, M.E., Ampleman, G., Thiboutot, S., Walker, D.D., 2006. Comparison of explosives residues from the blow-in-place detonation of 155-mm high-explosive projectiles. ERDC/CRREL TR-06-13. U.S. Army Engineer Research and Development Center, Hanover, NH.

Wang, D., Lin, Y., Du, W., Liang, J., Ning, Y., 2013. Optimization and characterization of lignosulfonate biodegradation process by a bacterial strain, *Sphingobacterium* sp. HY-H. Int. Biodeter. Biodegr. 85, 365-371.

Yang, D., Qiu, X., Pang, Y., Zhou, M., 2008. Physicochemical properties of calcium lignosulfonate with different molecular weights as dispersant in aqueous suspension. J. Disper. Sci. Technol. 29. 1296-1303.

Zhang, B., Cox, S.B., McMurry, S.T., Jackson, W.A., Cobb, G.P., Anderson, T.A., 2008. Effect of two major N-nitroso hexahydro-1, 3, 5-trinitro-1, 3, 5-triazine (RDX) metabolites on earthworm reproductive success. Environ. Pollut. 153(3), 658-667.

Zhao, J.S., Paquet, L., Halasz, A., Manno, D., Hawari, J., 2004. Metabolism of octahydro-1,3,5,7-tetranitro-1,3,5,7-tetrazocine by *Clostridium bifermentans* strain HAW-1 and several other H_2-producing fermentative anaerobic bacteria. FEMS Microbiol. Lett. 237, 65-72.

CHAPTER 4. BATCH STUDIES OF TNT AND RDX SORPTION IN NATURAL AND LIGNOSULFONATE AMENDED SOILS

4.1 Introduction

2,4,6-trinitrotoluene (TNT) and hexahydro-1,3,5-trinitro-1,3,5-triazine (RDX; royal demolition explosive) are representative explosive compounds typically found on military training ranges. They can be deposited on range soils after low-order (partial) detonations and can slowly leach from unexploded ordinance (UXO) (Brannon and Pennington 2002; Fuller et al. 2004; Walsh et al. 2006). TNT and RDX deposited on the ranges can be transported to groundwater by infiltrating rainfall.

TNT and RDX are moderately soluble in water (130 and 42 mg/L, respectively) and are reported to weakly bind to soil (Brannon and Pennington 2002; Hatzinger et al. 2004; Jaramillo et al. 2011). Brannon and Pennington (2002) reported soil/water partitioning coefficients (K_d) of 0 - 11 L/kg for TNT and 0 - 8.4 L/kg for RDX in surface soil. TNT is biodegradable under aerobic condition, while RDX is resistant to aerobic biodegradation (Lee and Brodman 2004). Biodegradation of both TNT and RDX is enhanced under anoxic conditions (Hawari et al. 2000; Kwon and Finneran 2006).

When biotic and abiotic degradation rates are slow, sorption can enhance removal by providing additional contact time for degradation to occur. TNT and/or RDX sorption can

potentially occur through hydrophobic partitioning, hydrogen bonding, ion exchange, and chemisorption (Pichtel 2012) and can be influenced by the soil and pore water physicochemical properties including clay content, soil organic carbon (SOC), ionic strength, pH, cation exchange capacity (CEC), and pore water composition (Kalderis et al. 2011).

TNT and RDX sorption are reported to be correlated with the soil organic carbon fraction (Yamamoto et al. 2004; Dontsova et al. 2009; Sharma et al. 2013). Dontsova et al. (2009) and Sharma et al. (2013) also suggested that SOC was more important than clay content in sorption of TNT and RDX. However, Haderlein et al. (1996) showed the importance of exchangeable cations on TNT sorption to clays, with increased sorption in the presence of K^+ or NH_4^+ compared to Na^+, Ca^{2+}, Mg^{2+}, and Al^{3+}. Cattaneo et al. (2000) found that TNT sorption was two orders of magnitude greater for montmorillonite than kaolinite, demonstrating the important role of clay mineralogy in HE sorption.

Several different modeling approaches have been employed to describe RDX and TNT sorption. Selim and Iskandar (1994), Myers et al. (1998), and Brannon et al. (2002) reported that a linear model provided a good fit for RDX sorption to soil. However, other investigators reported nonlinear sorption of RDX to clayey soil and activated carbon (Townsend et al. 1996; Morley and Fatemi 2010; Hatzinger et al. 2004). Similarly, Yamamoto et al. (2004) and Chappell et al. (2011) demonstrated linear sorption of TNT to soils, while other studies (Pennington and Patrick 1990; Selim and Iskandar 1994; Hatzinger et al. 2004) have reported nonlinear sorption.

Farling (2013) proposed the use of a mixture of waste glycerin (GL) and lignosulfonate (LS) as an alternative for stimulating bioremediation of explosives in soil. GL

and LS could be spray applied to the contaminated range without exposure of worker to UXO since these materials are highly water soluble. LS is produced through reaction with metal bisulfites and other reagents during wood pulping for paper production and contains high molecular weight polymeric organic carbon, similar to natural soil humics. The GL would be rapidly consumed in soil due to its ready biodegradability. However, the slowly biodegradable LS would be present longer in soil and potentially sorb to soil during transport through the vertical soil profile. The sorbed LS was hypothesized to increase soil organic carbon, enhancing HE sorption. Hence, it is important to understand the impact of LS addition to soil on TNT and RDX sorption and transport of explosives in soils treated with the substrate mixture.

Objectives of this work are to: 1) understand sorption behavior of LS in representative soils; 2) determine the extent of TNT and RDX sorption in soils; and 3) evaluate the impact of LS addition on sorption of TNT and RDX in soils. These results will improve our understanding of explosives transport in range soils and the impact of LS amendments on transport.

4.2 Material and Methods

Two soils collected from near Fort Bragg, NC were used in this work. Grenade range soil (RS) used in the sorption experiments was collected from 0 to 1.0 m below the ground surface (bgs) in Bay C within hand grenade range RG40 at Fort Bragg. Field sand (FS) was obtained from the Four-O-One Sand quarry, located approximately 27 km from the RG40 grenade range at Fort Bragg. Soils were air-dried, passed through a No.4 (4.76 mm) mesh

sieve, and homogenized prior to use. Selected properties were measured on homogenized samples (Table 4.1). Soil organic carbon (OC), cation exchange capacity (CEC), humic matter (HM), and silt-clay fraction were higher in RS than those in FS. Explosive concentrations were 0.012 ± 0.005 mg/kg for RDX and 0.015 ± 0.006 mg/kg for TNT in RS, while all explosives were below the detection limits (< 0.002 mg/kg) in FS.

Table 4.1. Selected properties of soils used in sorption isotherm study.

Properties		**Field Sand (FS)**	**Range Soil (RS)** ‡
Organic Carbon	**(%)**	0.06	0.19
Cation Exchange Capacity	**(meq/100 cm^3)**	0.9	1.6
Base Saturation	**(%)**	48	44
Humic Matter	**(%)**	0.04	0.12
Sand	**(%)**	96.3	85.0
Silt-Clay	**(%)**	3.7	15.0
pH		4.6	4.9

‡ Average values for range soils from 0 to 1 m bgs.

Calcium lignosulfonates (Ultrazine CA and Norlig A) used in this study were from Lignotech USA (Rothschild, WI). TNT and RDX were from AccuStandard, Inc. (New Haven, CT) and prepared by dissolution in deionized water prior to use. Artificial groundwater was used for the sorption isotherm to minimize the effect of carbon present in actual groundwater. The chemical composition of artificial groundwater used in this study is shown in Table 4.2.

Table 4.2. Chemical composition of artificial groundwater.

Chemical	mmol/L
$Ca(NO_3)_2*4H_2O$	0.136
$MgCl_2*6H_2O$	0.080
$Al_2(SO_4)_3*18H_2O$	0.001
$FeSO_4*7H_2O$	0.001
$Mn(NO_3)_2*4H_2O$	0.003
$NaHCO_3$	0.300
$KHCO_3$	0.030
$CaSO_4*2H_2O$	0.076

Sorption isotherm experiments for Ultrazine CA (UCA) were conducted in both field sand (FS) and range soil (RS) to estimate sorption coefficients and evaluate the effect of UCA dose and equilibration period. UCA sorption isotherm bottles were prepared by addition of 100 g of FS or RS, 100 mL of artificial groundwater, and varying amounts of UCA (0.001 to 0.1 g). To examine the effect of biological activity in UCA sorption, a group of bottles was autoclaved prior to UCA addition at 121 ºC and 20 psi for an hour. Bottles were then shaken on a tumbler for 1, 7, 14, or 30 days to examine the effect of equilibration period. Sorption isotherms were measured for RS with 1, 7, and 14-day equilibration periods. The supernatant from each bottle was collected, centrifuged at 2500 rpm for 20 min, and passed through 0.45 μm PTFE syringe filters. The dissolved organic carbon (DOC) content of the filtered supernatants was measured with a Shimadzu TOC-5000A Total Organic Carbon. Bottle controls without sediment were also prepared and operated in parallel, but sorbed amount was negligible. A measurable amount of DOC was released from the soil in sediment controls constructed with sediment and groundwater without LS addition. Sorbed

LS concentration was calculated as (initial DOC - (supernatant DOC - sediment control DOC))/soil mass.

For the Norlig A (NA) sorption experiments, only the effect of NA dose was examined. To improve the convenience and effectiveness of separating supernatant from sediment, 50 mL disposable glass centrifuge tubes were used for NA sorption tests instead of 500 mL amber borosilicate bottles. NA sorption tubes were prepared by addition of 25 g of FS, 40 mL of artificial groundwater, and varying amount of NA (0.001 to 0.1 g). Tubes were mixed on a tumbler for 14 days, based on results from the UCA tests which showed no significant difference between 14-day and 30-day equilibration periods.

Sorption isotherm experiments for TNT and RDX were conducted using both FS and RS, with and without Norlig A (NA) to evaluate the effect of NA on HE sorption. Amended field sand was prepared by addition of 500 g FS and 500 mL of 1,000 mg/L NA solution into a 1 L borosilicate bottle, and mixing on a tumbler for two days. Washed field sand was prepared in parallel by mixing 500 g of FS with 500 mL deionized water for two days. To remove NA that had not sorbed to the soil, the supernatant of both bottles was replaced with fresh 500 mL deionized water and mixing for another two days. This process was repeated three times, then the liquids were drained off and sediments were air-dried. In preliminary work, addition of 1000 mg/L of NA to RS resulted in relatively small increase in soil organic carbon. Consequently, the TNT and RDX sorption measurements were conducted on RS that was treated with a higher concentration of NA (70,000 mg/L DOC), and the bottles were mixed for a week prior to removal of the supernatant. The washing process to remove NA that was not sorbed to the RS was repeated ten times, until DOC concentration in the

supernatant was less than 20 mg/L. In washing process, liquids were gently decanted to minimize loss of clay or silt material. Washed RS was prepared in parallel following an identical washing procedure. After washing, liquids were drained off and sediments were air-dried.

Explosive sorption measurements were conducted in 50 mL disposable glass centrifuge tubes containing 25 g of soil, 40 mL artificial groundwater, and varying amounts of TNT and RDX (10 to 5,000 μg/L). When spiking TNT and RDX, TNT degradation products (2-amino-4,6-dinitrotoluene (2-ADNT), 2,6-dinitrotoluene (2,6-DNT), 2,4-dinitrotoluene (2,4-DNT)) were also added since explosives mixture was used in this sorption test. To inhibit biological activity, all tubes were autoclaved at 121 ºC and 20 psi for an hour prior to spiking TNT and RDX. Triplicate tubes were prepared for each concentration in each soil. Tubes were capped, sealed with parafilm, and shaken on a tumbler for 14 days, then centrifuged at 2500 rpm for 20 min, followed by decantation of aqueous phase. The collected water samples at 0 and 14 day were extracted using toluene by the modified frozen micro extraction (FME) method (Li et al. 2011). The extracts were analyzed by Agilent 7890A gas chromatograph (GC) with an electron capture detector (ECD). The detailed procedures for FME and analytical method by GC-ECD are described in Appendix I. The amount sorbed to soils was determined by mass lost from the aqueous phase. The extracts were stored at - 20 ºC until analyzed by GC-ECD. Tube controls were run in parallel containing 40 mL artificial groundwater and 100 μg/L of explosives, but their sorption was negligible. The amounts of explosives released from sediment itself was also negligible.

Sorbed concentration was calculated as (initial aqueous concentration - final aqueous concentration)/soil mass.

Desorption of TNT and RDX was not evaluated due to loss of clay and silt material while supernatant was removed after centrifugation, and difficulties in resuspending sediment with fresh water. The Linear, Freundlich, and Langmuir isotherm models were fit to experimental results for lignosulfonates (LS) and explosives sorption. The Linear isotherm has the form:

$$S_i = K_d C_i$$

where S_i is the sorbed concentration (μg/g), C_i is the aqueous concentration (μg/mL), and K_d is the linear sorption coefficient (mL/g). The Freundlich isotherm has the form:

$$S_i = K_F C_i^n$$

where S_i is the sorbed concentration (μg/g), C_i is the aqueous concentration (μg/mL), and K_F is the Freundlich sorption coefficient ($mL^n \mu g^{1-n}/g$), and n is a constant. The Langmuir isotherm has the form:

$$S_i = (KC_i)/(1 + nC_i)$$

where S_i is the sorbed concentration (μg/g), C_i is the aqueous concentration (μg/mL), K is the ratio of sorbed and solute concentrations, and n is the equilibrium constant (mL/μg). Coefficients for Linear, Freundlich, and Langmuir isotherms were obtained by fitting the model to the observed sorption results for each soil using the GRG Nonlinear solver in MS Excel to minimize root-mean-square error (RMSE) of log transformed sorbed concentrations. RMSE was defined as $[\Sigma(\text{Log } S_{estimated} - \text{Log } S_{observed})^2/n]^{0.5}$ which gives approximately equal weight to low and high concentration data. Goodness of fit was determined by the Nash-

Sutcliffe model efficiency coefficient (*E*) indicating that the highest *E* is considered as the best model (Nash and Sutcliffe 1970; Bolster and Hornberger 2007). 95 % confidence interval (CI) and t-test with 95 % confidence level were applied to determine the statistical significance. 95 % CI was defined as [$S_{estimated}$ ± critical t x residual standard error (SE) of $S_{observed}$]. SE was computed by dividing the sum of squares of the residuals by the degrees of freedom, and critical t-value was calculated by Excel built-in function (TINV) to minimize underestimation of the true uncertainty in nonlinear estimation (Hossain et al. 2013).

4.3 Experimental Results

4.3.1 *Sorption of Lignosulfonates in Soils*

Sorption isotherm experiments for two lignosulfonates (LS), Ultrazine CA (UCA) and Norlig A (NA), were conducted using field sand (FS) and range soil (RS) obtained from the sand quarry and Fort Bragg, NC respectively, to determine the extent of LS sorption and identify the effect of LS dose and equilibration period.

Figure 4.1 shows sorbed concentrations as function of equilibration time for varying initial UCA concentrations in field sand (FS). At initial concentrations less than 100 mg/L, sorption equilibrium for UCA was reached within 1 day. However, a 14-day equilibration period was required at initial concentrations above 500 mg/L. Autoclaving did not influence UCA sorption to FS at concentrations over 500 mg/L, with overlapping 95 % confidence intervals (CI) for UCA sorbed to autoclaved and untreated FS (Figure S-8). However, at low initial concentrations < 500 mg/L, UCA more weakly sorbed to autoclaved FS. This result is consistent with prior studies which found decreased sorption capacity in autoclaved soils for

chemical compounds and bacteria (Won et al. 2007; Serrasolses et al. 2008). Based on these results, all further sorption isotherms were developed with a 14-day equilibration period using autoclaved soil.

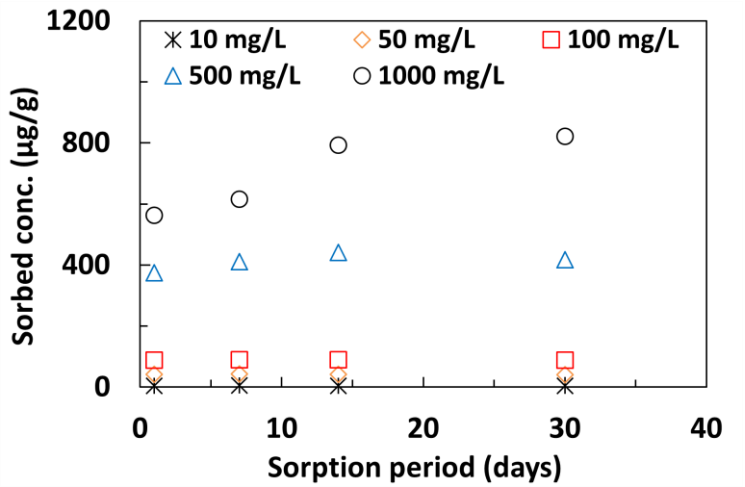

Figure 4.1. Concentrations of Ultrazine CA (UCA) sorbed to field sand (FS) for varying equilibration times and initial concentrations.

The sorption data for UCA and NA in soils were used to estimate parameters for Linear, Freundlich, and Langmuir sorption isotherm models (Table 4.3 and Figure 4.2). The isotherm model that provided the best fit was identified using the model efficiency (E) as described by Bolster and Hornberger (2007). Sorption of UCA and NA in FS was better fit with the Freundlich model resulting in higher E values than Linear and Langmuir models indicating that the Freundlich is the superior model (Table 4.3). Isotherm models for UCA sorption to RS could not be compared due to small number of valid measurements. $E < 0$, i.e., negative values, for the Linear UCA and NA sorption isotherms in FS indicates that an average of the measurements could provide a better prediction compared to model (Bolster

and Hornberger 2007). Previous investigators (Grigg and Bai 2004; Bai et al. 2009) also found that the Freundlich isotherm provided a better fit for adsorption of calcium LS on Berea sandstone and dolomite. However, Qui et al. (2009) reported that a Langmuir isotherm provided a better fit for adsorption of LS on TiO_2 particles. The values of Freundlich constant (n) in both UCA (n = 0.43 ± 0.07) and NA (n = 0.56 ± 0.04) were significantly different from 1 (*p-value* < 0.05) indicating concentration dependent sorption.

Table 4.3. Regression parameters for Ultrazine CA and Norlig A sorption to field sand (FS) and/or range soil (RS) with 14-day equilibration period (± 95 % confidence limit). Bold values are parameters for the model with the best fit.

Model		**Linear**		**Freundlich**			**Langmuir**			
LS[†]	**Soils**[‡]	**K_d**	***E***[§]	**K_F**	**n**	***E***	**K**	**N**	**S_{max}**	***E***
UCA	**FS**	18.9 ± 8.1	-21	**76.2 ± 22.3**	**0.43 ± 0.07**	**0.98**	120 ± 181	0.23 ± 0.38	525	0.73
UCA	**RS**	53.0 ± 10.3	1	47.5 ± N/A	1.04 ± N/A	1	51 ± N/A	-0.003 ± N/A	15,397	1
NA	**FS**	2.7 ± 0.9	-4	**22.7 ± 12.3**	**0.56 ± 0.04**	**0.98**	10 ± 16	0.012 ± 0.02	849	0.65

[†] LS = lignosulfonate, UCA = Ultrazine CA, NA = Norlig A.
[‡] FS = field sand, RS = range soil.
[§] *E* = model efficiency; 1 = perfect fit to the measurements, *E* < 0 = average of the measurements better than model prediction.
[¶] Unit; K_d = L/kg, K_F = $mL^n\mu g^{1-n}/g$, K = L/kg, Langmuir n = mL/μg, S_{max} = μg/g.
[#] CIs for Freundlich and Langmuir isotherms in UCA sorption to RS were not applicable due to lack of sample population.

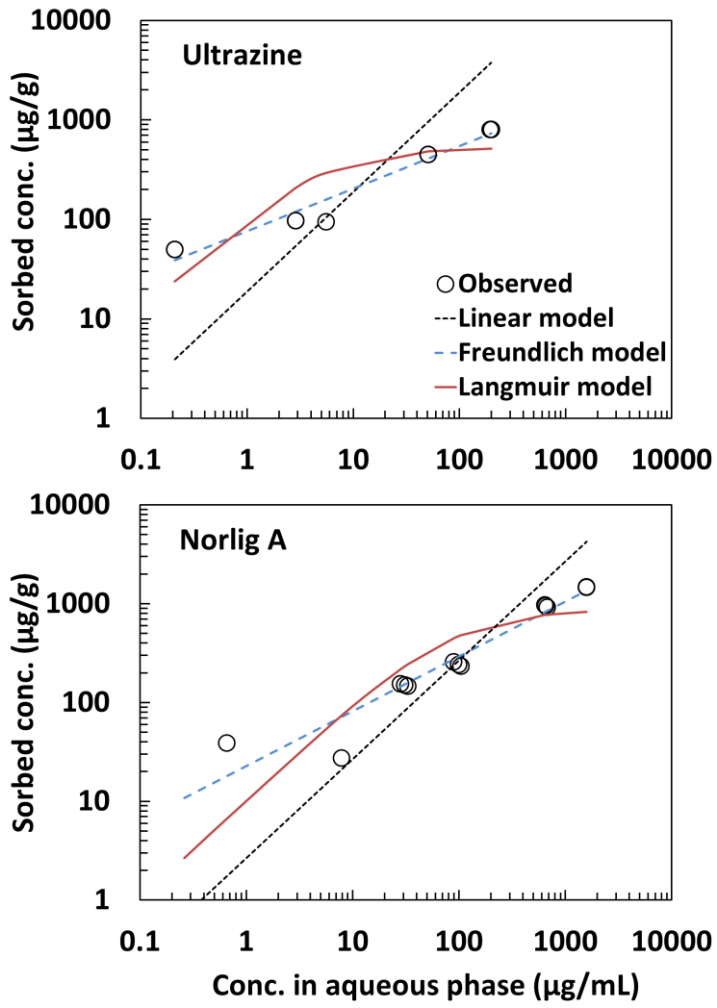

Figure 4.2. Freundlich and Langmuir sorption isotherms for Ultrazine CA (UCA) and Norlig A (NA) on field sand (FS).

UCA appears to sorb more strongly to RS than FS (Figure 4.3), probably due to higher OC, CEC, and/or clay content in RS (Table 4.1). At initial concentrations over 500 mg/L, linear partition coefficients (K_d) for UCA were six- to ten-fold higher in RS (52.2 - 53.8 L/kg) than that in FS (4.0 - 8.8 L/kg) (data not shown). Freundlich model parameters could not be reliably estimated for sorption to RS due to small number of valid measurements. *E* values for UCA sorption to RS was 1 in all isotherm models, indicating a

perfect fit to the measurements, because only two data points were available for parameter estimation after data correction for controls.

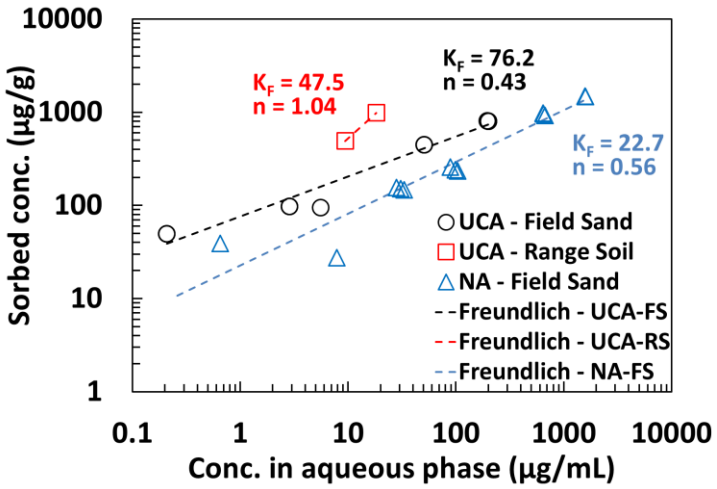

Figure 4.3. Freundlich isotherms for Ultrazine CA (UCA) and Norlig A (NA) on field sand (FS) and range soil (RS).

Freundlich K_F values for UCA sorption to FS were significantly greater than NA sorption (Table 4.3, *p-value* < 0.05), indicating stronger sorption of UCA, especially at lower concentrations (Figure 4.3). However, at concentrations > 1,000 mg/L, the sorption isotherms converge and no significant difference is expected between NA and UCA, as indicated by the overlap in the 95 % CIs (Figure S-9).

The differences in UCA and NA sorption to FS may be due to differences in the chemical properties of these lignosulfonates. NA is a full sugar, hardwood lignosulfonate that contains a mixture of low and medium molecular weight materials. UCA is a spruce wood lignosulfonate that has been fermented to remove sugars and other more readily biodegradable low molecular weight materials. The higher UCA sorption was likely due to

the higher concentration of high molecular weight materials. Farling (2013) showed relatively higher molar UV absorptivity at 280 nm (ε_{280}) of UCA (269 L/cm/mol) than that of NA (148 L/cm/mol), which is positively correlated with the degree of aromaticity (Chin et al. 1994). Increasing aromaticity and decreasing polarity is reported to result in increased sorption of aromatic compound in soil (Liu et al. 2002).

Zeta potential measurements were conducted on FS, UCA and NA for pH values from 2 to 12 (Figure S-6). The zeta potential of both UCA and NA was negative throughout the measured pH range, consistent with prior research (Wang et al. 2013). The zeta potential of FS varied from +10 mV at low pH to -40 mV at high pH, with a point of zero charge (PZC) of 4.0 to 4.5 consistent with isoelectric values for gibbsite and hematite (Park 1965). The ambient pH of FS is 4.6 so UCA addition (pH = 5.8) should result in a pH greater than or equal to the PZC, and the FS would have a net negative charge. Under these conditions, anion exchange of the negatively charged UCA would be limited.

4.3.2 *TNT and RDX Sorption to FS and RS*

Sorption of TNT and RDX to field sand (FS) and range soil (RS) with and without NA amendment was examined to determine sorption extent and identify the impact of NA addition on HE sorption. Sorbed concentrations and modeling results for TNT and RDX in FS and RS are shown in Figure 4.4 and 4.5 respectively. The best fit sorption isotherms for both TNT and RDX are strongly non-linear (Table 4.4) consistent with prior research (Ainsworth et al. 1993; Selim and Iskandar 1994; Sharma et al. 2013). Based on the *E* values, the Freundlich model provided the best fit for both TNT and RDX sorption to RS, while the

Langmuir model provided the best fit for TNT and RDX sorption to FS. However, the 95% confidence intervals overlap for most of the measured concentration range (Figure S-10 and S-11), indicating one model is not significantly better than the other.

Table 4.4. Regression parameters for TNT and RDX sorption to field sand (FS) and range soil (RS) with 14-day equilibration period (± 95 % confidence limit). Bold values are parameters for the model with the best fit.

HE	Soil†	Linear		Freundlich			Langmuir			
		K_d	E‡	K_F	n	E	K	n	S_{max}	E
TNT	**FS**	1.17 ± 0.52	-6	0.84 ± 0.54	0.80 ± 0.16	0.33	**2.15 ± 1.07**	**0.94 ± 0.62**	**2.28**	**0.96**
	RS	10.98 ± 5.07	-110	**2.16 ± 6.09**	**0.56 ± 0.29**	**0.92**	22.83 ± 19.76	6.65 ± 6.63	3.43	0.85
RDX	**FS**	1.16 ± 0.54	-9	0.73 ± 0.39	0.73 ± 0.14	0.49	**2.60 ± 1.28**	**1.83 ± 1.13**	**1.42**	**0.97**
	RS	9.37 ± 3.84	-21	**3.06 ± 2.75**	**0.67 ± 0.15**	**0.96**	18.25 ± 25.38	4.67 ± 7.77	3.91	0.75

† FS = field sand, RS = range soil.

‡ E = model efficiency; 1 = perfect fit to the measurements, $E < 0$ = average of the measurements better than model prediction.

§ Unit; K_d = mL/g, K_F = $mL^n\mu g^{1-n}/g$, K = mL/g, Langmuir n = mL/μg, S_{max} = μg/g.

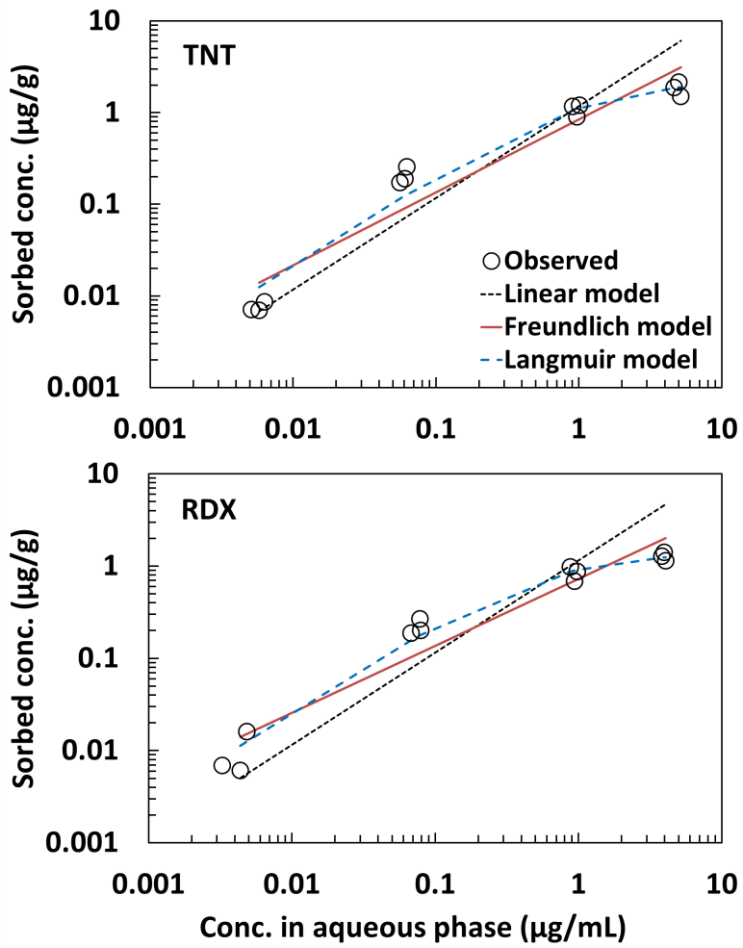

Figure 4.4. Linear, Freundlich, and Langmuir sorption isotherms for TNT and RDX on field sand (FS).

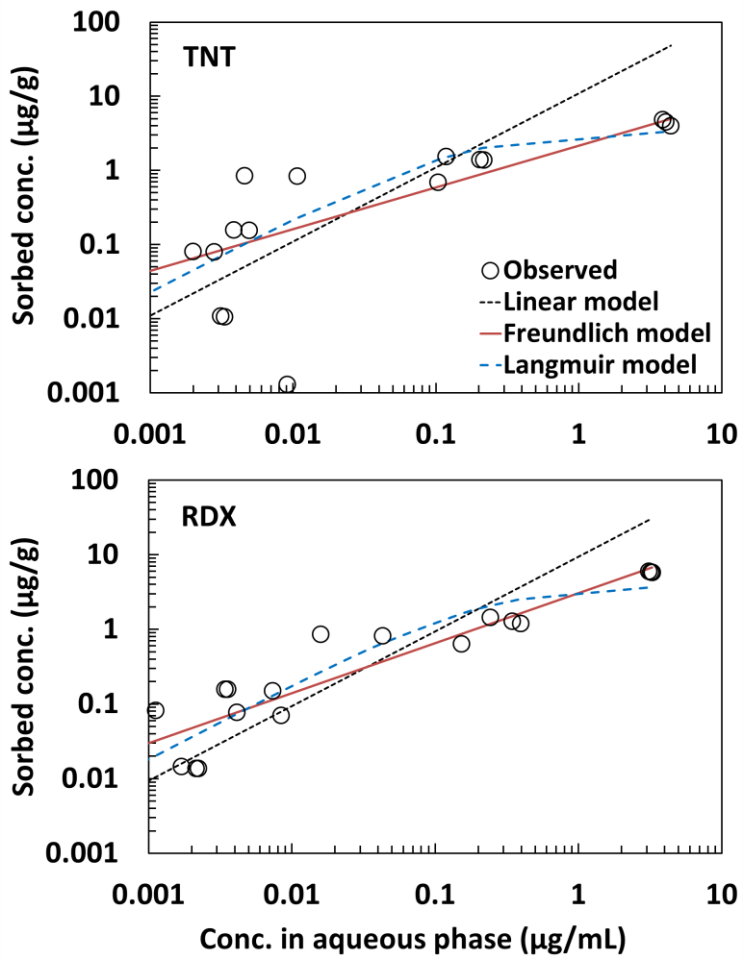

Figure 4.5. Linear, Freundlich, and Langmuir sorption isotherms for TNT and RDX on intact range soil (RS).

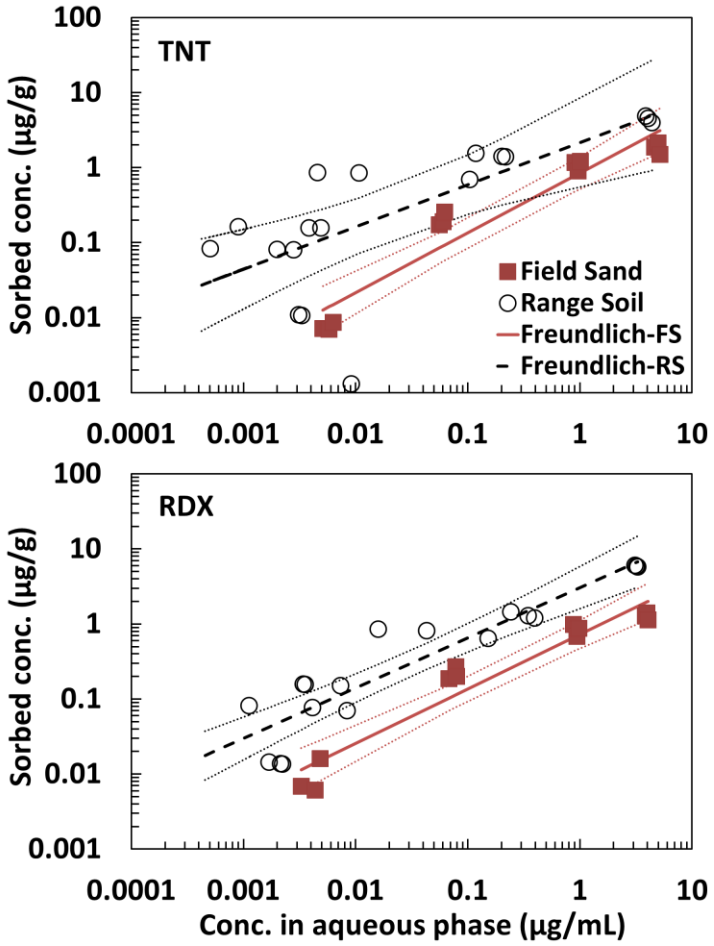

Figure 4.6. Freundlich sorption isotherms for TNT and RDX on field sand (FS) and range soil (RS). Dotted lines are upper and lower 95 % confidence intervals for each estimated Freundlich isotherm model.

Figure 4.6 shows the Freundlich isotherms and 95% confidence intervals (CI) for TNT and RDX sorption to FS and RS. TNT appears to sorb more strongly to RS at initial concentrations < 0.1 µg/mL without overlap in 95 % CIs. However, at higher concentrations, the sorption isotherms converge and there was no significant difference in TNT sorption between FS and RS with overlapping 95 % CIs. RDX also sorbed more strongly to RS compared to FS for most of the observed concentration range. K_F values for both TNT and

RDX were approximately three-fold higher in RS than in FS. K_F values were 2.16 ± 6.09 $mL^{0.56}\mu g^{0.44}/g$ for TNT and 3.06 ± 2.75 $mL^{0.67}\mu g^{0.33}/g$ for RDX in RS, but 0.84 ± 0.54 $mL^{0.8}\mu g^{0.2}/g$ for TNT and 0.73 ± 0.39 $mL^{0.73}\mu g^{0.27}/g$ for RDX in FS (Table 4.4). The greater scatter in the data at low concentrations in RS resulted in higher 95 % CIs for estimated parameters (Table 4.4) and wider 95 % CIs for sorbed concentrations (Figure 4.6). The stronger sorption of TNT and RDX to RS could be associated with higher OC, CEC, and/or clay content in RS compared to FS (Table 4.1).

TNT and RDX sorption were not significantly different from each other for the measured concentration range for each soil. Figure 4.7 shows observed TNT and RDX sorption in both FS and RS and model simulation results with 95 % CI. The best fit model based on *E* was plotted. The 95 % CIs for partition coefficients (K_F and K) and sorbed concentrations overlapped (Table 4.4 and Figure 4.7), indicating no significant difference between TNT and RDX sorption in both soils. In RS, K_F of TNT and RDX were 2.16 ± 6.09 $mL^{0.56}\mu g^{0.44}/g$ and 3.06 ± 2.75 $mL^{0.67}\mu g^{0.33}/g$ respectively. Similarly, K of TNT and RDX were 2.15 ± 1.07 and 2.60 ± 1.28 mL/g respectively in FS. The t-test analysis for the measurements also showed no significant difference in concentrations sorbed to RS between TNT and RDX at initial concentrations less than 1 μg/mL (*p-values* > 0.05), but significantly higher RDX sorbed concentrations than TNT at initial concentrations over 5 μg/mL (*p-values* < 0.05). However, the inverse trend was observed in FS presenting higher TNT sorbed concentrations at high initial concentrations.

There was more scatter in the data at low concentrations in RS than in FS (Figure 4.7) indicating more variability in RS. This is not clearly explainable, but may be associated with

higher soil heterogeneity of RS compared to FS (Sana and Jalila 2016), or due to lower relative precision of the GC-ECD measurements near the detection limit (1 µg/L). The greater spread in the data was probably not the result of desorption of HEs from the RS since preliminary dissolution tests using the same soil for 7 days showed no detectable HEs.

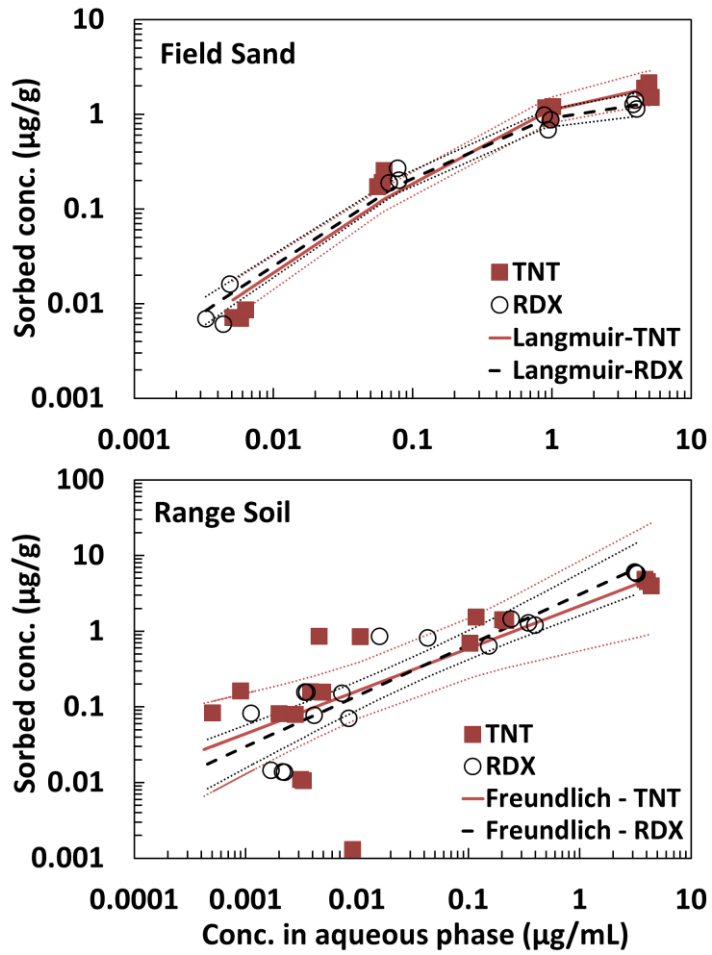

Figure 4.7. Sorption isotherms for TNT and RDX on field sand (FS) and range soil (RS). Dotted lines are upper and lower 95 % confidence intervals for each estimated Freundlich isotherm model.

In this work, sorption of RDX was found to be similar to TNT in both FS and RS. This differs from prior research which reported greater TNT sorption than RDX (Brannon and Pennington 2002; Hatzinger et al. 2004; Yamamoto et al. 2004; Jaramillo et al. 2011; Ariyarathna et al. 2016). Sheremata et al. (1999) proposed that decreased TNT sorption might be associated with competitive sorption of TNT in the presence of its degradation products. They demonstrated that sorption capacity increased with the increase of the number of amino groups (NH_2). Sorption capacity was 2,4-diamino-6-nitrotoluene (2,4-DANT) > 4-amino-2,6-dinitrotoluene (4-ADNT) > TNT (Sheremata et al. 1999). In this study, no substantial difference was observed in between TNT and its degradation products sorbed to RS (Figure S-12 and Table S-4). However, TNT sorption could have been reduced by competition for available sorption sites on the soil surface, since TNT degradation products were present in the mixture.

4.3.3 *TNT and RDX Sorption to Lignosulfonate Treated Soil*

Lignosulfonate (LS) addition to soil was hypothesized to increase sorption of TNT and RDX by increasing soil organic carbon (SOC). To examine the impact of LS addition, TNT and RDX sorption isotherm experiments were conducted in FS and RS amended with NA. Washed FS and RS were also examined to control for the loss of fines when the sediment was washed to remove aqueous NA.

Measured concentrations and Freundlich modeling results with 95 % CIs for TNT and RDX sorption in intact (IRS) and amended range soils (ARS) are presented in Figure 4.8. NA addition did not have a substantial impact on TNT and RDX sorption at most

concentrations, with the overlapping 95 % CIs (Figure 4.8) and no significant difference in Freundlich partition coefficients (K_F in Table 4.5). No significant difference was also observed in the estimated sorbed concentrations of both TNT and RDX in between ARS and WRS over all concentration range (Figure S-13). In addition, washing treatment did not impact TNT and RDX sorption in RS (Figure S-13 and S-14). It appears that NA amendment could not increase OC sufficiently to enhance sorption capacity for TNT and RDX since most OC initially sorbed to RS was desorbed during repeated washing, resulting in no significant OC mass loss in aqueous phase after washing (Figure S-15).

In FS, no significant impact of NA amendment was also observed in TNT and RDX sorption over all measured concentrations (Table 4.5 and Figure 4.9). The lack of measurable impact on TNT and RDX sorption in FS is probably due to the negligible increase in the OC to FS after washing (data not shown).

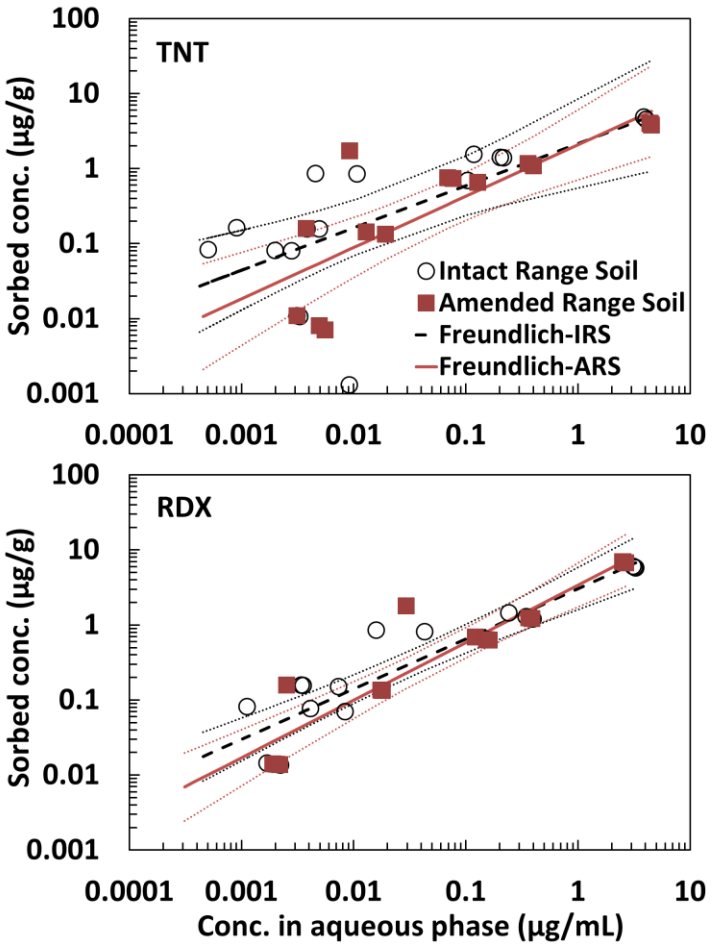

Figure 4.8. Freundlich sorption isotherms for TNT and RDX on intact (IRS) and amended range soil (ARS). Dotted lines are upper and lower 95 % confidence intervals for each estimated Freundlich isotherm model.

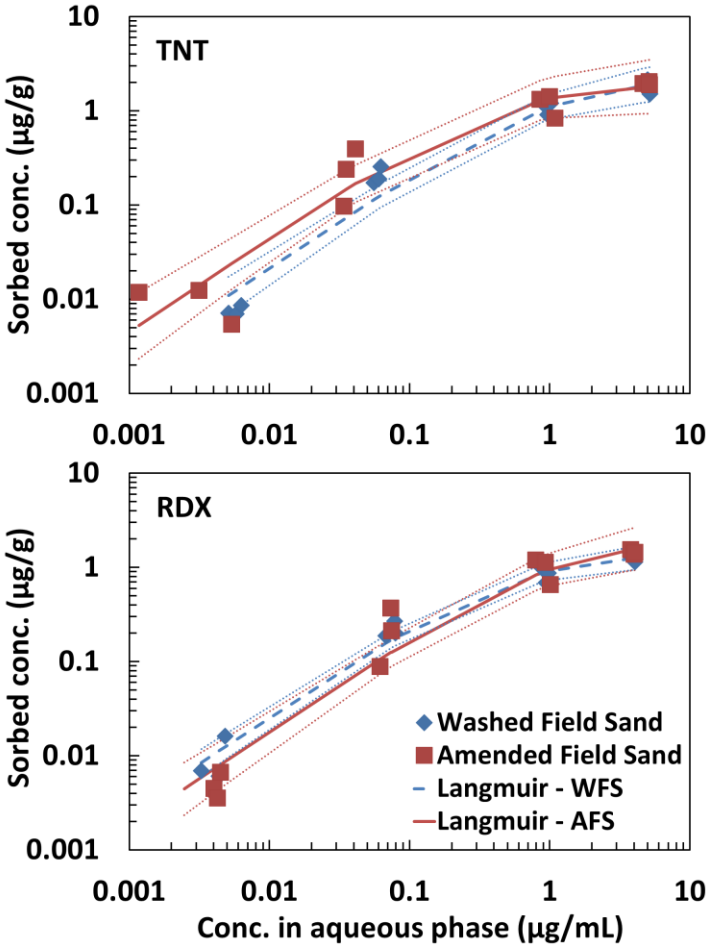

Figure 4.9. Langmuir sorption isotherms for TNT and RDX on washed (WFS), and amended field sand (AFS). Dotted lines are upper and lower 95 % confidence intervals for each estimated Langmuir isotherm model.

Table 4.5. Regression parameters of TNT and RDX sorption to washed (WFS) and amended field sand (AFS), intact (IRS), washed (WRS), and amended range soils (ARS) (± 95 % confidence limit). Bold values are parameters for the model with the best fit.

	Soil†	Treatment	Freundlich			Langmuir			
			K_F	n	*E*	K	n	S_{max}	*E*
TNT	FS	**Washed**	0.84 ± 0.54	0.80 ± 0.16	0.33	**2.15 ± 1.07**	**0.94 ± 0.62**	**2.28**	**0.96**
		Amended	0.95 ± 0.50	0.68 ± 0.12	0.63	**4.50 ± 3.91**	**2.32 ± 2.38**	**1.94**	**0.94**
	RS	**Intact**	**2.16 ± 6.09**	**0.56 ± 0.29**	**0.92**	22.83 ± 19.76	6.65 ± 6.63	3.43	0.85
		Washed	**2.53 ± 4.70**	**0.53 ± 0.23**	**0.68**	40.35 ± 76.89	15.08 ± 32.67	2.68	0.64
		Amended	2.07 ± 3.86	0.68 ± 0.29	0.60	**8.85 ± 7.45**	**2.35 ± 2.34**	**3.76**	**0.86**
RDX	FS	**Washed**	0.73 ± 0.39	0.73 ± 0.14	0.49	**2.60 ± 1.28**	**1.83 ± 1.13**	**1.42**	**0.97**
		Amended	0.79 ± 0.60	0.84 ± 0.18	0.12	**1.81 ± 1.22**	**0.91 ± 0.86**	**1.99**	**0.92**
	RS	**Intact**	**3.06 ± 2.75**	**0.67 ± 0.15**	**0.96**	18.25 ± 25.38	4.67 ± 7.77	3.91	0.75
		Washed	**2.98 ± 3.80**	**0.72 ± 0.22**	**0.86**	11.84 ± 15.38	2.62 ± 4.15	4.51	0.78
		Amended	**3.41 ± 3.20**	**0.77 ± 0.18**	**0.97**	9.94 ± 9.97	1.56 ± 2.11	6.36	0.85

† FS = field sand, RS = range soil.

‡ *E* = model efficiency; 1 = perfect fit to the measurements, *E* < 0 = average of the measurements better than model prediction.

§ Unit; K_d = mL/g, K_F = $mL^n\mu g^{1-n}/g$, K = mL/g, Langmuir n = mL/μg, S_{max} = μg/g.

4.4 Discussion

Batch sorption measurements showed nonlinear sorption of lignosulfonate (LS) indicating LS sorption in soils with higher partition coefficients at lower concentrations. LS sorption required 14 days to reach equilibrium and a longer equilibration period (30 day) did not result in a measurable increase in sorbed LS concentrations. Grigg and Bai (2004) and Bai et al. (2009) also reported nonlinear sorption of calcium LS (CLS) on different sediments. UCA and NA sorption to FS and RS (K_F = 23 - 76 mL/g or 0.06 - 0.20 L/cm^3, n = 0.43 - 1.05) was similar to CLS sorption to Berea sand stone (K_F = 0.031 L/cm^3 rock, n = 0.49,

Grigg and Bai 2004), but much stronger than CLS sorption to dolomite (K_F = m1 L/g, n = 0.67, Bai et al. 2009). Bai et al. (2009) also reported considerable desorption of CLS from dolomite. In this study, desorption of LS was not examined due to significant loss of clay and silt material when supernatant was removed, and difficulties in re-suspending sediment with fresh water after centrifugation.

Linear distribution coefficients for TNT and RDX sorption to FS and RS (Table 4.4) were in the range of values previously reported (K_d = 0.1 - 16.6 L/kg for TNT, K_d = 0.12 - 8.4 L/kg for RDX, Brannon et al. 1992; Ainsworth et al. 1993; Townsend and Myers 1996; Pennington et al. 1999; Yamamoto et al. 2004). However, the measured K_d values for TNT were generally on the low side of the reported range and RDX K_d values were on the high side.

The non-linear Freundlich and Langmuir models provided a significantly better fit (*p-value* < 0.05) than the linear model for both TNT and RDX sorption to FS and RS. The observed concentration dependent sorption behavior will result in increased retention at the low concentrations in typical training ranges. Equilibrium retardation factor R for non-linear sorption with the Freundlich isotherm can be calculated as (Zheng and Bennett, 1995)

$$R = 1 + \rho_b n K_F C^{n-1}/\theta$$

where K_F is the Freundlich distribution coefficient, n is a constant, and C is the aqueous concentration, ρ_b is the soil bulk density, and θ is the water filled porosity.

Figure 4.10 shows computed Retardation factors (R) for varying concentrations of TNT and RDX in range soil (RS) with ρ_b = 1.90 and θ = 0.27 (Chapter 5). At aqueous concentrations near solubility, R values approach 1 and sorption has minimal impact in

slowing TNT and RDX transport. However at the concentrations observed in the field at Fort Bragg (0.001 to 0.06 μg/mL for TNT, 0.001 to 0.45 μg/mL for RDX), retardation factors are much higher and may significantly reduce leaching.

Selim and Iskandar (1994) showed impact of linear and nonlinear TNT sorption in its leaching behavior presenting deviation from the breakthrough curve resulted from their column study. Spurlock et al. (1995) demonstrated that assuming linear sorption may generate considerable errors in predictions of solute transport in soil.

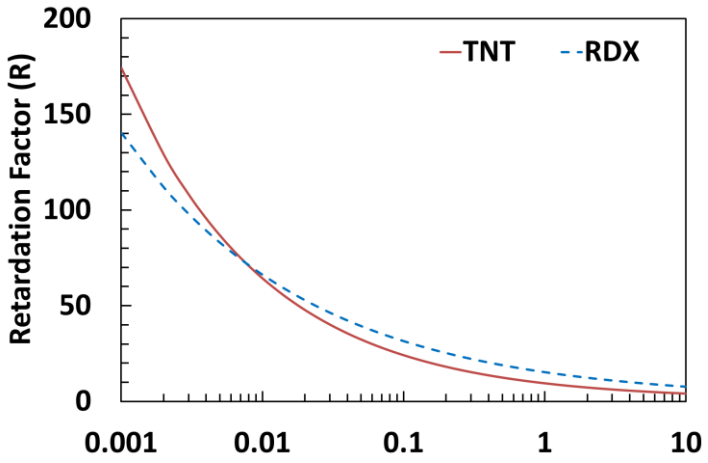

Figure 4.10. Retardation factors for varying concentrations of TNT and RDX in range soil (RS) which were computed with regression parameters determined by Freundlich sorption isotherm model.

Prior sorption studies reported that TNT sorbed more strongly to soils than RDX (Brannon and Pennington 2002; Hatzinger et al. 2004; Yamamoto et al. 2004; Jaramillo et al. 2011; Ariyarathna et al. 2016). However, in RS, RDX sorption was similar to TNT sorption. This might be associated with relatively higher affinity of RDX sorption to clay minerals compared to TNT. Sunahara et al. (2009) suggested that interactions with minerals in clay

might govern RDX and HMX sorption rather than association with OC in soil. Monteil-Rivera el al. (2003) also showed positive correlation between HMX sorption and clay content. Cattaneo et al. (2000) reported that the clay mineralogy could influence on RDX sorption. Additional research is needed to identify the cause of higher RDX sorption in RS.

4.5 Conclusions

Batch sorption experiment and isotherm model simulation clearly showed that both lignosulfonate (LS) and explosives examined in this study followed nonlinear sorption in field sand (FS) and range soil (RS). Sorption coefficients for UCA were six- to ten-fold greater in RS than in FS, and UCA sorbed more strongly to FS than NA.

RDX sorption was stronger in RS than in FS at most concentrations, presumably due to the higher OC, CEC, and clay content in RS. RDX sorption was similar to TNT in both FS and RS, inconsistent with prior research results. NA amendment did not significantly increase TNT and RDX sorption to either FS or RS.

Nonlinear sorption should be considered when predicting transport of LS or explosives in soil. Nonlinear sorption is concentration dependent, substantially influencing distribution coefficients and retardation factors of solutes.

4.6 References

Ainsworth, C.C., Harvey, S.D., Szecsody, J.E., Simmons, M.A., Cullinan, V., 1993. Relationship between the leachability characteristics of unique energetic compounds and soil properties. Battelle Memorial Inst., Pacific Northwest Labs.

Ariyarathna, T., Vlahos, P., Tobias, C., Smith, R., 2016. Sorption kinetics of TNT and RDX in anaerobic freshwater and marine sediments: Batch studies. Environ. Toxicol. Chem., 35(1), 47-55.

Bai, B., Wu, Y., Grigg, R.B., 2009. Adsorption and desorption kinetics and equilibrium of calcium lignosulfonate on dolomite porous media. J. Phys. Chem. C. 113(31), 13772-13779.

Brannon, J.E., Adrian, D.D., Pennington, J.C., Myers, T.E., 1992. Slow release of PCB, TNT, and RDX from soils and sediments. WES/TR/EL-92-38. Army Engineer Waterways Experiment Station. Vicksburg, MS.

Brannon, J.M., Pennington, J.C., 2002. Environmental fate and transport process descriptors for explosives. Final report for Strategic Environmental Research and Development Program. ERDC/EL TR-02-10. U.S. Army Engineer Research and Development Center, Vicksburg, MS.

Brannon, J.M., Price, C.B., Hayes, C., Yost, S.L., 2002. Aquifer soil cation substitution and adsorption of TNT, RDX, and HMX. Soil Sediment Contam. 11(3), 327-338.

Cattaneo, M.V., Pennington, J.C., Brannon, J.M., Gunnison, D., Harrelson, D.W., Zakikhani, M., 2000. Natural attenuation of explosives in remediation of hazardous waste contaminated soils. Marcel Dekker, New York, NY.

Chappell, M.A., Price, C.L., Miller, L.F., 2011. Solid-phase considerations for the environmental fate of nitrobenzene and triazine munition constituents in soil. Appl. Geochem. 26, S330-S333.

Dontsova, K.M., Hayes, C., Pennington, J.C., Porter, B., 2009. Sorption of high explosives to water-dispersible clay: Influence of organic carbon, aluminosilicate clay, and extractable iron. J. Environ. Qual. 38(4), 1458-1465.

Farling, S.R., 2013. Generation of biodegradation-sorption barriers for munitions constituents. MS thesis. North Carolina State University, Raleigh, NC.

Fuller, M.E., Hatzinger, P.B., Rungmakol, D., Schuster, R.L., Steffan, R.J., 2004. Enhancing the attenuation of explosives in surface soils at military facilities: Combined sorption and biodegradation. Environ. Toxicol. Chem. 23(2), 313-324.

Grigg, R.B., Bai, B., 2004. Calcium lignosulfonate adsorption and desorption on Berea sandstone. J. Colloid Interf. Sci. 279(1), 36-45.

Haderlein, S.B., Weissmahr, K.W., Schwarzenbach, R.P., 1996. Specific adsorption of nitroaromatic explosives and pesticides to clay minerals. Environ. Sci. Tech. 30(2), 612-622.

Hatzinger, P.B., Fuller, M.E., Rungmakol, D., Schuster, R.L., Steffan, R.J., 2004. Enhancing the attenuation of explosives in surface soils at military facilities: Sorption-desorption isotherms. Environ. Toxicol. Chem. 23(2), 306-312.

Hawari, J., Beaudet, S., Halasz, A., Thiboutot, S., Ampleman, G., 2000. Microbial degradation of explosives: biotransformation versus mineralization. Appl. Microbiol. Biotechnol. 54(5), 605-618.

Hossain, M. A., Ngo, H. H., Guo, W., 2013. Introductory of Microsoft Excel SOLVER function-spreadsheet method for isotherm and kinetics modelling of metals biosorption in water and wastewater. J. Water Sustain. 3(4), 223-37.

Jaramillo, A.M., Douglas, T.A., Walsh, M.E., Trainor, T.P., 2011. Dissolution and sorption of hexahydro-1, 3, 5-trinitro-1, 3, 5-triazine (RDX) and 2, 4, 6-trinitrotoluene (TNT) residues from detonated mineral surfaces. Chemosphere, 84(8), 1058-1065.

Kalderis, D., Juhasz, A.L., Boopathy, R., Comfort, S., 2011. Soils contaminated with explosives: Environmental fate and evaluation of state-of-the-art remediation processes. Pure Appl. Chem. 83(7), 1407-1484.

Kwon, M.J., Finneran, K.T., 2006. Microbially mediated biodegradation of hexahydro-1,3,5-trinitro-1,3,5-triazine by extracellular electron shuttling compounds. Appl. Environ. Microbiol. 72(9), 5933-5941.

Lee, S.Y., Brodman, B.W., 2004. Biodegradation of 1,3,5-Trinitro-1,3,5-triazine (RDX). J. Environ. Sci. Health A Tox. Hazard. Subst. Environ. Eng. 39(1), 61-75.

Li, M.Y., Conlon, P., Fiorenza, S., Vitale, R.J., Alvarez, P.J.J., 2011. Rapid analysis of 1,4-Dioxane in groundwater by frozen micro-extraction with gas chromatography/mass spectrometry. Ground Water Monit. R. 31(4), 70-76.

Liu, X., Song, C., Xing, B., 2002. Characteristics of the natural organic matter sorption affects of organic contaminants. J. Environ. Sci. 14(3). 351-356.

Monteil-Rivera, F., Groom, C., Hawari, J., 2003. Sorption and degradation of oxtahydro-1,3,5,7-tetranitro-1,3,5,7-tetrazocine in soil. Environ Sci Technol. 37(17): 3878-3884.

Morley, M. C., Fatemi, M., 2010. Adsorption of RDX and its nitroso metabolites onto activated carbon. Practice Periodical of Hazardous, Toxic, and Radioactive Waste Management, 14(2), 90-97.

Myers, T.E., Brannon, J.M., Pennington, J.C., Davis, W.M., Myers, K.F., Townsend, D.M., Ochman, M.K., Hayes, C.A., 1998. Laboratory studies of soil sorption/transformation of TNT, RDX, and HMX. Tech. Rep. IRRP-98-8. US Army Engineer Waterways Experiment Station. Vicksburg, MS.

Nash, J.E., Sutcliffe, J.V., 1970. River flow forecasting through conceptual models part I - A discussion of principles, J. Hydrol. 10 (3), 282–290.

Parks, G.A., 1965. The isoelectric points of solid oxides, solid hydroxides, and aqueous hydroxo complex systems. Chemical Reviews, 65(2), 177-198.

Pennington, J.C., Gunnison, D., Harrelson, D.W., Brannon, J.N., Zakikhani, M., 1999. Natural attenuation of explosives in soil and water systems at Department of Defense sites. WES/TR/EL-99-8. Army Engineer Waterways Experiment Station. Vicksburg, MS.

Pennington, J.C., Patrick, W.H., 1990. Adsorption and desorption of 2, 4, 6-trinitrotoluene by soils. J. Environ. Qual. 19(3), 559-567.

Pichtel, J., 2012. Distribution and fate of military explosives and propellants in soil: A review. Appl. Environ. Soil Sci. 2012, 1-33.

Qiu, X., Yan, M., Yang, D., Pang, Y., Deng, Y., 2009. Effect of straight-chain alcohols on the physicochemical properties of calcium lignosulfonate. J. Colloid Interf. Sci. 338(1), 151-155.

Sana, D., Jalila, S., 2016. Combined effect of unsaturated soil condition and soil heterogeneity on methylene blue adsorption/desorption and transport in fixed bed column: Experimental and modeling analysis. Journal of King Saud University-Science. In press.

Selim, H.M., Iskandar, I.K., 1994. Sorption-desorption and transport of TNT and RDX in soils. CRREL-94-7. Cold Regions Research and Engineering Lab, Hanover, NH.

Serrasolses, I., Romanyà, J., Khanna, P.K., 2008. Effects of heating and autoclaving on sorption and desorption of phosphorus in some forest soils. Biol. Fert. Soils, 44(8), 1063-1072.

Sharma, P., Mayes, M.A., Tang, G., 2013. Role of soil organic carbon and colloids in sorption and transport of TNT, RDX and HMX in training range soils. Chemosphere, 92(8), 993-1000.

Sheremata, T.W., Thiboutot, S., Ampleman, G., Paquet, L., Halasz, A., Hawari, J., 1999. Fate of 2,4,6-trinitrotoluene and its metabolites in natural and model soil systems. Environ. Sci. Technol. 33(22), 4002-4008.

Spurlock, F.C., Huang, K., van Genuchten, M.T., 1995. Isotherm nonlinearity and nonequilibrium sorption effects on transport of fenuron and monuron in soil columns. Environ. Sci. Technol. 29(4), 1000-1007.

Sunahara, G.I., Lotufo, G., Kuperman, R.G., Hawari, J., 2009. Ecotoxicology of explosives. CRC Press.

Townsend, D.M., Adrian, D.D., Myers, T.E., 1996. RDX and HMX sorption in thin disk soil columns. IRRP-96-8. US Army Engineer Waterways Experiment Station. Vicksburg, MS.

Townsend, D.M., Myers, T.E., 1996. Recent developments in formulating model descriptors for subsurface transformation and sorption of TNT, RDX, and HMX. WES/TR/IRRP-96-1. Army Engineer Waterways Experiment Station. Vicksburg, MS.

Walsh, M.R., Walsh, M.E., Ampleman, G., Thiboutot, S., Walker, D.D., 2006. Comparison of explosives residues from the blow-in-place detonation of 155-mm high-explosive projectiles. ERDC/CRREL TR-06-13. U.S. Army Engineer Research and Development Center, Hanover, NH.

Wang, Z., Zhu, J. Y., Fu, Y., Qin, M., Shao, Z., Jiang, J., Yang, F., 2013. Lignosulfonate-mediated cellulase adsorption: enhanced enzymatic saccharification of lignocellulose through weakening nonproductive binding to lignin. Biotechnol. Biofuels, 6(1), 1.

Won, J., Kim, J.W., Kang, S., Choi, H., 2007. Transport and adhesion of *Escherichia coli* JM109 in soil aquifer treatment (SAT): One-dimensional column study. Environ. Monit. Assess. 129(1-3), 9-18.

Yamamoto, H., Morley, M.C., Speitel, G.E. Jr., Clausen, J., 2004. Fate and transport of high explosives in a sandy soil: adsorption and desorption. Soil Sediment Contam. 13(5), 361-379.

Zheng, C., Bennett, G.D., 1995. Applied Contaminant Transport Modeling: Theory and Practice, VanNostrand Reinhold, New York, NY, 440p.

CHAPTER 5. LABORATORY COLUMN EVALUATION OF HIGH EXPLOSIVES DEGRADATION IN GRENADE RANGE SOILS

5.1 Introduction

High explosives (HEs) including 2,4,6-trinitrotoluene (TNT), hexahydro-1,3,5-trinitro-1,3,5-triazine (RDX; Royal Demolition Explosive), and octahydro-1,3,5,7-tetranitro-1,3,5,7-tetrazine (HMX; High Melting Explosive) are deposited on military ranges as part of training activities and have the potential to adversely impact groundwater (Brannon and Pennington 2002; Fuller et al. 2004). To date, only limited research has been conducted to identify cost effective remediation technologies for treating explosives deposited on ranges.

Prior to active remediation of HEs contaminated sites, we should first determine if the HEs will naturally attenuate under ambient site conditions. However, the conditions under which HEs naturally attenuate have not been sufficiently studied. TNT and its degradation products have been shown to naturally attenuate in groundwater at the Louisiana Army Ammunition Plant (LAAP), marine sediment, and sediment from a pond treatment of wastewater from explosives production (Harrelson et al. 1997; Pennington et al. 2001; Yang et al. 2008; Amaral et al. 2016). The high potential for TNT natural attenuation is due to its easy biodegradability under aerobic conditions and high sorption capacity. However, there is

limited evidence of RDX or HMX natural attenuation due to their resistance to biodegradation under aerobic conditions (Ringelberg et al. 2003; Bordeleau et al. 2013).

Previous research has identified conditions that are either favorable or unfavorable for natural attenuation of explosives. Ringelberg et al. (2003) showed RDX attenuation in sandy loam (silt-clay content = 42 %) under saturated conditions with a maximum degradation rate of 0.15 mg/L/d. Photolysis can potentially lead to RDX attenuation at the surface soil, with over half of the initial mass removed when there was no shielding of sunlight and small explosive particles (Bordeleau et al. 2013). Pennington et al. (2001) suggested that abundance of sulfate-, iron-, and sulfite-reducing bacteria in soil could enhance TNT and RDX mineralization. However, soils with very low organic carbon (OC, < 0.1 %) and high sand content (> 90 %) could lead to a low partition coefficient, resulting in low attenuation of explosives in soil (Pennington et al. 1999). Bradley and Chapelle (1995) suggested that natural attenuation of explosives is unlikely due to the inhibitory impact of high explosive concentrations on bacterial populations in the severely contaminated soil. In sandy soils from Massachusetts Military Reservation (MMR), groundwater dissolved oxygen (DO) and oxidation reduction potential (ORP) were the most important factors influencing RDX attenuation (Morris and Fallin 2008).

Prior research suggests that soil type could be an important factor in natural attenuation of HEs by influencing on geophysical and geochemical properties. Water saturation, OC, sand content, iron-reducing conditions, DO, and ORP can be directly influenced by soil type. Therefore, different transport behavior of explosives is expected in varying soil types. In clayey soil, the pores are likely water saturated leading to reducing

conditions, low DO and ORP, potentially enhancing natural attention of explosives. Further, higher surface area of clayey soils provides greater available sites for sorption of explosives.

Soil type could also influence the impact of organic substrate addition on oxygen status. Oxygen transport in soil is influenced by pore size and moisture retention, which are dominated by soil type. In sandy soil, application of organic substrate may not be effective in reducing oxygen concentration in soil due to rapid oxygen transport from atmosphere, resulting in negligible enhancement of explosive degradation. Farling (2013) showed no significant oxygen depletion in sandy soils when glycerin was added, with no substantial increase in RDX degradation.

In batch microcosms using grenade range soil from Fort Bragg, NC, a mixed organic substrate of crude glycerin (GL) and lignosulfonate (LS) was effective at increasing the oxygen consumption rate in soil. Anaerobic soil conditions could be established by rapid oxygen consumption of easily biodegradable GL, and then maintained by slow oxygen consumption with more slowly biodegradable LS. TNT was rapidly biodegraded under both aerobic and anaerobic conditions. RDX, HMX, and RDX daughter products did not significantly degrade under aerobic conditions. However under anaerobic conditions, RDX and HMX biodegraded, without accumulation of daughter products (Chapter 3).

In this work, we examine the transport and fate of HEs in soil from an active hand grenade range, and the impact of GL and LS addition on oxygen consumption and HEs biodegradation using laboratory scale columns. These results provide information on when natural attenuation of HEs is likely and how organic substrate can be used to limit HEs leaching.

5.2 Material and Methods

Calcium lignosulfonates (Norlig A) was purchased from Lignotech USA (Rothschild, WI) and crude glycerin was obtained from Piedmont Biofuels (Pittsboro, NC). Acetonitrile and toluene used in soil and water sample extractions for explosives were HPLC grade and purchased from J.T. Baker and Fisher Scientific respectively. Hydrochloric acid (HCl) and hydroxylamine hydrochloride ($NH_2OH \cdot HCl$) used in soil Fe(II/III) extraction were ACS grade and purchased from Fisher Scientific and Acros Organics.

Analytical standards for TNT, RDX, 2,4-DNT, 2,6-DNT, 2-ADNT, 4-ADNT, and HMX were purchased from AccuStandard, Inc. (New Haven, CT), and standards for RDX nitroso degradation products (MNX, DNX, and TNX) were purchased from SRI International (Menlo Park, CA) then prepared by dissolution in acetonitrile.

Soils used in this laboratory column study were collected from 0 - 1.5 m below the ground surface (bgs) of two adjoining hand grenade throwing bays at Fort Bragg, NC (Bays C and T). Overall, the physical and chemical properties of Bays C and T were similar. Soils in both bays were primarily sand with 9 - 18% silt and 1.4 - 2.6% clay. Soil pH varied from 5.0 to 5.6. Soil pH, silt content, and median grain size (D_{50}) were not statistically different between Bay C and T soils, showing averages of 5.4 ± 0.2 in soil pH, 13.4 ± 2.7 % in silt content, and 296 ± 70 μm in sediment D_{50}. Total iron content varied from 1.99 to 7.62 g/Kg with most of the iron present in the crystalline form. The majority of the non-crystalline iron was present as Fe(II) indicating the bays underwent periods of anoxic conditions. The only significant difference (*p-values* < 0.05) between soil in the two bays was the higher organic

carbon content and clay content of the Bay C soil (OC = 0.20 ± 0.06, clay = 2.3 ± 0.3 %) compared to Bay T soil (OC = 0.08 ± 0.03, clay = 1.9 ± 0.3 %).

RDX concentrations ranged from 0.03 to 1.03 mg/kg in Bay T and 0.01 to 0.04 mg/kg in Bay C soil. TNT concentrations varied from 0.009 to 0.018 mg/kg in Bay T and from 0.008 to 0.021 mg/kg in Bay C soil. While average RDX concentrations in Bay T were somewhat higher, the mean concentrations were not statistically different (*p-values* > 0.05). TNT and RDX concentrations of both Bays C and T were lower than average surface concentrations previously reported by Jenkins et al. (2006) for grenade bays (3.3 mg/Kg TNT and 5.8 mg/Kg RDX). Due to the comparatively low TNT and RDX concentration in the surface soil (Jenkins et al. 2006), the surface of each column was amended with 50 g of soil containing TNT and RDX associated with Comp B high explosive.

Experimental columns were constructed with 5 cm diameter x 1.5 m long clear PVC and packed with 0.15 m of coarse sand and 0.1 m of washed fine sand as a water drainage layer, followed by 1 m of soils from 0 to 1.2 m bgs in grenade throwing bays (Bays C and T) at Fort Bragg, NC. Prior to use in columns, soils were passed through a No. 4 (4.76 mm) sieve to remove clumps. Soils were packed with 0.25 m vertical increment in the same order as the grenade range. 0.64 cm inner diameter x 0.2 m long LDPE tubing connected the bottom of columns and to sampling vials to minimize oxygen inflow from the bottom. Soil gas sampling ports were installed at 0.25, 0.5, 0.75, and 1 m below the soil surface. Four replicate columns were prepared for each throwing bay soil (Bays C and T), followed by biweekly NC groundwater application. Three months after water application, all columns received 50 g of contaminated soil prepared by mixing with composition B explosive (Comp

B) in the laboratory. The columns were wrapped with aluminum foil to prevent the photoreduction of Fe(III) and photodegradation of explosive compounds (Brannon and Pennington 2002). Two leaching columns were prepared with a water drainage layer (0.15 m coarse sand + 0.1 m fine sand) and received the same amount of Comp B contaminated soil as other columns. These leaching columns were operated and monitored in parallel with the columns containing active range soils to measure the explosives concentrations released by the Comp B contaminated soil. Photographs of laboratory soil columns are shown in Figure S-16 in Appendix IV.

40.6 mL of NC groundwater was applied biweekly on the soil surface in columns, which is equivalent to 52 cm per year. At 56 days after addition of the Comp B amended soil, 0.15 g/cm^2 crude glycerin (GL) and 0.15 g/cm^2 Norlig A (NA, lignosulfonate) were applied to the soil surface. The GL and NA loading rates are the same as employed in a field evaluation of substrate addition being conducted at the grenade range at Fort Bragg (Chapter 6). Experimental treatments evaluated include: 1) Bay C soils with no amendment, (2) Bay C soils with GL + NA, (3) Bay T soils with no amendment, and (4) Bay T soils with GL + NA. Duplicates were prepared for each treatment. Column effluents and soil gases were monitored monthly for explosives (RDX, TNT, HMX, and their degradation products), anions (Cl, NO_3, Br, NO_2, and SO_4), cations (Mn and Fe), total organic carbon (TOC), pH, and gas concentrations (N_2, O_2, CO_2 and CH_4). At the end of column operation, columns were cut into 0.1 m sections, homogenized, and soils were analyzed for explosives, TOC, Fe(II/III), moisture, volatile solids, and ash contents.

Analytical methods were as described in Appendix I. Briefly, explosives concentrations were determined by gas chromatography (GC) with electron captured detector (ECD) following U.S. Environmental Protection Agency (EPA) Method 8095 to minimize interferences with humic materials and lignin present in soil and aqueous samples. Prior to GC-ECD analysis, water samples were extracted in toluene by the modified frozen micro-extraction (FME) method (Li et al. 2011). 300 g soil samples were dried at room temperature, ground by puck mill for 60 seconds to reduce the particle size to less than 75 μm, homogenized by random subsampling, and then extracting with acetonitrile for 18 hr. in a cooled ultrasonic bath. The filtered supernatant was then analyzed by GC-ECD. Total organic carbon (TOC) was analyzed using Shimadzu 5000A TOC analyzer. Anions (Cl, NO_3, Br, NO_2, and SO_4) were analyzed by ion chromatography (IC) following EPA Method 9056A (SW-846). Cations (Fe and Mn) were analyzed on a Perkin-Elmer Plasma II Inductively Coupled Plasma Atomic Emission Spectrometry (ICP-AES) following methods equivalent to EPA Method 6010C (SW-846).

Soil particle size distribution was measured using a Beckman Coulter LS 13-320 laser particle size analyzer equipped with a Universal Liquid Module. Soil total carbon (TC) content was analyzed using Perkin Elmer 2400 CHNS Analyzer. Soil moisture content and volatile solids were determined by weight losses on drying at 105 °C for 24 hours and ignition in a muffle furnace at 550 °C for 2 hours respectively. Water retention was measured at 0, 30, 60, 100, 333, and 500 cm of H_2O. Saturated hydraulic conductivity was determined using repacked ring samples with dimensions of 7.6 cm diameter by 7.6 cm tall. Soil samples for iron analysis were extracted using 0.25 M hydrochloric acid (HCl) for Fe(II)

and 0.25 m HCL + 0.25 M hydroxylamine hydrochloride ($NH_2OH \cdot HCl$) for total Fe(II + III). Extractions were performed in 40 mL EPA vials flushed with nitrogen gas to minimize Fe oxidation, then the extracts were analyzed by ICP-AES. Samples were extracted for 30 minutes to measure poorly crystalline and sediment-bound iron oxides, and for 96 hours to measure crystalline reactive iron oxides.

5.3 Experimental Results

5.3.1 *Leaching Columns*

Two leaching columns were constructed with a water drainage layer (0.15 m coarse sand + 0.1 m fine sand) and 50 g of the Comp B impacted soil. Two centimeters of water (40.6 mL) was applied to the column surface biweekly. The leaching columns were operated and monitored in parallel with the other soil columns to distinguish between the HE leached from the added Comp B and from the Fort Bragg range soils.

Figure 5.1 shows the average biweekly effluent volume and average concentrations of total organic carbon (TOC), nitrate (NO_3), nitrite (NO_2), RDX, and TNT in effluents of duplicate leaching columns. HMX concentrations (data not shown) reached a maximum of 0.23 mg/L at about 150 days and then gradually declined with time to 0.05 mg/L (average over monitoring period = 0.11 mg/L).

Effluent flowrates varied seasonally with the lowest flowrates observed during the winter when the evaporation from the open columns was a maximum, due to the dry indoor air of the laboratory. 66 % of water applied was recovered as effluent in leaching columns with 3 % of water retained in soil and 31 % of water evaporated. TOC, NO_2, TNT and RDX

concentrations varied with effluent flowrate, reaching a maximum when evaporation was highest. However, the mass of these constituents did not vary with effluent volume indicating most of this variability was associated with concentration of the solutes by evaporation. Approximately 51 % of the TOC released from the leaching columns was dissolved TNT, RDX, HMX, and monitored degradation products. Nitrate (NO_3) initially present in the soil was quickly leached from the soil and then remained below the detection limit (0.5 mg/L) for the most of monitoring period. In contrast, NO_2 was continuously observed in the leaching column effluents, potentially associated with loss of nitro functional groups (-NO_2) from the TNT aromatic ring under aerobic conditions (Martin et al. 1997; Stenuit et al. 2006; Smith et al. 2015b). TNT concentrations varied from 5.7 to 56.4 mg/L (ave. = 23.4 mg/L). Some portion of the TNT likely degraded since TNT degradation products (ADNTs and 2,4-DNT) were consistently observed in the effluent (Figure S-19). RDX concentrations varied from 6.0 to 31.4 (ave. = 27.8 mg/L). MNX, DNX, and TNX gradually declined over time, suggesting these degradation products were initially present in the soil and leached out over time.

Figure 5.2 shows the cumulative mass of RDX, TNT, HMX, and RDX/TNT degradation products discharged in the effluent and mass present in the soil at the end of the leaching column experiments. Total mass recovered in the duplicate columns was similar, but not identical. This is not surprising given the high variability in HE concentrations in explosive impacted soil, even after soil mixing (Jenkins et al. 1997; Crockett et al. 1998; Clausen et al. 2004; USEPA 2014b). Masses of RDX and TNT degradation products were 0.6 % and 1.2 % of their parent compounds respectively, indicating very limited degradation

of RDX and TNT in leaching columns. However, amount of inorganic nitrogen (NO_2-N + NO_3-N) in effluent (0.10 mmol N) was somewhat higher than N mass derived from TNT and RDX degradation products (0.04 mmol N). The higher N mass might be associated with degradation of TNT or RDX to other degradation products which are not monitored in this study, or further mineralization of degradation products observed in this study. HMX degradation products were not monitored in this study.

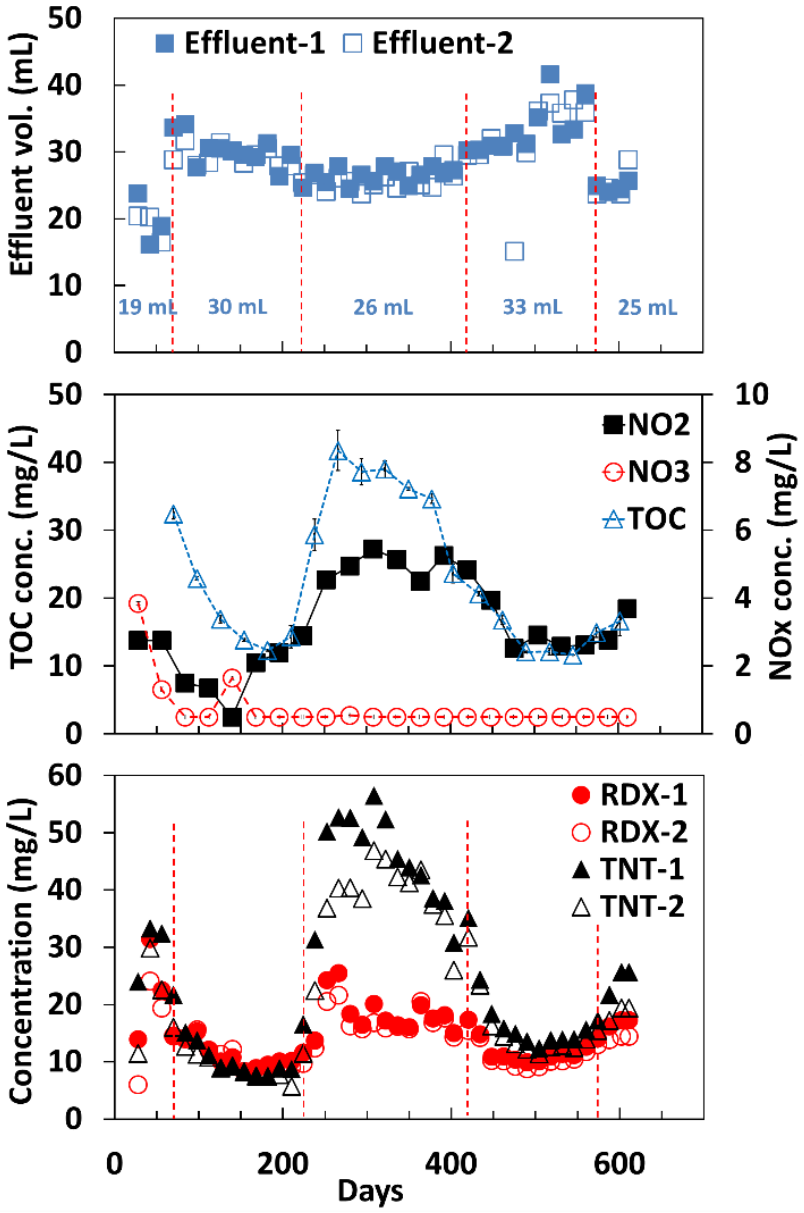

Figure 5.1. Average biweekly effluent volume and average concentrations of total organic carbon (TOC), nitrate (NO_3), nitrite (NO_2), RDX, and TNT in effluents of the duplicate leaching columns. Error bars represent range of values in duplicate columns. Where not visible, error bars are smaller than symbol size.

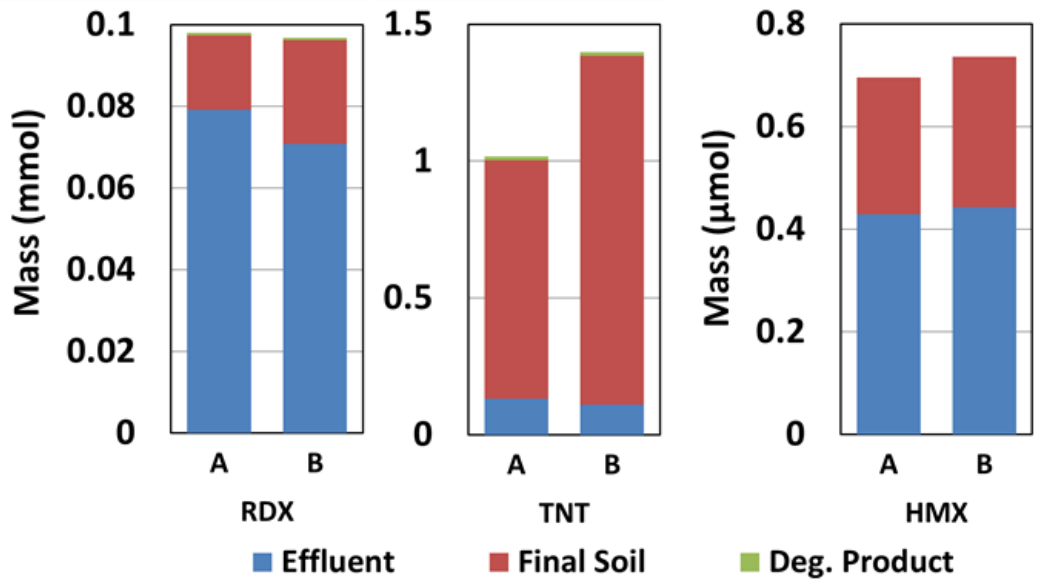

Figure 5.2. Masses of RDX, TNT, HMX, and degradation products in effluent and soils of duplicate leaching columns. HMX degradation products were not monitored in this study.

5.3.2 *Soil Column Hydraulics*

Two centimeters of water was applied to the surface of each soil column every other week over the course of the experiment. The applied water was not allowed to runoff and remained on the column surface consistent with the observed presence of ponded water in numerous craters on the Fort Bragg grenade ranges. After 26 to 86 weeks after start of the experiment, water began to pond on the surface of the Bay C columns. The greater ponding in the Bay C soils is consistent with the higher computed hydraulic retention times (HRT) that were associated with the lower saturated hydraulic conductivity (K_{sat}) of the soils. Average column hydraulic properties are shown in Table 5.1. The lower K_{sat} can be inferred from the much lower effluent volumes in Bay C columns. The lower K_{sat} of the Bay C soils

is probably due to the somewhat higher clay content and higher bulk density. The same procedure was used to compact the laboratory test cylinders, so the higher ρ_b of the Bay C soils suggests greater ease of compaction.

Table 5.1. Average column hydraulic properties.

Columns		**Control Bay C**		**Treated Bay C**		**Control Bay T**		**Treated Bay T**	
Replicate	**Units**	**A**	**B**	**A**	**B**	**A**	**B**	**A**	**B**
Sum H_2O Leached	cm	23.4	18.7	9.4	16.0	54.5	55.1	48.1	50.3
Ave. Porosity	-	0.28	0.26	0.26	0.27	0.30	0.30	0.29	0.29
Ave. Water Filled Porosity	-	0.27	0.26	0.26	0.26	0.21	0.21	0.23	0.23
ρ_b	g/cm^3	1.87	1.91	1.93	1.89	1.83	1.83	1.86	1.84
V during last year	cm/yr	17.9	12.5	5.9	9.4	35.9	37.5	29.1	33.5
HRT during last year	d	699	966	1,972	1,273	273	258	366	314

Total porosity (θ) and water-filled porosity (θ_w) were calculated from soil bulk density, moisture content, and specific gravity measured at the end of the monitoring period (Figure 5.3 and Table S-6). θ was relatively consistent in all Bay C columns (range = 0.25 to 0.34), but more variable in the Bay T columns (0.24 to 0.41). The reason for this variability is not known, since identical procedures were used to pack all the columns.

At the end of the monitoring period, the Bay C soil columns were nearly saturated with $\theta_w/\theta > 95\%$ throughout the profile, while θ_w/θ was below 82% throughout the Bay T soil columns. The average θ_w in Bay C soils was significantly higher than Bay T soils at the end of column experiment (*p-values* < 0.05), resulting in lower air-filled porosities (< 0.02). The higher water-filled porosities in Bay C soils are probably associated with relatively higher

clay and organic carbon fraction leading to lower saturated hydraulic conductivities (K_{sat}). Rawls et al. (2003) reported a positive relationship between organic carbon content and water retention in soil, exhibiting higher correlation in sandy and silty soils.

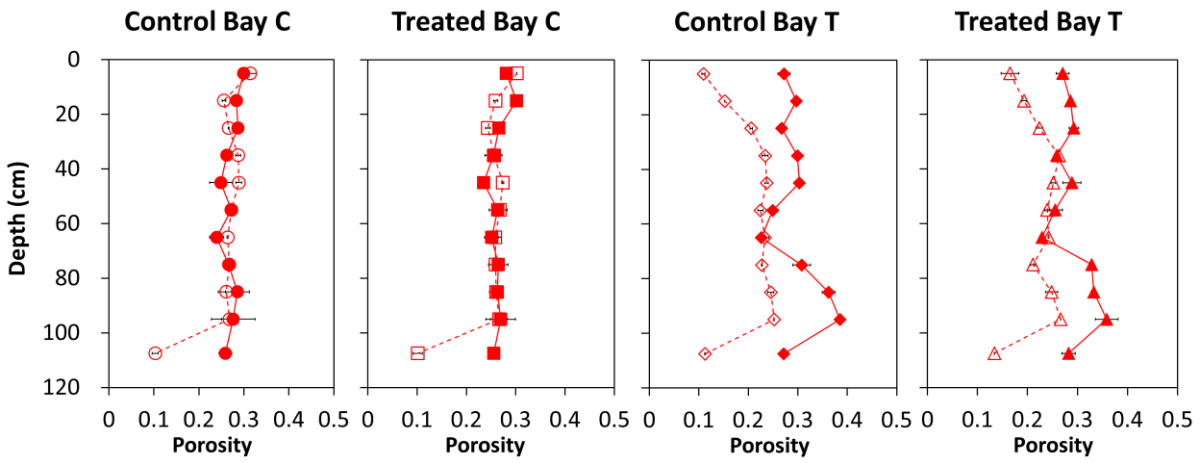

Figure 5.3. Total porosities (closed marks) and water-filled porosities (open marks) along the vertical soil profile in soil columns at the end of monitoring period. Error bars represent range of values in duplicate columns. Where not visible, error bars are smaller than symbol size.

Organic amendment addition resulted in a substantial increase in θ_w in the upper half of the Bay T columns, with the greatest increase in the top layer (0 - 20 cm) (*p-values* < 0.05), presumably due to enhanced water retention and/or lower K_{sat} associated with lignosulfonate addition. This increased θ_w and reduced air-filled porosity is expected to have reduced oxygen transport through the soil surface of the amended Bay T columns, increasing the likelihood of anaerobic conditions. Amendment addition did not have a substantial impact on θ_w in the Bay C columns, presumably due to the very high θ_w in the Bay C controls.

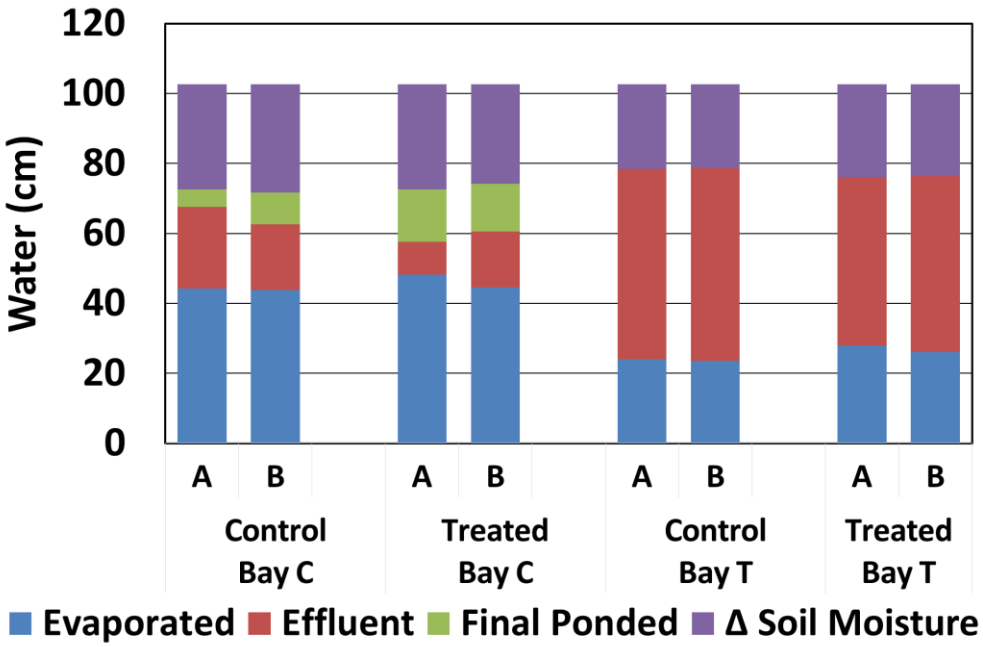

Figure 5.4. Soil column water balance over 695 day operating period. [Evaporated = Applied - (Effluent + Ponded + Δ Soil moisture)].

Figure 5.4 and Table S-7 present results of a water balance for each column for the 695-day monitoring period including the initial water present in the soil, water applied, water discharged in the column effluent, ponded water, water present in the soil at the end of the experiment, and water lost due to evaporation. Water lost due to evaporation was calculated as the difference between the water applied and total water recovered.

The presence of ponded water increased evaporation from the Bay C columns, reducing the total amount of water discharged in the effluent, compared to the Bay T columns. Similarly, the higher water retention in the surface layer of the amended Bay T columns appears to have somewhat enhanced evaporation and reduced the amount of water discharged from these columns (Figure S-17 and Table S-7). During the last year of the

experiments, the average flowrate was 15 cm/yr (range = 12.5 - 17.9) in the Bay C columns and 37 cm/yr (35.9 – 37.5) in the Bay T columns. These values are reasonably consistent with the net groundwater recharge rate of 32 cm/yr for the Fort Bragg area reported by Heath (1994).

Average hydraulic retention times (HRT) during last year were 265 days in the control Bay T columns, 340 days in the amended Bay T columns, 833 days in the control Bay C columns, and 1,623 days in the amended Bay C columns. The larger HRTs were the result of higher water retention in these columns combined with greater evaporation (reduced discharge).

5.3.3 *Oxygen Distribution in Soil Columns*

To identify the impact of soil texture and organic amendment addition on redox conditions, soil gases were monitored monthly. Figure 5.5 illustrates variation in oxygen (O_2) concentrations at four depths of laboratory soil columns over the monitoring period.

In the both duplicate control Bay T columns, oxygen concentrations remained close to atmospheric throughout the monitoring period. In both duplicate treated Bay T columns, oxygen concentrations rapidly declined at a depth of 50 cm following organic amendment addition. In one of the treated Bay T replicates (column T-A), oxygen concentrations remained below 5 % by volume at the 75 and 100 cm depths for over 280 days. However, in the treated Bay T-B replicate column, oxygen levels rebounded to near atmospheric levels by 200 days. The large difference in observed oxygen levels in the duplicate soil columns may be associated with more rapid oxygen transport through slightly higher air-filled porosities in

the top layer (0 - 30 cm) of the treated Bay T-B column (0.09 - 0.14) compared to the treated Bay T-A column (0.05 - 0.08). However, air-filled porosities at the end of the monitoring period were not significantly different at the 95% level (*p-values* = 0.06).

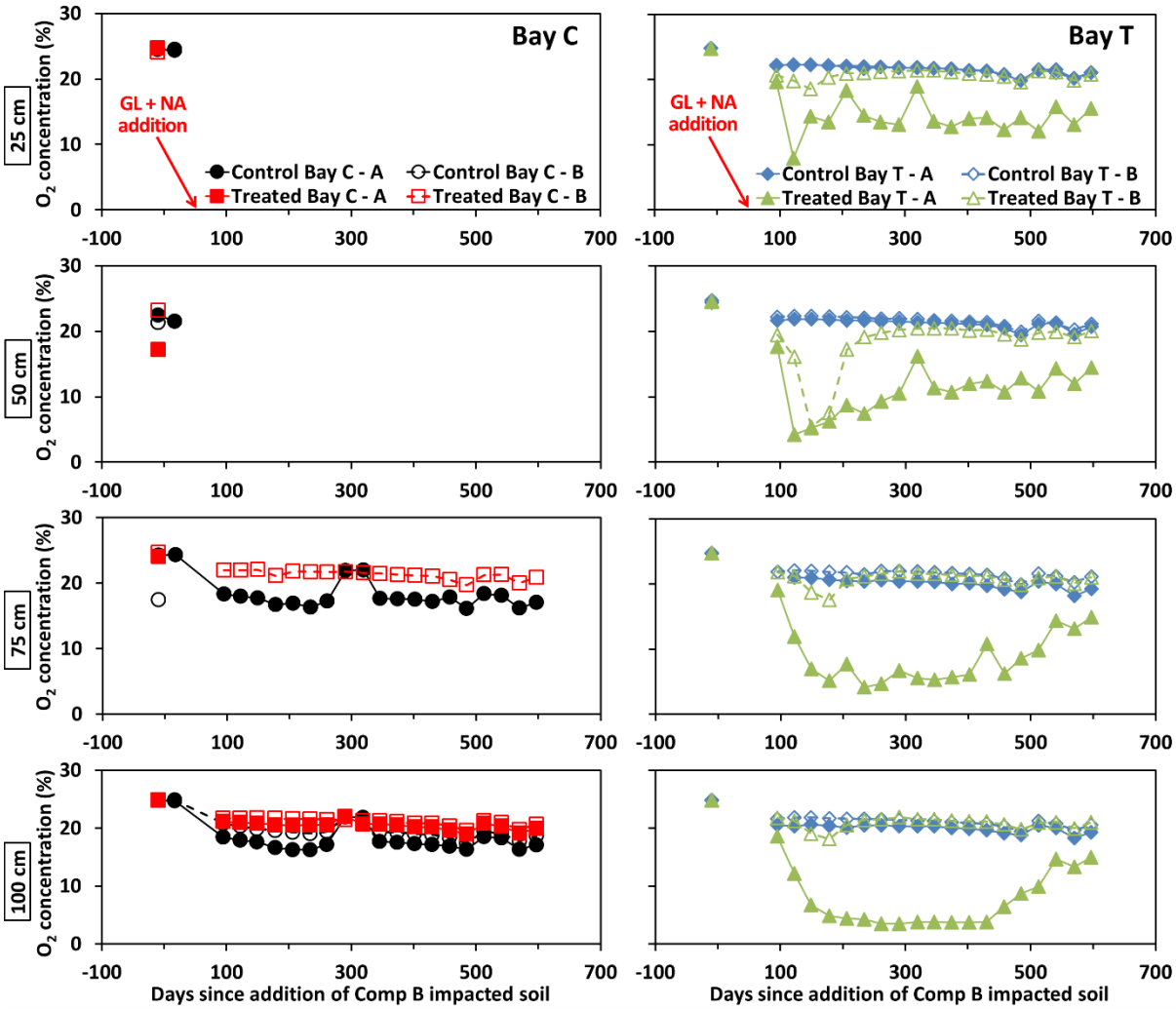

Figure 5.5. Oxygen concentrations at 25, 50, 75, and 100 cm below the soil surface in soil columns over the monitoring period.

In Bay C soils, gas samples could not be collected from the 25 cm and 50 cm sampling ports due to nearly water saturated soil conditions (Figure 5.2). The measured

oxygen levels at 75 and 100 cm depths in Bay C soils were close to the atmospheric, probably due to air entry through the bottom of columns. Oxygen transport through the upper portion of the Bay C columns was limited due to the high water saturation, greatly increasing the potential for development of anoxic conditions. However, the bottom half of the Bay C columns remained aerobic for the most monitoring period.

5.3.4 *Soil Column Geochemistry*

Column effluents were monitored monthly to evaluate the impact of organic amendment addition on geochemical parameters including TOC, pH, anions (Cl, NO_3, Br, NO_2, and SO_4), and cations (Mn and Fe). Carbon content and Fe(II/III) in soils packed in columns were also measured at the end of monitoring period. The average pH of the column effluents was pH 8.0 ± 0.2 over monitoring period, which is comparable with pH of groundwater applied (7.8 ± 0.1) (data not shown). One of the untreated Bay C soil columns showed pH decline up to 6.4 then rebounded back up to a pH range close to the groundwater applied, probably due to combined influence of low water transport and initial soil pH (5.4 ± 0.2).

Figure 5.6 shows the variation in chloride (Cl), TOC, nitrate (NO_3), and manganese (Mn) concentrations in the soil column effluents. TOC concentrations were initially elevated, potentially due to release during column packing. In the treated Bay T columns, average Cl present in the waste glycerin (2.7 % Cl) began arrive in the effluent at 280 days, increasing to a maximum of 283 mg/L at 420 days (364 days after glycerin addition), which is consistent with the computed average HRT of 410 days. By this time, TOC concentrations were low

(0.9 to 12.7 mg/L) indicating negligible organic carbon transport through the columns. However, there were significant variations in Cl migration between duplicate treated Bay T columns as shown in Figure 5.6. Cl concentration in effluent reached a maximum more rapidly in the T-A column (283 mg/L at 420 days) compared to the T-B column (151 mg/L at 588 days). This difference might be resulted from slightly lower θ_w at the top layer soils (0 - 30 cm) in the T-B column (ave. = 0.18, range = 0.15 - 0.22) than the T-A column (ave. = 0.20, range = 0.18 - 0.23) since Cl migrates through the water-filled potion of soil pores.

In the treated Bay C columns, low concentrations of Cl appeared to break through in the treated Bay C columns at 504 days after amendment addition, which is much more rapid than would be expected based on the computed HRT of 1,891 days. Similar to the other columns, organic carbon breakthrough in the Bay C columns was negligible. In all treated columns, less than 1% of the added carbon was discharged in the effluent. In contrast, over 60,000 mg/L of TOC was discharged in the effluent of washed sand (3.7 % silt-clay) columns amended with glycerin (Farling 2013). The much more limited TOC breakthrough in the Fort Bragg soil columns is presumably due to the higher silt-clay content (15.1 ± 3.5 % silt-clay) and longer HRT.

Nitrite (NO_2) was initially detected in the effluent of all columns at concentrations ranging from 0.7 to 1.8 mg/L and then declined below detection (< 0.5 mg/L) within 168 days (data not shown). NO_2 concentrations in the leaching column effluent varied from 0.5 to 5.5 mg/L, indicating substantial NO_2 attenuation in Bay C and T columns, either by oxidation to NO_3 or anaerobic NO_2 reduction.

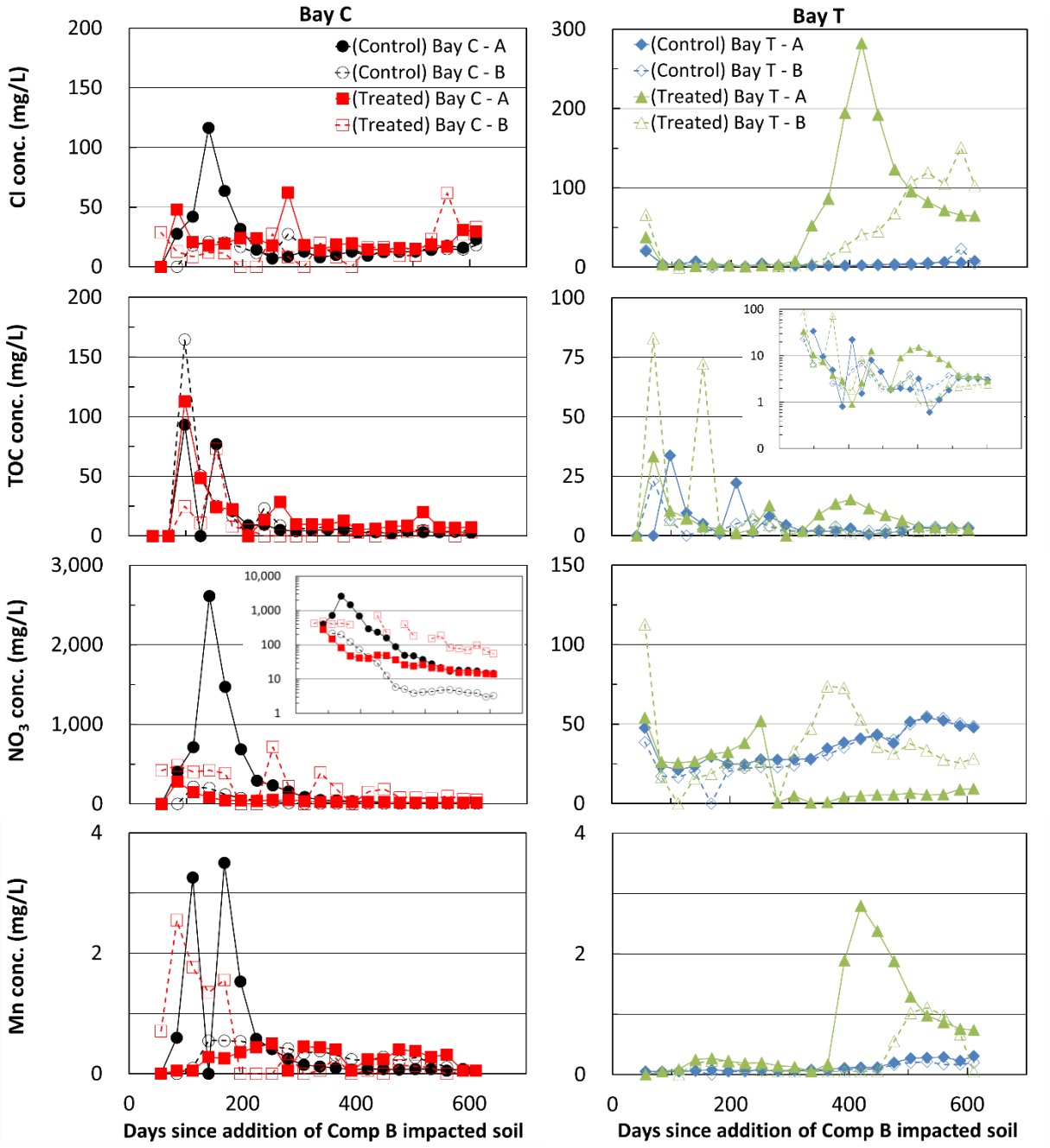

Figure 5.6. Average chloride (Cl), TOC, nitrate (NO_3), and manganese (Mn) concentrations in effluents of soil columns over monitoring period.

In both control Bay T columns and one treated Bay T column (B), NO_3 concentrations increased over the course of the experiment, presumably due to oxidation of NO_2 released from the Comp B on the column surface. However, in the treated Bay T-A column, NO_3 concentrations slightly increased by 252 days then declined over time, presumably due to denitrification under anoxic conditions (Figure 5.5). Initial NO_3 concentrations in both the treated and control Bay C effluents were much higher than in the Bay T columns. The reason for this difference is not obvious, but it might be associated with deposition of considerable amount of NO_3 in the Bay C soil through NO_2 release during natural explosives degradation followed by nitrification under aerobic condition. Over time, NO_3 concentrations in all the Bay C effluents declined.

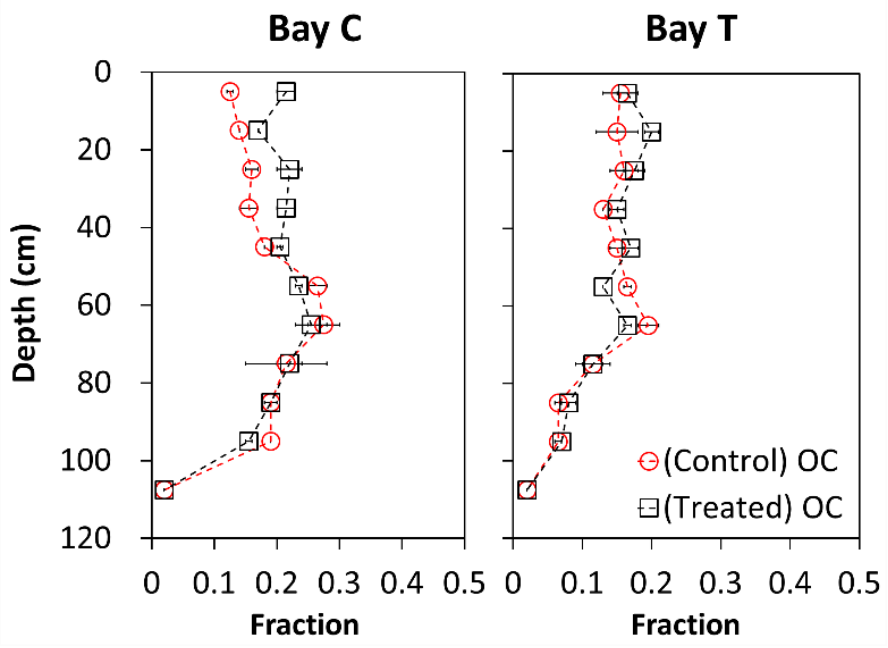

Figure 5.7. Organic carbon (OC) contents along the vertical soil profile in columns at the end of monitoring period. Error bars represent range of values in replicate columns. Where not visible, error bars are smaller than symbol size.

Manganese (Mn) concentrations were increased from 336 days since addition of organic amendment at 56 days in treated Bay T-A column, consistent with the breakthrough of Cl. This suggests the establishment of Mn reducing conditions in the treated Bay T soils, but not Fe reducing conditions demanding much negative redox potential, i.e., higher reducing power.

Organic carbon (OC) levels in soil at the completion of the experiment are shown in Figure 5.7. Amendment addition appears to have increased the soil OC content in the upper portion of both the Bay C and T soils, compared to the controls (*p-values* < 0.05). The greater increase in the Bay C columns is likely due to the reduced water flow and oxygen transport in these columns.

Figure 5.8 and Table S-8 present an analysis of the cumulative mass of nitrogen present in the effluent and soils for the leaching columns and soil columns. Inorganic N includes NO_2 and NO_3. Explosive-N includes TNT, RDX, HMX and their degradation products. Most of the nitrogen present in the leaching column soil was present as TNT with much lower amounts of RDX. The mass of nitrogen recovered in the Bay C and Bay T effluents and soils was much lower, due to extensive leaching and degradation of both TNT and RDX. The mass of inorganic nitrogen (NO_3) released from the all Bay C and Bay T columns was greater than that released from the leaching columns (NO_2), supporting oxidation of the HEs or their degradation products. However, a substantial portion of the N present in the leaching columns could not be accounted for. The unaccounted for N could be in the form of NH_3, NH_4, N_2O, and N_2 produced through explosives degradation and/or denitrification processes (Bhushan et al. 2002; Smith et al. 2015a; Smith et al. 2015b).

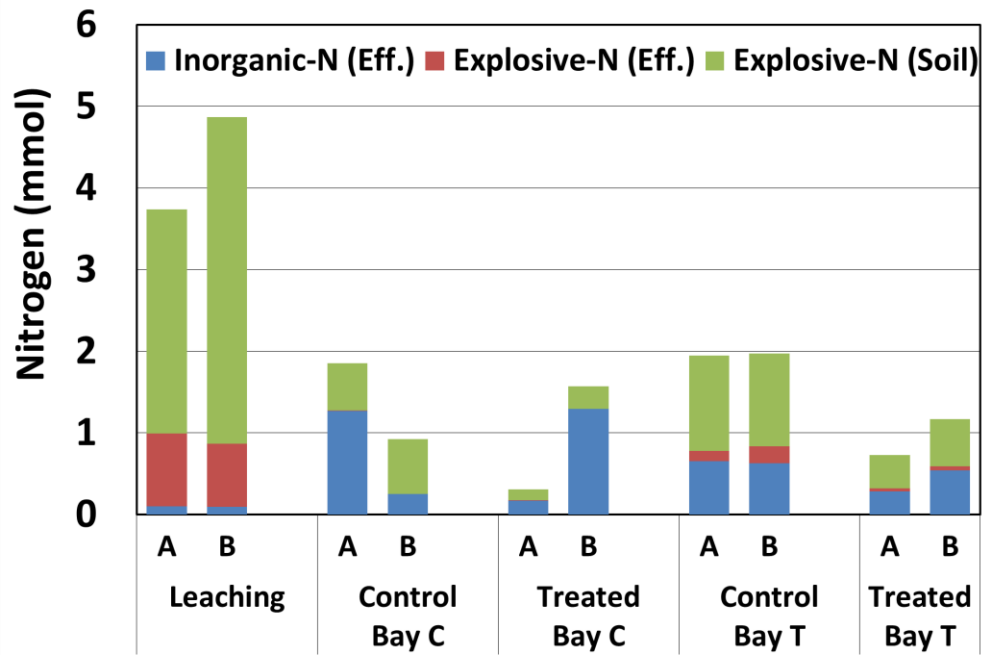

Figure 5.8. Masses of nitrogen in effluent and soils of laboratory columns. Inoganic-N (Eff.) = (NO_2-N + NO_3-N) discharged. Exploisive-N (Eff.) = explosives-N discharged. Exploisive -N (Soil) = explosives-N sorbed to soils.

Organic amendment addition did not result in a measurable increase in dissolved Fe in either the Bay C or Bay T columns, with dissolved Fe concentrations remaining below the analytical detection limit of 0.05 mg/L in all column effluents throughout the monitoring period (data not shown). However, organic amendment addition did result in a statistically significant increase (*p-values* < 0.05) in levels of poorly crystalline Fe(II) in the upper 50 cm of the Bay C columns and a small increase in poorly crystalline Fe(II) from 50 - 80 cm in the Bay T columns (Figure 5.9). Amendment addition did not result in a measurable increase in crystalline Fe(II) for either soil.

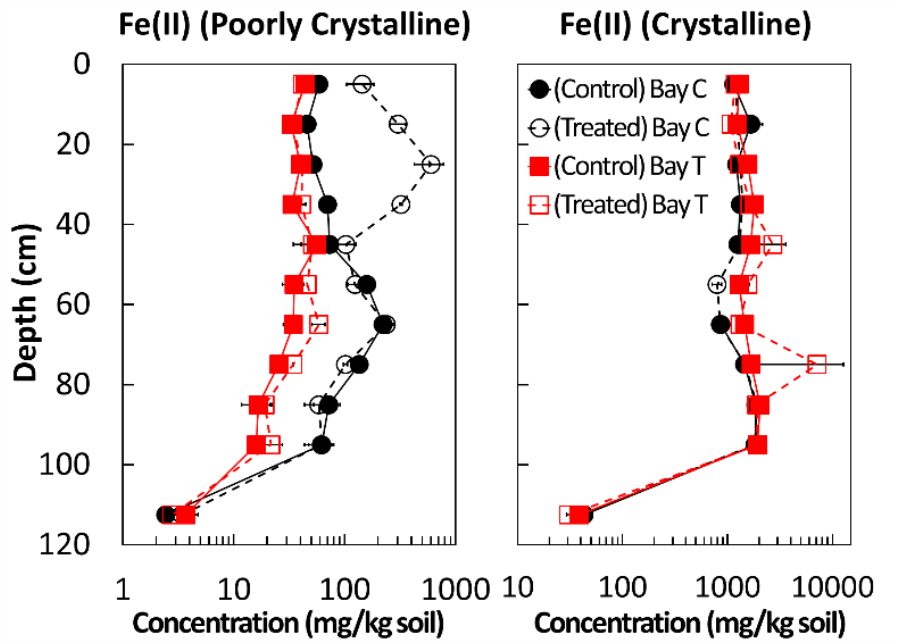

Figure 5.9. Concentrations of poorly crystallized and crystallized Fe(II) along the vertical soil profile in columns at the end of monitoring period. Error bars represent range of values in replicate columns. Where not visible, error bars are smaller than symbol size.

5.3.5 *Explosives in Soil Columns*

Column effluents were analyzed monthly by GC-ECD after liquid-liquid extraction in toluene to evaluate the impact of soil texture and organic amendment addition on changes in explosives concentrations (Figure 5.10). At the completion of the experiment, the columns were cut into 10 cm intervals, dried at room temperature, ground by puck mill, extracted in acetonitrile, then analyzed on GC-ECD. Figure 5.11 shows vertical distribution of HEs in column soils at the end of monitoring period. Cumulative masses of HEs and degradation products in the effluent and soils for each column are presented in Figure 5.12 and Table S-9.

TNT was extensively degraded in both Bay C and T soils with effluent concentrations consistently below the detection limit (< 1 µg/L) (Figure S-19). TNT daughter product

concentrations also remained low. DNTs (2,4-DNT and 2,6-DNT) were below the detection limit (< 2.5 µg/L) and concentrations of ADNTs (2-ADNT and 4-ADNT) were less than 10 µg/L in all columns over the most monitoring period (Figure S-19). The total mass of TNT discharged in the Bay C and Bay T soils was less than 0.1% of the mass released from the leaching columns for both organic amended (treated) and control columns (Figure 5.12).

TNT concentrations in soil were highest at the soil surface and then declined with depth in all columns (Figure 5.11). In both the Bay C and Bay T soils, soil bound TNT levels were significantly lower (*p-values* < 0.05) in the columns treated with the amendment than the untreated, indicating organic substrate (GL + NA) addition enhanced TNT degradation in both Bay C and T soils. These low levels of TNT and its degradation products in the effluent and soil are consistent with results from biodegradation experiment in microcosms using Bay C and T soils (Chapter 3).

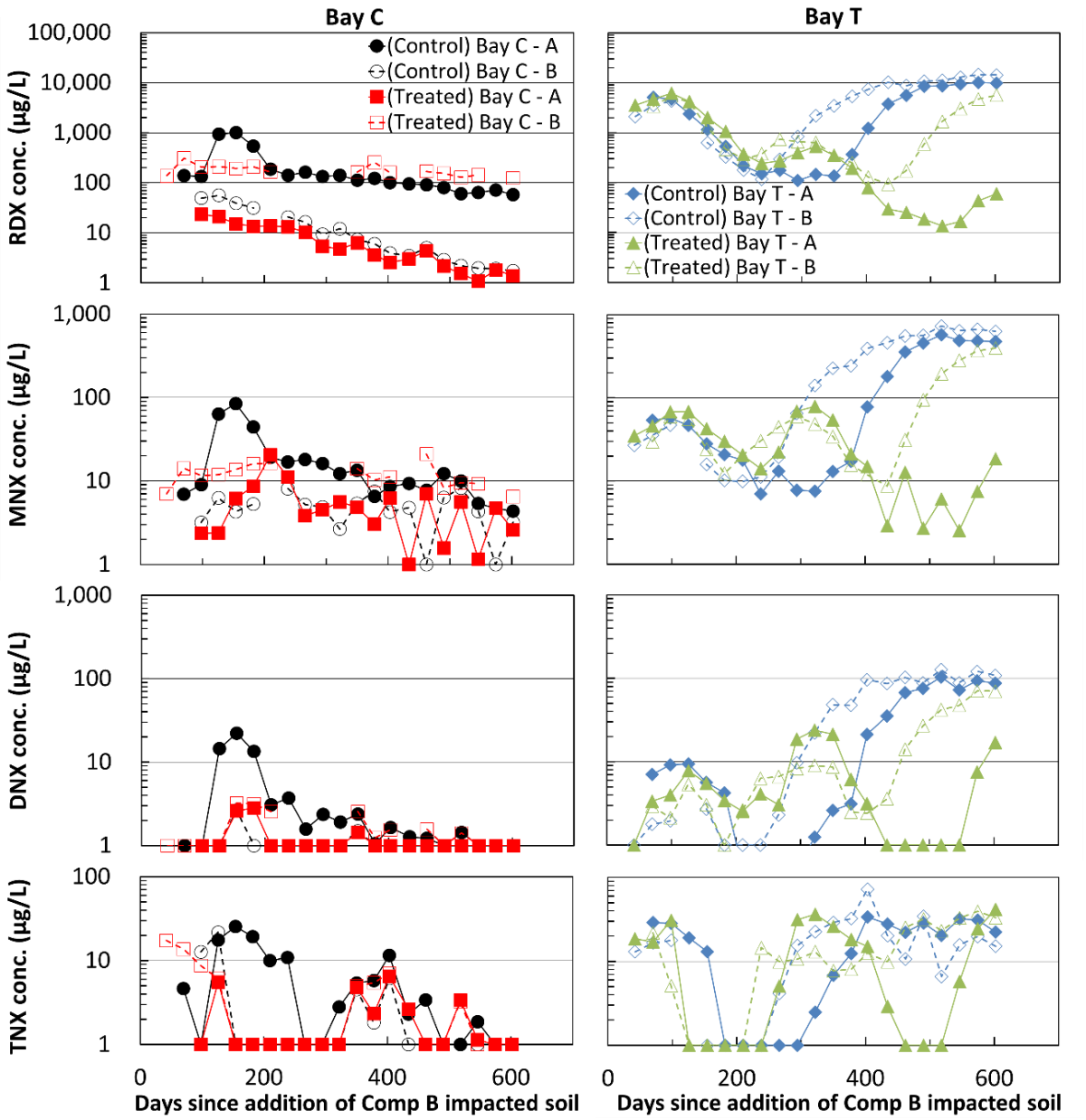

Figure 5.10. Concentrations of RDX and RDX nitroso degradation products (MNX, DNX, and TNX) in column effluents over the monitoring period. TNT and TNT degradation products were less than 36 µg/L in all effluent samples.

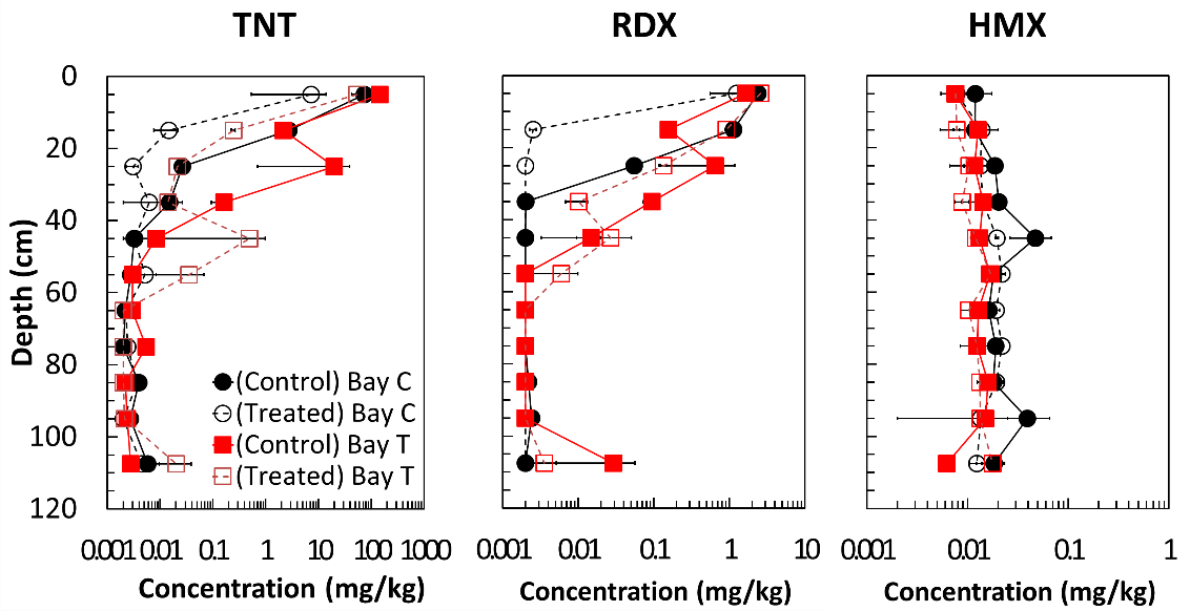

Figure 5.11. Vertical distribution of HEs in column soils at the end of monitoring period. Error bars represent range of values in replicate columns. Where not visible, error bars are smaller than symbol size.

RDX leaching behavior was significantly different between Bay C and T soil columns. Figure 5.10 shows variation in concentrations of RDX and RDX nitroso degradation products (MNX, DNX, and TNX) in column effluents over the monitoring period.

In the treated and control Bay T columns, RDX, MNX, DNX and TNX were relatively consistent over the first 250 days, reaching a maximum at approximately 100 days and then declining. In the control Bay T columns, RDX concentrations began to increase at 250 days to 350 days, reaching a maximum of ~10,000 µg/L by the end of the experiment, similar to the RDX concentrations discharged from the leaching columns. In the treated bay T columns, RDX concentrations began to rebound at about 450 days in treated Bay T-B column and at 550 days in treated Bay T-A column. The more rapid rebound in column B was likely due to the more rapid return to oxidizing conditions in this column (Figure 5.5).

Similar results were observed for MNX and DNX, where organic amendment addition appeared to delay degradation product increases in the Bay T column effluents by about 200 days.

There was much more variability in RDX concentrations in the Bay C column replicates. In one control column (A) and one treated column (B) with Bay C soil, RDX concentrations were relatively high (100 - 1000 µg/L) and remained almost constant with time. In the other replicate Bay C column, RDX concentrations were lower and declined more rapidly with time. As a result, total mass of RDX released from the Bay C treated and control columns were similar (Figure 5.12 and Table S-9).

In Bay C columns, RDX concentrations were highest near the soil surface and declined rapidly with depth (Figure 5.11). Mass analysis results shown in Figure 5.12 demonstrate that RDX was extensively degraded in both the control and treated Bay C columns, with 10 to 22 % of the RDX recovered as nitroso degradation products. RDX removal was slightly higher in the treated columns than the controls. However, RDX degradation product mass was higher in the treated columns so overall removal of RDX and degradation products was similar in the treated and control columns. The large majority of the degradation products recovered were sorbed to the soil with TNX present in the highest concentrations, followed by MNX and DNX.

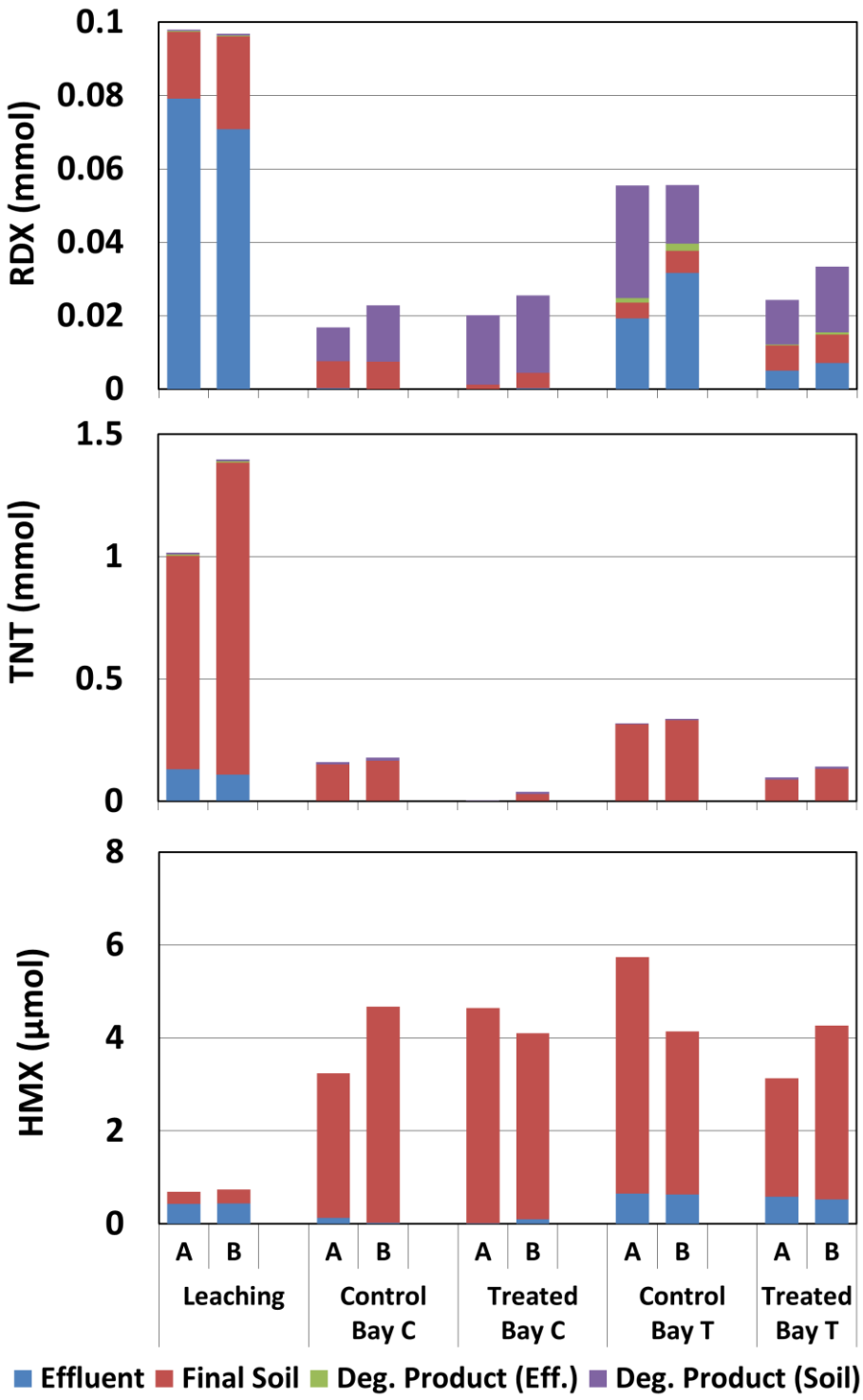

Figure 5.12. Masses of RDX, TNT, HMX, and degradation products in effluent and soils of laboratory columns. HMX degradation products were not monitored in this study.

The distribution of RDX and its degradation products in the Bay T soil at the end of the experiment was similar to the Bay C columns (Figure 5.11). The highest RDX concentrations were present near the soil surface, and levels declined rapidly with depth. 13 to 33 % of the RDX mass was recovered as nitroso degradation products sorbed to soil (Figure 5.12), with TNX present in the highest concentrations. In the Bay T columns, amendment addition reduced both the mass of RDX released in the column effluent and the mass of RDX degradation products in the soil.

Amendment addition did not have a significant impact on HMX leaching or final HMX concentrations in the soil, for either the Bay C or Bay T soils (Figure S-22). The limited HMX removal is probably due to high RDX concentrations which inhibit biodegradation of HMX (Uchimiya et al. 2010).

5.4 Discussion

High concentrations of TNT and RDX were leached from Comp B impacted soils in laboratory leaching columns. TNT leaching was more limited in the leaching columns compared to RDX, consistent with prior research results (Furey et al. 2008; Rylott et al. 2011). Extensive leaching of TNT and RDX could be a contaminate in groundwater (Spain et al. 2000; Lynch et al. 2001; Pennington and Brannon 2002). TNT and RDX degradation products are also a concern due to their toxic potentials (Lachance et al. 2004; Lotufo and Lydy 2005; Zhang et al. 2008). Clausen et al. (2004) showed widespread contamination of soil and groundwater by leaching of explosives and their degradation products at Camp Edwards, Massachusetts Military Reservation (MMR).

In columns packed with grenade range soils, TNT leaching was extensively reduced and a small amount of TNT remained in surface soil regardless of soil type and organic substrate addition, possibly due to natural attenuation. However, natural attenuation of RDX was quite variable with minor differences in soil properties. Control Bay T soil columns were unsaturated and remained aerobic, resulting in low Mn concentrations in the effluent. RDX concentrations reached the concentrations discharged from the leaching columns after approximately 546 and 430 days in the replicates, which are somewhat later than computed HRT during last year (273 and 258 days). This later RDX breakthrough is not surprising since its average retardation factors (R) are 37.0 at low concentrations (= 114 μg/L) and 8.7 at high concentrations (= 12,345 μg/L), which are estimated with Freundlich partition coefficient (K_F = 3.06 L/kg, n = 0.67) for RDX sorption to Bay C soils (Chapter 4), indicating increased retention at low concentrations. Most RDX residual was discharged in effluent with small portion of RDX sorbed onto soils. On the contrary, significant portion of RDX degradation products were observed in soils rather than effluent (Figure 5.12). The considerable amount of MNX and TNX present in soil indicates that RDX was degraded in control Bay T soils, probably occurred in nearly water saturated segment at 50 - 70 cm depth with average $\theta_w/\theta > 97$ % (Figure 5.3). RDX concentrations were highest at top soil and declined rapidly with depth (Figure 5.11).

In control Bay C soils with relatively higher clay and organic carbon contents than Bay T soils, it appears that anoxic condition was established in upper portion of columns by nearly water saturated soil conditions, while the lower portion remained aerobic (Figure 5.3 and Figure 5.5). Very little RDX was discharged in effluent (< 0.5 % of leaching column

effluent) with small amount sorbed to Bay C soils (Figure 5.12). The mass of RDX discharged in effluent was expected to be low, based on the long HRT of the column (833 days). However, the mass remaining in the soil was also low, indicating the majority of RDX was degraded. As a result of RDX degradation, RDX degradation products were elevated in soil (Figure S-21). MNX and TNX were distributed throughout vertical soil profile, while DNX rapidly declined with depth with highest concentration at top soils (Figure S-22).

Mass balance results showed significant RDX removal (Figure 5.12) in the control Bay T columns that were aerobic for the most monitoring period (Figure 5.5). The observed RDX degradation might be associated with the short term anoxic conditions. Despite RDX degradation potential under aerobic conditions, RDX degradation was significantly enhanced under water saturated soil conditions presumably generating anoxic conditions. Prior research also showed more extensive RDX attenuation in sandy loam (silt-clay content = 42 %) under the saturated condition compared to limited degradation under unsaturated conditions (Ringelberg et al. 2003). RDX is typically more resistant to aerobic biodegradation than TNT (Bradley and Chapelle 1995; Hawari et al. 2000; Felt et al. 2009). Farling (2013) showed extensive TNT removal and no substantial RDX degradation in his aerobic columns study using sandy soil.

The mixture of crude glycerin (GL) and Norlig A (lignosulfonate, NA) was selected as an organic amendment in this study. The readily biodegradable GL, produced as a byproduct of biodiesel production, was intended to rapidly consume oxygen in soil, generating anoxic conditions and leading to enhanced anaerobic biodegradation of explosives. The NA, produced during paper production, was expected to much slowly consume oxygen

due to its slow biodegradability, helping to maintain anoxic conditions established by GL degradation. GL and NA are highly water soluble and could be applied to the contaminated site by spraying without entering the range to remove unexploded ordnance (UXO). The amendment applied would be transported into the soil by rainfall or artificial irrigation.

The impact of amendment addition was variable between replicates in Bay T soil columns. In one replicate (T-A), organic amendment rapidly migrated through the column with a travel time of 366 days, generating anoxic conditions at the bottom half of the column for about a year (Figure 5.5 and Figure 5.6). With the arrival of Cl present in the GL at the bottom of column, TOC and Mn concentrations increased, while RDX and its degradation products substantially declined with significant NO_3 decrease, indicating that enhanced RDX biodegradation under the generated anoxic conditions. In contrast, another replicate (T-B) showed no establishment of anoxic conditions, with oxygen levels close to atmosphere for the most of the experiment (Figure 5.5). Cl was much gradually discharged with negligible TOC and lower Mn concentrations in effluent. NO_3 initially increased with Cl breakthrough then gradually declined, but the concentration was still high at the end of monitoring (Figure 5.6). RDX was discharged with some delay compared to control Bay T columns. However, advantageous impact of amendment was limited, presenting two orders of magnitude higher concentration in effluent at the end of experiment (Figure 5.10).

In Bay C columns, amendment addition was not effective in reducing RDX leaching since very little amount of RDX was discharged even in controls. However, it appears that amendment led to enhanced reductive degradation of RDX, exhibiting smaller amount of RDX, similar MNX, smaller DNX, and higher TNX present in treated soils compared to

controls at the end of experiment (Figure 5.12 and Figure S-21). There was no evidence of benefit by amendment addition in reducing HMX leaching and enhancing degradation.

5.5 Conclusions

A laboratory column evaluation demonstrated that extensive TNT degradation can occur under both aerobic and anaerobic conditions in soil, and TNT degradation is less sensitive to changes in soil properties. Experimental results also showed that some RDX will naturally attenuate even in soils that appear to be aerobic. However, natural attenuation of RDX is more dependent on site characteristics, especially soil moisture status. Extensive RDX removal can occur under saturated soil conditions, typically occurring in soils with high silt-clay content. Further research is needed to better understand site conditions controlling monitored natural attenuation (MNA).

Application of substrate mixture containing waste glycerin and Norlig A was effective in generating anoxic conditions in grenade range soil, significantly reducing RDX leaching. The best RDX removal occurred when easily biodegradable carbon penetrated the soil profile. For the successful remediation of range soil, carbon needs to be transported with water to contaminated area before completely consumed.

5.6 References

Amaral, H.I., Gama, A.C., Gonçalves, C., Fernandes, J., Batista, M.J., Abreu, M., 2016. Long-term TNT and DNT contamination: 1-D modeling of natural attenuation in the vadose zone: case study, Portugal. Environ. Earth Sci. 75(1), 1-15.

Bhushan, B., Halasz, A., Spain, J.C., Hawari, J., 2002. Diaphorase catalyzed biotransformation of RDX via N-denitration mechanism. Biochem. Bioph. Res. Co. 296(4), 779-784.

Bordeleau, G., Martel, R., Ampleman, G., Thiboutot, S., 2013. Photolysis of RDX and nitroglycerin in the context of military training ranges. Chemosphere, 93(1), 14-19.

Bradley, P.M. and Chapelle, F.H., 1995. Factors affecting microbial 2,4,6-trinitrotoluene mineralization in contaminated soil. Environ. Sci. Technol. 29, 802-806.

Brannon, J.M. and Pennington, J.C., 2002. Environmental fate and transport process descriptors for explosives. Final report for Strategic Environmental Research and Development Program. ERDC/EL TR-02-10. U.S. Army Engineer Research and Development Center, Vicksburg, MS.

Brannon, J.M., Price, C.B., Hayes, C., and Yost, S.L., 2002. Aquifer soil cation substitution and adsorption of TNT, RDX, and HMX. Soil Sediment Contam. 11(3), 327-338.

Clausen, J., Robb, J., Curry, D., Korte, N., 2004. A case study of contaminants on military ranges: Camp Edwards, Massachusetts, USA. Environ. Pollut. 129(1), 13-21.

Crockett, A.B., Jenkins, T.F., Craig, H.D., Sisk, W.E., 1998. Overview of on-site analytical methods for explosives in soil. CRREL-SR-98-4. Cold Regions Research and Engineering Lab, Hanover, NH.

Farling, S.R., 2013. Generation of biodegradation-sorption barriers for munitions constituents. MS thesis. North Carolina State University, Raleigh, NC.

Felt, D.R., Bednar, A., Arnett, C., and Kirgan, R., 2009. Bio-geochemical factors that affect RDX degradation. Proceedings of the Annual International Conference on Soils, Sediments, Water and Energy. 14(17), 207-215.

Fuller, M.E., Hatzinger, P.B., Rungmakol, D., Schuster, R.L., and Steffan, R.J., 2004. Enhancing the attenuation of explosives in surface soils at military facilities: Combined sorption and biodegradation. Environ. Toxicol. Chem. 23(2), 313-324.

Furey, J.S., Fredrickson, H.L., Richmond, M.J., Michel, M., 2008. Effective elution of RDX and TNT from particles of Comp B in surface soil. Chemosphere, 70(7), 1175-1181.

Harrelson, D.W., Pennington, J.C., Adcock, S.C., Stroud, K.W., 1997. Natural attenuation of explosives at the Louisiana Army Ammunition Plant, Minden, Louisiana.

Hawari, J., Beaudet, S., Halasz, A., Thiboutot, S., and Ampleman, G., 2000. Microbial degradation of explosives: biotransformation versus mineralization. Appl. Microbiol. Biotechnol. 54(5), 605-618.

Heath, R.C., 1994. Ground-Water Recharge in North Carolina. N.C. Dept. of Environment and Natural Resources, DEQ Groundwater Section, Raleigh.

Jenkins, T.F., Topp, G.C., Hewitt, A.D., Grant, C.L., Thiboutat, S., Ampleman, G., Walsh, M.E., Ranney, T.A., Ramsey, C.A., Palazzo, A.J., Pennington, J.C., 2006. Identity and distribution of residues of energetic compounds at army live-fire training ranges. Chemosphere 63(8):1280–1290.

Jenkins, T.F., Walsh, M.E., Thorne, P.G., Thiboutot, S., Ampleman, G., 1997. Assessment of sampling error associated with collection and analysis of soil samples at a firing range

contaminated with HMX. CRREL-SR-97-22. Cold Regions Research and Engineering Lab, Hanover, NH.

Lachance, B., Renoux, A.Y., Sarrazin, M., Hawari, J., Sunahara, G.I., 2004. Toxicity and bioaccumulation of reduced TNT metabolites in the earthworm *Eisenia andrei* exposed to amended forest soil. Chemosphere, 55(10), 1339-1348.

Li, M.Y., Conlon, P., Fiorenza, S., Vitale, R.J., and Alvarez, P.J.J., 2011. Rapid analysis of 1,4-Dioxane in groundwater by frozen micro-extraction with gas chromatography/mass spectrometry. Ground Water Monit. R. 31(4), 70-76.

Lotufo, G.R., Lydy, M.J., 2005. Comparative toxicokinetics of explosive compounds in sheepshead minnows. Arch. Environ. Contam. Toxicol. 49(2), 206-214.

Lynch, J.C., Myers, K.F., Brannon, J.M., Delfino, J.J., 2001. Effects of pH and temperature on the aqueous solubility and dissolution rate of 2,4,6-trinitrotoluene (TNT), hexahydro-1,3,5-trinitro-triazine (RDX), and octahydro-1,3,5,7-tetranitro-1,3,5,7-tetrazocine (HMX). J. Chem. Eng. Data. 46(6), 1549-1555.

Martin, J.L., Comfort, S.D., Shea, P.J., Drijber, R.A., Kokjohn, T.A., 1997. Denitration of 2, 4, 6-trinitrotoluene by *Pseudomonas savastanoi*. Can. J. Microbiol. 43(5), 447-455.

Morris, M.W. Fallin, L., 2010. Effects of reducing conditions on the fate and transport of RDX in groundwater; A multivariate approach. Proceedings of the Annual International Conference on Soils, Sediments, Water and Energy. 13(13).

Pennington, J.C., Brannon, J.M., 2002. Environmental fate of explosives. Thermochim. Acta. 384(1), 163-172.

Pennington, J.C., Brannon, J.M., Gunnison, D., Harrelson, D.W., Zakikhani, M., Miyares, P., Jenkins, T.F., Clarke, J., Hayes, C., Ringleberg, D., Perkins, E., and Fredrickson, H., 2001. Monitored natural attenuation of explosives. Soil Sediment Contam. 10, 45-70.

Rawls, W.J., Pachepsky, Y.A., Ritchie, J.C., Sobecki, T.M., Bloodworth, H., 2003. Effect of soil organic carbon on soil water retention. Geoderma, 116(1), 61-76.

Ringelberg, D.B., Reynolds, C.M., Walsh, M.E., Jenkins, T.F., 2003. RDX loss in a surface soil under saturated and well drained conditions. J. Environ. Qual. 32(4), 1244-1249.

Rylott, E.L., Budarina, M.V., Barker, A., Lorenz, A., Strand, S.E., Bruce, N.C., 2011. Engineering plants for the phytoremediation of RDX in the presence of the co-contaminating explosive TNT. New Phytologist, 192(2), 405-413.

Smith, R.W., Tobias, C., Vlahos, P., Cooper, C., Ballentine, M., Ariyarathna, T., Fallis, S., Groshens, T. J., 2015a. Mineralization of RDX-derived nitrogen to N_2 via denitrification in coastal marine sediments. Environ. Sci. Technol. 49, 2180-2187.

Smith, R.W., Vlahos, P., Bohlke, J.K., Ariyarathna, T., Ballentine, M., Cooper, C., Fallis, S., Groshens, T.J., Tobias, C., 2015b. Tracing the cycling and fate of the explosive 2, 4, 6-trinitrotoluene in coastal marine systems with a stable isotopic tracer, ^{15}N-[TNT]. Environ. Sci. Technol. 49(20), 12223-12231.

Spain, J.C., Hughes, J.B., Knackmuss, H.J., 2000. Biodegradation of nitroaromatic compounds and explosives. Lewis Publishers.

Stenuit, B., Eyers, L., Rozenberg, R., Habib-Jiwan, J.L., Agathos, S.N., 2006. Aerobic growth of Escherichia coli with 2, 4, 6-trinitrotoluene (TNT) as the sole nitrogen source

and evidence of TNT denitration by whole cells and cell-free extracts. Appl. Environ. Microbiol. 72(12), 7945-7948.

Uchimiya, M., Gorb, L., Isayev, O., Qasim, M.M., and Leszczynski, J., 2010. One-electron standard reduction potentials of nitroaromatic and cyclic nitramine explosives. Environ. Pollut. 158, 3048-3053.

U.S. Environmental Protection Agency (EPA). 2014. TNT Fact Sheet (on-line), available from URL https://www.epa.gov/sites/production/files/2014-03/documents/ffrrofactsheet_contaminant_tnt_january2014_final.pdf

Yang, H., Halasz, A., Zhao, J.S., Monteil-Rivera, F., Hawari, J., 2008. Experimental evidence for in situ natural attenuation of 2, 4-and 2, 6-dinitrotoluene in marine sediment. Chemosphere, 70(5), 791-799.

Zhang, B., Cox, S.B., McMurry, S.T., Jackson, W.A., Cobb, G.P., and Anderson, T.A., 2008. Effect of two major N-nitroso hexahydro-1, 3, 5-trinitro-1, 3, 5-triazine (RDX) metabolites on earthworm reproductive success. Environ. Pollut. 153(3), 658-667.

CHAPTER 6. NATURAL AND ENHANCED ATTENUATION OF EXPLOSIVES ON A HAND GRENADE RANGE

6.1 Introduction

Military personnel routinely train on use of hand grenades on small ranges that are few hectares in size, containing several throwing bays. In the US, the M67 fragmentation grenade is common, containing 185 g of Composition B (Comp B) high explosive (HE). Comp B contains approximately 59.5% RDX (hexahydro-1,3,5-trinitro-1,3,5-triazine or Royal Demolition Explosive), 39.4% TNT (2,4,6-trinitrotoluene), 1% wax binder, and HMX (octahydro-1,3,5,7-tetranitro-1,3,5,7-tetreazocine), a major impurity in commercial RDX. When the grenades function as designed and undergo a high order detonation, greater than 99.99% of the explosive is consumed and very little is deposited on the range (Pennington et al. 2003; Hewitt et al. 2005). However, when the munition undergoes a low-order (partial) detonation, then a substantial portion of the explosive load may be deposited on the range as particles of explosive material or as un-exploded ordinance (UXO) (Jenkins et al. 2006).

Jenkins et al. (2006) measured HE concentrations in surface soil at multiple active and closed hand grenade ranges. In the more highly contaminated sites (9 out of 15), TNT levels varied from 0.12 to 36 mg/Kg (ave. = 5.5) and RDX varied from 0.45 to 51 mg/Kg (ave. = 9.6). However, in 6 out of 15 sites, contamination levels were much lower (ave. TNT = 0.04 mg/Kg, RDX = 0.01 mg/Kg).

Accumulation of TNT and RDX on ranges is a concern, since both compounds are classified as possible human carcinogens (C classification) by U.S. Environmental Protection Agency (EPA 2014) with a recommended lifetime drinking water levels of 2 μg/L. TNT and RDX are moderately soluble in water (130 and 56 mg/L, respectively) and weakly bind to soil (Brannon and Pennington 2002; Hatzinger et al. 2004; Jaramillo et al. 2011). At the Massachusetts Military Reservation, large plumes of RDX contaminated groundwater have been identified. While concentrations in groundwater are typically low (RDX < 20 μg/L), concentrations approaching 400 μg/L have been observed (Yamamoto et al. 2004).

TNT and RDX transport to groundwater can be limited by natural and enhanced biodegradation. TNT is biodegradable under both aerobic and anaerobic conditions. Under aerobic conditions, TNT can serve as both a carbon and nitrogen source (Kalderis et al. 2011). Under anaerobic conditions, transport is limited by covalent binding of transformation products to soil surfaces (Szecsody, et al. 2007; Kalderis et al 2011). In laboratory microcosms, extensive removal of TNT was observed under both aerobic and anaerobic conditions (Chapter 3).

Under aerobic conditions, RDX can be used as a nitrogen source by certain organisms (*Stenotrophomonas maltophilia*, *Rhodococcus* sp. Strain DN22 and *Rhodococcus rhodochrous* strain 11Y) under aerobic conditions (Cupples et al. 2010; Kalderis et al. 2011). However, RDX removal rates are often low or zero in aerobic environments (Boopathy and Manning 1996; Hawari et al. 2000; Pennington and Brannon 2002; Bhushan et al. 2006; Kwon and Finneran 2008; Kalderis et al. 2011). Under anaerobic conditions, RDX can be degraded by (a) reduction to hexahydro-1-nitroso-3,5-dinitro-1,3,5-triazine (MNX),

hexahydro-1,3-dinitroso-5-nitro-1,3,5-triazine (DNX), and hexahydro-1,3,5-trinitroso-1,3,5-triazine (TNX) followed by ring cleavage (Hawari et al. 2000); and (b) direct ring cleavage, producing methylenedinitramine (MEDINA) and bis(hydroxymethyl)nitramine that can be further degraded to nitrous oxide (N_2O) and formaldehyde (HCHO) by spontaneous chemical decomposition (Hawari et al. 2001).

In microcosms constructed with soil from Grenade Bays C and T at Fort Bragg, NC, RDX did not significantly biodegrade under aerobic conditions (Chapter 3). However, under anaerobic conditions, RDX rapidly biodegraded without accumulation of MNX, DNX, or TNX. RDX half-lives varied from 5 to 14 days with more rapid degradation with added glycerin (GL) and/or Norlig A (NA) lignosulfonate. In variably saturated column experiments without added organic amendments, extensive RDX removal was observed in columns containing Bay C soil, but lower removal in columns with Bay T soil (Chapter 5). Addition of GL and NA to the surface of the Bay T columns, significantly increased RDX removal.

While there is extensive research demonstrating that TNT and RDX are biodegradable, there is only limited information on the natural and enhanced attenuation of these compounds in the environment. In this project, we evaluate the transport and attenuation of TNT, RDX and HMX in variably saturated soils at an active hand grenade range located at Ft. Bragg, NC. Two different management approaches are evaluated: a) monitored natural attenuation (MNA); and b) organic substrate enhanced attenuation (OSEA). MNA is most effective in fine textured soils that occasionally become saturated during high rainfall periods, reducing oxygen transfer through gas filled soil pores. OSEA involves

addition of soluble, biodegradable organic substrates that increase oxygen consumption. Both approaches can result in anoxic periods that stimulate HE biodegradation, potentially reducing leaching to the water table.

6.2 Material and Methods

This field evaluation was conducted in active hand grenade throwing bays on Range RG40 at Fort Bragg, NC. The spatial distribution of HEs in the soil immediately surrounding the grenade targets in each bay was first determined by excavating a 0.4 m wide x 9 m long x 1.5 m deep trench down the approximate centerline of the throwing area (Figure S-23). Throughout the excavation process, the soil was monitored for the presence of unexploded ordinance (UXO). Soil samples collected from these trenches were analyzed for explosives, metals, and soil characteristics. During excavation, the soil was segregated in 0.3 m lifts, then backfilled in the same sequence (Figure S-24). During backfill, instrumentation clusters were installed at four locations along the length of each trench (Figure S-24). Each cluster consisted of two bucket lysimeters (Soil Moisture Equipment, CA, top of bucket at 0.9 and 1.5 m below ground surface (bgs)), one suction lysimeter with the intake at 1.2 m bgs (Model 1922 Ultra Soil Water Samplers, Soil Moisture Equipment), two electrical resistance moisture sensors (Irrometer Model 200SS WATERMARK at 1.2 and 1.5 m bgs), and two oxidation-reduction potential (Eh) probes at 1.2 m and 1.5 m bgs (Vepraskas and Cox 2002) (Figure S-25). No instrumentation was installed shallower than 0.9 m bgs to prevent damage by grenades during ongoing training exercises. Sampling and monitoring lines were run to the central berm to allow continued monitoring without entering the throwing bays. Samples

could not be collected from some bucket lysimeters during certain monitoring events due to low water volume. During those events, averages were computed from the lysimeters that could be sampled.

After monitoring pore water for 3 months to establish baseline conditions, a 15 m x 30 m area in one of the bays (designated Bay T) was treated by spray application of 755 kg of crude glycerin (Piedmont Biofuels, Pittsboro, NC), 800 kg of Norlig A lignosulfonate (Lignotech USA, Rothschild, Wisconsin.) and 542 L of water, resulting in a net application of 1.7 kg/m^2 of lignosulfonate, 1.6 kg/m^2 of glycerin, and 0.5 cm of fluid (mixture of lignosulfonates, glycerin and water) (Figure S-26). Another throwing bay (Bay C) was treated with an equal volume of NaBr solution and served as an untreated control to evaluate natural attenuation of explosives under ambient conditions. Several hours after amendment addition, there was an intense summer rainstorm and a portion of the applied amendment might have run off. Bay T was selected for amendment addition because the initial Eh, TNT and RDX concentrations were higher. NaBr was not added to the organic amendment applied to Bay T since the crude glycerin contains a substantial amount of KCl that can be used as a tracer. After monitoring soil pore water concentrations for 24 months, the trenches in both bays were re-excavated and sampled to evaluate changes in HE in the soil. Saturated hydraulic conductivity (K_{sat}) was measured in the laboratory (Mohanty et al. 1994) on intact 7.5 cm dia. x 7.5 cm long cores collected at two locations and three depths within each trench.

Analytical methods are described in Appendix I. Briefly, explosives concentrations were determined by gas chromatography (GC) with electron captured detector (ECD) following U.S. Environmental Protection Agency (EPA) Method 8095 to minimize

interferences with humic materials and lignin present in soil and aqueous samples. Prior to GC-ECD analysis, water samples were extracted in toluene by a modified frozen micro-extraction (FME) method (Li et al. 2011). 300 g soil samples were dried at room temperature, ground by puck mill for 60 seconds to reduce the particle size to less than 75 µm, homogenized by random subsampling, and then extracting with acetonitrile for 18 hr in a cooled (< 4 °C) ultrasonic bath following EPA Method 8330b. The filtered supernatant was then analyzed by GC-ECD. Total organic carbon (TOC) was analyzed using Shimadzu 5000A TOC analyzer. Anions (Cl, NO_3, Br, NO_2, and SO_4) were analyzed by ion chromatography (IC) following EPA Method 9056A (SW-846). Cations (Fe and Mn) were analyzed on a Perkin-Elmer Plasma II Inductively Coupled Plasma Atomic Emission Spectrometry (ICP-AES) following methods equivalent to EPA Method 6010C (SW-846).

Soil particle size distribution was measured using a Beckman Coulter LS 13-320 laser particle size analyzer equipped with a Universal Liquid Module. Soil total carbon (TC) content was analyzed using Perkin Elmer 2400 CHNS Analyzer. Soil moisture content and volatile solids were determined by weight losses on drying at 105 °C for 24 hours and ignition in a muffle furnace at 550 °C for 2 hours respectively. Soils samples for iron analysis were extracted using 0.25 M hydrochloric acid (HCl) for Fe(II) and 0.25 m HCL + 0.25 M hydroxylamine hydrochloride ($NH_2OH{\cdot}HCl$) for total Fe (II + III). Extractions were performed in 40 mL EPA vials flushed with nitrogen gas to minimize Fe oxidation, then the extracts were analyzed by ICP-AES. Samples were extracted for 30 minutes to measure poorly crystalline and sediment-bound iron oxides, and for 96 hours to measure crystalline reactive iron oxides.

6.3 Experimental Results

6.3.1 *Field Site Characteristics*

The field demonstration was conducted at hand grenade range RG40 at Fort Bragg, NC, which has been in active use for over twenty years. The two throwing bays (Bay C and Bay T) monitored are ~15 m wide by ~60 m long and separated by a single ~15 m wide soil berm. Throwing targets are typically located in the approximate center of each bay, 30 m from the throwing box. Soils in the area are mapped as Vaucluse loamy sand (fine-loamy, kaolinitic, thermic Fragic Kanhapludults). A typical profile for Vaucluse loamy sand consists of sandy loam (0 to 0.4 m), sandy clay loam (0.4 to 1.5 m), underlain by sandy loam (USDA, 2012). However, much of the Ap and E horizons have been removed from the bays and used to form blast containment berms.

At the start of this project, trenches were excavated down the approximate centerline of two throwing bays with the middle of each trench coinciding with the grenade targets. The trenches were excavated in lifts with composite samples collected at each depth and analyzed for a range of physical and chemical parameters. The first throwing bay was designated as Bay C and was operated as an untreated control. The 2nd bay, designated Bay T, was treated with glycerin (GL) and lignosulfonate (LS).

Figure 6.1 shows soil characterization results including saturated hydraulic conductivity (K_{sat}), silt fraction, clay fraction, organic carbon content, poorly-crystalline and crystalline Fe(II) fraction and total Fe concentrations over the vertical soil profile. Overall, the physical and chemical properties of Bays C and T were similar. Soils in both bays were primarily sand with 9 - 16% silt and 1.4 - 2.6% clay. Soil pH varied from 5.0 to 5.6. Soil pH

(5.4 ± 0.2), silt content (13.4 ± 2.7 %), and median grain size (D_{50} = 296 ± 70 μm) were not statistically different between Bay C and T soils. However, organic carbon (OC), and clay content were significantly higher in Bay C (*p-values* < 0.05). Total iron content varied from 2 to 8 g/Kg with the large majority of the iron present in the crystalline form (Table S-10). Much of the poorly crystalline iron was present as Fe(II) consistent with the soils undergoing periods of anoxic conditions.

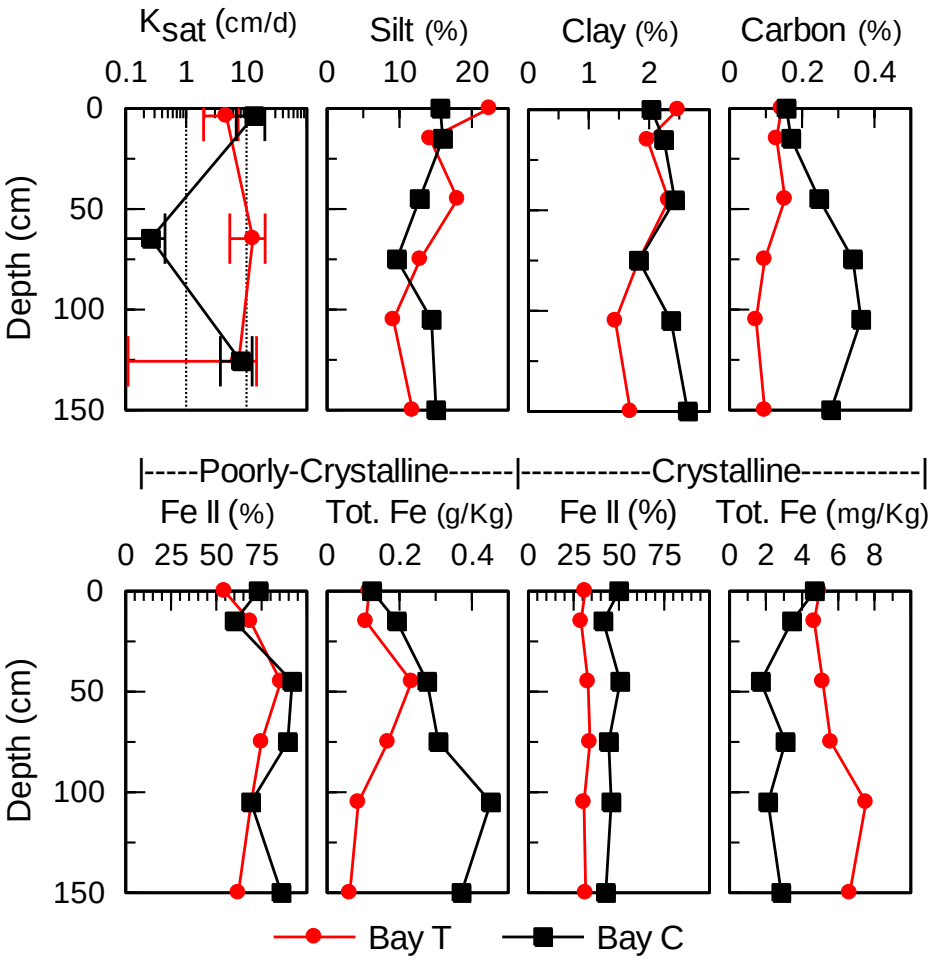

Figure 6.1. Saturated hydraulic conductivity (K_{sat}), silt fraction, clay fraction, organic carbon content, poorly-crystalline and crystalline Fe(II) fraction and total Fe versus depth in Bays T and C.

6.3.2 *Site Hydrology and Biogeochemistry*

Temporal variations in precipitation and evapotranspiration had a significant influence on infiltration and soil moisture. This in turn, influenced oxygen transfer through air filled soil pores and soil redox potential. Figure 6.2 shows cumulative rainfall and cumulative infiltration rates over time in the bucket lysimeters installed in Bay C and Bay T. Infiltration rates were measured by monitoring the total volume of water recovered from each bucket lysimeter normalized to the bucket surface area. Rainfall and evaporation data are from weather station NFBR – Fort Bragg, located 2.2 km north of RG40 (data from the State Climate Office of North Carolina (SCONC)).

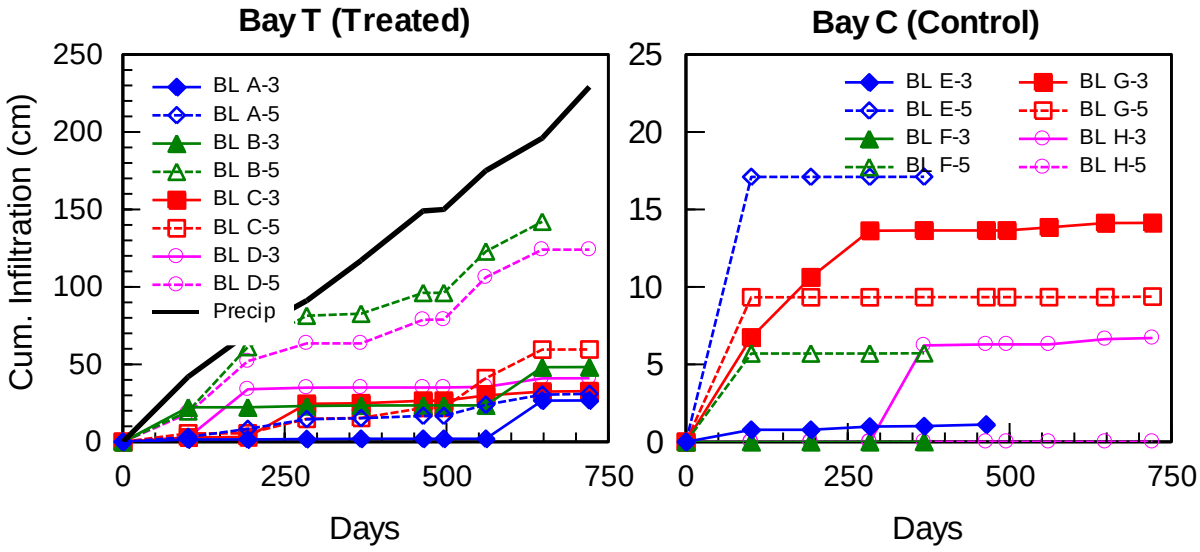

Figure 6.2. Cumulative infiltration measured in bucket lysimeters in throwing bays in comparison to cumulative rainfall.

There were large variations in infiltration rates within each bay and between the two throwing bays. Measured infiltration rates in Bay T bucket lysimeters B-5 and D-5 were

very high, equivalent to 60 - 70% of cumulative rainfall, while other Bay T lysimeters (A-3, A-5, B-3, C-3, C-5, and D-3) were much lower (equivalent to 12 - 26% of rainfall). The cause of the large differences is likely the result of grenade detonation craters that formed over different lysimeters, focusing infiltration in different locations.

In Bay C, there were also significant variations in infiltration between the different bucket lysimeters. However, total infiltration rates were much lower, with cumulative infiltration varying from less than 1% to up to 6% of cumulative rainfall. The low infiltration rates in Bay C are presumably due to the lower permeability of soils in this bay.

Figure 6.3 shows precipitation, reference crop evapotranspiration (ET) and soil moisture for the study period. Electrical resistance in the moisture sensors was converted to water tension using a standard curve generated with their correlation. Climate data are for weather station NFBR – Fort Bragg. ET was estimated using the Modified Penman-Monteith equation (Allen et al. 1998).

High rainfall and low ET in winter and spring of 2013 resulted in high soil moisture contents in both Bays C and T. June 2013 was very wet (total precipitation = 27 cm) resulting in near saturated soil conditions during substrate application. Drier conditions in August through October 2013 allowed the soil in Bay T to drain, while moisture content remained high in Bay C. High ET and relatively low rainfall from April 2014 through October 2014 resulted in a decline in soil moisture in both Bays C and T. Higher rainfall with low ET caused soil moisture to rebound in Winter and Spring of 2015.

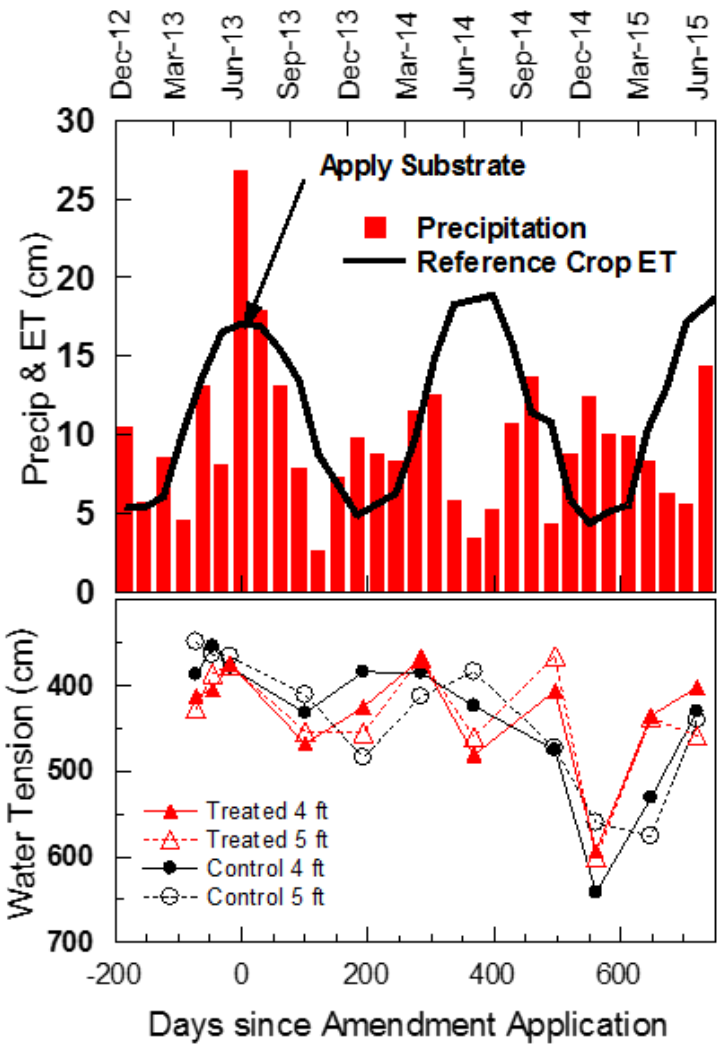

Figure 6.3. Precipitation, potential ET, and soil moisture for December 2012 to June 2015.

Figure 6.4. shows average concentrations of Cl and Br in bucket lysimeters at 0.9 and 1.5 m bgs and suction lysimeters at 1.2 m. In the treated bay, Cl and Br present in the waste glycerin began to breakthrough at 1.2 m after 90 days, reaching a peak at one year after amendment addition. In the control Bay, Br breakthrough from the tracer addition was more variable with two separate pulses observed in the 0.9 m bucket lysimeters. Samples could not be collected from the control bay 1.5 m bucket lysimeters during most sampling events,

so Br breakthrough could not be monitored at this depth. Cl was not applied to the control bay, so concentrations remained low (8 ± 2 mg/L).

Organic carbon breakthrough in the treated bay followed a similar pattern to Cl and Br, with peak TOC concentrations observed at about one year after amendment application (Figure 6.4). TOC concentrations in the control bay were more variable and did not follow any clear pattern. The elevated levels of TOC in Bay C are presumably associated with the higher organic carbon content of these soils (Figure 6.1).

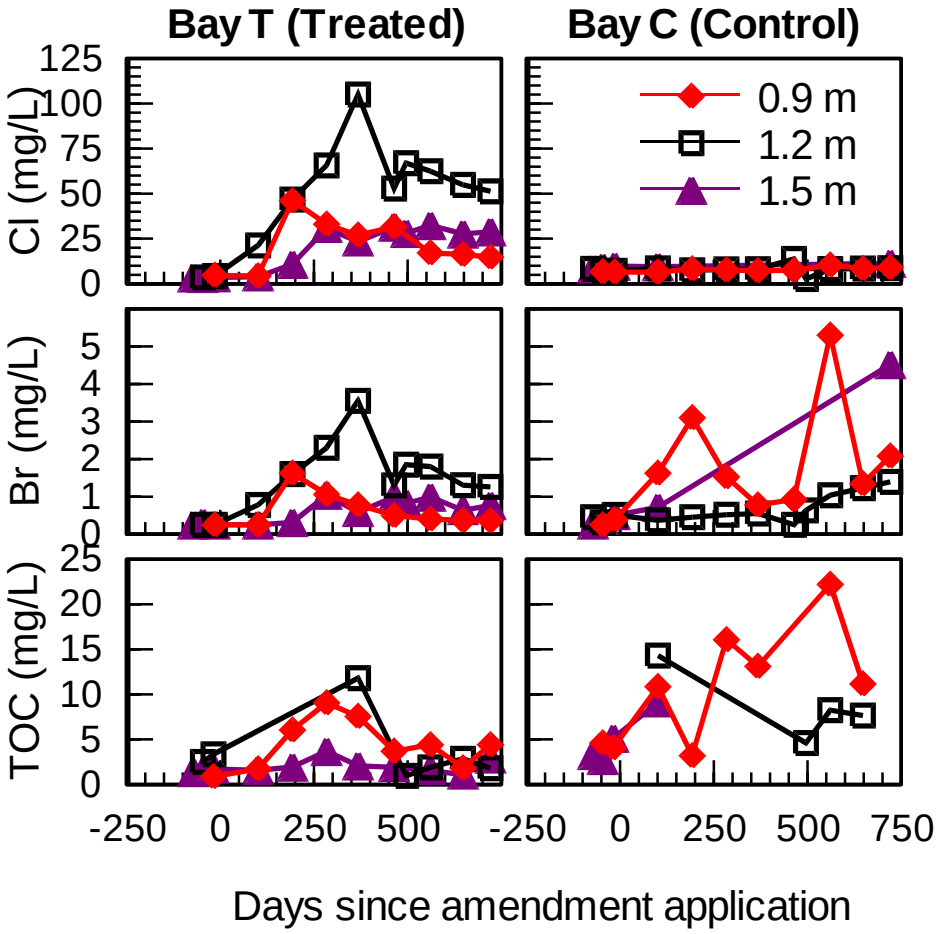

Figure 6.4. Temporal variations in chloride (Cl), bromide (Br) and TOC in throwing bays at 0.9, 1.2 and 1.5 m bgs.

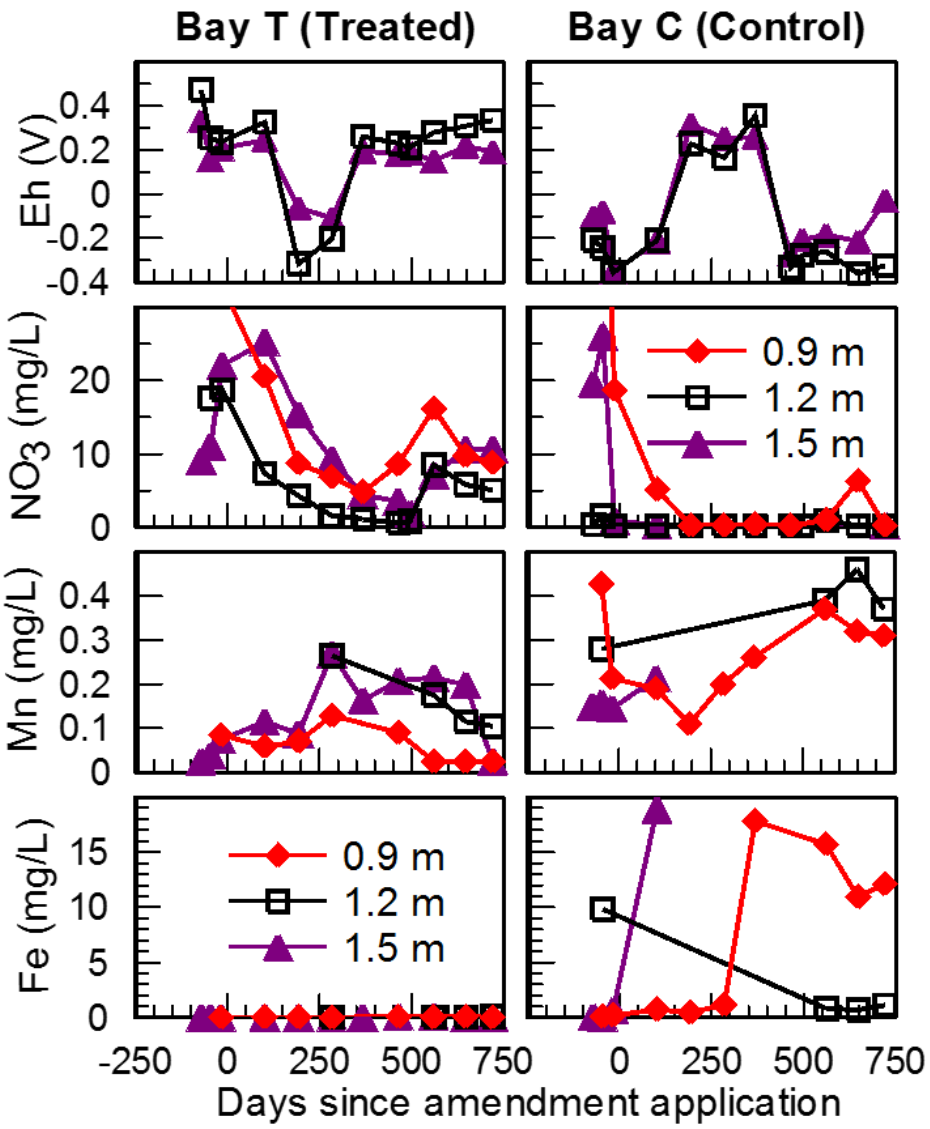

Figure 6.5. Temporal variations in Eh, nitrate (NO_3), manganese (Mn), and iron (Fe) in throwing bays at 0.9, 1.2 and 1.5 m bgs.

Substantial variations in soil oxidation-reduction potential (Eh), NO_3, Mn and Fe (Figure 6.5) were observed in response to variations in soil moisture and amendment application. In Bay C (control), Eh initially declined (reducing conditions) with a concurrent drop in NO_3, presumably due to the high soil moisture, warmer summer temperatures, and

higher organic carbon content of the Bay C soils. In Bay T, Eh declined with the arrival of organic carbon (Figure 6.5) following organic amendment application, and then rebounded as TOC declined. NO_3 followed a similar pattern to Eh in Bay T, but changes in NO_3 lagged Eh by several months. Mn increased in Bay T concurrent with the NO_3 decline. Fe concentrations in Bay T remained below 0.15 mg/L throughout the monitoring period, indicating only moderately reducing conditions. In Bay C, Mn and Fe were occasionally elevated, indicating more strongly reducing conditions. However, there was no obvious pattern to the variations in Mn and Fe over time. There was no significant change in the fraction of Fe(II) present in the poorly-crystalline or crystalline phases in either bay, in soil profiles measured in March 2013 (prior to amendment application) and July 2015 (two years after amendment application) (data not shown).

6.3.3 *Explosives*

Figure 6.6 presents the number of grenades thrown per bay per month and a linear trend of the numbers. Much higher number of grenades were thrown during the periods of installation of monitoring and sampling instrumentation (Mar 2013) and organic substrate application (July 2013). Less than average number of grenades (158.5) were thrown on the Bays C and T during 71 % of the entire monitoring period. However, the amount of explosives deposited on the surface soil is not proportional to the number of grenades thrown on the bays since they are typically deposited on the range when grenades undergo a low-order (partial) detonation (Jenkins et al. 2006). The exact amount of HE deposited is

unknown. However, a substantial amount of HE was likely deposited on the Bays C and T due to constant use of the Bays for the military training.

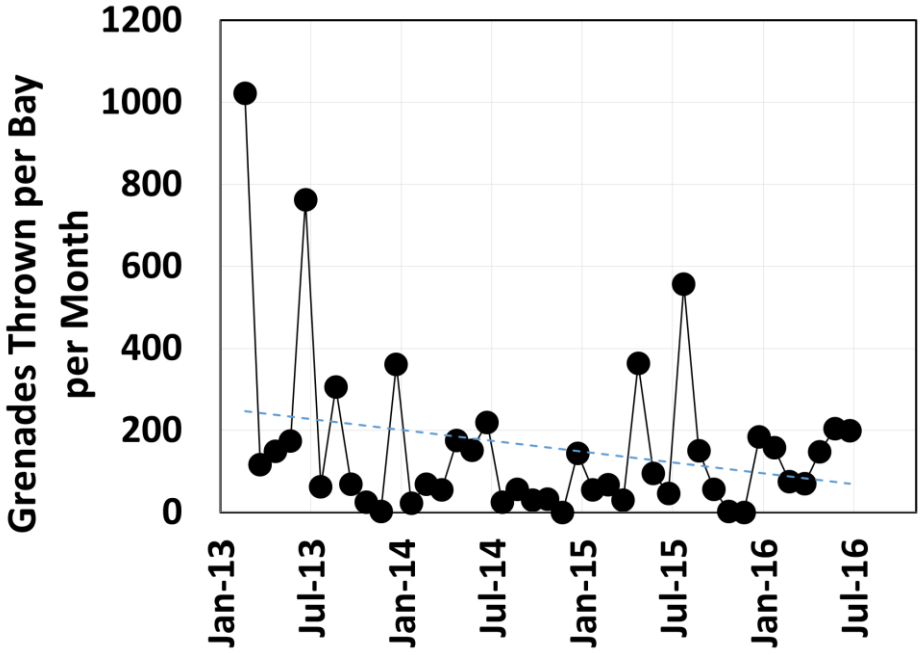

Figure 6.6. Number of grenades thrown per Bay per month. Dashed line presents a linear trend of the numbers.

Figure 6.7 shows the variation in the average concentrations of TNT, RDX, HMX, MNX, DNX and TNX in the bucket lysimeters (0.9 and 1.5 m) and suction lysimeters (1.2 m) in Bays T and C. Detectable levels of TNT were initially observed in several different lysimeters in both bays. However, TNT levels dropped below the detection limit (1 µg/L) in all samples by 100 days, and concentrations remained near or below the detection limit for the remainder of the project.

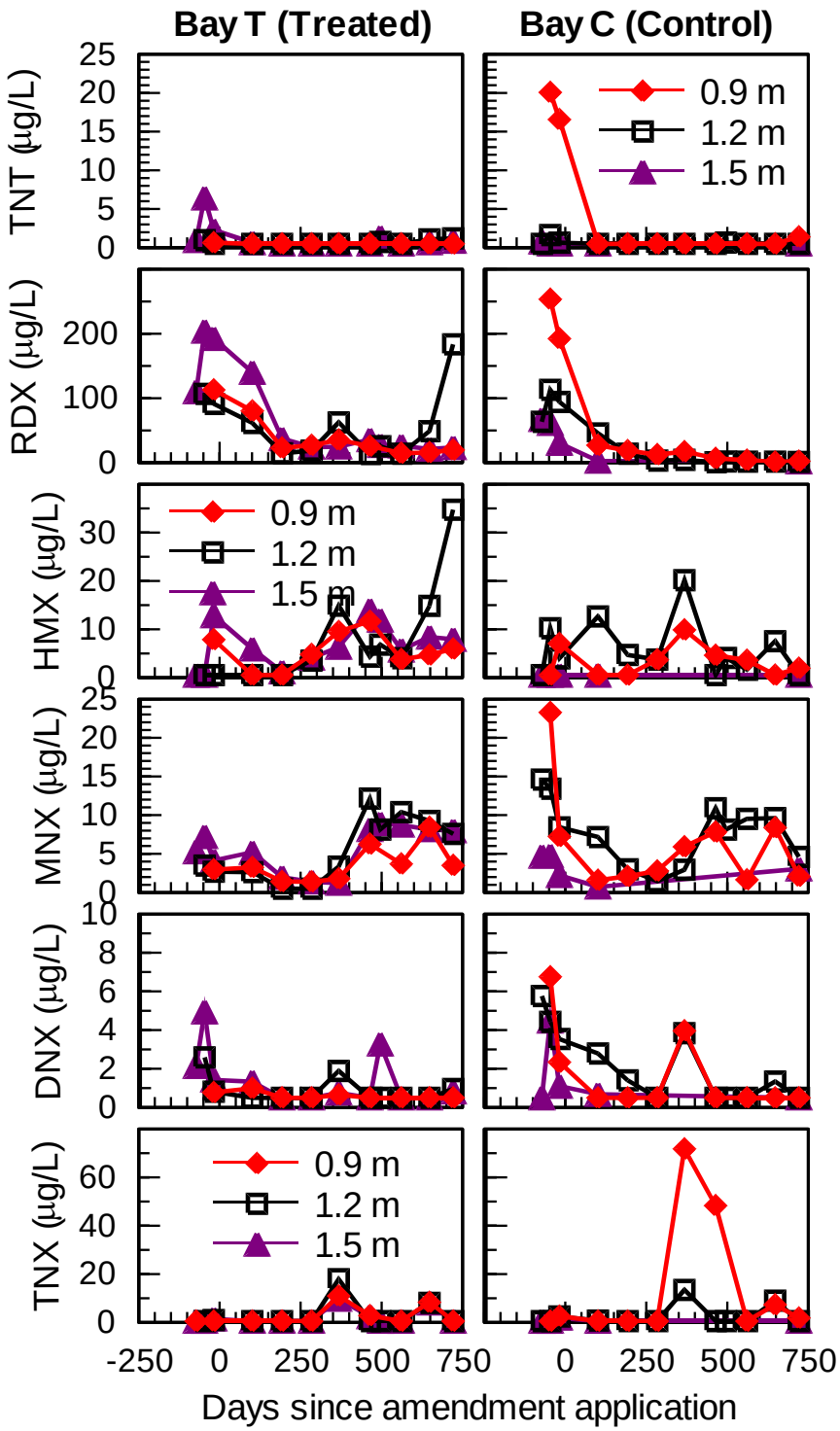

Figure 6.7. Temporal variations in TNT, RDX, HMX, MNX, DNX, and TNX in throwing bays at 0.9, 1.2 and 1.5 m bgs.

RDX was also present in pore water samples collected throughout both Bay T and C at the start of the project. In Bay C, RDX levels declined with the onset of reducing conditions and remained low for the duration of the project. In Bay T, RDX levels declined with the arrival of TOC from the organic amendment and depletion of NO_3. Low levels of RDX nitroso degradation products (MNX, DNX and TNX) were detected throughout the monitoring period in both bays, indicating anaerobic biotransformation of RDX. HMX levels varied throughout the monitoring period in both bays and did not follow any obvious patterns.

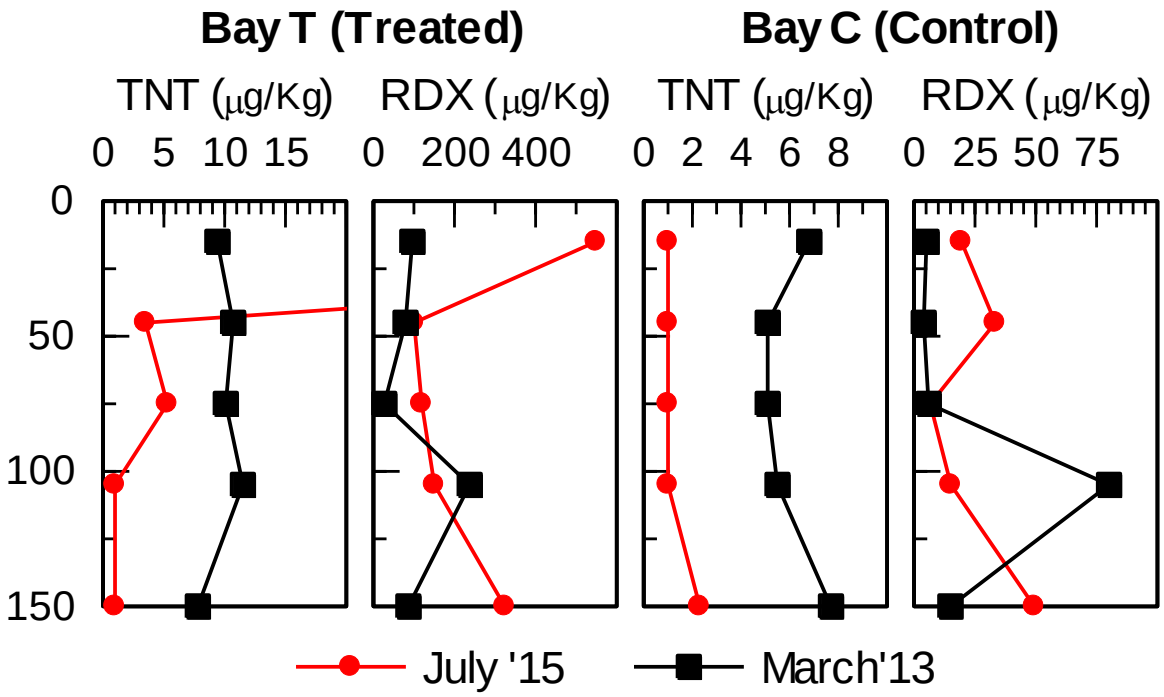

Figure 6.8. TNT and RDX concentrations in soil in Bays T and C in Marcy 2013 - prior to amendment application and July 2015 – two years after amendment application.

Figure 6.8 shows average TNT and RDX concentrations in soils from Bays T and C in March 2013 - prior to amendment addition, and in July 2015 - two years after amendment addition. In March 2013, average RDX and TNT concentrations were higher in Bay T than Bay C soil (*p-value* < 0.05). However, in July 2015, there was no significant difference between the two bays. Between 2013 and 2015, average TNT concentrations declined in Bay C (*p-value* < 0.05), but there was no significant change in average RDX in Bay C or average RDX and TNT concentrations in Bay T.

6.4 Discussion

Ongoing use of hand grenade ranges for training can result in accumulation of TNT, RDX, and other material in surface soil. While the Comp B explosive present in fragmentation grenades is approximately 39% TNT, TNT concentrations in pore water were below detection (<1 µg/L) for most of the monitoring period. This is consistent with laboratory microcosm results which showed extensive removal of TNT in both aerobic and anaerobic laboratory microcosms containing soil from Bay C, Bay T and a nearby sand quarry (Chapter 3). Similar results were found at two grenade bays at Fort Jackson, SC where TNT concentrations in soil were very low and TNT in pore water samplers were consistently < 1 µg/L (Larsen et al. 2008).

RDX, the other major component of Comp B, was initially detected at significant concentrations in both Bays C and T. During the first 3 months of monitoring, RDX levels in bucket and suction lysimeters varied between 1 and 454 µg/L. In control Bay C, reducing conditions resulted in a rapid decline in NO_3, increase in dissolved Mn, and decline in RDX.

Similar results were observed in laboratory column experiments containing Bay C soil, where saturated, anoxic conditions reduced RDX leaching by 93% (Chapter 5). Larsen et al. (2008) observed similar results at Fort Jackson, SC, where RDX levels varied from < 1 µg/L to 3,200 µg/L (ave. = 435 ug/L) in suction lysimeters installed below an untreated grenade bay. Similar to Bay C at Fort Bragg, RDX levels were high in winter and spring, declining to low levels in summer. Concurrent with the decline in RDX, redox potential decreased and soluble Fe increased (Larsen et al. 2008).

In Treated Bay T, Cl, Br and TOC associated with glycerin (GL) and Norlig A (NA) lignosulfonate addition was observed in bucket and suction lysimeters several months after amendment application. With the arrival of TOC, the pore water became reducing with a decline in Eh and NO_3, increase in Mn and decline in RDX. Similar results were observed in Bay T soil column experiments, where Cl and small amounts of TOC discharged in the column effluent at 6 - 12 months after GL and NA addition (Chapter 5). Shortly after TOC breakthrough, NO_3 declined, Mn increased, and RDX declined. However, once TOC was depleted, NO_3 recovered, Mn declined, and RDX started to rebound. While the GL+NA addition did not provide permanent treatment, the total mass of RDX discharged was reduced by an average of 76% compared to untreated control columns.

The average annual mass loadings of RDX collected in the deep bucket lysimeters varied from 8 to 63 µg/m^2/yr in Bay T (ave. = 40 µg/m^2/yr) and from 1 to 56 µg/m^2/yr in Bay C (ave. = 15 µg/m^2/yr). Average RDX concentrations were somewhat higher in Bay T, much of this variation was associated with the higher infiltration rates at some locations (21 to 85

cm/yr in Bay T, 6 to 35 cm/yr in Bay C) believed to be associated with blast craters that formed around the grenade targets.

6.5 Conclusions

Relatively small differences in soil physical and chemical properties between the two bays, resulted in large differences in infiltration rates, biogeochemical conditions, and RDX leaching. Additional research is needed to better understand the interrelationships between these processes and develop methods to identify when natural attenuation processes are sufficient to control RDX leaching.

Addition of GL and NA resulted in anoxic conditions and reduced RDX leaching for about one year after amendment addition in Bay T. Additional research is needed to identify soil conditions where this approach will be effective in reducing leaching and to identify alternative substrates that are more effective and long-lasting.

6.6 References

Allen, R.G., Pereira, L.S., Raes, D., Smith, M., 1998. Crop evapotranspiration - Guidelines for computing crop water requirements - FAO Irrigation and drainage paper 56, Food and Agriculture Organization of the United Nations, Rome.

Boopathy, R., Manning, J.F., 1996. Characterization of partial anaerobic metabolic pathway for 2,4,6-trinitrotoluene degradation by a sulfate-reducing bacterial consortium. Can. J. Microbiol. 42(12), 1203-1208.

Brannon, J.M. and Pennington, J.C., 2002. Environmental fate and transport process descriptors for explosives. Final report for Strategic Environmental Research and Development Program. ERDC/EL TR-02-10. U.S. Army Engineer Research and Development Center, Vicksburg, MS.

Bhushan, B., Halasz, A., Hawari, J., 2006. Effect of iron(III), humic acids and anthraquinone-2,6-disulfonate on biodegradation of cyclic nitramines by Clostridium sp. EDB2. J. Appl. Microbiol., 100(3), 555-563.

Cupples, A.M., 2010. Development of biomarkers for assessing in situ RDX biodegradation potential. Michigan State University East Lansing College of Engineering.

Hawari, J., Beaudet, S., Halasz, A., Thiboutot, S., Ampleman, G., 2000. Microbial degradation of explosives: biotransformation versus mineralization. Appl. Microbiol. Biotechnol. 54(5), 605-618.

Hawari, J., Halasz, A., Beaudet, S., Paquet, L., Ampleman, G., Thiboutot, S., 2001. Biotransformation routes of octahydro-1, 3, 5, 7-tetranitro-1, 3, 5, 7-tetrazocine by municipal anaerobic sludge. Environ. Sci. Technol. 35(1), 70-75.

Kwon, M.J., Finneran, K.T., 2008. Biotransformation products and mineralization potential for hexahydro-1,3,5-trinitro-1,3,5-triazine (RDX) in abiotic versus biological degradation pathways with anthraquinone-2,6-disulfonate (AQDS) and Geobacter metallireducens. Biodegradation. 19(5), 705-715.

Szecsody, J.E., Crocker, F.H., Comfort, S., Girvin, D.C., Fredrickson, H.L., Resch, C.T., Boparai, H.K., Shea, P., Devary, B.J., Fischer, A.E., Thompson, F., Durkin, L.M., Phillips, J.L., 2007. Enhancement of In Situ Bioremediation of Energetic Compounds by Coupled

Abiotic/Biotic Processes. PNNL-16754. Engineer Research and Development Center. Vicksburg, MS.

Hatzinger, P.B., Fuller, M.E., Rungmakol, D., Schuster, R.L., Steffan, R.J., 2004. Enhancing the attenuation of explosives in surface soils at military facilities: Sorption-desorption isotherms. Environ. Toxicol. Chem. 23(2), 306-312.

Hewitt, A.D., Jenkins, T.F., Walsh, M.E., Walsh, M.R., Taylor, S., 2005. RDX and TNT residues from live-fire and blow-in-place detonations. Chemosphere 61, 888–894.

Jaramillo, A.M., Douglas, T.A., Walsh, M.E., Trainor, T.P., 2011. Dissolution and sorption of hexahydro-1, 3, 5-trinitro-1, 3, 5-triazine (RDX) and 2, 4, 6-trinitrotoluene (TNT) residues from detonated mineral surfaces. Chemosphere, 84(8), 1058-1065.

Pennington, J.C., Jenkins, T.F., Ampleman, G., Thiboutot, S., Brannon, J.M., Lynch, J., Ranney, T.A., Stark, J.A., Walsh, M.E., Lewis, J., Hayes, C.H., Mirecki, J.E., Hewitt, A.D., Perron, N.M., Lambert, D.J., Clausen, J., Delfino, J.J., 2003. Distribution and fate of energetics on DoD test and training ranges: Interm Report 3. Technical Report ERDC TR-03-2. US Army Engineer Research and Development Center, Vicksburg, MS.

Jenkins, T.F., G.C. Topp, A.D. Hewitt, C.L. Grant, S. Thiboutat, G. Ampleman, M.E. Walsh, T.A. Ranney, C.A. Ramsey, A.J. Palazzo, J.C. Pennington. 2006. Identity and distribution of residues of energetic compounds at army live-fire training ranges. Chemosphere 63(8):1280–1290.

Kalderis, D., Juhasz, A.L., Boopathy, R., Comfort, S., 2011. Soils contaminated with explosives: Environmental fate and evaluation of state-of-the-art remediation processes. Pure Appl. Chem. 83(7), 1407-1484.

Larson, S.L., Davis, J.L., Martin, W.A., Felt, D.R., Nestler, C.C., Fabian, G., O'Connor, G., Zynda, G. Johnson, B.A., 2008. Grenade range management using lime for dual role of metals immobilization and explosives transformation. Field demonstration at Fort Jackson, SC. ERDC/EL-TR-08-24. Engineer Research and Development Center, Vicksburg, MS.

Mohanty, B.P., Kanwar, R.S., Everts, C.J., 1994. Comparison of saturated hydraulic conductivity measurement methods for a glacial-till soil. Soil Science Society of America Journal, 58(3), 672-677.

Pennington, J.C., Brannon, J.M., 2002. Environmental fate of explosives. Thermochimica acta. 384(1), 163-172.

U.S. Environmental Protection Agency (EPA). 2014. RDX Fact Sheet (on-line), available from URL http://www2.epa.gov/sites/production/files/2014-03/documents/ffrrofactsheet _contaminant _rdx_january2014_final.pdf

U.S. Environmental Protection Agency (EPA). 2014. TNT Fact Sheet (on-line), available from URL https://www.epa.gov/sites/production/files/2014-03/documents/ffrrofactsheet_contaminant_tnt_january2014_final.pdf

U.S. Department of Agriculture (USDA), 2012. Natural Resources and Conservation Service, Web Soil Survey (WSS) http://websoilsurvey.nrcs.usda.gov/app/HomePage.htm, Data downloaded on 12/27/11.

Vepraskas, M.J., Cox, J.L., 2002. Redox potential measurements, North Carolina State University. Soil Science Department. Raleigh, NC.

Yamamoto, H., Morley, M.C., Speitel, G.E. Jr., Clausen, J., 2004. Fate and transport of high explosives in a sandy soil: adsorption and desorption. Soil Sediment Contam. 13(5), 361-379.

CHAPTER 7. CONCLUSIONS AND RECOMMENDATIONS FOR FURTHER RESEARCH

7.1 Conclusions

Soil microcosm, batch sorption, laboratory soil column, and field pilot studies were conducted to improve our understanding of processes controlling leaching of high explosives (HE) at grenade ranges, including the impact of crude glycerin (GL) and lignosulfonate (LS) addition on HE biodegradation, sorption of TNT and RDX to field sand and range soil, and the impact of LS addition on sorption.

Microcosm results demonstrated rapid TNT biodegradation under both aerobic and anaerobic conditions regardless of organic amendment addition. Under aerobic conditions, there was no significant biodegradation of RDX, HMX, or RDX degradation products. However, RDX and HMX were significantly biodegraded under anaerobic condition, without accumulation of TNT or RDX daughter products. Addition of GL and LS enhanced oxygen consumption in microcosms containing grenade range soil, increasing the oxygen consumption rate more than 200 % over untreated soils. Results indicate that organic amendment (GL + LS) addition can potentially be effective in generating anoxic conditions and stimulating anaerobic HE biodegradation.

Sorption batch studies showed that both LS and HE sorption followed nonlinear sorption in soils used in this study. Greater sorption of Ultrazine CA (UCA) was observed in range soil (RS) compared to field sand (FS). UCA also more strongly sorbed to FS than NA.

NA was weakly bound to RS, and desorbed easily during repeated washing of the sediment, indicating it could potentially migrate deeper into the soil stimulating biodegradation. RDX more strongly sorbed to RS than FS, with similar sorption capacity to TNT. NA amendment did not substantially increase overall TNT and RDX sorption to both RS and FS. Nonlinear sorption needs to be considered as an important factor influencing HE transport since HE retention is concentration dependent.

Soil column experiment results showed that TNT was rapidly and extensively degraded under both aerobic and anaerobic conditions, consistent with results from the prior microcosm study. Although some RDX natural attenuation was observed in columns that were usually aerobic, removal was more rapid under anoxic conditions. Soil moisture status is a major control on the development of anoxic conditions and resulting RDX biodegradation. However, further research is needed to better understand the impact of site conditions on monitored natural attenuation (MNA) of HEs.

The experimental results showed that organic amendment (GL + LS) addition was effective in generating anoxic conditions in one soil column, significantly reducing RDX leaching. However, the added organic amendment was consumed in about one year. Extensive RDX removal occurred when TOC from amendment addition was present in the column effluent. Further research will be necessary to improve treatment longevity and reduce amendment reapplication frequency.

Field monitoring results demonstrated that relatively minor changes in soil properties resulted in major changes in geophysical and geochemical conditions in two grenade bays, influencing RDX leaching. When range soils periodically become anaerobic, RDX leaching

will be reduced. However, further research is needed to improve our understanding of the factors controlling natural attenuation. Organic amendment application reduced RDX leaching in one grenade bay, concurrent with transition from aerobic to anaerobic conditions. However, the amendment addition only reduced soil redox for about a year, consistent with the column results. Additional research is needed to improve amendment longevity and identify soil conditions where this remediation technology will be effective in reducing explosives leaching.

7.2 Recommendations for Further Research

The column and field study showed that soil moisture status is a major factor controlling natural attenuation of HE in soil. Prior research has shown that precipitation and clay content can strongly influence soil moisture. Numerical modeling studies would be useful to evaluate the impact of soil properties, climate and organic amendment addition on redox status and RDX attenuation. Important parameters required for model simulations were generated as part of this study. The conditions which can lead to saturated soil conditions could be determined by simulating various scenarios including varying clay contents and precipitation. The model results could then be validated by comparison with the column or field results generated in this study.

This study demonstrated that addition of GL + LS was effective in generating anoxic conditions and reducing leaching of HEs in soil. However, column and field evaluation results showed that the organic amendment and the associated reduction in explosive leaching lasted about one year. Additional research is needed to identify soil conditions

where this amendment will be more effective in reducing HEs leaching and improve the longevity of treatment. For better treatment longevity, alternative organic substrates should be considered. GL is rapidly biodegradable and LS is slowly biodegradable. Organic substrate that biodegrade at a rate intermediate between GL and LS would be useful. Potential alternatives could be evaluated in soil microcosm studies and compared to oxygen consumption by GL.

Amending soil with GL and LS could also be applied to treat other contaminants that are more degradable under anoxic conditions. However, site characterization will be required prior to the field application. Oxygen consumption and transport rates should be determined for the target site to determine an appropriate loading rate for the organic amendment.

APPENDICES

APPENDIX I. Experimental and Analytical Methods

I.I. Water Sample Extraction and Analytical Method for Explosives

All explosives concentrations were determined by gas chromatography (GC) with an electron capture detector (ECD) following U.S. Environmental Protection Agency (EPA) Method 8095 to minimize interferences with humic materials and lignin present in aqueous samples. Water samples containing explosives were extracted prior to GC-ECD analysis by the revised frozen micro-extraction (FME) method. Approximately 5 mL of water sample was filtered through a 0.2 µm PTFE syringe filter and the first 2 mL of filtrate was discarded. The remained 1 mL of the filtered sample was transferred into a 4 mL Teflon-capped target vial followed by addition of 1 mL toluene. Vials were mixed by a vortex for 30 seconds and shaken on a table shaker for 2 hours after packed in an insulated box filled with ice to minimize thermal decomposition of explosives. Vials then were placed in a - 80 ºC for 30 min to separate toluene by freezing water. After freezing, the toluene was transferred to amber target vials and stored at - 20 ºC until analyzed by GC-ECD.

Explosives were analyzed by GC-ECD by injecting 2 µL extract in toluene into an Agilent 7890A GC equipped with a cool-on-column inlet, 7.5 m long-0.53 mm diameter-1.5 µm film thickness DB-5ms column, and 1.0 m Restek retention gap column, with helium as the carrier gas (10 mL/min) and nitrogen as the makeup gas (60 mL/min). The detector temperature was 325 ºC. The different analytes were separated with the following temperature program: 75 ºC for 0.1 min, increased at 15 °C per min to 200 ºC, then increased at 20 ºC per min to 300 °C, then held for 5.5 min. The autosampler tray was cooled to ~ 4 ºC

to minimize thermal decomposition of the samples. The cool-on-column injector was used to minimize decomposition of RDX and HMX. However, some losses still occurred. To further minimize this effect, a series of stock standards in toluene were analyzed to fill any active sites on the column prior to running any experimental samples. All experimental samples were run in duplicate. If the differences between duplicates were greater than 10 %, the samples were rerun until consistent results were obtained. Analytical standards and blanks were analyzed at the beginning, middle, and end of each run.

I.II.Analytical Methods for Carbon, Anions, and Cations

Total carbon and inorganic carbon were analyzed using Shimadzu 5000A TOC analyzers following manufacturer's instructions. Anions (nitrate, nitrite, chloride, bromide, and sulfate) were analyzed by ion chromatography (IC) following EPA methods 314.0 and SW-846 9056. Cations (Fe and Mn) were analyzed on a Perkins Elmer Plasma II Ion Coupled Plasma Atomic Emission Spectrometer (ICP-AES) following methods equivalent to SW-846 6010C.

I.III. Analytical Methods for Gas Samples

Soil gas samples were collected by attaching a syringe with 3-way valve, opening the valve to collect gas, and then closing the valve. Soil gas samples were analyzed by gas chromatography (GC) with a thermal conductivity detector (TCD) and flame ionization detector (FID).

Head space gas samples were collected by attaching a syringe with 3-way valve to the rubber stopper on a serum bottle, opening the valve to collect gas, and then closing the valve. Head space gas samples were also analyzed by GC-TCD and FID.

I.IV. Column Destruction and Analytical Methods for Soil Samples

All columns were cut into eleven, 10 cm long segments, using a large pipe cutter, including drain layer composed of fine and coarse sands at the bottom of each column. Soil samples collected from each section of columns were homogenized and stored in clean mason jars. Samples for Fe(II/III) analysis were subsampled into 40 mL EPA vials immediately after soil sample collection from the column destruction, flushed with nitrogen gas to minimize oxidation of iron content in soil, and stored in a freezer for later pretreatment and analysis.

Moisture content was measured on the same day of column destruction to minimize experimental errors by change in moisture over time. 20 g of each soil sample was placed in aluminum weighing dishes and moisture content was determined by measuring weight loss on drying at 105 °C for 24 hours. 10 g of the soil samples dried at 105 °C was subsampled into crucibles and volatile solids was measured by weight loss on ignition in a muffle furnace at 550 °C for 2 hours. Ash content was determined by measuring the remaining solid content after ignition at 550 °C. Total carbon content of each soil section was analyzed using Perkin Elmer 2400 CHNS Analyzer by Environmental and Agricultural Service (EATS) in Department of Soil Science at NCSU. Organic carbon content of soil was analyzed by the same method for total carbon after inorganic carbon was removed by solution containing

sulfuric acid (H_2SO_4) and ferrous sulfate heptahydrate ($FeSO_4*7H_2O$). All samples were analyzed in duplicate and samples were reanalyzed if difference in duplicate is over 10 %.

For explosive analysis, approximately 300 g of each sample was dried at room temperature. The dried samples were ground by puck mill for 60 seconds to reduce the particle size to less than 75 µm. The entire ground soil was spread out on a clean aluminum foil, and then 10 g of the ground soil was subsampled by randomly collecting more than 30 increments. The subsample was placed in 40 mL Teflon-capped EPA vial, followed by addition of 20 mL acetonitrile. Vials were placed in a cooled (< 4 °C) ultrasonic bath and sonicated for 18 hours, and then were allowed to settle for 30 min. Supernatant was filtered through 0.2 µm syringe filters and collected in 2 mL clear target vials after discard of 5 mL filtrate. Then the extract was stored at - 20 °C until analyzed by GC-ECD.

Samples for Fe(II/III) analysis were extracted using HCl and HAHCl reagents, following the method used by Farling (2013). Detailed extraction method is described below. The extracts were analyzed by ICP-AES.

I.V. Characterization of Soil Samples

Particle size distribution was measured using a Beckman Coulter LS 13-320 laser particle size analyzer equipped with a Universal Liquid Module by the Department of Marine, Earth and Atmospheric Science at NCSU. Total carbon was analyzed using Perkin Elmer 2400 CHNS Analyzer. Heavy metals were measured by acid digestion following method EPA 3050 B using a 1:1 ratio of 12.1 N HCl to 15.8 N HNO_3 and 30% H_2O_2, followed by ICP-AES analysis. The Fe(II/III) content was determined by extraction using 0.25 M

hydroxylamine hydrochloride in 0.25 M HCl (HAHCl) and 0.25 M HCl with two extraction periods (30 minutes and 96 hours), then the extracts were analyzed by ICP-AES. The different extraction techniques were applied for the following iron forms: (1) 30-minute extractions – poorly crystalline and sediment-bound iron oxides, (2) 96-hour extractions – crystalline reactive iron oxides, (3) HAHCl extractions – total [Fe(II) and Fe(III)] iron oxides, and (4) HCl extractions – ferrous [Fe(II)] iron oxides. Water retention was measured at 0, 30, 60, 100, 333, and 500 cm of H_2O. Saturated hydraulic conductivity was determined using intact ring samples with dimensions of 7.6 cm diameter by 7.6 cm tall. TC, heavy metals, Fe(II/III), water retention, and saturated hydraulic conductivity were measured by EATS in the Department of Soil Science at NCSU. Cation exchange capacity (CEC) was determined by the Agronomic Services Division in NC Department of Agriculture and Consumer Services.

I.VI. Monitoring Instrumentation at a Hand Grenade Range

The bucket lysimeters (Part 1960, Soil Moisture Equipment, CA) consist of a 5-gallon pail with a porous top allowing infiltrating water to enter the bucket and collect over time, allowing estimation of infiltration rates and to monitor chemical constituents. The suction lysimeter (Model 1922 Ultra Soil Water Samplers, Soil Moisture Equipment) is a cylindrical device consisting of a porous ceramic cup (to withdraw soil pore water using a vacuum); a reservoir; and a two-hole stopper assembly for pulling a vacuum and retrieving the sample. After installation below ground level, vacuum is applied to the bucket and suction lysimeters through tubing leading from the lysimeter to the sampling station located between the

throwing bays at ground surface. The negative air pressure created inside the lysimeter draws pore water into the lysimeter through the porous section of the lysimeter. After allowing the sample collection reservoir to fill with water for several hours, the pore water is transported to the surface by applying positive pressure to the lysimeter through a second tube. At the surface, the pore water is collected directly into a laboratory prepared sample container appropriate for the analytical method being used. The moisture sensors are Irrometer Model 200SS WATERMARK sensors with 25 ft long leads. The redox probes were custom manufactured as described by Vepraskas and Cox (2002) and were installed in parallel with a Ag/AgCl reference electrode (Fisher Scientific) and monitored by measuring the voltage generated between the redox probe and reference electrode with a standard voltmeter (Fisher Scientific). All monitoring equipment was assembled and tested prior to installation in the field.

APPENDIX II. Supplementary Material for Batch Study

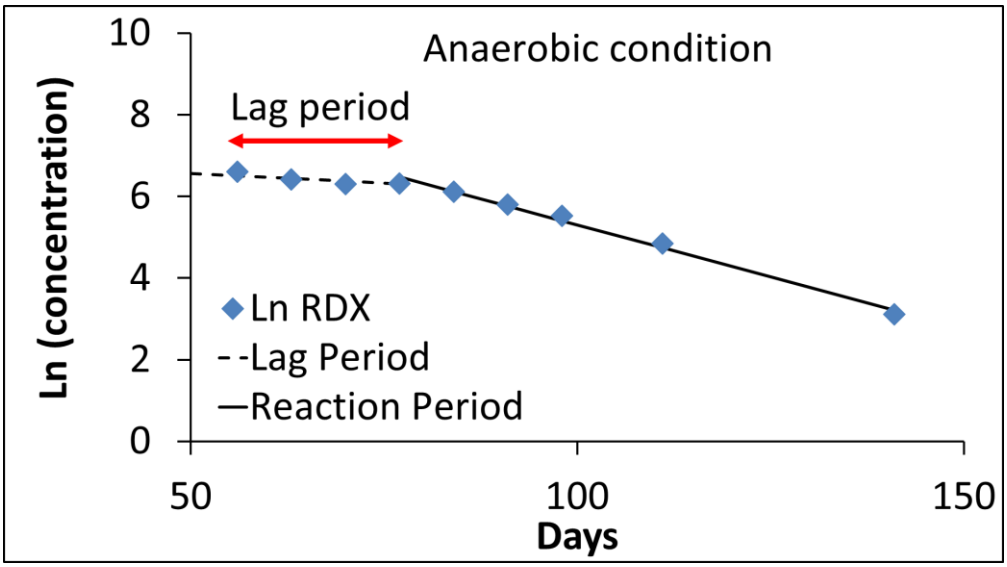

Figure S-1. Example of first-order RDX degradation rate estimated by searching for regression that generated highest F-statistic.

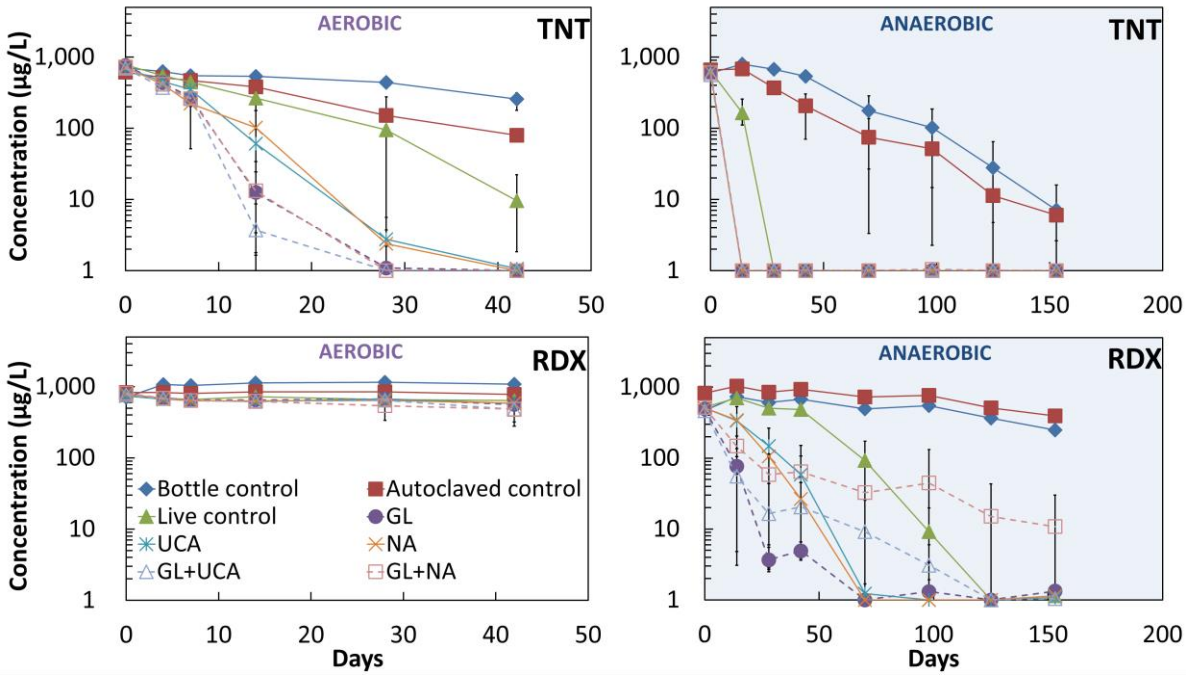

Figure S-2. Concentrations of TNT and RDX in field sand microcosms with various treatments under aerobic and anaerobic conditions. Error bars represent range of values in replicate columns. Where not visible, error bars are smaller than symbol size.

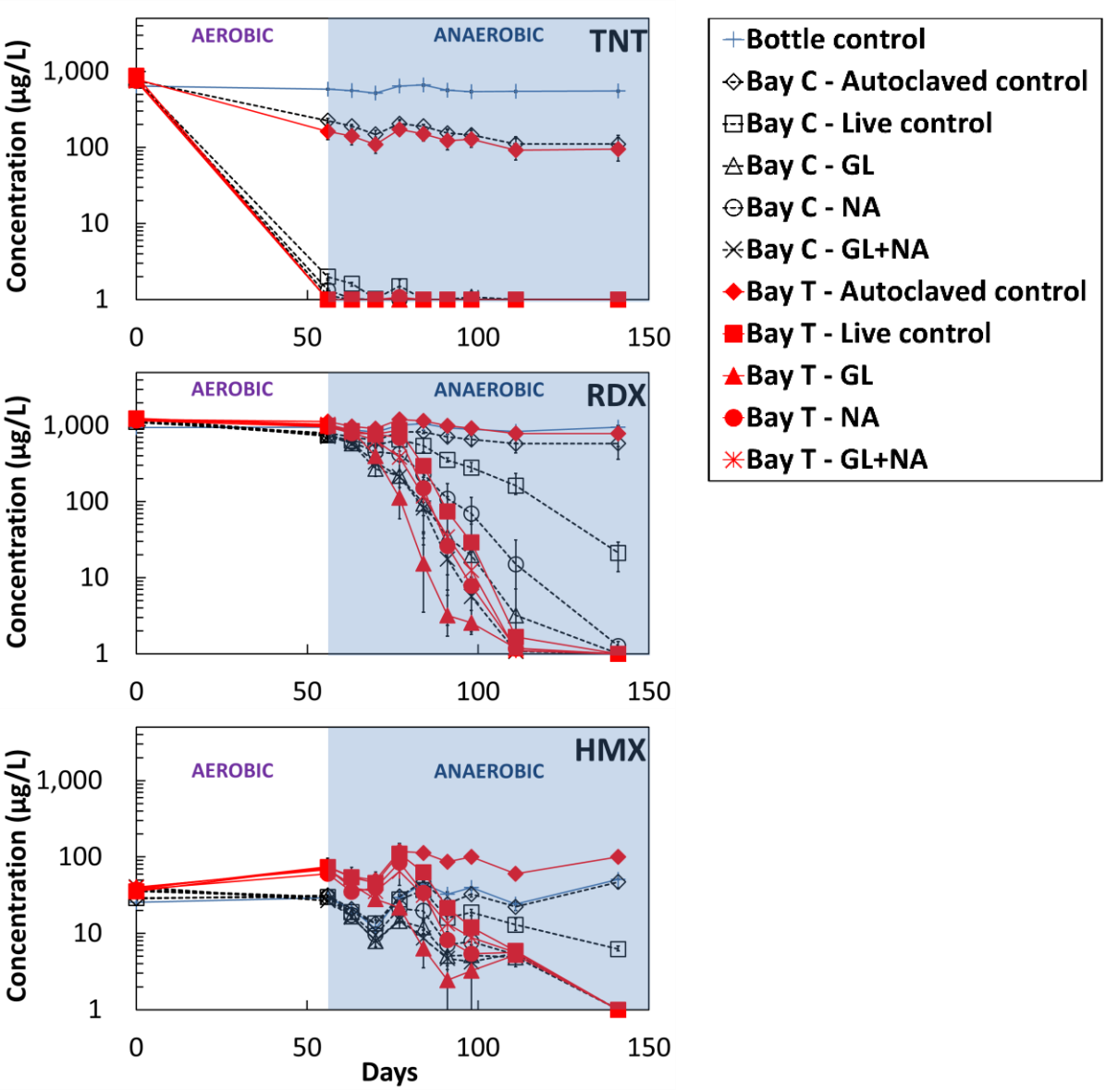

Figure S-3. Concentrations of high explosives (RDX, TNT, and HMX) in Bay C and T soil microcosms for all treatments under aerobic and anaerobic conditions. Error bars represent range of values in replicate columns. Where not visible, error bars are smaller than symbol size.

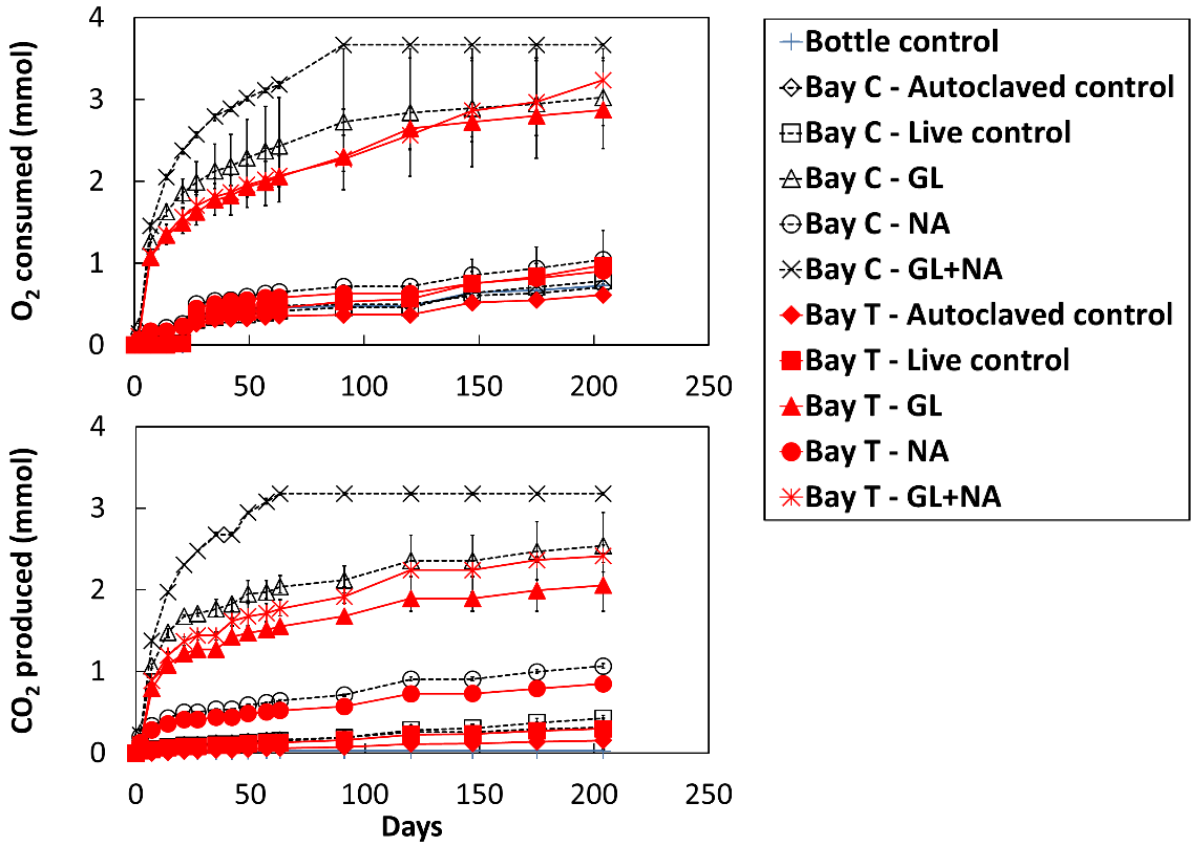

Figure S-4. Cumulative oxygen consumption and carbon dioxide production in Bay C and T soil microcosms for all treatments. Error bars represent range of values in replicate microcosms. Where not visible, error bars are smaller than symbol size.

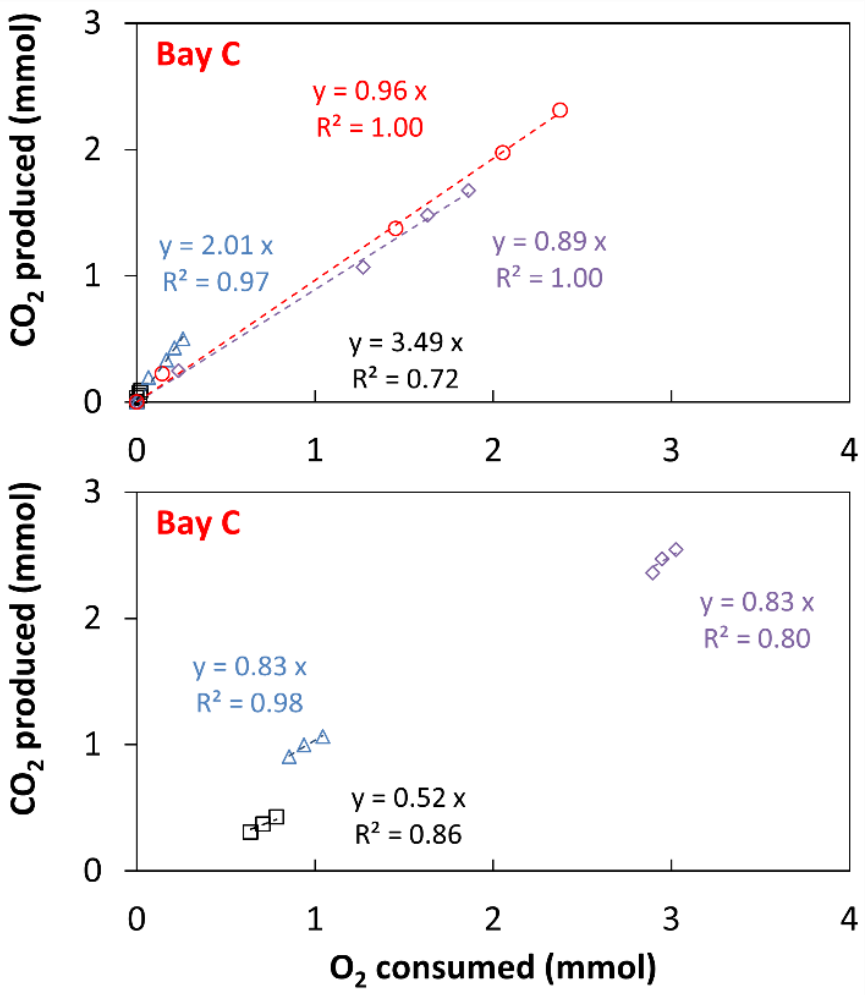

Figure S-5. Correlations between cumulative masses of oxygen consumed and carbon dioxide produced during first 27 days (top) and last 57 days (bottom) of monitoring period in Bay C soil microcosms with no treatment (□), addition of GL only (◊), NA only (Δ), and GL+NA (○). Dash lines represent linear correlation for each treatment.

APPENDIX III. Supplementary Material for Sorption Study

Table S-1. Main physicochemical properties of Ultrazine CA and Norlig A (Farling 2013).

Compound	Ultrazine CA (UCA)	Norlig A (NA)
Chemical formula[†]	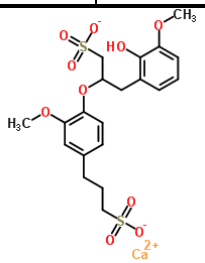 $C_{20}H_{24}CaO_{10}S_2$	
Molecular weight[‡] (g/mol)	528.6	
Water solubility at 20 ºC (mg/L)	> 95 %	> 95 %
ε_{280}[§] (L/cm/mol)	269	148

[†] Downloaded from www.chemspider.com.
[‡] Molecular weight for an average calcium lignosulfonate.
[§] Molar UV absorptivity at 280 nm.

Table S-2. Main physicochemical properties of TNT and RDX (Brannon and Pennington 2002).

Compound	**TNT**	**RDX**
Chemical formula[†]	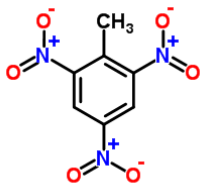 $C_7H_5N_3O_6$	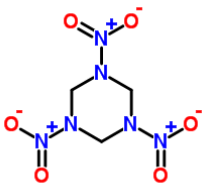 $C_3H_6N_6O_6$
Molecular weight (g/mol)	227.13	222.26
Water solubility at 20 ºC (mg/L)	130	42
Specific gravity	1.5-1.6	1.89
Octanol/water partitioning coefficient (K_{OW})	1.86	0.86

[†] Downloaded from www.chemspider.com.

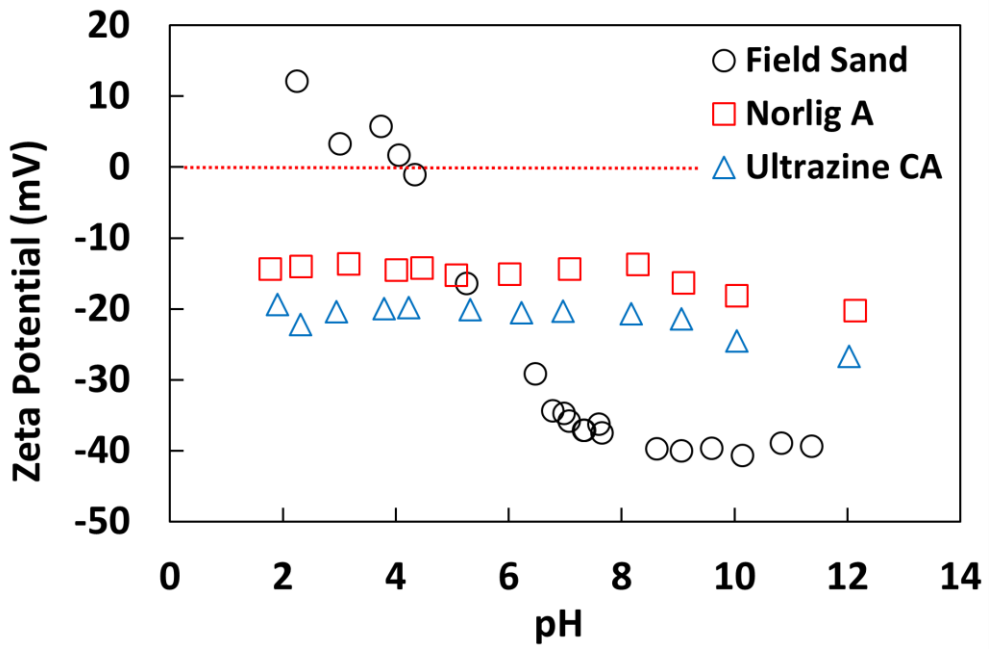

Figure S-6. Zeta potentials of field sand (FS) and lignosulfonates (Norlig A and Ultrazine CA) over pH 2 - 12.

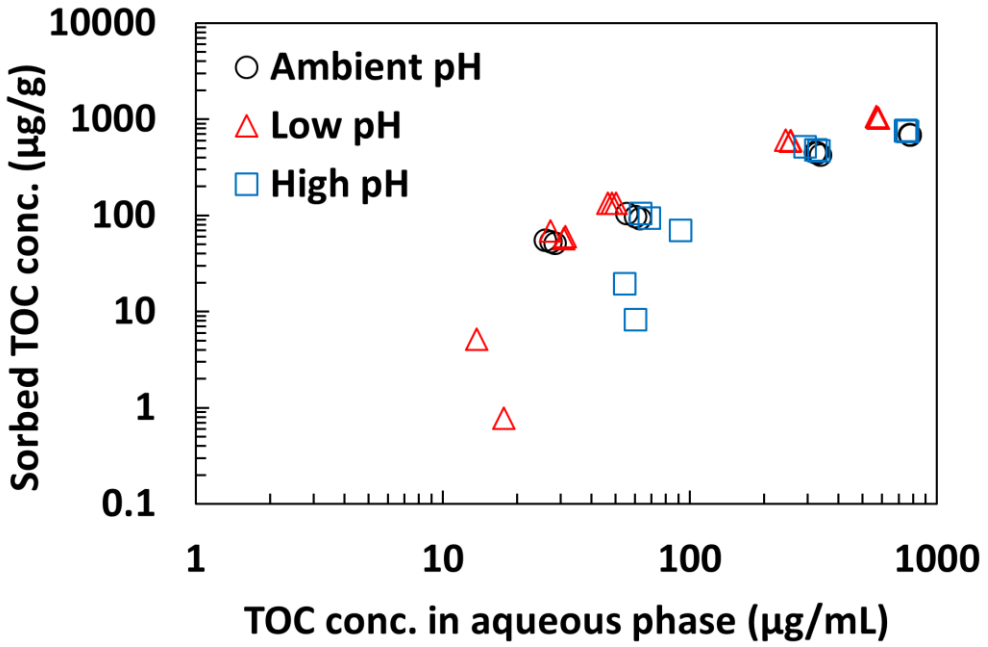

Figure S-7. pH effect in sorption of Norlig A (NA) in field sand (FS). Low pH; Initial pH = 2.53 ± 0.05 (after 2hrs for equilibrium), final pH 4.14 ± 0.09 (after 14-day sorption period). High pH; Initial pH 7.89 ± 1.10, final pH 6.59 ± 0.55.

Table S-3. Regression parameters for experimental lignosulfonate sorption results in field sand (FS) and range soil (RS).

LS[†]	Soil[‡]	Sorption period	Linear		Freundlich			Langmuir		
			K_d	*E*[§]	K_F	n	*E*	K	n	*E*
UCA	FS	1 day (autoclaved)	2.36	-0.3	3.89	0.85	0.77	4.04	0.005	0.96
		1day	5.93	-16	56.26	0.40	0.99	42.94	0.083	0.94
		7 days	7.65	-11	64.38	0.41	0.88	39.03	0.062	0.91
		14 days	18.87	-21	76.16	0.43	0.98	119.80	0.228	0.73
		30 days	11.00	-2	35.01	0.60	0.99	25.17	0.032	0.90
	RS	14 days	52.95	1	47.52	1.04	1	50.54	-0.003	1
NA	FS	14 days	2.68	-4	22.66	0.56	0.98	10.19	0.012	0.65

[†] LS = lignosulfonate, UCA = Ultrazine CA, NA = Norlig A.

[‡] FS = bulk field sand, RS = grenade range soil.

[§] *E* = model efficiency; 1 = perfect fit to the measurements, $E < 0$ = average of the measurements better than model prediction.

[¶] Unit; Kd = mL/g, KF = mLnμg1-n/g, K = mL/g, Langmuir n = mL/μg.

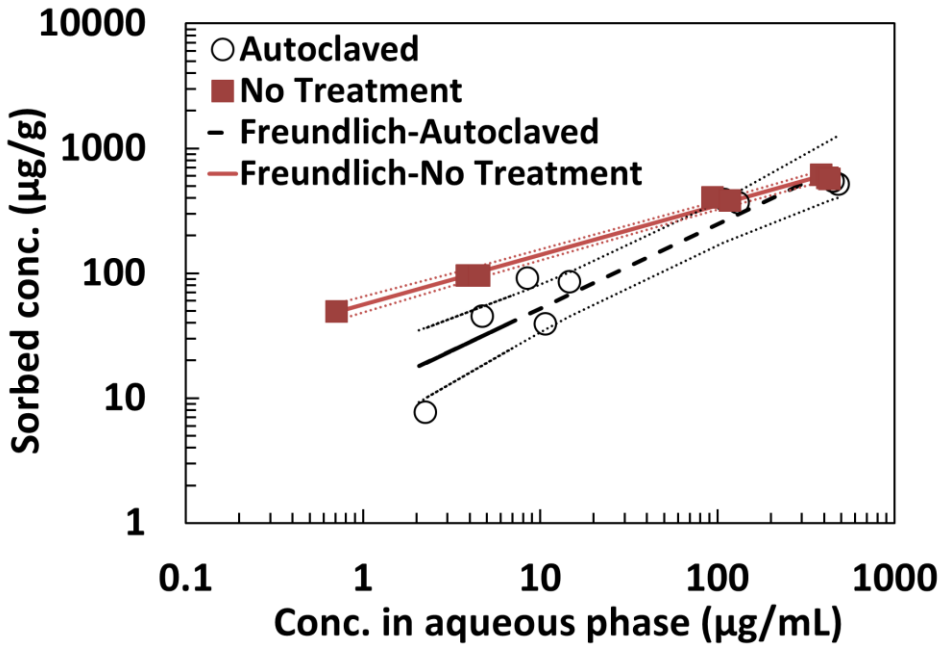

Figure S-8. Freundlich sorption isotherms for Ultrazine CA (UCA) on autoclaved and untreated field sand (FS). Dotted lines are upper and lower 95 % confidence intervals for each estimated Freundlich isotherm model.

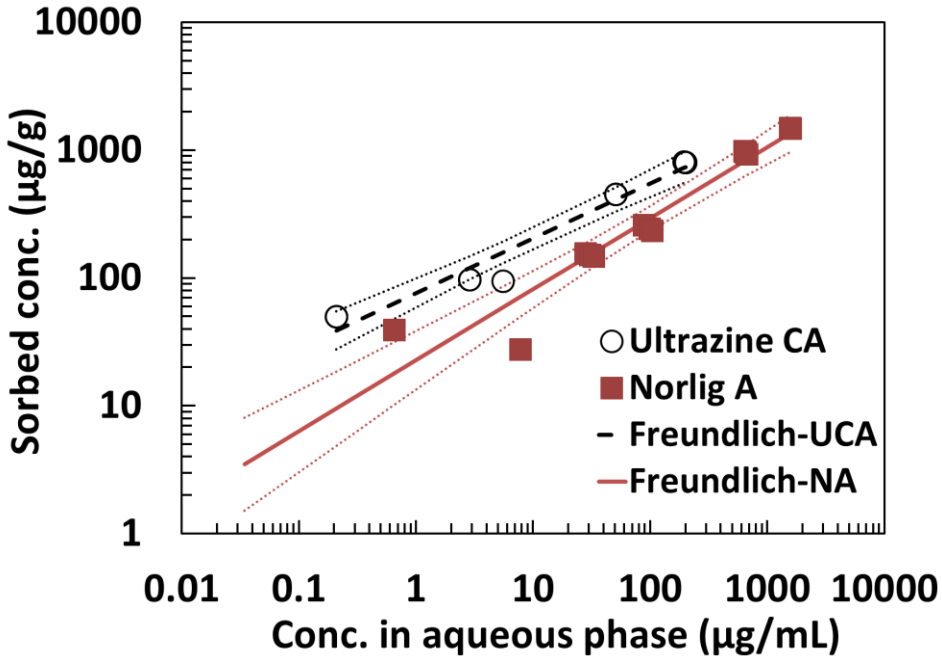

Figure S-9. Freundlich sorption isotherms for Ultrazine CA (UCA) and Norlig A (NA) on field sand (FS). Dotted lines are upper and lower 95 % confidence intervals for each estimated Freundlich isotherm model.

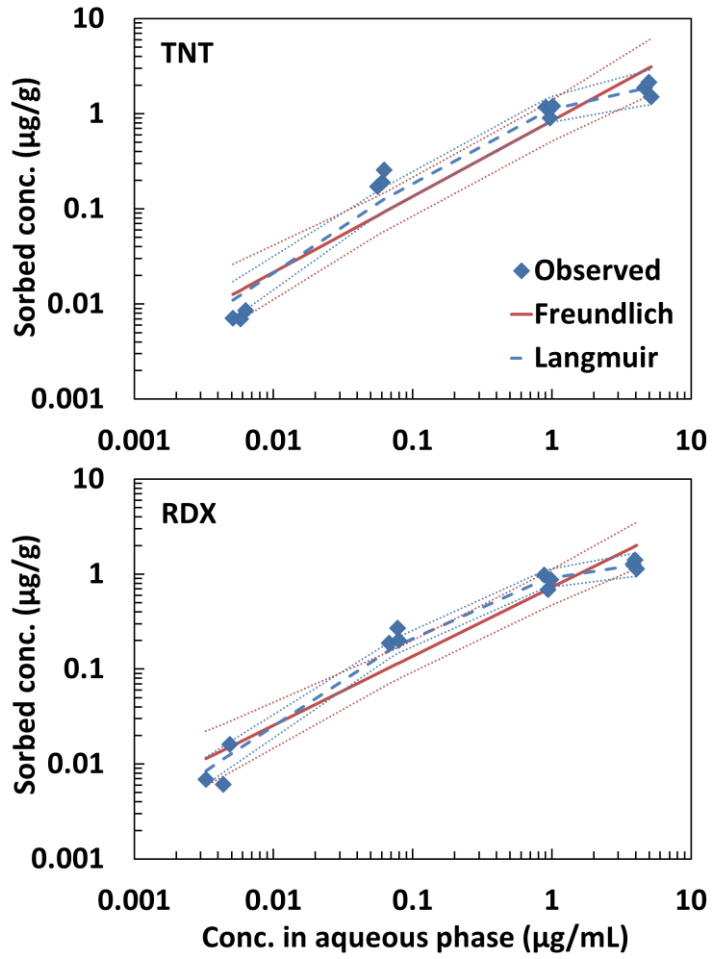

Figure S-10. Freundlich and Langmuir sorption isotherms for TNT and RDX on field sand (FS). Dotted lines are upper and lower 95 % confidence intervals for each estimated isotherm model.

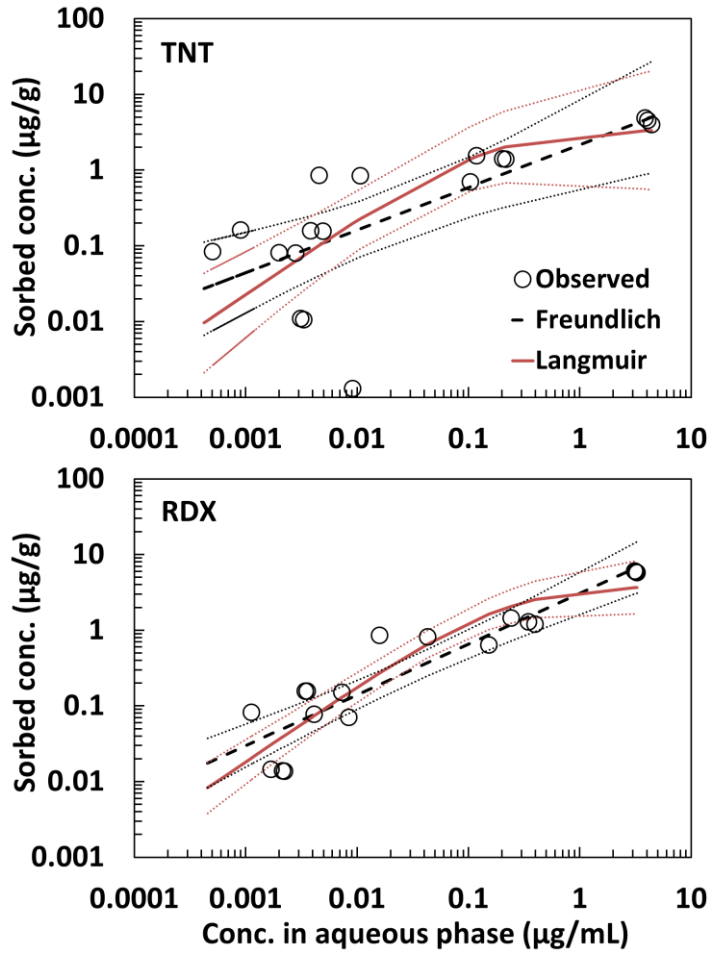

Figure S-11. Freundlich and Langmuir sorption isotherms for TNT and RDX on range soil (RS). Dotted lines are upper and lower 95 % confidence intervals for each estimated isotherm model.

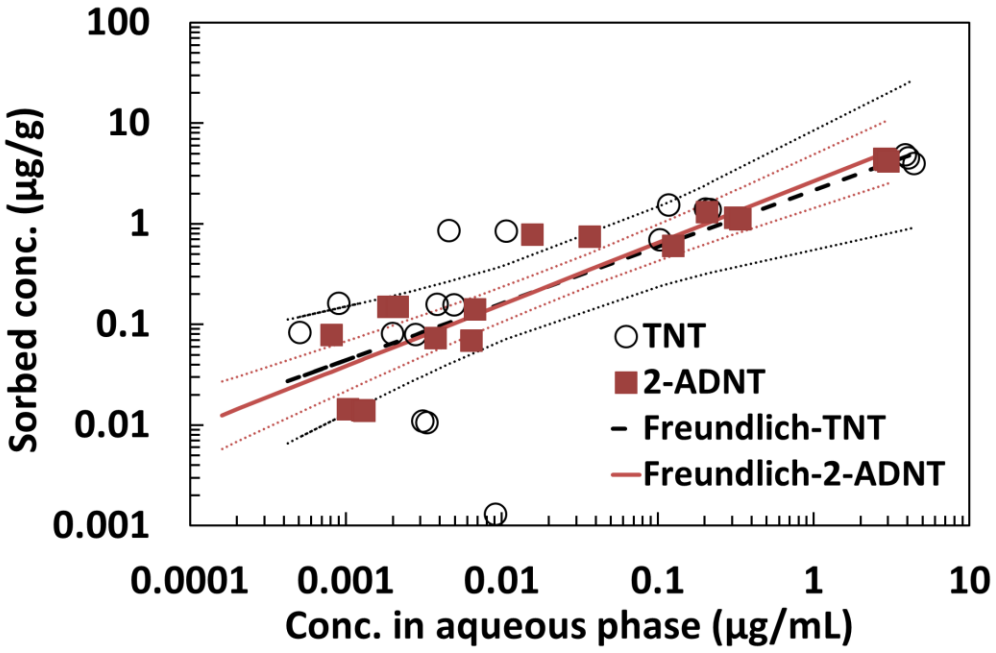

Figure S-12. Freundlich sorption isotherms for TNT and 2-ADNT on range soil (RS). Dotted lines are upper and lower 95 % confidence intervals for each estimated Freundlich isotherm model.

Table S-4. Regression parameters of 2,6-DNT, 2,4-DNT, and 2-ADNT sorption to intact (IRS), washed (WRS), and amended range soils (ARS).

	Soil†	Treatment	Linear		Freundlich			Langmuir			
			K_d	*E*‡	K_F	n	*E*	K	n	S_{max}	*E*
2,6-DNT	**RS**	**Intact**	5.96	-62	1.55	0.58	0.95	15.00	7.14	2.10	0.63
		Washed	4.44	-33	1.56	0.61	0.85	11.08	4.83	2.29	0.58
		Amended	2.16	-5	1.15	0.71	0.89	3.81	1.39	2.73	0.71
2,4-DNT	**RS**	**Intact**	9.48	-136	1.91	0.55	0.90	27.84	13.92	2.00	0.67
		Washed	6.51	-71	1.89	0.58	0.71	19.05	9.11	2.09	0.60
		Amended	3.92	-23	1.71	0.66	0.74	8.35	3.09	2.70	0.83
2-ADNT	**RS**	**Intact**	10.88	-54	2.66	0.61	0.93	25.83	9.70	2.66	0.71
		Washed	6.72	-22	2.67	0.69	0.69	13.84	4.25	3.26	0.78
		Amended	4.24	-6	2.01	0.71	0.92	7.91	2.55	3.10	0.75

† FS = field sand, RS = range soil.

‡ *E* = model efficiency; 1 = perfect fit to the measurements, $E < 0$ = average of the measurements better than model prediction.

¶ Unit; K_d = mL/g, K_F = $mL^n\mu g^{1-n}/g$, K = mL/g, Langmuir n = mL/µg, s_{max} = µg/g.

Table S-5. Regression parameters of TNT and RDX sorption to washed (WFS) and amended field sand (AFS), intact (IRS), washed (WRS), and amended range soils (ARS) (± 95 % confidence limit). Bold values are parameters for the model with the best fit.

	Soil†	Treatment	Linear		Freundlich			Langmuir			
			K_d	E‡	K_F	n	E	K	n	S_{max}	E
TNT	FS	**Washed**	1.17 ± 0.52	-6	0.84 ± 0.54	0.80 ± 0.16	0.33	**2.15 ± 1.07**	**0.94 ± 0.62**	**2.28**	**0.96**
		Amended	1.74 ± 0.88	-16	0.95 ± 0.50	0.68 ± 0.12	0.63	**4.50 ± 3.91**	**2.32 ± 2.38**	**1.94**	**0.94**
	RS	**Intact**	10.98 ± 5.07	-110	**2.16 ± 6.09**	**0.56 ± 0.29**	**0.92**	22.83 ± 19.76	6.65 ± 6.63	3.43	0.85
		Washed	12.79 ± 6.79	-214	**2.53 ± 4.70**	**0.53 ± 0.23**	**0.68**	40.35 ± 76.89	15.08 ± 32.67	2.68	0.64
		Amended	4.76 ± 2.22	-27	2.07 ± 3.86	0.68 ± 0.29	0.60	**8.85 ± 7.45**	**2.35 ± 2.34**	**3.76**	**0.86**
RDX	FS	**Washed**	1.16 ± 0.54	-9	0.73 ± 0.39	0.73 ± 0.14	0.49	**2.60 ± 1.28**	**1.83 ± 1.13**	**1.42**	**0.97**
		Amended	1.05 ± 0.44	-4	0.79 ± 0.60	0.84 ± 0.18	0.12	**1.81 ± 1.22**	**0.91 ± 0.86**	**1.99**	**0.92**
	RS	**Intact**	9.37 ± 3.84	-21	**3.06 ± 2.75**	**0.67 ± 0.15**	**0.96**	18.25 ± 25.38	4.67 ± 7.77	3.91	0.75
		Washed	6.44 ± 2.70	-10	**2.98 ± 3.80**	**0.72 ± 0.22**	**0.86**	11.84 ± 15.38	2.62 ± 4.15	4.51	0.78
		Amended	6.45 ± 2.16	-2	**3.41 ± 3.20**	**0.77 ± 0.18**	**0.97**	9.94 ± 9.97	1.56 ± 2.11	6.36	0.85

† FS = field sand, RS = range soil.

‡ E = model efficiency; 1 = perfect fit to the measurements, $E < 0$ = average of the measurements better than model prediction.

§ Unit; K_d = mL/g, K_F = $mL^n\mu g^{1-n}/g$, K = mL/g, Langmuir n = mL/μg, S_{max} = μg/g.

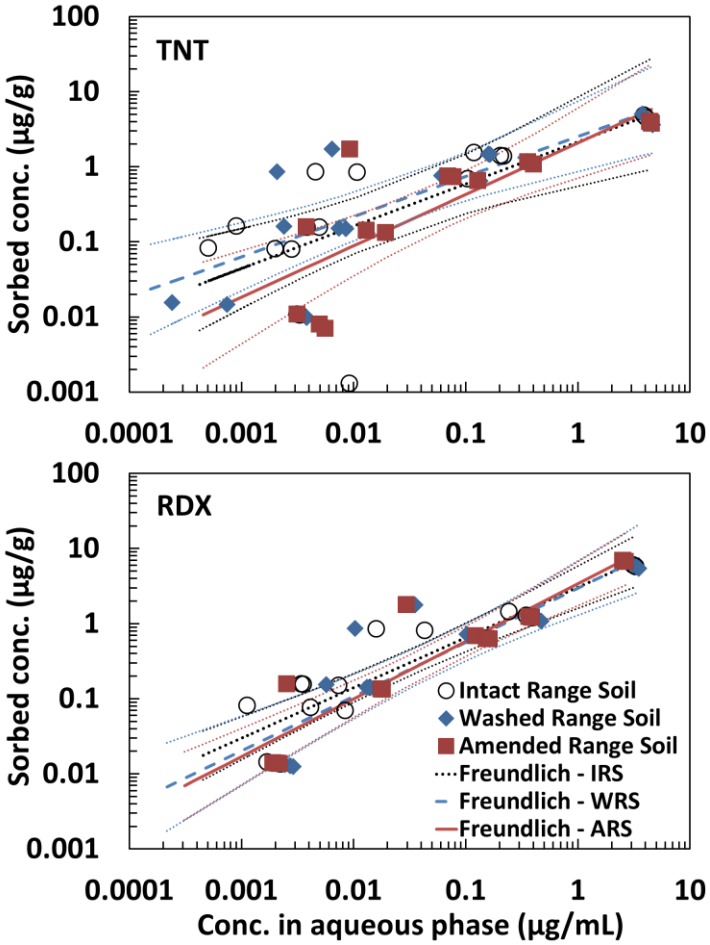

Figure S-13. Freundlich sorption isotherms for TNT and RDX on intact (IRS), washed (WRS), and amended range soil (ARS).

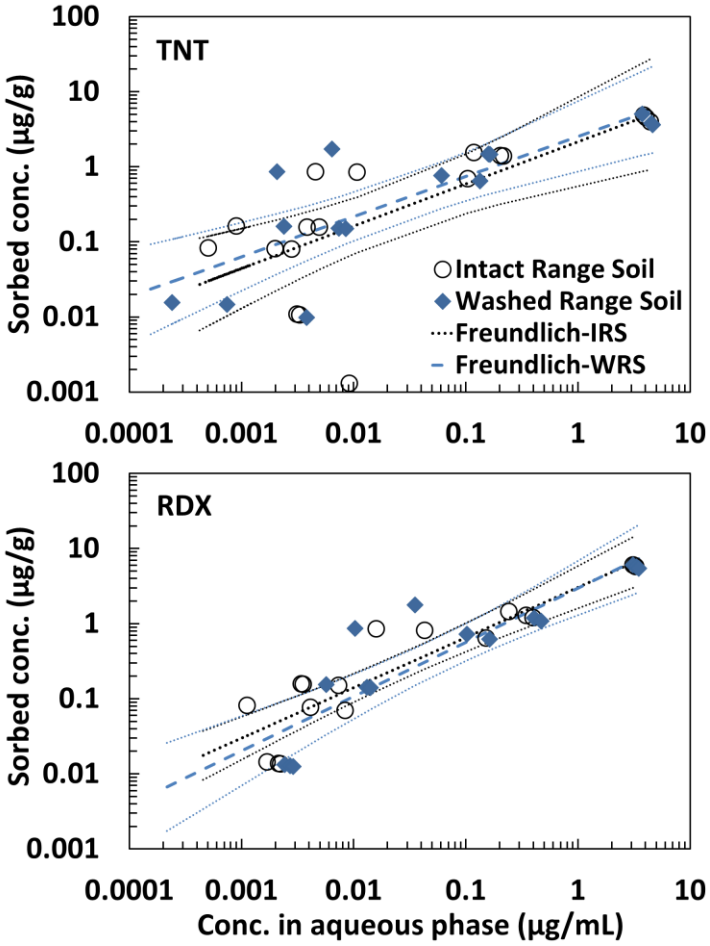

Figure S-14. Freundlich sorption isotherms for TNT and RDX on intact (IRS) and washed range soil (WRS). Dotted lines are upper and lower 95 % confidence intervals for each estimated Freundlich isotherm model.

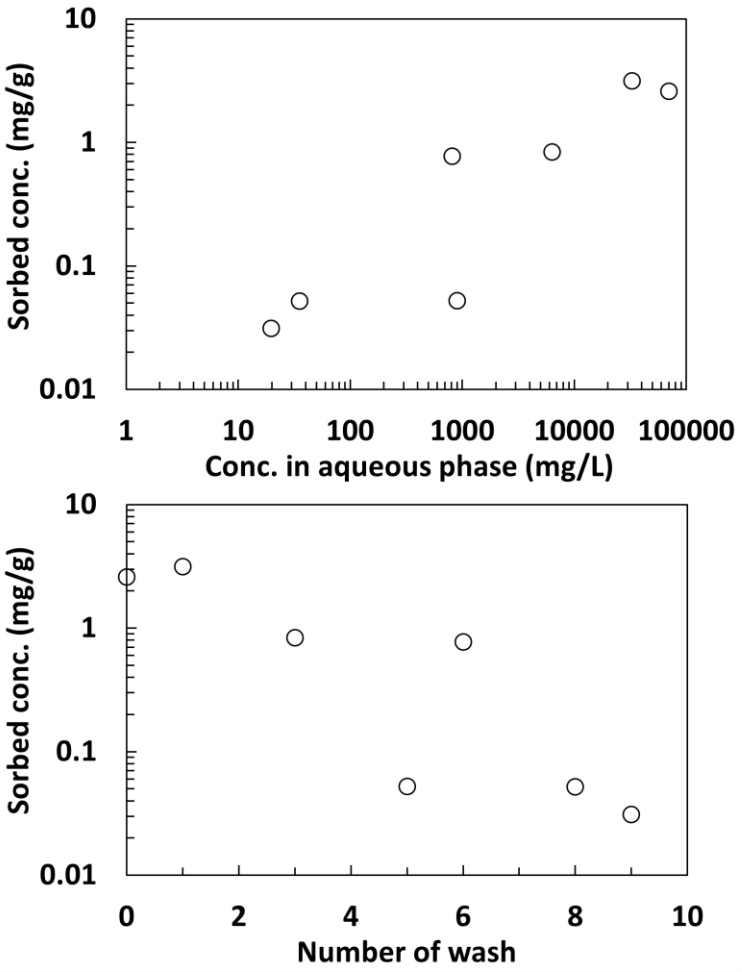

Figure S-15. Desorption of Norlig A (NA) during washing process in pretreatment of grenade range soil (RS) prior to sorption experiment for TNT and RDX.

APPENDIX IV. Supplementary Material for Column Study

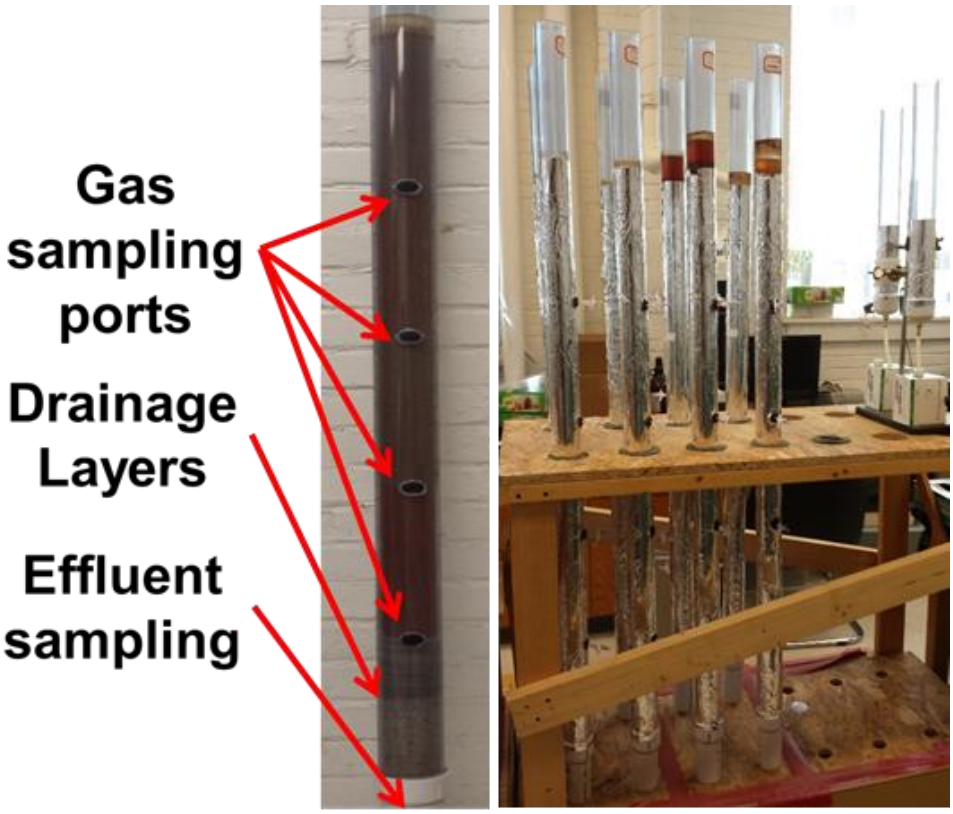

Figure S-16. Photographs of soil columns. Column series included: 1) Bay C soils with no amendment, (2) Bay C soils with GL + NA, (3) Bay T soils with no amendment, and (4) Bay T soils with GL + NA. Relatively smaller columns on top of the rack were leaching columns with a water drainage layer only (0.15 m coarse sand + 0.1 m fine sand).

Table S-6. Hydraulics of soil columns measured at the termination of monitoring.

Columns		Volume (cm^3)	Bulk Density		Particle Density (g/cm^3)	Porosity (Φ)	Volumetric Moisture Content (θ, cm^3/cm^3)	Air-filled Porosity (Φ_a)
			Wet Bulk Density (g/cm^3)	Dry Bulk Density (g/cm^3)				
Control Bay C	A	2,027	2.15	1.87	2.57	0.279	0.274	0.005
	B	2,027	2.19	1.91	2.57	0.265	0.265	0
Treated Bay C	A	2,027	2.21	1.93	2.57	0.256	0.256	0
	B	2,027	2.15	1.89	2.57	0.273	0.262	0.012
Control Bay T	A	2,027	2.04	1.83	2.57	0.298	0.214	0.083
	B	2,027	2.04	1.83	2.57	0.296	0.212	0.084
Treated Bay T	A	2,027	2.09	1.86	2.57	0.286	0.234	0.053
	B	2,027	2.07	1.84	2.57	0.294	0.230	0.063

Table S-7. Water balance in soil columns over monitoring period.

Columns		Leaching		Control Bay C		Treated Bay C		Control Bay T		Treated Bay T	
Parameters	**Cumulative days**[†]	A	B	A	B	A	B	A	B	A	B
Cumulative applied groundwater (mL)	-84	-	-	0	0	0	0	0	0	0	0
	0	0	0	284	284	284	284	284	284	284	284
	56	214	214	458	458	458	458	458	458	458	458
	611	1,838	1,838	2,082	2,082	2,082	2,082	2,082	2,082	2,082	2,082
Cumulative effluents (mL)	56	59	57	0	0	0	19	9	15	12	3
	611	1,228	1,191	474	379	191	325	1,105	1,116	975	1,019
	Fraction (%)	67	65	23	18	9	16	53	54	47	49
Water retained in soil (mL)	611	57[‡]	57[‡]	612	629	611	577	491	487	541	535
	Fraction (%)	3	3	29	30	29	28	24	23	26	26
Water ponded on the top (mL)	611	N/A	N/A	99	184	304	278	N/A	N/A	N/A	N/A
	Fraction (%)	-	-	5	9	15	13	-	-	-	-
Water evaporated (mL)	611	553	590	896	889	976	902	486	478	566	528
	Fraction (%)	30	32	43	43	47	43	23	23	27	25

[†] Cumulative days since application of Comp B impacted soil. Start of groundwater application at -84 days, application of Comp B impacted soil at 0 day, application of waste glycerin and Norlig A (lignosulfonate) at 56 days, and termination of groundwater application at 611 days.

[‡] Estimated by water volume retained in soils for drain layer at the bottom of soil columns.

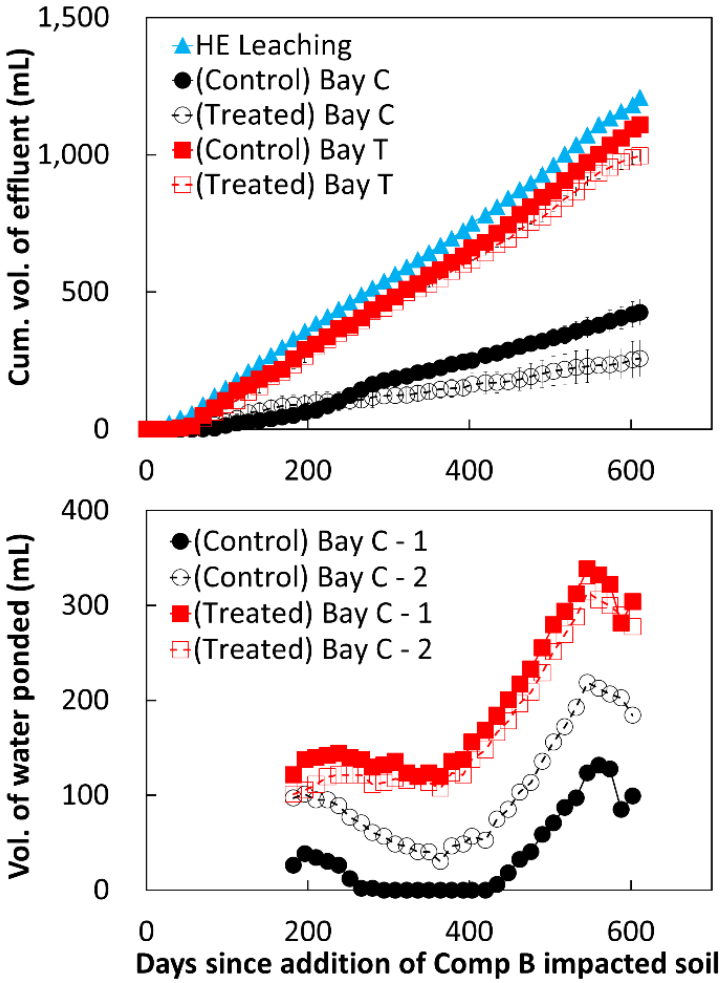

Figure S-17. Cumulative volumes of column effluents and volumes of water ponded on the top of column soils over the monitoring period. Error bars in cumulative volumes of effluent represent range of values in replicate columns. Where not visible, error bars are smaller than symbol size.

Table S-8. Mass balance results of nitrogen in soil columns.

Columns		Leaching		Control Bay C		Treated Bay C		Control Bay T		Treated Bay T	
	Media	**A**	**B**	**A**	**B**	**A**	**B**	**A**	**B**	**A**	**B**
N (mmol)	†Inorg.-N_{eff}	0.1	0.1	1.3	0.2	0.2	1.3	0.7	0.6	0.3	0.5
	‡Exp.-N_{eff}	0.89	0.77	0.003	0	0	0.003	0.13	0.21	0.04	0.05
	§Exp.-N_{soil}	2.74	4.00	0.58	0.67	0.13	0.27	1.17	1.14	0.41	0.58
	Total	3.74	4.87	1.85	0.93	0.31	1.57	1.95	1.98	0.73	1.17

† Inorg.-N in effluent = NO_2 + NO_3.
‡ Exp.-N in effluent = explosives-N discharged.
§ Exp.-N in soil = explosives-N sorbed to soil.

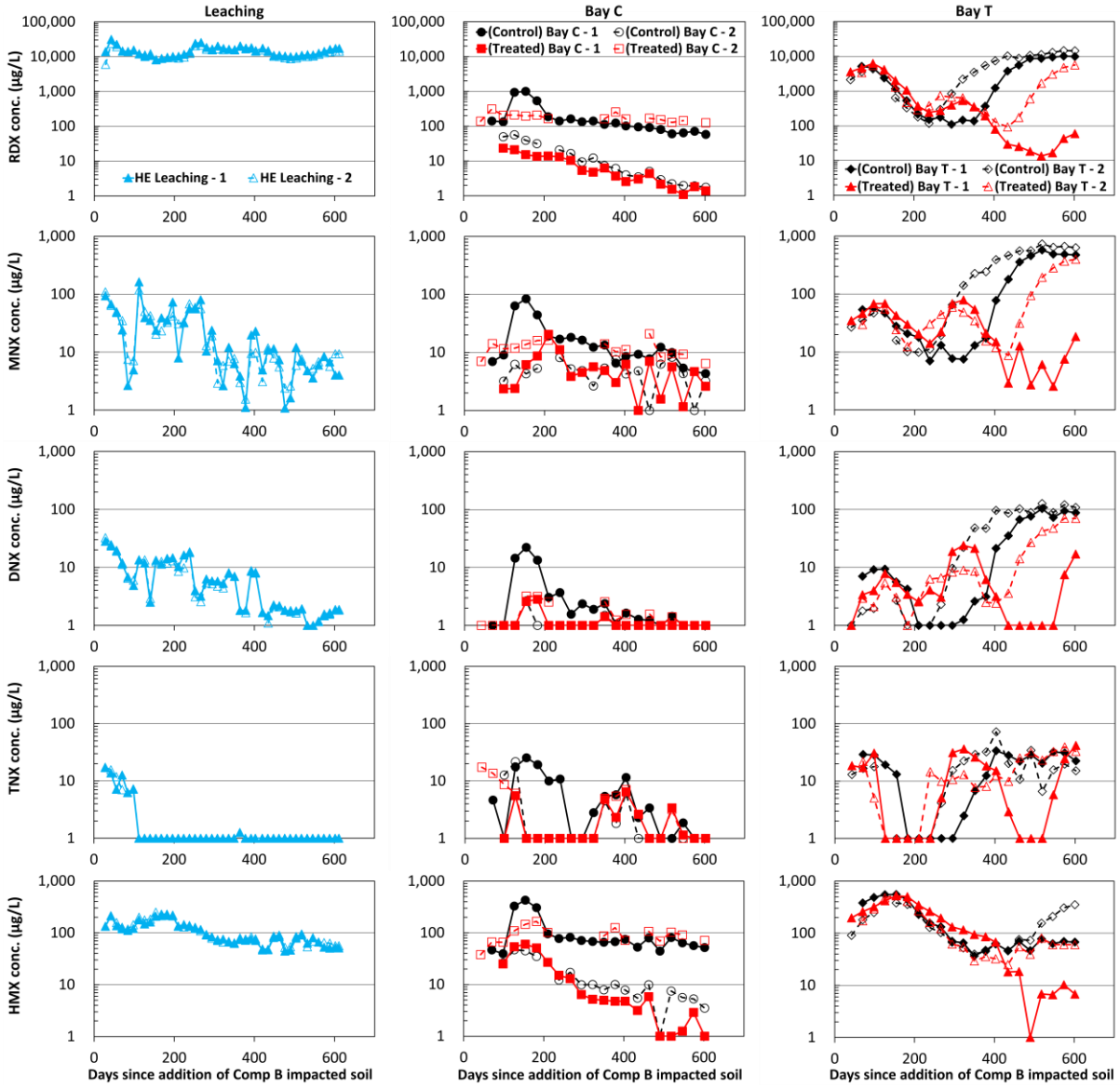

Figure S-18. Concentrations of RDX, MNX, DNX, TNX and HMX in column effluents over the monitoring period.

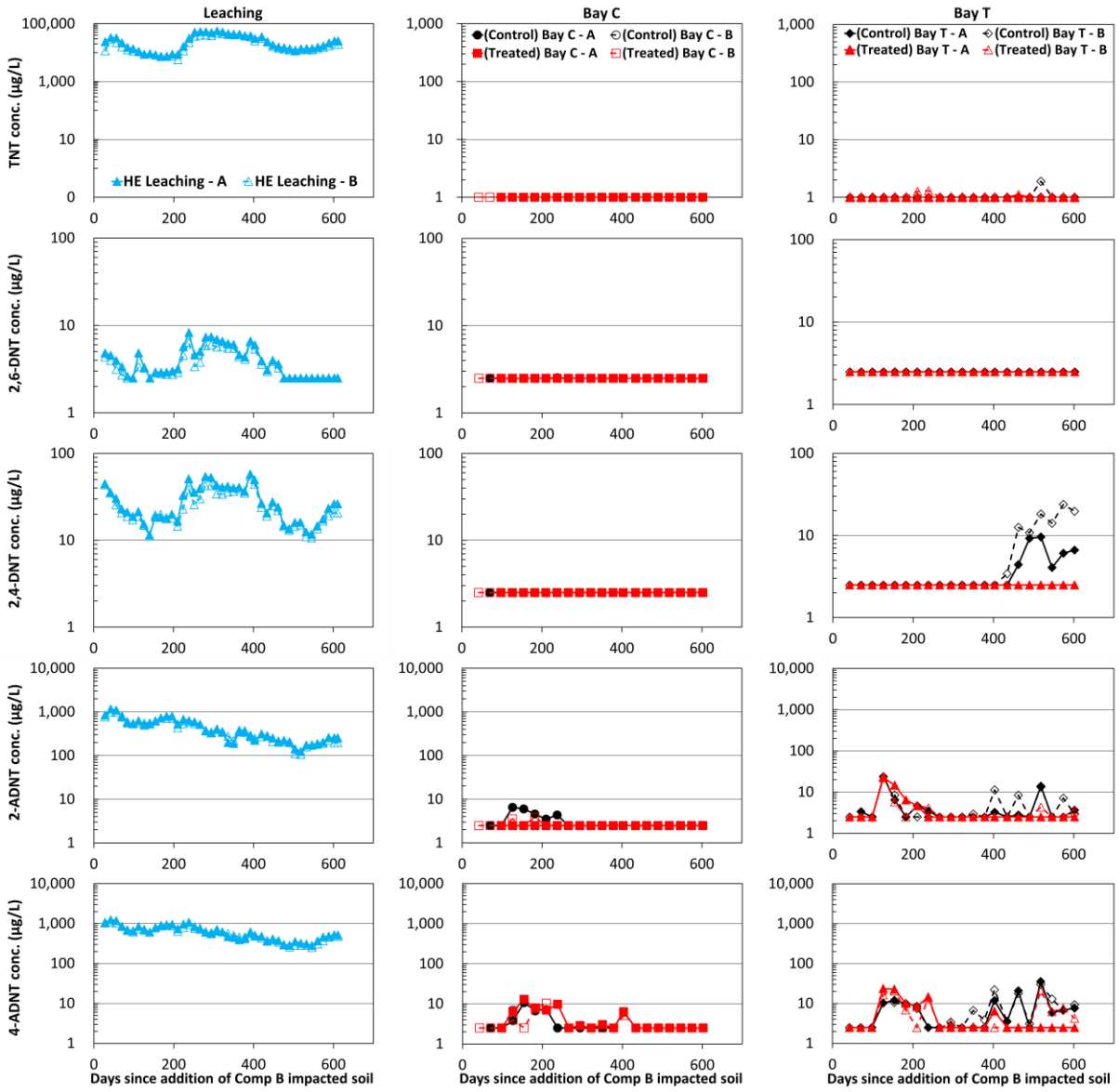

Figure S-19. Concentrations of TNT, 2,6-DNT, 2,4-DNT, 2-ADNT and 4-ADNT in column effluents over the monitoring period.

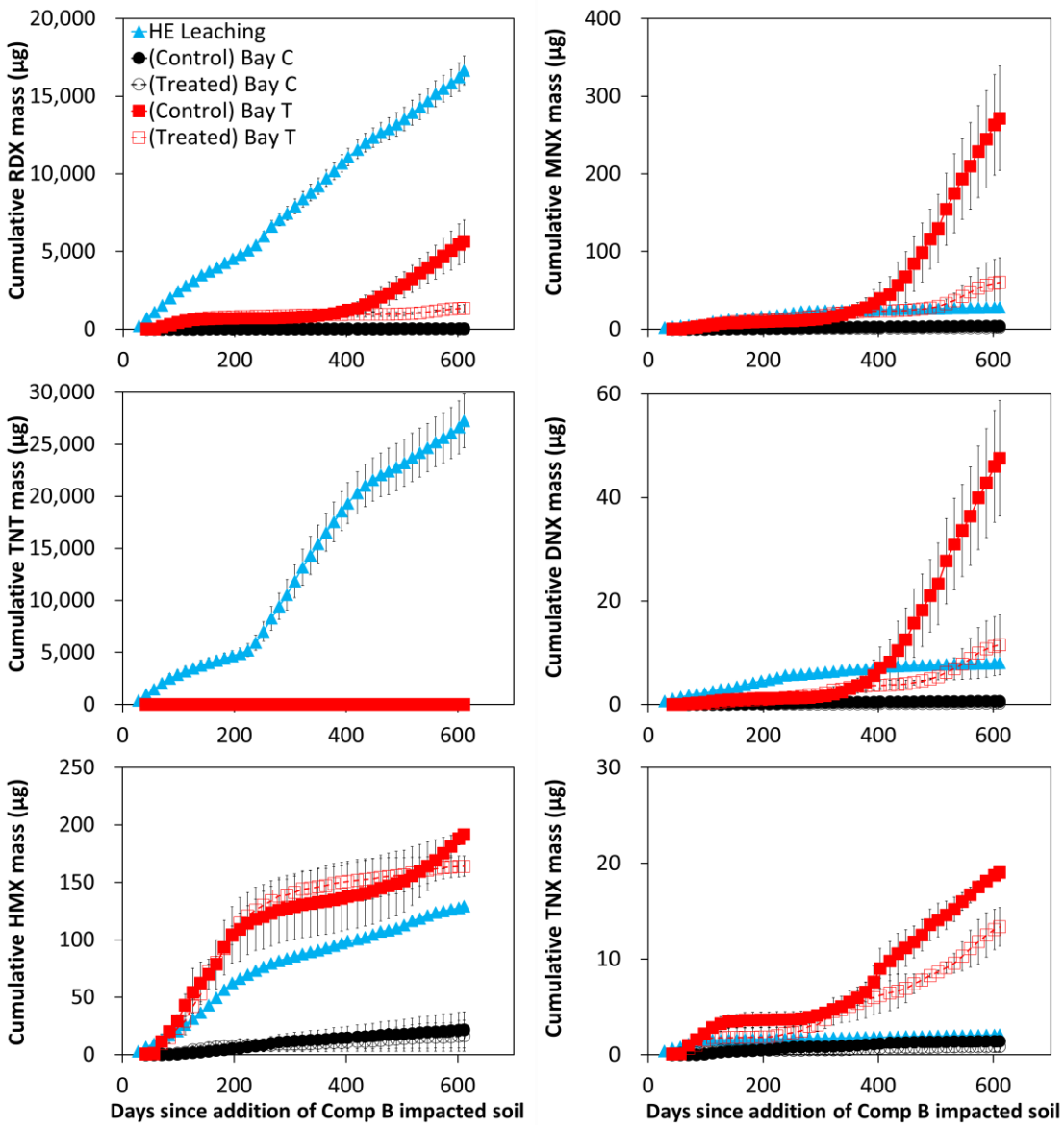

Figure S-20. Cumulative masses of RDX, TNT, HMX, and RDX degradation products (MNX, DNX, and TNX) over the monitoring period.

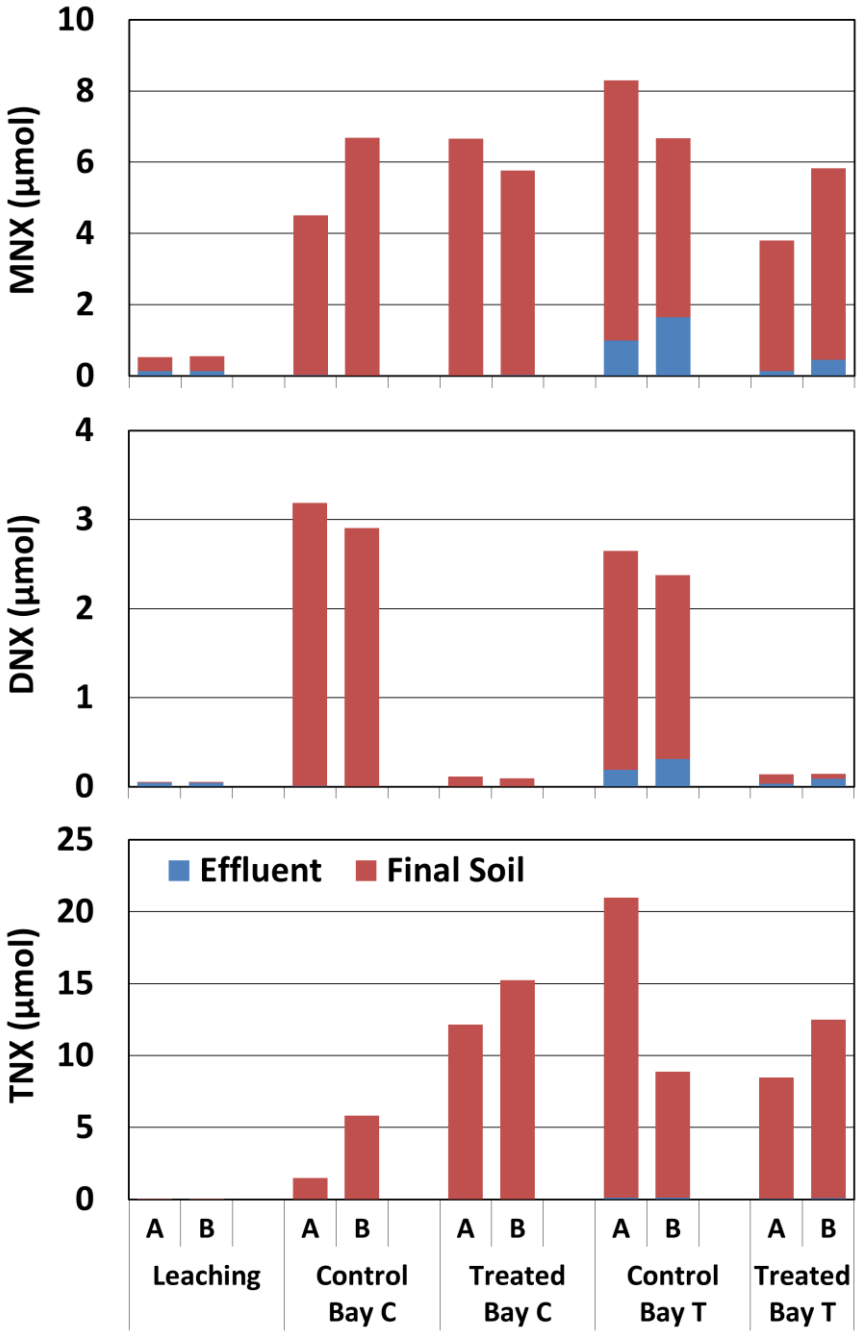

Figure S-21. Masses of MNX, DNX, and TNX in effluent and soils of laboratory columns.

Table S-9. Masses of OC, RDX, TNT, HMX, and RDX degradation products (MNX, DNX, and TNX) in soil columns.

Columns		Leaching		Control Bay C		Treated Bay C		Control Bay T		Treated Bay T	
Parameters	**Media**	**A**	**B**	**A**	**B**	**A**	**B**	**A**	**B**	**A**	**B**
OC (g)	Effluents	0.03	0.03	0.005	0.006	0.005	0.004	0.007	0.005	0.008	0.009
	Soils	2.13	2.13	8.23	8.82	9.16	9.64	5.71	6.03	6.30	6.17
	Total	2.15	2.15	8.24	8.82	9.16	9.64	5.72	6.04	6.31	6.18
RDX (mg)	Effluents	17.59	15.72	0.07	0.006	0.002	0.06	4.27	7.03	1.11	1.57
	Soils	4.04	5.64	1.63	1.66	0.28	0.94	0.96	1.33	1.54	1.73
	Total	21.63	21.36	1.69	1.66	0.28	0.99	5.23	8.36	2.65	3.31
TNT (mg)	Effluents	29.83	24.65	0	0	0	0	0.001	0.001	0.001	0.001
	Soils	197.90	289.71	34.26	37.54	0.29	6.69	71.56	75.23	19.91	29.91
	Total	227.72	314.36	34.26	37.54	0.29	6.69	71.56	75.23	19.91	29.91
HMX (mg)	Effluents	0.13	0.13	0.04	0.006	0.003	0.03	0.19	0.19	0.17	0.16
	Soils	0.02	0.01	0.13	0.11	0.09	0.08	0.06	0.06	0.07	0.06
	Total	0.15	0.14	0.16	0.11	0.09	0.11	0.25	0.25	0.25	0.21
MNX (mg)	Effluents	0.03	0.03	0.006	0.002	0.001	0.004	0.20	0.34	0.03	0.09
	Soils	0.68	0.91	0.92	1.38	1.37	1.18	1.51	1.04	0.75	1.11
	Total	0.71	0.94	0.93	1.38	1.37	1.19	1.71	1.38	0.78	1.20
DNX (mg)	Effluents	0.008	0.008	0.001	0	0	0	0.04	0.06	0.006	0.02
	Soils	0.002	0.002	0.61	0.55	0.02	0.02	0.47	0.39	0.02	0.01
	Total	0.01	0.01	0.61	0.55	0.02	0.02	0.50	0.45	0.03	0.03
TNX (mg)	Effluents	0.002	0.002	0.002	0.001	0	0.001	0.02	0.02	0.01	0.02
	Soils	0.002	0.002	0.26	1.01	2.12	2.66	3.63	1.53	1.46	2.16
	Total	0.004	0.004	0.26	1.01	2.12	2.66	3.65	1.54	1.47	2.17

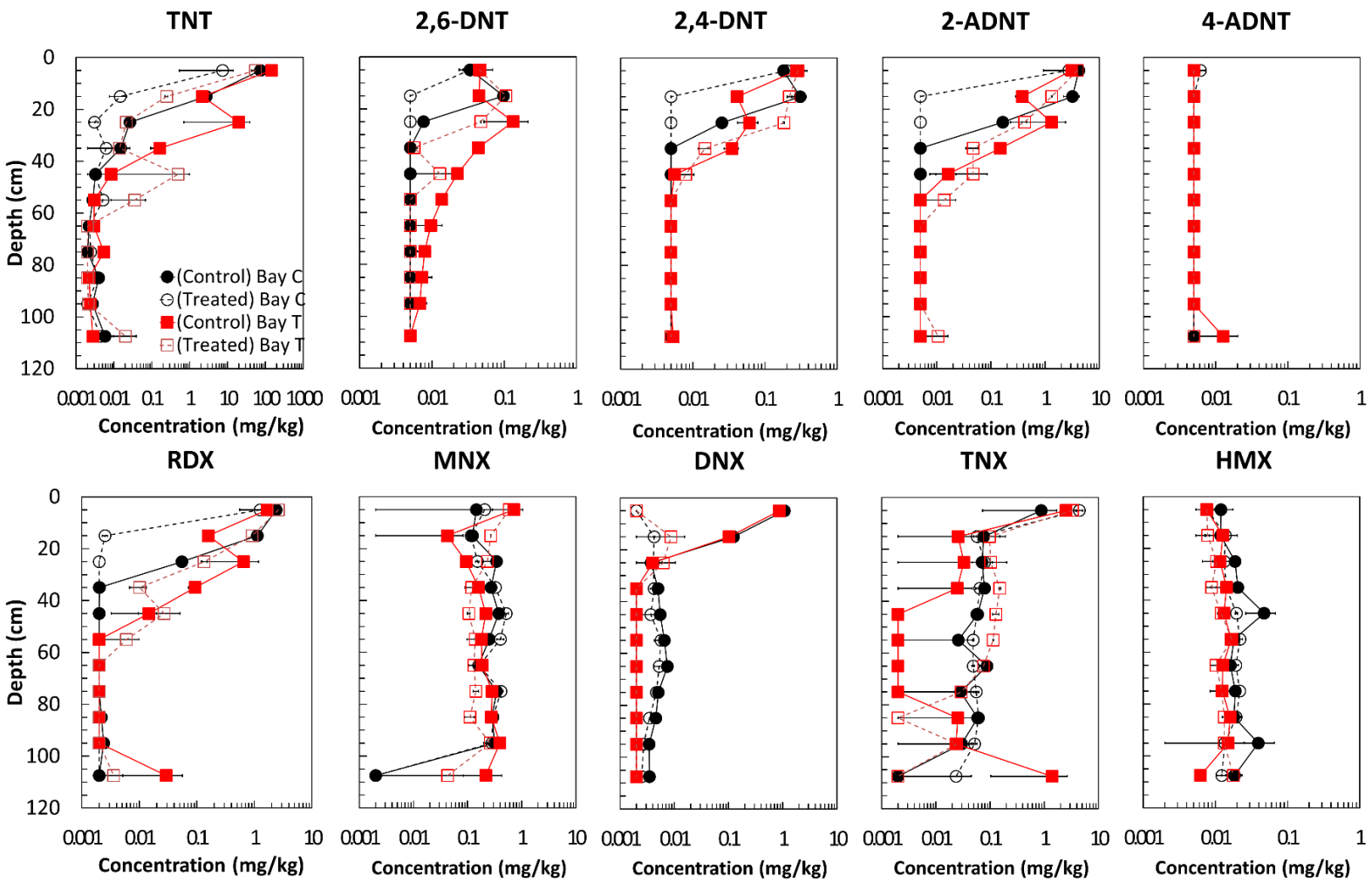

Figure S-22. Vertical variation of explosives concentrations in soil columns at the end of monitoring period.

APPENDIX V. Supplementary Material for Field Study

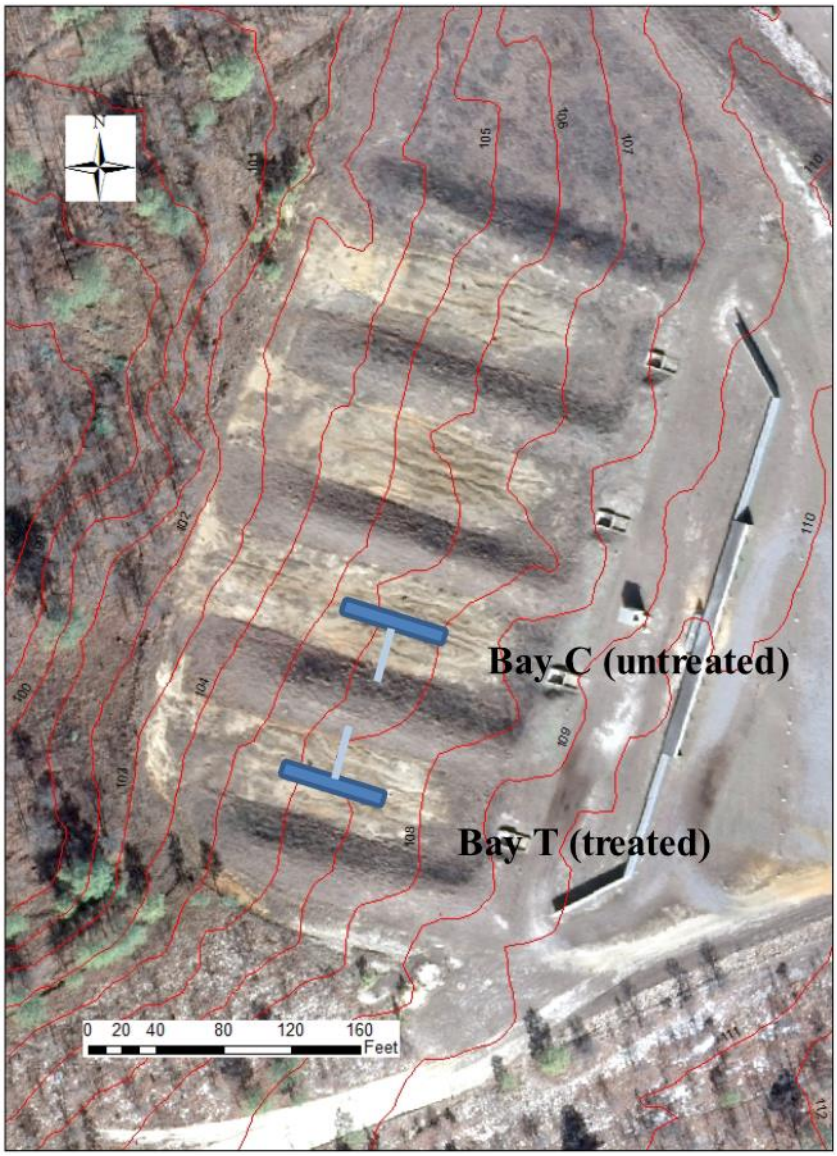

Figure S-23. Hand grenade range (RG40) at Fort Bragg.

Figure S-24. Trench excavation and open trench in hand grenade range at Fort Bragg.

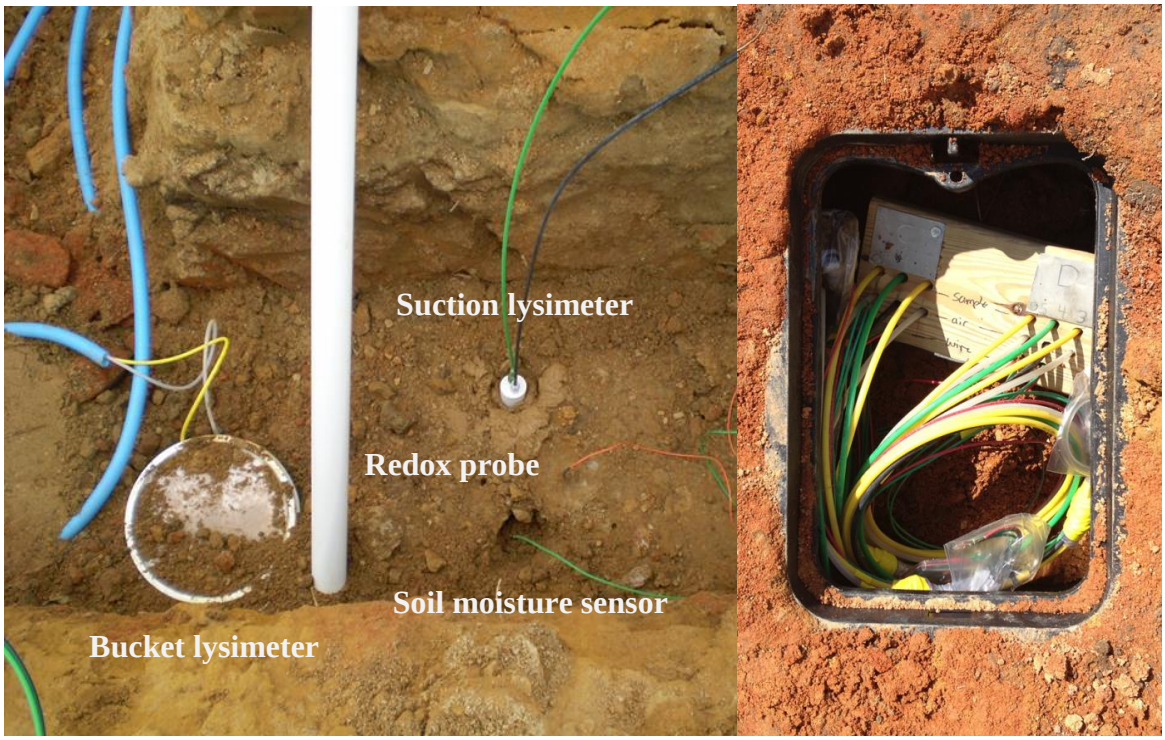

Figure S-25. Monitoring instrumentation during installation in grenade bays and sampling access point.

Figure S-26. Craters in grenade throwing bay, organic amendment application by impact sprinkler, and organic amendment application by spray nozzle.

Table S-10. Characterization results of different depth grenade range soils.

Parameters		Soils	0 - 1 ft	1 - 2 ft	2 – 3 ft	3 – 4 ft	4 – 6 ft	Mean
Organic Carbon (%)		Bay T	0.08	0.11	0.09	0.04	0.09	0.08 ± 0.03
		Bay C	0.10	0.19	0.27	0.19	0.24	0.20 ± 0.06
Total Fe (g/kg)	**Non-Crystalline**	Bay T	0.11	0.23	0.17	0.09	0.06	0.13 ± 0.07
		Bay C	0.19	0.28	0.31	0.45	0.37	0.32 ± 0.10
	Crystalline	Bay T	4.67	5.14	5.59	7.53	6.64	5.91 ± 1.16
		Bay C	3.44	1.72	3.08	2.13	2.86	2.64 ± 0.71
Total Fe(II) (g/kg)	**Non-Crystalline**	Bay T	0.07	0.20	0.13	0.06	0.04	0.10 ± 0.07
		Bay C	0.12	0.25	0.28	0.31	0.32	0.26 ± 0.08
	Crystalline	Bay T	1.36	1.70	1.90	2.31	2.10	1.88 ± 0.37
		Bay C	1.42	0.87	1.37	0.98	1.22	1.17 ± 0.24
Fe(II) / Total Fe (%)	**Non-Crystalline**	Bay T	69	86	75	69	62	72 ± 9
		Bay C	60	92	89	69	86	79 ± 14
	Crystalline	Bay T	29	33	34	31	32	32 ± 2
		Bay C	41	51	44	46	43	45 ± 4
Sediment D_{50} (µm)		Bay T	253	180	358	359	337	297 ± 79
		Bay C	205	246	384	322	319	295 ± 70
Silt Fraction (%)		Bay T	14.2	18.0	12.9	9.2	11.8	13.2 ± 3.2
		Bay C	16.0	12.8	9.7	14.4	15.1	13.6 ± 2.5
Clay Fraction (%)		Bay T	2.0	2.3	1.8	1.4	1.7	1.9 ± 0.3
		Bay C	2.2	2.4	1.8	2.4	2.6	2.3 ± 0.3
pH		Bay T	5.5	5.5	5.5	5.6	5.5	5.5 ± 0.1
		Bay C	5.6	5.0	5.1	5.4	5.3	5.3 ± 0.2
RDX (mg/kg)		Bay T	1.03	0.03	0.16	0.21	0.09	0.30 ± 0.41
		Bay C	0.02	0.01	0.01	0.01	0.04	0.02 ± 0.01
TNT (mg/kg)		Bay T	0.018	0.013	0.009	0.013	0.014	0.013 ± 0.003
		Bay C	0.015	0.008	0.021	0.016	0.021	0.016 ± 0.005